THE TRANSIENT BEHAVIOUR OF PLAIN CONCRETE AT ELEVATED TEMPERATURES

by

ABDERRAHIM BALI

Thesis submitted for the degree of

Doctor of Philosophy

The University of Aston in Birmingham

April 1984

This thesis is dedicated

to the memory of

my father Achour.

To my mother, sisters

and brothers.

The University of Aston in Birmingham

The Transient Behaviour of Plain Concrete at Elevated Temperatures

By
ABDERRAHIM BALI

Thesis submitted for the degree of Doctor of Philosophy
April 1984

Summary

This thesis describes an investigation of the effect of elevated temperatures upon the properties of plain concrete containing a siliceous aggregate. A complete stress-strain relationship and creep behaviour are studied. Transient effects (non-steady state) are also examined in order to simulate more realistic conditions. A temperature range of 20-700°C is used, corresponding to the temperatures generally attained during an actual fire.

In order to carry out the requisite tests, a stiff compression testing machine has been designed and built. The overall control of the test rig is provided by a logger/computer system by developing appropriate software, thus enabling the load to be held constant for any period of time. Before outlining any details of the development of the testing apparatus which includes an electric furnace and the associated instrumentation, previous work on properties of both concrete and steel at elevated temperatures is reviewed.

The test programme comprises four series of tests :-
- stress-strain tests (with and without pre-load)
- transient tests (heating to failure under constant stress)
- creep tests (constant stress and constant temperature),

where 3 stress levels are examined : 0.2, 0.4 & 0.6 f'_c.

The experimental results show that the properties of concrete are significantly affected by temperature and the magnitude of the load. The slope of the descending portion branch of the stress-strain curves (strain softening) is found to be temperature dependent.

After normalizing the data, the stress-strain curves for different temperatures are represented by a single curve. The creep results are analysed using an approach involving the activation energy which is found to be constant. The analysis shows that the time-dependent deformation is sensibly linear with the applied stress. The total strain concept is shown to hold for the test data within limits.

Key words :- Fire, concrete, stress, strain, time-dependence.

ACKNOWLEGEMENTS

I wish to express my gratitude to Dr. J.A. Purkiss for his constant help, encouragement and valuable guidance throughout this investigation.

Also thanks are due to the Technicians who made this research possible by manufacturing and assembling the majority of the test rig.

I am deeply indebted to all the members of my family namely, Hamid, Madjid & Hocine, for their continual encouragement throughout the duration of the research.

I also wish to thank Mr M. Forghani for typing this thesis, and Miss. C. Dittli for her encouragement and the enduring task of typing the titles to all the diagrams.

Finally, I would like to thank the Ministry of Higher Education and Scientific Research of ALGERIA for the total financial support during the period of the research.

The equipment was built under an SERC grant.

LIST OF CONTENTS

LIST OF FIGURES

LIST OF TABLES

LIST OF PLATES

CHAPTER 1

INTRODUCTION

Concrete is widely used in all types of construction mainly due to the fact that it has been generally more economic when compared to structural steel work. It is also recognized as an excellent fire-resistant and non-combustible material, which implies that concrete members have been thought to retain their function without extra protective measures for a certain period of time under fire and that no toxic fumes are emitted (Neville (1981)). However exposure to a fire has consequences which can in severe cases lead to damage to the structure causing, sometimes, a total collapse of the buildings elements, and to a loss of human life.

The damage resulting from a fire can be, in general, attributed to bad detailing and to poor design of the structure for fire resistance. This is mainly due to a lack of sufficient knowledge of the structural behaviour as against the member considered as an isolated unit under fire conditions. There has been an important effort in fire research to overcome this difficulty. By the prediction of member performance, fire regulations are being established in most countries to provide the members with an adequate degree of fire protection to enable fire fighting to take place and the evacuation of the occupants.

Despite all the regulations on structural behaviour a high number of fires occur every year resulting in many casualties mostly due to asphyxiation or release of toxic gases. However this does not mean that an imperative need to introducing measures in detailing and design for fire resistance is not necessary. Since the existing

methods ('deemed to satisfy' clauses) which have resulted from tests on isolated members, are not economical and therefore do not provide a satisfactory design, since continuity is seldom considered. Sullivan & Dougill (1983) have outlined the deficiencies of these methods.

Design methods are therefore being developed to assess fire resistance of structural members in more realistic conditions. It is becoming the practice to design building elements under fire loading by using rational methods. These approaches are fully reported in the Institution of structural Engineers & the Concrete Society Reports (1975 & 1978), and in the FIB/CEB Report (1978).

The limit state concept for structural design has been implemented to overcome the inadequacies of the empirical rules based on tabulated data. The adoption of a rational design method is required because this approach provides the designer with more confidence. A rational approach to fire design is based on limit state principles and validated by data obtained from fire tests. This design method considers three factors :-

a) limit state of stability : resistance to collapse and excessive deformation.

b) limit state of integrity : resistance to the passage of flames.

c) limit state of insulation : restriction of excessive heat transfer.

These three limit states are fully defined in Malhotra (1982). At present this method has only been developed for single elements with limited internal force redistribution, and no account is taken of full

member interaction or element instability mainly when slender vertical members are considered. Instability can only be considered using a computer model, since an actual test is impractical.

As mentioned earlier, the limit state approach uses the data validated by conducting standard fire tests in accordance with BS 476 : part 8 : 1972 based on ISO-834 specifications, in addition to some data on material behaviour. Furnace tests are usually carried out on individual structural members and the collected results provide useful information on the behaviour of single elements of a structure in fire conditions. The test data are used to establish the standard fire resistance required for separate elements in a building. This method, however, does not evaluate the fire resistance of a whole structure, since the effect of restraint and continuity is not realistically considered because of the difficulty to conduct tests on complete buildings. Purkiss (1972) described some fire tests as carried out by the PCA. He also reported the inconsistencies of the standard fire test which does not reflect the structural behaviour in actual fire conditions. Dougill (1966) had already considered this for the standard column test. A furnace test does not necessarily reproduce the real fire severity in a structure and there is no direct relationship between the fire test and the actual conditions in a building. Because of these anomalies, it is essential to introduce an alternative approach to the standard test, to predict the structural behaviour in a fire, based on analysis and calculations. However to

develop such analytical models more consistent material data obtained from experimental work are needed.

The development of computer models will lead to better structural design and will enable a more realistic assessment of fire safety in buildings. The same needs for introducing improved mathematical modelling in fire conditions have been highlighted by many of the papers presented in 1983 at the conference "Three Decades of Structural Fire Safety" held at the Fire Research Station.

Although there are already some data on the properties of steel and concrete available, it is not possible to adopt all those findings for concrete to formulate general models because of the differences in the results obtained by different investigators. The main reasons for these differences include the testing methods, the equipment used to conduct the experiments and varying mix designs. An important requirement for setting up a valid model is to obtain a properly coordinated set of data for the behaviour of concrete at elevated temperatures. To simulate realistic conditions, transient high temperature exposure requires to be adequately investigated.

It is thus the purpose of the present work to obtain such data on the stress/strain behaviour (including the descending branch), thermal expansion and transient behaviour at elevated temperatures. A typical siliceous aggregate concrete is used since it is more common in the U.K., although some limestone aggregate is used.

Before describing the testing programme envisaged and the special equipment used to carry out the requisite tests, the available data on

the properties of structural concrete subjected to elevated temperatures are reviewed in the next chapter.

CHAPTER 2

LITERATURE REVIEW

2.1 INTRODUCTION :

Fire in a building can occur suddenly and then rapidly develop, spreading at an increasing rate, causing losses of life and serious damage to the structure. Most fires are reported to be caused by negligence and carelessness as outlined by the FIP/CEB report (1978). The fire statistics for 1973 reported by the Institution of Structural Engineers and the Concrete Society (1975) give the total number of fires in the U.K. as 331164 and indicate that most fatal casualties occured in domestic dwellings. These constructions which suffer most, have little chance to survive a fire due mainly to a lack of proper fire protection and bad detailing. It is thus, necessary to provide a structure with appropriate fire resistance. BS 476 (1932) as reported by Malhotra (1982), defined the fire resistance as "the property by virtue of which an element of a structure as a whole, functions satisfactorily for a specified period whilst subjected to a prescribed heat influence and load".

Present regulations are based on results of standard furnace tests performed on single small structural elements. The main concepts used in these tests are identified by Bizri (1973) as :

a) the fire endurance is uniquely dependent on the fire severity as defined in the area under the time-temperature curve for the compartment during the fire.

b) the fire severity is a unique function of the fire load density.

This seems to imply that short duration, intensive fires are equivalent to long but less intensive fires as pointed out by Harmathy & Lie (1970) and reported in Bizri (1973).

There is now a substantial quantity of published work dealing with the behaviour of structural concrete members in fire, which has tended to develop new approaches to structural design and detailing. Proposals, such as extensions of limit state and rational approaches as presented in the report of the Institution of Structural Engineers and the Concrete Society (1975), have been introduced to assess more realistically the fire resistance of buildings elements. These procedures, however, do not predict easily the fire performance of an overall structure. At present none of these methods is recognized by the regulatory bodies (Malhotra (1982)). Four different approaches to satisfy safety requirements are presented by Malhotra (1982) as shown in Fig. 2.1.

Method 1 represents the classical approach, in which the standard fire resistance tests are the current way of satisfying the regulatory control. This method lacks flexibility and does not provide good design (FIP/CEB Report (1978)). In this approach, tabulated data on minimum member sizes are provided.

The assessment of fire resistance using empirical relationships is the objective of Method 2 in which either interpolation or extrapolation techniques (2a) or analytical methods on individual elements (2b) can be used.

Fire resistance in Method 3 can be specified using three possibilities, direct test data (3a), interpolation techniques (3b) or analytical approach (3c).

Aston University

Illustration removed for copyright restrictions

FIG. 2.1 DIFFERENT LEVELS OF SOPHISTICATION IN PROVIDING FIRE RESISTANCE (MALHOTRA 1982)

The fourth approach (Method 4), more sophisticated, is fully analytical which takes account of the heat transfer and the structural behaviour. Computer programs can be designed to cope with the transient heating conditions. Knowledge of material properties at elevated temperatures has increased and permits a better level of sophistication in the analysis of structural behaviour in a real fire.

The current approach used in the U.K. is Method 1 where the fire resistance of a building is determined by conducting tests on simple elements in accordance with BS476 : Part 8 : 1972. The limitations of the standard test arise mainly from the difficulty of predicting the behaviour of a structure in fire conditions. Only isolated members are tested without considering the effect of restraint and continuity, ie. no account is taken of the relation to the surrounding structures.

This approach (Method 1) has provided tabulated data for the assessment of the fire resistance of a structural element as reported in the FIP/CEB report (1978) in terms of size of the member and cover to the reinforcement steel. Sullivan & Dougill (1983) point out the deficiencies of this tabular method. Although it is relevant to simply supported members, this approach is uneconomic and too restrictive on design when highly redundant structures are considered. Sullivan & Dougill then argue an analytical approach to structural design in fire should be used.

Empirical methods based on tests do not provide sufficient knowledge of the performance of structures in transient heating conditions. Studies of the prediction of the fire resistance of buildings elements in a real fire are engaged in modern research where

the development of fire, fire load and ventilation are taken into account.

Analytical modelling and calculations of fire resistance are less expensive and less time consuming than any test procedure. This has been demonstrated by some investigators such as Lie & Allen (1972) when they assessed the fire resistance of reinforced concrete columns by calculations and produced a set of empirical rules.

2.2 CONCEPT OF HEAT EXPOSURE AND STRUCTURAL MODELS :

The present regulations for design in fire conditions have some weaknesses especially when assuming the temperature rise and the fire duration and when estimating the fire resistance from furnace tests on single members. Because of this, extensive research has been undertaken to obtain economically more uniform safety. Moreover, Witteveen (1983) has insisted on the introduction of probabilistic design procedures in structural fire engineering design. This probabilistic design, according to Witteveen, includes a methodology by which all relevant factors, such as safety considerations from both the human and economic point of view, probability of flash-over, uncertainties in fire exposure and structural fire response, the effect of fire brigade actions and sprinklers can be dealt with systematically.

2.2.1 Fire exposure :

The time/temperature relationship of the fire as shown in Fig. 2.2 defines the standard fire exposure as introduced by ISO-834 and adopted by BS476 : Part 8 : 1972. The curve can be expressed mathematically as :

$$T - T_o = 345 \log_{10}(8t + 1) \qquad (2.1)$$

where t = time of test in minutes.

T = furnace temperature in ^{o}C at time t, and

T_o = initial furnace temperature in ^{o}C.

This standard time/temperature curve does not necessarily represent the actual development of temperatures in a real fire, as the intensity and duration of fires in buildings may considerably differ from that of the standard fire test.

The fire severity, however, depends upon several parameters. The main factors are the fire load, the ventilation and the characteristics of the compartment. Figure 2.3 shows the temperature development in a compartment with different ventilation. The effect of fire load is shown in Fig. 2.4 (reproduced from Malhotra (1982)). These parameters are fully discussed by Law (1983) when reviewing the main results and conclusions of some experiments on building fires.

Considering the factors affecting the fire exposure, a relationship to express the real fire severity has been proposed by the Fire Research Station (the Institution of Structural Engineers (1975)) and is of the following type :

$$t_f = k\,(L/A_F)(A_F/(A_F A_W A_T)^{1/2}) \qquad (2.2)$$

where t_f = equivalent fire resistance in minutes.

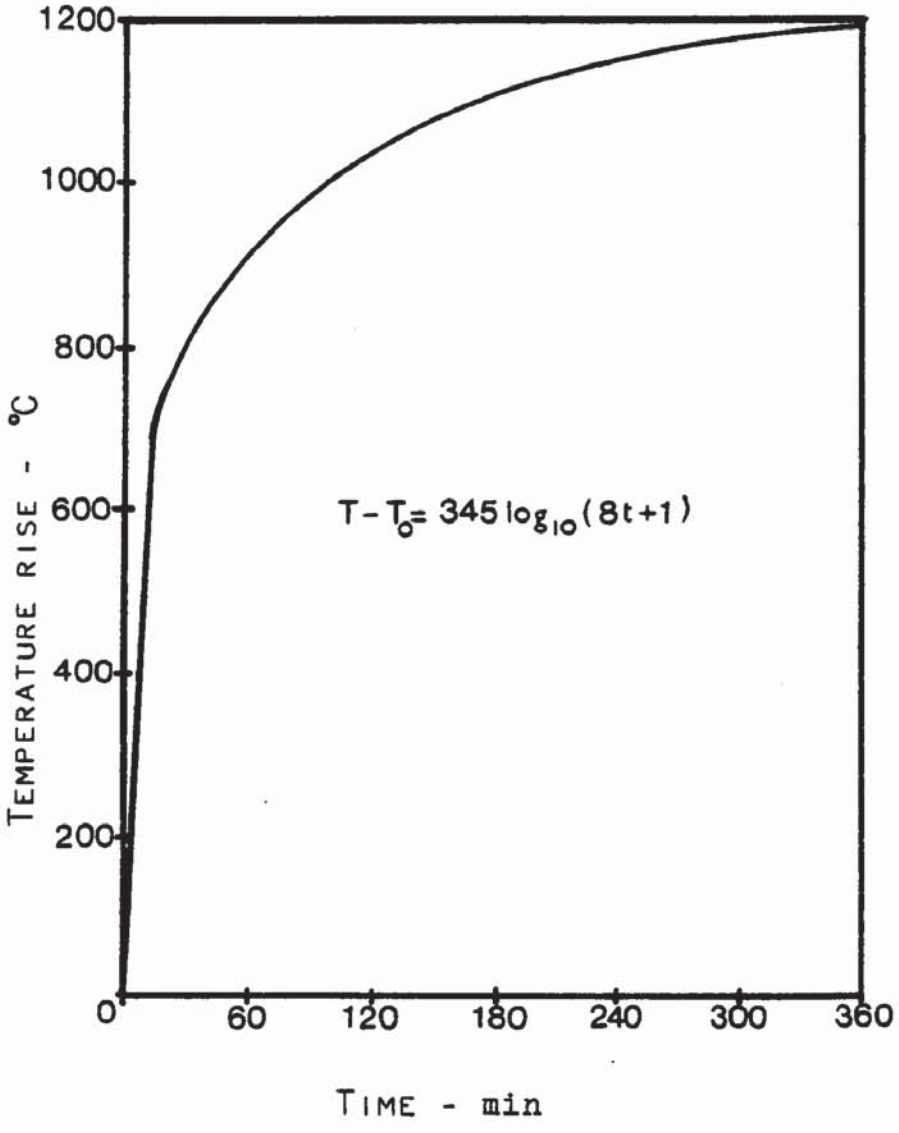

FIG. 2.2 STANDARD TEMPERATURE CURVE FROM BS 476:PART 8:1972.

FIG. 2.3 TEMPERATURE DEVELOPMENT IN A COMPARTMENT WITH DIFFERENT VENTILATION. (MAGNUSSON 1970)
FIRE LOAD q = 500MJ/m^2 (WOOD CRIBS)

(60(1/2) = FIRE LOAD 60 KG/m^2 FLOOR AREA AND VENTILATION 50% OF ONE WALL).

FIG. 2.4 EFFECT OF FIRE LOAD DENSITY AND VENTILATION ON FIRE TEMPERATURES. (THOMAS 1970)

L/A_F = fire load density (L = fire load in Kg, and A_F = floor area in m^2).

$A_F/(A_W A_T)^{1/2}$ = ventilation factor (A_W = window area, A_T = area of wall, floor and celling surfaces in m^2).

k = fuel distribution factor, which varies between Ø.7 and 1.5.

The fire severity in a building can be estimated more realistically using the above relationship, thus enabling a more realistic assessment of the fire resistance.

2.2.2 Heat exposure and Structural models :

The development of analytical modelling has been stimulated by the lack of accuracy and uncertainty of the standard fire test. The deficiencies of the present testing method have been reported by Sullivan & Dougill (1983) and by some other investigators, namely Bizri (1973) and Lie & Allen (1972).

Recently, attempts have been made to improve the regulations and design methods for structural fire engineering design. Witteveen (1983) has described in his paper the available improved models consisting mainly of heat exposure models (H) and structural models (S) which are considered to be probabilistic design methods. The two types of methods with their appropriate components are shown in Fig. 2.5.

FIG. 2.5 MATRIX OF HEAT EXPOSURE AND STRUCTURAL MODELS IN SEQUENCE OF IMPROVED SCHEMATIZATION. (WITTEVEEN 1983)

The heat exposure model (H) is used for the determination of the rise of temperature as a function of time. The different (H) models have been developed consequent on the type of thermal exposure, and are reported in Witteveen's paper. The temperature rise in (H1) and (H2) are determined in accordance with ISO-834. The duration of the temperature rise in the former is equal to "the required time of fire duration" as expressed in building regulations, but in the latter it is equal to "the equivalent time of fire exposure" which relates an actual fire exposure to the standard time/temperature curve. These two models are based on an experimental approach. In the third model (H3), the determination of the rise of the temperature is obtained by an analytical approach, based on the gas-temperature time curve of a fully developed fire in a compartment.

The heat transfer and the ultimate load capacity of the structure can be determined experimentally or analytically using the structural model (S). The load bearing structure is determined in three different (S) models depending on the type of structural system. When considering only single members with simplified restraint conditions, model (S1) which can be either experimental or analytical approach is used. Model (S2) which is mainly based on an analytical method is concerned with sub-assemblies such as beam-column systems. Finally, the analysis of a whole structure can be dealt with using model (S3).

Figure 2.5 shows a classification of different combinations representing design procedures. The current design method used in building codes is that represented by H1 - S1 and occasionally H1 - S2 with experimental and possible analytical verification of the fire resistance. The heat exposure models (H2) and (H3) are being more and

more used in many countries. Witteveen (1983) continues by discussing the difficulty in using some of the combinations such as H1 - S3 and H3 - S1 which cannot be considered as design methods for general application due to the different levels of sophistication of both models. The combinations H2 - S3 and H3 - S3 are not recognized operational design procedures for regular practice since the highly complex structural analysis of model (S3) requires computer solutions.

The design procedures resulting from the combinations of heat exposure models (H1) and (H2) and structural models (S1) and (S2) can be verified either experimentally or analytically. However, as mentioned by Witteveen, both types of verifications should be made compatible in order to render the same degree of reliability.

2.3 DATA FOR STRUCTURAL MODEL :

The development of a structural model requires a knowledge of the behaviour of structures in fire conditions. The performance of concrete structures exposed to high temperatures is influenced by the effect of temperature on both basic materials : concrete and steel.

In this section only the properties of concrete are dealt with. The effect of elevated temperatures on concrete has been the subject of intensive research and the results of some investigators are reviewed here.

Malhotra (1982) divided into four groups the different material properties, i.e. thermal, chemical, physical and mechanical.

The properties of concrete at high temperatures are, however, influenced by the type of aggregate. Carbonate, siliceous and

lightweight constitute the usual structural concretes. Carbonate aggregates including limestone and dolomite undergo chemical changes. Siliceous aggregates including granite, quartz and sandstones, expand considerably at elevated temperatures and the important physical change of these aggregates is the α-to-β quartz transformation at 575°C which is accompanied by a large increase in volume. With lightweight aggregates such as clays, expanded shales and fly ash, lower losses of strength can be achieved.

2.3.1 Thermal properties :

2.3.1.1 Thermal conductivity :

The thermal conductivity (k) of concrete is controlled by that of its constituents, thus depending upon the aggregate type and the cement type. Below 100°C, the thermal conductivity is influenced by the moisture content, but at high temperatures the water is driven out.

Harmathy (1970) examined various concretes and obtained two bands as indicated in Fig. 2.6. His results show that for dense concrete conductivity decreases with increasing temperature, but for lightweight aggregate concrete no significant decrease is observed. Similar trends have been obtained by other investigators such as Zoldners (1960), who tested ordinary Portland cement concrete made with three types of aggregates (gravel, limestone and sandstone), and Maréchal (1970).

FIG. 2.6 EFFECT OF TEMPERATURE ON THERMAL CONDUCTIVITY OF CONCRETE. (HARMATHY 1970)

2.3.1.2 Specific heat :

The specific heat (c) also changes with increasing temperature and is dependent on the type of aggregate. Figure 2.7 as reported in Malhotra (1982) shows the variation of the specific heat with temperature for different type of concrete as obtained by different researchers. It can be seen that the values increase slowly with increasing temperature. The specific heat is affected by moisture. This is shown by Colette's results (1976) on lightweight concrete (Fig. 2.7) where an important increase is observed at 100 °C caused mainly by the evaporation of free water.

2.3.1.3 Thermal diffusivity :

The conduction of heat within the concrete is controlled by the thermal diffusivity ($k/\rho c$) which is more dependent on the conductivity (k) than on the density (ρ) or the specific heat (c). Consequently a reduction in the conductivity will lead to a reduction in the diffusivity. It would be therefore more advantageous to use materials with low conductivity. Figure 2.8, as produced by Harmathy (1970), shows the decrease in diffusivity with increasing temperature. It can be seen that with lightweight concrete, the heat transfer is considerably lower than with normal dense concrete.

2.3.2 Mechanical properties :

2.3.2.1 Stress-strain relationships :

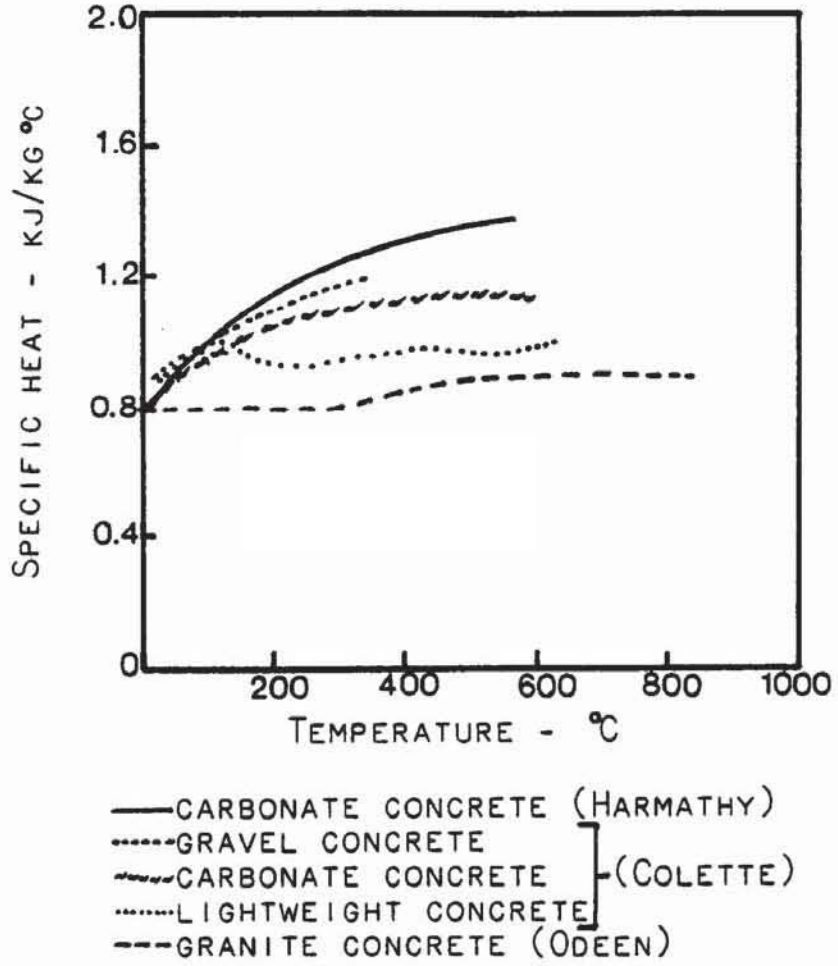

FIG. 2.7 EFFECT OF TEMPERATURE ON SPECIFIC HEAT OF CONCRETE.

FIG. 2.8 EFFECT OF TEMPERATURE ON THERMAL DIFFUSIVITY OF CONCRETE.(HARMATHY 1970)

A complete stress-strain curve for concrete at elevated temperature was first obtained by Furamura (1966) in Japan. He conducted his experiments on cylindrical specimens using a testing machine which was stiff enough to allow the descending branch to be followed. Because of the experimental difficulties, only the initial portion of the stress-strain curve was measured in previous investigations by Harmathy & Berndt (1966). The failure in their attempt to record the complete stress-strain curve was most likely due to the soft testing machine used.

A complete stress-strain curve as shown in Fig. 2.9 has also been obtained by Purkiss (1972). And more recently some attempts to obtain similar results have been made by Schneider (1976).

Furamura's results plotted in Fig. 2.10 indicate that the stress-strain curve at high temperatures has the same form as that observed at normal temperature. The peak stress, however, is reduced and the strain range is considerably increased at elevated temperatures. On the other hand the maginitude of the slope of the descending portion decreases with increasing temperature. These conclusions have been confirmed by Purkiss (1972) and some other researchers although they only considered the effect of heating on the peak stress and modulus of elasticity.

Baldwin & North (1973) reviewed Furamura's results to show, in spite of the complexity of the relationship, that if the data are normalized, the stress-strain curves are of the form :

$$\sigma/\sigma_{max} = f\,(\epsilon/\epsilon_{max}) \qquad (2.3)$$

where f : is a function independent of temperature.

FIG. 2.9 STRESS-STRAIN CURVES FOR CONCRETE TESTED IN COMPRESSION AT HIGH TEMPERATURES. (PURKISS 1972)

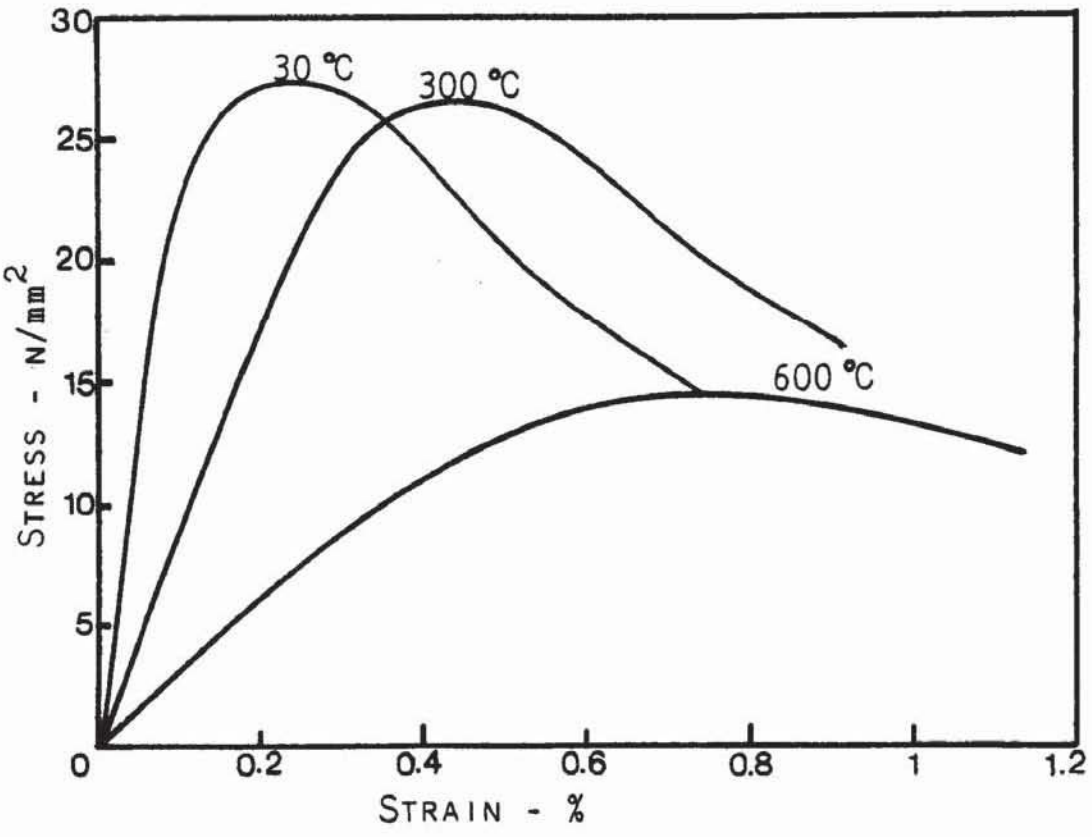

FIG. 2.10 TYPICAL STRESS-STRAIN CURVES OF FURAMURA AT DIFFERENT TEMPERATURES.

σ_{max} : stress at the peak of the stress-strain for a given temperature.

ϵ_{max} : strain at the peak of the stress-strain for a given temperature.

The data may be represented by the equation :

$$\frac{\sigma}{\sigma_{max}} = \frac{\epsilon}{\epsilon_{max}} \exp\left(1 - \frac{\epsilon}{\epsilon_{max}}\right) \qquad (2.4)$$

Due to the fact that the function f is independent of temperature Baldwin & North obtained a significant result which implies that the stress-strain curve for concrete at high temperatures can be derived from the stress-strain curve at normal temperature. The maximum of the stress-strain at high temperatures can similarly be located. The study undertaken by Baldwin & North is based on results obtained using concrete specimens carrying no load during heating. This form of non-dimensional plot was confirmed by Purkiss (1972).

The influence of a pre-load during heating on the stress-strain curves has been examined in some recent work by Schneider (1976). He conducted his tests on relatively large specimens (80 x 300 mm with a maximum aggregate size of 16 mm) which were pre-loaded to two stress levels (10% and 30% of the peak stress at room temperature). Some of his results are plotted in Fig. 2.11 together with some results of unloaded specimens for comparison purposes. It can be seen that a significant increase in peak stress is observed with pre-loaded specimens; and the high temperature strains of pre-loaded specimens decrease with the total load during heating.

FIG. 2.11 STRESS-STRAIN RELATIONSHIP OF ORDINARY CONCRETE SPECIMENS UNIAXIALLY LOADED DURING HEATING. (SCHNEIDER 1976)

Similar trends have been reported in some earlier work by Fischer (1970). He used the same type of aggregate (quartz) and a water/cement ratio of 0.6. The specimens were stressed to about 0.33 f'_c during heating. No attempt was made to measure the complete stress-strain curve, since he was only interested in the initial portion to investigate the influence of temperature upon the elasticity of concrete.

2.3.2.2 Strength and elasticity of concrete at high temperatures :

The modulus of elasticity and the compressive strength of concrete at elevated temperatures, have been covered in a number of investigations. The results obtained by some notable authors are reviewed in this section. Regarding the tensile strength, only some work has been undertaken (Zoldners (1960)).

The main conclusions reported by all of the researchers is that the three properties mentioned above decrease with increase in temperature. However the differences between the values produced by each investigator are mainly due to the different methods of testing used and the materials to make the concrete.

These properties are influenced by the moisture, the mix characteristics and the test conditions. The decrease in strength and Young's modulus is reported to be caused by the moisture content and by the decomposition of the Calcium hydroxide $Ca(OH)_2$ resulting in a desintegration of the whole microstructure (Schneider (1976)). The main factors affecting the tensile strength are dehydration and

deterioration of the cement-aggregate bond caused by heating (Zoldners (1960)).

i) Strength of concrete at elevated temperatures :

The effect of temperature on the compressive strength of concrete has been widely studied. The results obtained from various investigations have been compared and presented in Fig. 2.12. Most workers have reported that the strength decreases continuously with increasing temperature, however some others have shown an increase in strength rather than a decrease at around 300 °C. They give credit for this increase to the importance of curing and moisture conditions of concrete during the early stages of heating. Below 300 °C, there is a possible presence of some free moisture in the specimen leading therefore to an increase in strength, but beyond this temperature, when the water removal is complete, the deydration will start, thus leading to a decrease in strength.

Maréchal (1970) examined the effect of temperature on the compressive strength of concrete incorporating different aggregates. His results indicated that concrete made with siliceous aggregate had a lower strength. On the other hand, he showed that the age had an effect on the strength at a temperature up to 130 °C, then this effect became negligible at high temperatures.

Malhotra (1956) studied more extensively the effects of heating upon the compressive strength of concrete. He examined the differences between the hot and residual strength previously reported by other

workers. He also investigated the influence of a pre-load during heating on the strength. He conducted his experiments on concrete specimens (50 x 100 mm) made with river-gravel aggregates using three testing conditions :- loaded crushed hot, unloaded crushed hot, and unloaded crushed cold. He used three mix proportions (1:3, 1:4.5 & 1:6) with four different water/cement ratios (0.4, 0.45, 0.5 & 0.65). The main results showed a loss in strength at high temperatures in all cases considered. But the concrete specimens carrying a load during heating exhibited a smaller reduction in strength than the non-loaded specimens. Malhotra also reported that the residual strength, measured immediately after cooling was less than that obtained at high temperatures. This finding was earlier produced by Lea in 1920 as indicated in Dougill (1965). Malhotra found that the strength was not significantly affected by the water/cement ratio, but was influenced by the aggregate/cement ratio, and as a result the proportional reductions are smaller for lean mixes than for rich mixes. Some results from Malhotra are shown in Fig. 2.13.

Abrams (1968) reported some results on the effect of high temperatures (up to 871 ^{o}C) upon the compressive strength of concrete. He used three types of aggregates (carbonate, siliceous and lightweight). The test procedure was basically the same as that used by Malhotra. Although both authors obtained similar trends, some differences are however apparent due to the slight modification in testing adopted by Abrams. When the test temperature was reached, he allowed the concrete specimens to soak before loading them to failure.

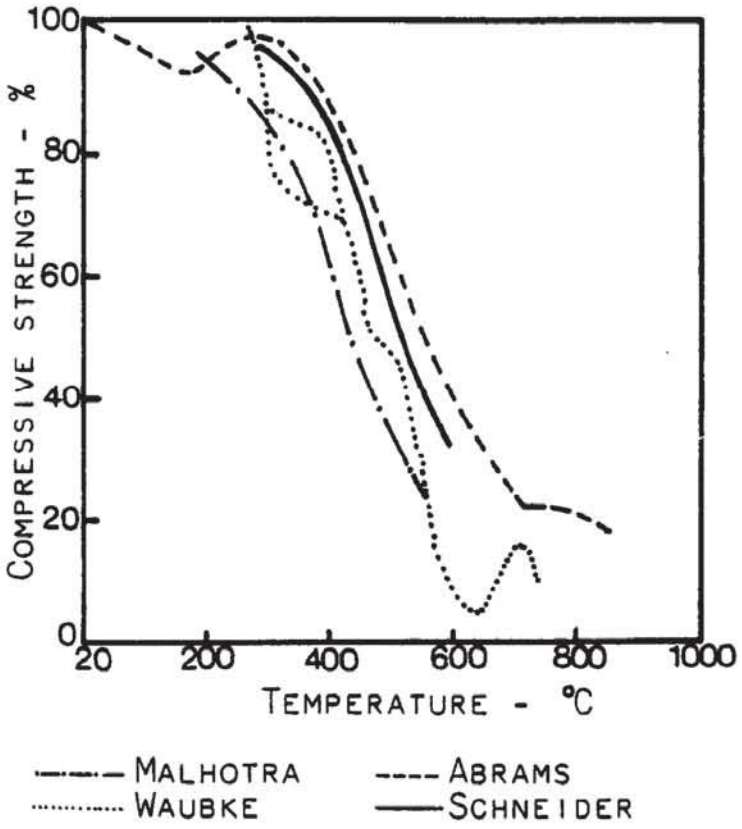

FIG. 2.12 COMPRESSIVE STRENGTH OF DENSE CONCRETE AT HIGH TEMPERATURES. (NO PRE-LOAD)

FIG. 2.13 EFFECT OF TESTING CONDITIONS ON CONCRETE STRENGTH (DENSE AGGREGATE). (MALHOTRA 1956)

The results obtained showed lesser reduction in compressive strength than those of Malhotra .

The residual strength was examined by Abrams in a different way. After heating to the required temperature the specimens were allowed to cool slowly to room temperature and then stored in air at 70 to 80% R.H for seven days. The results showed as expected that the strength of these specimens was lower than that of the hot specimens. But, despite the possible rehydration which could have occured in humid storage condition, Abrams reported a smaller loss in strength than Malhotra. On the other hand, both authors reported more loss in unstressed residual strength than Zoldners (1960) who used a different testing technique. After the slow cooling to room temperature, Zoldners eliminated the moisture content by desicating his specimens for four hours and then tested them in compression.

The aggregate type has a significant effect on the strength of concrete at high temperatures. It has been shown that corbonate aggregate concrete and lightweight concrete exhibit less reduction in strength than siliceous aggregate concrete. As reported by Abrams, the former two concretes retained 75% of their original strengths at 649 °C, while the latter retained 75% of its original strength only at 427 °C. The specimens stressed during heating showed high strengths (5 to 25%) than the non-loaded specimens. This is mainly due to the delay in crack formation. Figure 2.14 shows the results of the three different tests conducted by Abrams on concrete specimens made with siliceous aggregate.

Abram's work has been complementary to Malhotra's investigation on the compressive strength of concrete exposed to elevated temperatures. Some other researchers obtained similar trends and provided an additional information to the existing data. The influence of a pre-load, for instance, has been examined by Schneider (1976) and earlier by Fischer (1970). The latter performed several tests on specimens which were heated under constant load. His findings are similar to that already reported in the literature. It is to be noted that Fischer also examined the effect of the curing conditions on the residual strength (see Fig. 2.15). He reported a further loss in strength of concrete specimens stored in air resulting from a possible decomposition of the hydration products. On the other hand, a regain in strength was observed with specimens stored in water. As explained earlier, the humid storage condition leads to some rehydration of the Portland cement.

The results reviewed so far on the effect of heating upon the compressive strength have been concerend only with a short-time exposure to high temperatures (2 to 4 hours). Carette et al (1982) investigated the variation in strength of concrete after long-term exposure to sustained temperatures ranging from 75 to 600 ^{o}C. Three types of concretes made with normal Portland cement, normal Portland cement and blast furnace slag, and normal Portland cement and fly ash were used for the purpose of the investigation. Two water/cement ratios were used and the aggregates consisted of crushed dolomitic limestone and natural sand. The changes in strength of all concrete specimens under long-term exposure were observed mainly during the

FIG. 2.14 EFFECT OF TEMPERATURE ON THE COMPRESSIVE STRENGTH OF A SILICEOUS AGGREGATE CONCRETE (f'_c = 275 KG/cm^2). (ABRAMS 1968)

FIG. 2.15 RESIDUAL STRENGTH OF FAST COOLED CONCRETE SPECIMENS UNDER DIFFERENT STORAGE CONDITIONS. (FISCHER 1970)

first month for the 150°C temperature exposure. A significant loss in compressive srength (10 to 20%) was reported for all specimens. The tensile strength also decreased and the recorded loss was of the same order.

ii) Effect of temperature on the modulus of elasticity :

The modulus of elasticity of concrete when subjected to elevated temperatures is affected in a similar way as strength. Despite the various techniques used, most investigators reported a steady decrease in Young's modulus with increasing temperature. Some authors such as Saemann & Washa (1957) reported in Bizri (1973), showed an increase up to 205°C then beyond this temperature a continuous decrease is observed.

Philleo (1958) obtained the dynamic modulus of elasticity by determining the resonant frequency of the specimen in flexural vibration inside the furnace. Elgin aggregate concretes with three different water/cement ratios (0.4, 0.6 & 0.8) were tested. He reported that on heating to 760°C the modulus of elasticity was reduced to less than half its value at 24°C and was independent of age or curing conditions for a given water/cement ratio. However, the lower the water/cement ratio, the higher the modulus of elasticity after dehydration. Some typical results from Philleo are shown in Fig. 2.16.

The values of Young's modulus reported by Cruz (1966) were obtained from tests using torsional bending. To compute this results

FIG. 2.16 EFFECT OF TEMPERATURE ON YOUNG'S MODULUS OF CONCRETE. (PHILLEO 1958)

an elastic analysis method was used. Cruz suggested that the variation of the modulus of elasticity with temperature could be fitted by an exponential function. When comparing Philleo's dynamic method with the results of Young's modulus as obtained by Cruz for the same concrete,it appears that the reduction in the modulus of elasticity is independent of the test method (see Fig. 2.17).

The uniaxial loading procedure has been employed by Maréchal (1970). His results showed that Young's modulus of quartz-aggregate concrete, at 400 °C, decreased to about half its original value.

Some more recent work undertaken by Schneider (1976) and Thelandersson & Anderberg (1976) confirmed the results reported in the literature and consequently showed similar trends. Figure 2.18 shows a comparison between results from different investigators.

The influence of pre-load on the effect of heating on stiffness has been investigated by Fischer (1970). He conducted his tests on quartz-aggregate concrete specimens made with ordinary Portland cement and a water/cement ratio of 0.6. The specimens were pre-loaded to about one third of their cold strength during the whole heating period. He found that the modulus of elasticity slightly increased between 150 and 300 °C, then clearly decreased at 450 °C. As with strength, less loss in stiffness has been reported in pre-loaded specimens.

Some workers while investigating the modulus of elasticity at elevated temperature, have examined the effect of heating on Poisson's ratio. Philleo (1958), for instance, reported a general tendency for Poisson's ratio to decrease as the temperature rose. Cruz (1966),

FIG. 2.17 MODULUS OF ELASTICITY (E) OF ELGIN SAND AND GRAVEL CONCRETE BY OPTICAL AND DYNAMIC METHODS. (CRUZ 1966)

because of the erratic results obtained, failed in his attempt to indicate a general trend on the effect of temperature on this coefficient. On the other hand, Maréchal (1970) showed a decrease in Poisson's ratio with increase in temperature. The results obtained with a quartz-aggregate concrete indicated that after a slight increase at 50 °C, Poisson's ratio decreased steadily with temperature and at 300 °C was reduced to about half its original value (see Fig. 2.19).

2.3.2.3 Creep :

The time-dependent deformation of concrete has been extensively investigated at ambient or moderately elevated temperatures (up to around 150 °C). However, for the last few years, a number of workers have attempted to produce reasonable information on creep behaviour at high temperatures. At normal temperatures, creep can be defined as the increase in strain with time under a sustained stress (Neville (1981)). This phenomenon is however accelerated by an increase in the temperature or the stress as outlined in the literature. The influence of the stress on creep is still a matter of controversy. Some investigators such as Gross (1973) reported creep as a sensibly linear function of stress and some others produced results showing the opposite. Freudental & Roll (1958) have demonstrated that above a stress of 0.3 times the concrete strength, creep and stress are no longer linearly interelated. On the other hand it is unanimously agreed that large creep strains are obtained at elevated temperatures.

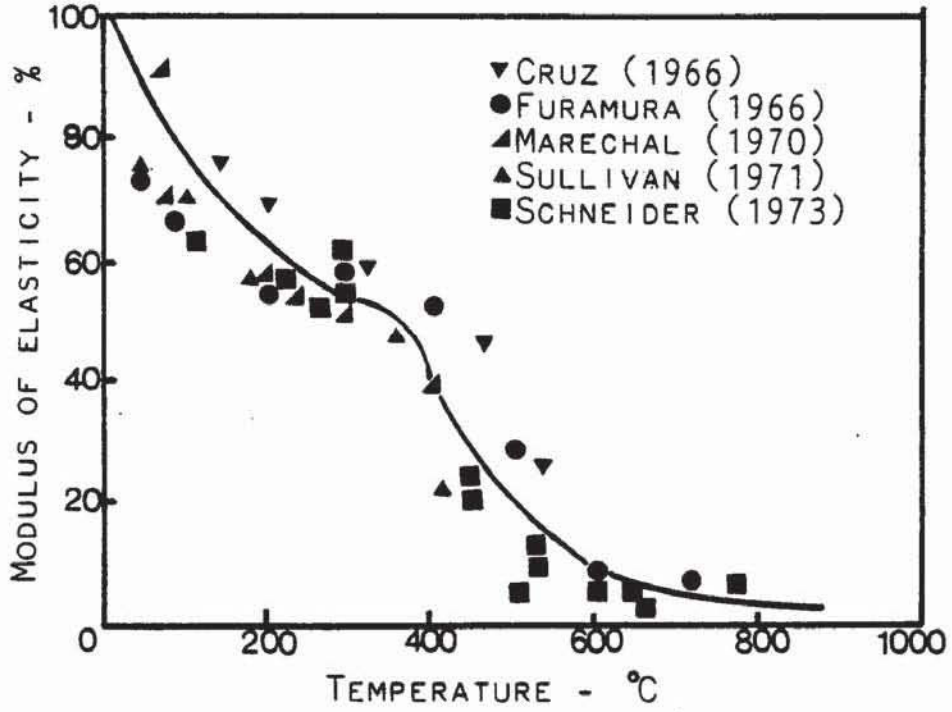

FIG. 2.18 UNIT MODULUS OF ELASTICITY OF NORMAL CONCRETE BASED ON PORTLAND CEMENT AT HIGH TEMPERATURES.

FIG. 2.19 EFFECT OF TEMPERATURE ON POISSON'S RATIO (QUARTZITE-AGGREGATE CONCRETE). (MARECHAL 1970)

In order to provide data on the inelastic behaviour of concrete at high tempratures, Cruz (1968) performed his first creep tests on 50 x 100 mm specimens. He used a gravel-aggregate concrete made of Ordinary Portland cement with a water/cement ratio of 0.56. The creep tests were conducted at five different temperature levels (27, 149, 315, 482 and 649 °C). The concrete cylinders were first heated to the required temperature then loaded to 0.45 f'_c which was maintained constant during the five hour testing period. The creep strains as measured by Cruz are shown in Fig. 2.20. These typical results indicate that creep of concrete increases significantly as the temperature increases and the creep strains measured at high temperatures are exceedingly larger than those recorded at room temperature. It can be seen from Fig. 2.20 that the creep strain achieved in five hours at 482 °C is 15 times higher than that obtained at 27 °C. Cruz performed his short-term creep tests under one stress level only.

Lately Gillen (1981) at the Portland Cement Association investigated the creep behaviour of concretes made with various aggregates (calcareous, siliceous, and expanded shale). The specimens were tested at different load levels (0.3, 0.45 & 0.6 f'_c) under temperatures ranging from 22 °C to 649 °C. The tests were conducted for each combination of load and temperature which were kept constant over the testing period of five hours. The creep curves obtained were similar to those reported by other investigators. Gillen's results showed that creep was not a linear function of stress and the relation between strain and temperature was not linear either. Gillen reported

FIG. 2.20 TIME-DEPENDENT STRAINS IN CONCRETE MAINTAINED UNDER LOAD AT HIGH TEMPERATURES (APPLIED STRESS: 12.5 N/mm^2).(CRUZ 1968)

that during every test, the rate of creep strain decreased with time, and the age of concrete and the specimen size had no significant effects on creep. The time-dependent deformation was, however, strongly influenced by the effects of moisture content at around $100\,^{o}C$, the aggregate type and the temperature dependence of compressive strength of concrete. The data obtained by Gillen compared favourably with three mathematical models commonly used to describe concrete creep behaviour. Figure 2.21 shows the comparison of the three creep models to selected test data.

More work has been undertaken in order to develop comprehensive models for creep of concrete at elevated temperatures. The model formulated by Thelandersson & Anderberg (1976) was based on data obtained from creep tests conducted over a period of three hours under sustained load and temperature. The model gives an expression of creep as a function of time, temperature and stress. The development of this model is based on the assumption that creep is proportional to the ratio between the actual stress and the concrete strength.

The creep model as presented by Thelandersson & Anderberg (1976) is of the form :

$$\epsilon_{cr} = \beta_o \frac{\sigma}{\sigma_u(T)} \left(\frac{t}{t_r}\right)^{p} e^{k1(T-20)} \qquad (2.5)$$

where $\beta_o = -0.53 \times 10^{-3}$

$\sigma_u(T)$ = Peak stress at current temperature

t = time

t_r = 3 hours

p = 0.5

FIG. 2.21 COMPARISON OF VARIOUS CREEP MODELS TO TYPICAL TEST RESULTS (SERIES II.c, 204 °C, 0.45 f'_c). (GILLEN 1981)

$k_1 = 3.04 \times 10^{-3}\ C^{-1}$

T = temperature.

The values of β_o and p were determined experimentally at two stress levels (0.225 & 0.45 f'_c) for concrete made of Ordinary Portland cement and quartzite aggregate. The determination of the different coefficients is fully reported in Thelandersson & Anderberg (1976).

For any given combination of temperature and stress, creep can be expressed by Eq. (2.5). However for temperature and stress varying with time, the basic creep is evaluated on the basis of the strain hardening principle.

Maréchal (1969 & 1970) has undertaken the most extensive work on high temperature creep using pre-dried specimens. He showed that the time-dependent deformation can be assessed by using an approach involving the equation of Arrhenius. He also reported that the activation energy was constant and stress independent. Bazant & Panula (1978) confirmed Maréchal's conclusion and used the same approach to express the temperature effect on creep. Maréchal conducted his tests on specimens made of concrete incorporating various aggregates. Two stress levels were used and the temperature ranged from 20 to 400 °C. The analysis of his results led to the following equation :

$$\dot{\epsilon}_{cr} = A.e^{-\frac{U_a}{KT}} \qquad (2.6)$$

where : $\dot{\epsilon}_{cr}$ = creep rate

U_a = activation energy

K = Boltzman's constant

T = Temperature (^{o}K)

A = constant depending on the stress.

Maréchal results were obtained after relatively a long-term creep test (56 days), but did not give any information about the activation energy at temperatures above 575 ^{o}C at which phase changes in quartz take place when siliceous aggregate is used.

Schneider (1976) investigated creep of concrete under transient temperature condition. The only available data on time-dependent deformation at high temperatures are generally obtained by conducting creep tests at constant load under sustained temperature. He reported that with uniaxially loaded concrete specimens under tansient conditions, creep strains observed during very short heating periods were higher than those creep values derived at constant temperatures. He conducted his experiments on quartzite-aggregate concrete specimens. Two load levels (0.15 & 0.30 f'_c) and three test temperatures (135, 300 & 450 ^{o}C) were used. The transitional creep strains were measured over a period of 168 hours consisting of 120 hours heating time under constant temperature and 48 hours cooling period. Creep as reported by Schneider is influenced by accelerated moisture diffusion, dehydration and microcrack formation. A comparison between Schneider's results and the creep data of some other workers is shown in Fig. 2.22 which indicates also the significant influence of the load level on the creep values. This effect is attributed to the reduction in strength with increasing temperature.

2.3.3 Physical Properties :

SYMBOL	β	DURATION OF THE TEST	AGGREGATE	WORKER
○	0.20	7 d	QUARTZ	GROSS
●	0.40	7 d	--"--	--"--
□	0.45	5 h	LIMESTONE	CRUZ
△	0.14	20 d	QUARTZ	MARECHAL
▲	--"-	5 d	--"--	--"--
▼	0.28	--"--	PORPHYRE	--"--
▽	0.15	5 d	QUARTZ	SCHNEIDER
■	0.30	--"--	--"--	--"--

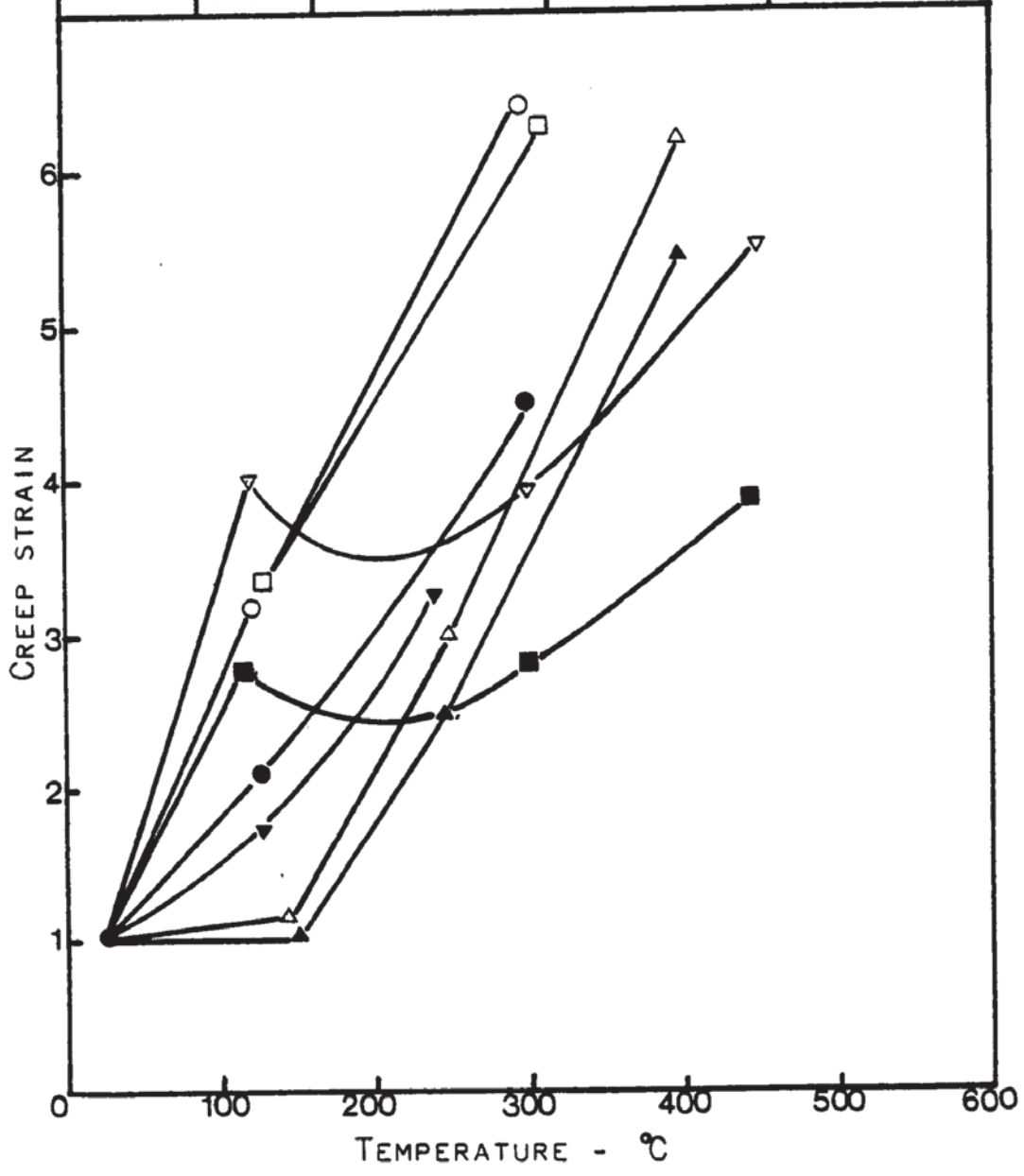

FIG. 2.22 UNIT CREEP STRAINS OF CONCRETE AT HIGH TEMPERATURES.

2.3.3.1 Density :

Malhotra (1982) reported that the effect of temperature on the density is not significant and can be neglected. However it is to be noted that the density decreases with increasing temperatures. This effect is caused by two main factors. The loss in weight due to drying, dehydration and disintegration, increases with temperature (Fischer (1970)). On the other hand, with quartzite-aggregate, the α-to-β quartz transformation is accompanied by an important increase in volume. This will obviously result in a decrease in density.

2.3.3.2 Thermal deformation :

There has been a large amount of work done on the unrestrained volume changes by Zoldners (1960), Maréchal (1970), Fischer (1970), Purkiss (1972), et al. Figure 2.23 shows the thermal expansion of an unrestrained-non-loaded specimen as obtained by Purkiss (1972). This result is typical concerning the behaviour in transient conditions. The specimen used in the test was heated slowly (2.9 ^{o}C/min) to the required temperature, was maintained at this temperature for three hours, then allowed to cool to room temperature. At the early stages of heating shrinkage occured due to drying then was inhibited as the temperature rose by the thermal expansion. The shrinkage was not recovered on cooling.

Thermal expansion of concrete is controlled by that of the cement paste and the aggregate. At elevated temperatures cracking occurs due

to stresses developed during heating leading to a breakdown between the aggregate and the cement paste. As a result, the thermal expansion of concrete is increased and approaches that of the aggregate. The large residual expansion reported by Purkiss was mainly due to the amount of cracking which was irreversible.

Although depending on the moisture, the thermal expansion is dominated by the mineralogical character of the aggregate, but the latter depends on the aggregate content in the concrete mix (Neville (1981)). With a large quantity of aggregate, the contraction of the cement paste due to heating will tend to stop and turn into expansion leading to a breakdown between the constituents, as reported by Purkiss (1972).

Cruz & Gillen (1980) investigated the thermal expansion of concrete at high temperatures and observed the influence of the cement paste and aggregate on the deformation of concrete. Some of their results are illustrated in Fig. 2.24. It can be seen that a contraction of the Portland cement paste is observed from 204 to 871 °C, but during the early stages of heating (up to 149 °C) the cement paste expanded likely because of the presence of the free moisture. On the other hand, all mortars and concretes tested expanded with increasing temperatures, and their thermal expansion was dominated by that of the aggregate type, which was, in turn, moderated by the contraction of the cement paste. For the same water/cement ratio (0.4), Philleo (1958) already reported similar results on the expansion of gravel-concrete and cement paste.

FIG. 2.23 TRENDS IN UNRESTRAINED THERMAL EXPANSION OF CONCRETES (DIAGRAMATIC). (PURKISS 1972)

1. PORTLAND CEMENT PASTE
2. ELGIN SAND MORTAR
3. OTTAWA SAND MORTAR
4. ELGIN SAND AND GRAVEL CONCRETE
5. ELGIN SAND AND CRUSHED DOLOMITE CONCRETE
6. DOLOMITE ROCK

FIG. 2.24 COMPARISON OF THERMAL STRAINS. (CRUZ & GILLEN 1980)

Some earlier work on thermal expansion of concretes incorporating different aggregates has been undertaken by Schneider & Haksever (1976) and reported in the FIP/CEB Report (1978). Figure 2.25 shows their typical results. It can be seen that higher expansion is obtained with siliceous aggregate resulting from the significant physical changes that occur at high temperatures, i.e., disintegration and the α-to-β quartz transformation at 575 ^{o}C.

Fischer (1970) showed that the deformation of concrete is influenced by the level of the applied load during heating. It has been already noted that the thermal expansion of concrete depends on whether aggregate or cement dominates. A quartz-aggregate concrete made of Ordinary Portland cement with a water/cement ratio of 0.6 was used by Fischer. His specimens were loaded first to different load levels (β=0, 1/6, 1/3 & 1/2) before being heated to 600 ^{o}C, were maintained at this temperature for three hours then were allowed to cool to room temperature. Figure 2.26 illustrates some of his results. It can be seen that the presence of load reduces significantly the expansion. With increasing load, the expansion tends to be pevented and turns into contraction. This suggests that the occurence of cracking due to thermal incompatibility is delayed by the compressive strains developed by the applied load.

Some recent work by Thelandersson & Anderberg (1976) and Schneider (1976) confirmed Fischer's results. In his tests, Schneider used a quartz-aggregate concrete with a water/cement ratio of 0.54. The specimens were loaded then heated to failure. The thermal expansion was superimposed by compressive strains depending on the

FIG. 2.25 THERMAL EXPANSION OF CONCRETE WITH VARIOUS AGGREGATES.
(SCHNEIDER & HAKSEVER 1976)

FIG. 2.26 STRAINS MEASURED ON CONCRETE SPECIMENS HEATED AND COOLED UNDER LOAD.
(SOAKING PERIOD : 3 HOURS AT 600°C)
(FISCHER 1970)

load level. For instance, at 50% compressive load the expansion was fully compensated by the compressive strains. Thelandersson & Anderberg obtained the same result at a stress equal to 40%. The difference may almost certainly be explained by the different aggregate/cement ratios used by either workers. The total aggregate/cement ratio used by Schneider was 5.41 whereas Thelandersson's was 4.8. Figure 2.27 shows the results as obtained by Schneider. The critical temperatures are slightly higher than that reported by Thelandersson & Anderberg. Another aspect of the thermal expansion has been observed by Schneider. The cyclic heating and cooling of concrete showed a different deformation behaviour as illustrated in Fig. 2.28. The specimen tested was first loaded to 15% of the ultimate load and heated to 600 ^{o}C. The expansion observed was as expected compensated by the transitional deformations. Because of this, compressive strains appeared on cooling to room temperature. These compressive strains increased after each temperature cycle.

2.3.3.3. Spalling :

Spalling defined as the separation of surface material from heated concrete can be divided into three groups : general or destructive, sloughing off and local spalling (Institution of Structural Engineers (1975)). The occurence of spalling which is generally unpredictable is mainly caused by the build-up of steam pressure within the concrete resulting in reduction in fire resistance and consequently leading to damage to the concrete structures.

FIG. 2.27 TOTAL DEFORMATION UNDER DIFFERENT LOAD LEVELS. (SCHNEIDER 1976)

FIG. 2.28 DEFORMATION OF A CONCRETE SPECIMEN UNDER CONSTANT LOAD DURING CYCLIC HEATING AND COOLING. (SCHNEIDER 1976)

It has been shown that continuous structures would withstand local damage more satisfactorily than simply supported members. But high restraint may lead to instability associated with general spalling causing early collapse of the structure. This has been demonstrated by Dougill (1972a & b) when he investigated analytically the occurence of general spalling in restrained concrete panels exposed to fire.

The general or destructive spalling is violent and occurs during the early part of exposure. Dougill reported its occurence within the first 30 minutes of a standard fire test in the form of local breakdown.

The local spalling includes surface spalling, aggregate splitting and corner separation. The surface spalling consists mainly on local removal of surface material. The cause for this type of spalling is attributed to the moisture, although differences in opinion are reported in the literature. The aggregate splitting is caused by failure of the aggregate near the surface due to physical changes in the crystalline structure at high temperatures. This type of spalling is frequently observed with dense concretes made of gravel aggregates with high silica content. The corner separation can be violent and is defined as the removal of external corners from beams or columns. This type of spalling which occurs with dense concrete is caused by a tensile stress leading to splitting across the corner.

"Sloughing off" is the third type of spalling which occurs after a prolonged heating leading to weak surface layers which are gradually separated from the concrete members resulting from the development of cracks.

To avoid the danger of collapse which could occur following a general spalling, precautions should be taken in the design of concrete structures. Malhotra (1982) reported the following preventive measures against spalling.

1- use of aggregate resistant to spalling (e.g. limestone and lightweight materials).

2- use of aerating agents.

3- elimination of sharp corners and sudden changes in cross-section.

4- insertion of anti-spalling reinforcement in the concrete cover.

5- use of plaster or other finishes to prevent a steep temperature gradient across the section.

The mechanism of spalling is not completely understood and appears to need an exhaustive study to evaluate the phenomenon.

2.3.4 Concept of total strain model :

This has been introduced by Thelandersson & Anderberg (1976) when they developed a constitutive model to describe the mechanical behaviour of concrete at transient high temperatures conditions. The formulation of this model was consequent to data obtained from the different tests they performed, maily concerned with the stress-strain characteristics, thermal expansion and creep behaviour.

Thelandersson & Anderberg used an hereditary approach which relates the stress and strain with full account of the history of stress, strain and temperature up to the particular time being

considered. This constitutive law for concrete may be expressed as follows :

$$\epsilon = \epsilon\,(\sigma(t),\ T(t),\ \tilde{\sigma}) \qquad (2.7)$$

where : ϵ = total strain at time t.

σ = stress

$\tilde{\sigma}$ = stress history

T = temperature.

This model as considered is based on the concept of the total deformation . For practical applications, Thelandersson & Anderberg have shown that the total strain of concrete during heating consists of four components. This result has been confirmed by Schneider (1976). The total strain may be written as :

$$\epsilon = \epsilon_{th}(T) + \epsilon_{\sigma}(\tilde{\sigma}, \sigma, T) + \epsilon_{cr}(\sigma, T, t) + \epsilon_{tr}(\sigma, T) \qquad (2.8)$$

where : ϵ = total strain

ϵ_{th} = thermal strain, including shrinkage measured on unrestrained specimens under variable temperature.

ϵ_{σ} = instantaneous, stress-related strain, based on stress-strain curves obtained under constant stabilized temperature.

ϵ_{cr} = creep-strain, recorded under constant stress at constant stabilized temperature.

ϵ_{tr} = transient strain caused by heating under stress derived from tests under constant stress and variable temperature.

Figure 2.29 shows the four components of the total strain for a concrete specimen heated under a load equal to 35% of initial ultimate

FIG: 2.29 DIFFERENT COMPONENTS OF THERMAL STRAIN.
(THELLANDERSSON 1976)

load. The concrete used was made of Ordinary Portland cement and quartzite aggregate. The evaluation of each of the strain components is based on the test results obtained by the authors and reported in the literature. The four different strains are discussed in this section and the complete description of the model is given in Thelandersson & Anderberg (1976) and reported in the FIP/CEB Report (1978).

The thermal strain is a function of the temperature and is determined by performing a simple thermal expansion test. A typical curve of the thermal expansion corresponds to Ø% in Fig. 2.29. It is to be noted that the thermal strain depends on the initial moisture content since the drying shrinkage is included.

The instantaneous stress-related-strain is the response of the material as a result of a change in stress. The stress-strain curve at a given time is considered as a function of the temperature and the stress history as presented in Eq. (2.8).

The creep strain is obtained from tests at constant stress and constant temperature, whereas the transient strain is evaluated from tests on concrete specimens which are heated to failure under sustained load.

2.3.5 Transient Strain :

The predominance of such a strain is illustrated in Fig. 2.29. As mentioned earlier, transient strains develop under compressive stresses as the temperature increases. They occur only under the first heating of concrete and are essentially irrecoverable. Thelandersson &

Anderberg (1976) evluated the transient strain from tests conducted on specimens under constant stress and heated to failure. ϵ_{tr} is obtained using the following relation :

$$\epsilon_{tr} = \epsilon - \epsilon_{th} - \epsilon_{\sigma} - \epsilon_{cr} \qquad (2.9)$$

The components are determined as follows :

ϵ_{th} is evaluated from the measured thermal expansion whereas ϵ_{σ} and ϵ_{cr} are calculated using the models developed for this purpose. The transient strain is obtained as a function of temprature but independent of time. From tests carried out by Thelandersson & Anderberg, it has been found that ϵ_{tr} is approximately linear with stress.

Thus ϵ_{tr} can be expressed as :

$$\epsilon_{tr} = - K_2 \frac{\sigma}{\sigma_{uo}} \cdot \epsilon_{th} \qquad (2.10)$$

where : K_2 = is a dimensionless constant. Regression analysis for the data gives $K_2 = 2.35$.

σ / σ_{uo} = is the stress/strength ratio

The model has been satisfactorily tested by Thelandersson and Anderberg using their data which were compared to those results obtained from other investigations. However some differences appeared for temperatures above 550° C. This discrepancy is most likely due to phase changes which occur at 575°C when using quartzite aggregate in the concrete.

2.4 STRUCTURAL RESPONSE AND MODELLING :

The response of structural elements in fire has been the subject of a large amount of work. But only limited information is available on structural members tested with simulated conditions of restraint and continuity to reproduce more realistically the behaviour in service. This, however, does not provide enough data to understand the overall response of a structure in fire conditions. Because of this, complete analytical models are needed to be incorporated into the design of structures operating at elevated temperatures, so that their actual fire resistance can be assessed.

When modelling structural behaviour, a good knowledge is required on the effect of heating on concrete structures whose performance at high temperatures is very much influenced by the effect of temperature on the basic materials : concrete and steel. The former has been described in the previous sections and the properties of the latter are briefly reviewed in the next paragraph.

2.4.1 Steel and bond strength at elevated temperatures :

The effects of temperature on the properties of steel have been studied by number of workers, namely Holmes et al (1982), Crook (1980), et al. The behaviour of reinforcing steel at high temperatures depends on the type of steel. The mechanical properties have been reported to decrease as the temperature increases. The thermal properties are also affected by heating. It has been shown that the thermal conductivity decreases with increasing temperature and depends

on the composition of the material. On the other hand, the specific heat which is independent of the nature of the steel, has been found to increase as the temperature rises, whereas the thermal diffusivity decreases more or less linearly (Malhotra (1982)).

As with concrete, due to the variations in the mechanical properties, steel becomes structurally weak when subjected to elevated temperatures. Tasmin (1975) discussed the influence of temperature on the material properties of steel and reported that the resistance to collapse in fire is greatly influenced by the strength-temperature characteristics of steel.

It has been shown that the tensile strength and the yield strength of steel are reduced under elevated temperatures. Some typical results are shown in Fig. 2.30 which indicates that the yield strength of steel first exhibits an increase at temperatures up to 300^{o}C, after which a progressive reduction in strength is observed.

The residual strength has also been examined and reported in some published work. Some typical results are shown in Fig. 2.31. It can be seen that the reinforcing steels almost regain their initial yield strength on cooling from temperatures of 500^{o}C - 600^{o}C. But on cooling from higher temperatures, e.g. 800 °C, there is a loss in yield strength for all steels. However the proportional reductions depend on the type of steel. Crook (1980) and Holmes et al (1982) investigated the effect of temperature on four types of steels and their results showed similar trends as those already reported.

The ultimate strength and Young's modulus are also significantly affected by temperature. The modulus of elasticity decreases with

FIG. 2.30 TYPICAL STRENGTH OF STEEL BARS TESTED AT ELEVATED TEMPERATURES. (BANNISTER 1968)

FIG. 2.31 TYPICAL YIELD STRENGTH OF REINFORCING BARS TESTED AT ROOM TEMPERATURE AFTER HEATING TO AN ELEVATED TEMPERATURE. (BANNISTER 1968)

increasing temperature as shown in Fig. 2.32 (reported in Crook (1980)). On the other hand the ultimate strength of Fig. 2.33 is generally greater at 300 ^{o}C than at normal temperature, then beyond this temperature is progressively reduced.

It has been intiated that creep of steel under elevated constant temperature can be divided into three regimes : primary, secondary and tertiary. Creep rupture occurs at the end of the third phase. Malhotra (1982) reported that up to a temperature of 450 ^{o}C creep strain due to primary and secondary creep was not very significant. But the amount of creep strain at higher temperature was influenced by the stress and temperature history.

The creep behaviour of steel can be assessed analytically. Creep models based on Dorn's creep theory (1954) have been developed mainly by Harmathy (1967). His model can predict the uniaxial time-dependent deformation of steel at increasing temperatures and varying stresses during the primary and secondary periods.

The total thermal deformation of steel at transient high temperatures can be expessed as the sum of three components. Anderberg (1983) reported the following constitutive equation :

$$\epsilon = \epsilon_{th}(T) + \epsilon_{\sigma}(\sigma,T) + \epsilon_{cr}(\ ,T,t) \qquad (2.11)$$

where ϵ = total strain

ϵ_{th} = thermal strain

ϵ_{σ} = instantaneous, stress-related strain based on stress-strain relations obtained under constant, stabilized temperature.

FIG. 2.32 MODULUS OF ELASTICITY OF SOME REINFORCING STEELS. (ANDERBERG 1978)

TEMPERATURE - °C

PROPORTION OF ROOM TEMPERATURE ULTIMATE STRENGTH

FIG. 2.33 TYPICAL ULTIMATE STRENGTHS OF REINFORCING AND PRESTRESSING STEELS AT ELEVATED TEMPERATURES.

ϵ_{cr} = creep strain or time dependent strain.

Anderberg in an earlier paper published in 1976, used Eq. (2.11) to develop a computer model to assess the mechanical behaviour of steel.

An increasing amount of information is becoming available on bond strength of steel and concrete at high tempratures. It has been shown that the bond strength depends upon the temperature level and on the other hand the influence of the surface and shape of the bar is very significant. Another important factor is associated with the type of concrete. As Malhotra (1982) reported, concretes with lower thermal strain characteristics retain higher bond strength values. Diederichs & Schneider (1981) conducted their experiments using siliceous-aggregate concrete and three different types of steel (ribbed steel bars, plain round bars and deformed prestressing bars). Some of their results are shown in Fig. 2.34. It can be seen that at a temperature up to 450 °C the lowest value of bond strength is obtained for the smooth bars, where only 20% of their bond strength at 20 °C is retained. Deformed bars behaved better and relatively higher values of the bond were retained. Diederichs & Schneider reported that the decrease in bond strength for ribbed bars at constant temperatures is of the same order of magnitude as the loss in compressive strength of concrete at high temperatues.

2.4.2 Structural response :

FIG. 2.34 REDUCTION OF BOND STRENGTH FOR DIFFERENT STEELS (DIEDERICHS 1981)

Tests on concrete structural elements have been performed to produce a basic information in designing for fire resistance. The flexural members (beams and floors) have been studied in more details in comparison with the compression members (columns and walls). However only few attempts have been made to carry out furnace tests under realistic structural conditions. Continuity and restaint can be obtained if real continuous structures are tested. But the realistic structural conditions as reported by Purkiss (1972) can be simulated by replacing continuity over the supports by deformation induced loads and moments. The difference between the behaviour of a specimen in a furnace test and that of an element in a building is mainly due to the boundary conditions.

The most important work on flexural members has been undertaken by the PCA in the United States, and is described in detail in Purkiss (1972). Gustaferro (1970) reported the results of some tests conducted on cantilevered beams. The redistribution of moments which occured resulted in an increase in moment over the supports and a decrease in a moment at mid span. It has been admitted that continuous concrete beams or slabs exhibit a higher fire resistance than simply supported members. On the other hand if the thermal expansion of such fluxural members is prevented by some degree of restraint their behaviour is even more improved.

The effect of restraint of the thermal expansion of the structural members has been examined by some investigators namely Selvaggio and Carlson (1963). Some methods for measuring the thermal restraint forces, have been developed by Issen et al (1970).

The Institution of Structural Engineers (1975) reports two types of restraint which can be applied to the members. Longitudinal restraint is a restriction to the expansion of the beam or the floor and will tend to impose direct compressive stresses on the cross section. These thermal stresses will increase the fire endurance of the element which is in fact prestressed by the applied restraint. However if an excessive restraint against expansion is provided, spalling of concrete can occur leading to damage to the structural members. The other type of restraint is provided by continuity or end fixity by applying a rotational restraint against movement caused by fire.

The influence of restraint on concrete compression members (columns and walls) and the effect of boundary conditions have not been extensively studied. Limited observations have been reported in the literature. The behaviour of columns exposed to fire attack depends on the type of concrete, the method of reinforcement, the column size, the applied load and the strength of concrete. Thomas & Webster (1953) showed that the smaller the load the greater is the endurance period, and with higher concrete strength an increased fire resistance is achieved. But the occurence of spalling in large columns reduces significantly the endurance period. Dougill (1975) reported that failure of an unrestrained column heated under load occurs when the strength is reduced by heating to the value of the constant applied load. Thomas & Webster assessed the fire resistance of concrete columns experimentally. More recently, Lie & Allen (1972) suggested a method to obtain, by calculation the fire resistance of reinforced concrete columns as a function of size, load intensity,

slenderness of the column and cover thickness to the steel. The method developed is not very satisfactory because it is based on assumptions made in a standard fire test. The test is conducted on an isolated unrestrained member subjected to heating corresponding to the standard fire temperature curve. Lie & Allen (1974) attempted to overcome the difficulty by undertaking a further study taking account of the effect of restraint in actual fire conditions.

Dougill (1966) investigated the effect of restraint applied to load-bearing members under heating. The thermal expansion of a column in a multi-storey structure, is restricted by the axial restraint as provided by the surrounding structure. In his analysis, he reported that due to the restraint, an additional load is induced in the column and increases with the number of floors above the heated compression member. When the total load of the column reaches its maximum load capacity, failure can occur leading to reduction in fire resistance caused by the excessive restraint. The transient effect of the whole structure has not been considered by Dougill (1966). He considered the heating on the column only and assumed the remainder of the structure unaffected by heating, and only considred axial restraint. This obviously does not reproduce realistic conditions, but the predicted trends will be correct.

Later work by Dougill (1972a & b) has shown the influence of restraint and loading on the occurence of instabilities in concrete panels. Dougill has put forward an analysis to study the instability corresponding to the incidence of general spalling of plain concrete panels. This mode of failure depends upon the boundary conditions of loading and restraint applied to the panel. He has also suggested that

failure due to spalling is analogous to a failure caused by strain softening in a standard compression test.

Dougill (1972b) has pointed out the difference between the behaviour of axially restrained and flexurally restrained panels. The former will tend to fail in a flexural mode with a sudden increase in curvature.

The mode of failure that might occur in a concrete panel is reported to be influenced by the extent of cracking and the form of stress-strain curve in compression. Cracking may be beneficial as it leads to increased fire resistance of the panel resulting from the limited development of thermal stresses. During heating, tensile stress develops and due to the tensile cracking induced, the rate of expansion is reduced and consequently the section unloads and therefore the failure is prevented and the panel partly cracked survives. This observation has also been reported in a following paper by Dougill (1975). However, instability in fire conditions, is likely to occur with extensive cracking. In order to perform effectively, the panel should be less damaged and it is therefore necessary to limit this cracking by using a small amount of reinforcement in the panel to hold the fractured concrete and to distribute the cracks. The role of reinforcement in panel structures has not been investigated by Dougill. He reported, however, that a large quantity of steel in the panel could be harmful and could promote instability and consequently collapse of the structure.

2.4.3 Computer modelling :

Computer programs for the complete analysis of concrete elements under fire conditions have been developed by number of workers.

Bizri (1973) developed a computer program for the study of the non-linear behaviour of reinforced concrete structures. His model is based on finite element methods. The specific application of the model is to predict the fire response of reinforced concrete columns. The formulation of Bizri's approach is based on approximations used to describe the material behaviour as well as the material properties.

This analysis has been extended in some later work undertaken by Becker et al (1974a) to develop an improved computer model (FIRES-T) for Fire Response of Structures-Thermal. In a following report by Becker et al (1974b) a complementary computer program has been introduced to evaluate the structural response of reinforced concrete frames in fire environments.

FIRES-T is a computer model based on a two-dimensional non-linear thermal analysis. It evaluates the temperature distributions of structures cross-sections subjected to fire attack, using a finite element formulation. This computer program is used in conjunction with FIRES-RC, a program for predicting the Fire Response of Structures-Reinforced concrete frames. FIRES-RC is a non-linear analysis approach based on finite element methods.

The behaviour of actual building structures in fire conditions has been dealt with by Bannergee (1972) and reported in Sullivan (1972). The computer program developed takes into account the deterioration of concrete in compression and the effect of temperature on the mechanical properties of both concrete and steel as reported in Dougill & Sullivan (1983).

Some workers such as Allen & Lie (1974) and Lie (1983) developed analytical approaches to assess the fire resistance of single members, e.g. reinforced concrete columns.

A more complete computer model for the prediction of the structures in fire conditions is being developed at the University of Aston. The model should permit a comprehensive study of the instability of slender columns subjected to elevated temperatures. The computer program is based on an analysis using finite elements methods and will use the results to be reported later in this thesis as a basis of the concrete materials model.

The next chapter deals with the specifications of the testing machine developed for the purpose of the investigation.

CHAPTER 3

SPECIFICATION & DESIGN OF THE TEST RIG

3.1 INTRODUCTION :

The effect of high temperature exposure on concrete subjected to compressive loading has been the subject of some research work. However only few data are available on a complete stress-strain temperature behaviour model required to assess the fire performance of concrete. To obtain such data relevant to the design of concrete members, a special testing machine capable of operating at high temperatures has been developed.

Since it is difficult to express the material behaviour of concrete under compressive stresses and high temperatures by a single mathematical equation, which requires parameters to be found from experiments at the test conditions imposed, it is necessary to develop testing equipment that is capable of carrying out the main experimental work under both transient and steady state conditions. The transient effect is obtained when heating a concrete specimen to failure at constant stress, whereas in tests performed under steady state condition, the specimen is loaded at constant temperature.

The apparatus has been developed to measure the load and overall deformation of a specimen, thus enabling a complete stress-strain curve to be obtained at elevated temperatures.

The machine is based on a prototype developed by Purkiss (1972) and reported in Dougill & Purkiss (1973). The design has been modified and improved partly as a result of the decision to use larger specimens to avoid aggregate interference.

The testing machine consists of a system of elements connected together in such manner that they form a stable assembly. An essential

requirement of the testing machine is that it should possess sufficient stiffness to provide stability and accuracy for the test to be carried out. A general view of the apparatus may be seen in Plate 3.1. The main frame of the machine consists essentially of three rigid triangular crossheads connected by three prestressed vertical members.

The crossheads are mild steel plates. The top and the lower crossheads are 75 mm thick whereas the centre one is 50 mm thick. Figure 3.1 shows the test rig arrangement. The main columns are hollow mild steel cylinders which are stiff enough to provide stability of the system as a whole and prestressed by 3 No. 32 mm diameter Macalloy bars to ensure that contact is maintained between the columns and the platens during the loaded condition. Details on the Macalloy bars are outlined in Appendix One. Longitudinal and torsional instabilities are prevented by the use of a three column machine.

A screw-jack is mounted below the lower crosshead and is fixed by means of tensioned high-tensile steel bolts. A dynamometer placed under the centre crosshead is attached to a threaded portion of the lifting screw of the jack. The whole assembly is supported by three mild steel sub-columns which are welded to a steel base plate of 12 mm thickness. The machine is set on a concrete plinth to give ease of operation as is shown in Fig. 3.1 and Plate 3.1.

The possible vibration of the rig is prevented by placing a rubber mat between the base plate and the top of the concrete plinth.

The test specimen is placed between two fixed rigid smooth platens which are machined from a high temperature alloy "Nimonic 90". It is however necessary to carry out proving tests in order to establish the performance of the rig. The instrumentation used for

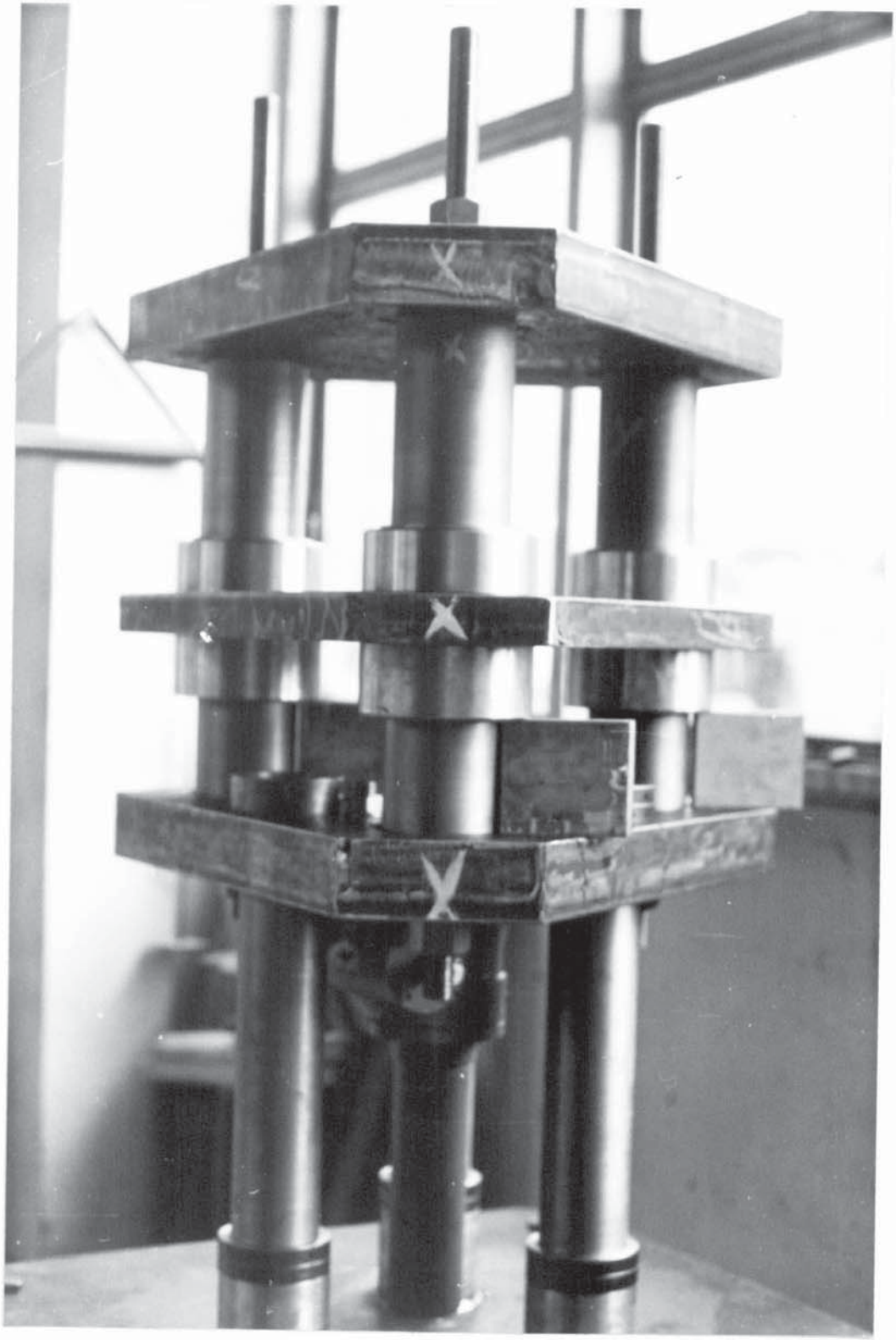

PLATE 3.1 TEST RIG

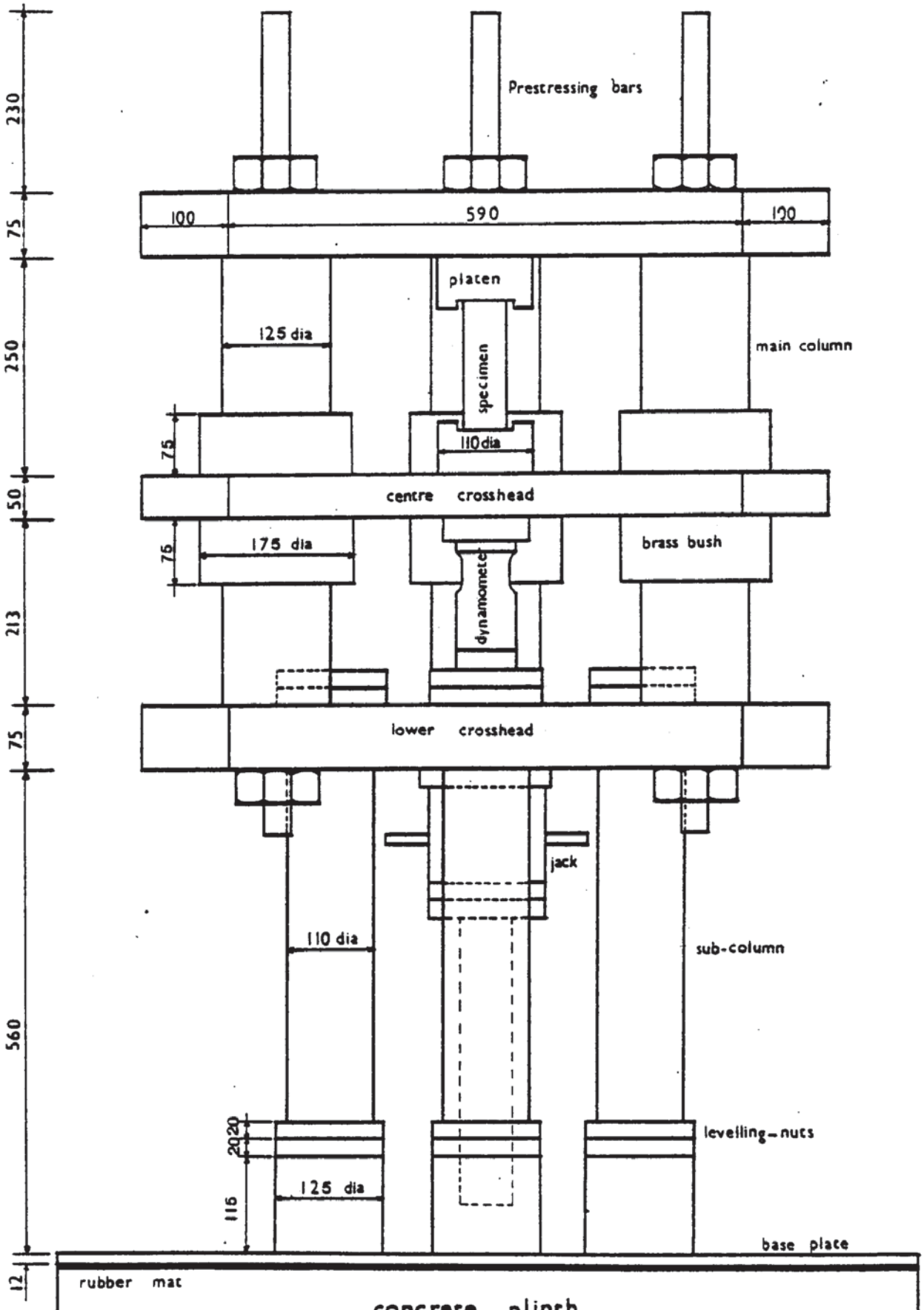

FIG. 3-1 : TEST RIG ARRANGEMENT

measuring and recording force, specimen displacement and temperature requires to be calibrated. The calibration tests are fully discussed in Appendix Two & Five.

3.2 SPECIMEN SIZE :

The preparation of the specimens is set out in the next Chapter. In order to obtain uniform temperatures in the test specimens, a small specimen size has been chosen for the purpose of the work. Once the specimen size has been selected the required machine stiffness can be calculated. The cylindrical test specimens are 50 mm in diameter and 150 mm in height. The aggregate size to be used is 10 mm to avoid problems of non-homogeneity caused by a large aggregate to specimen size ratio. The specimen stiffness will in fact tend to increase with decrease in aggregate size as noted by Hughes & Chapman (1966).

3.3 EXPERIMENTAL EQUIPMENT :

Plate 3.2 shows the complete testing equipment comprising the recording devices for temperature, specimen displacements and forces, the controlling system for the furnace, and the test rig but without the furnace. The measuring instruments of the test equipment are fully described in the following sections :-

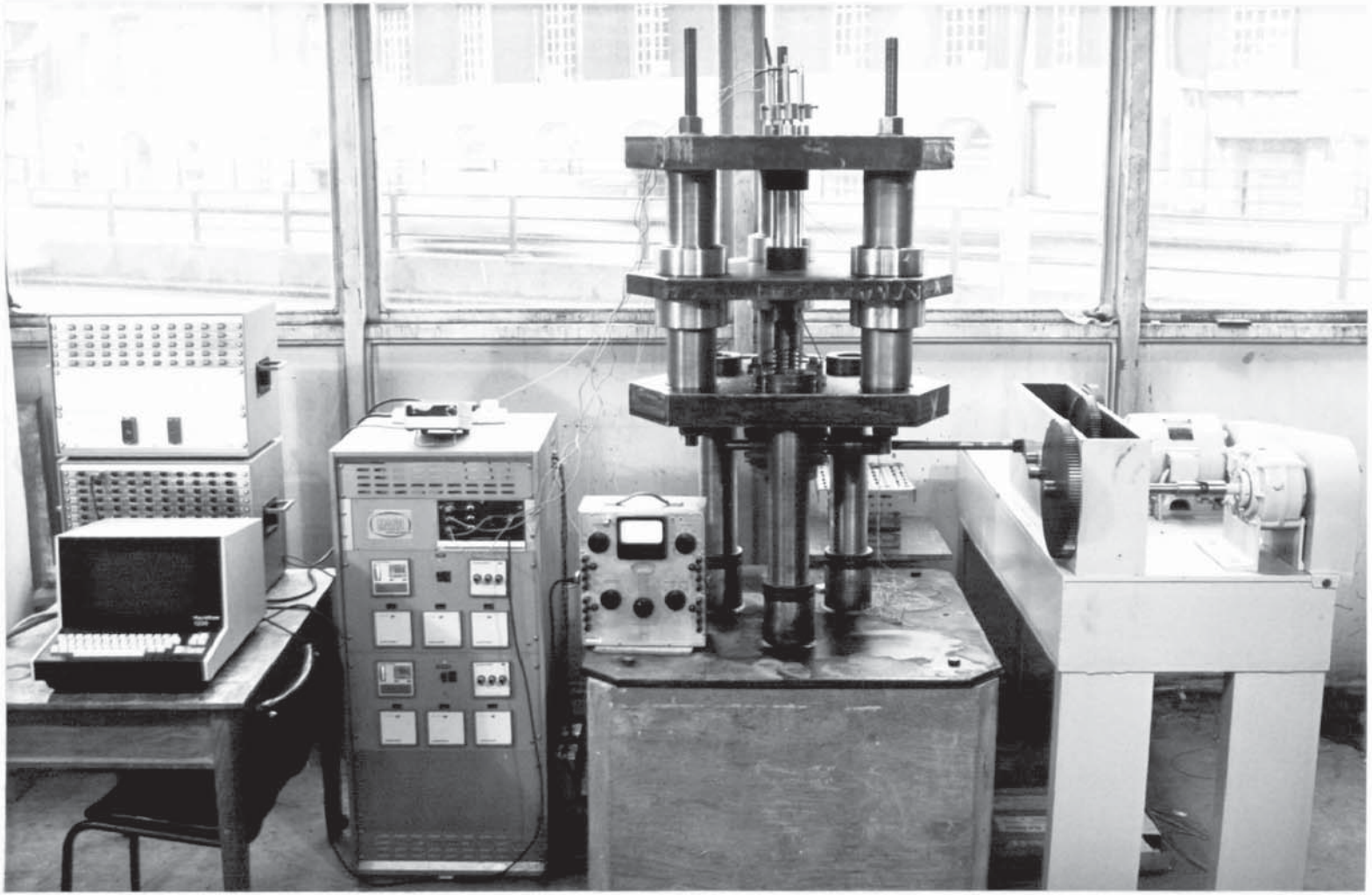

PLATE 3.2 TEST EQUIPMENT AND INSTRUMENTATION

3.3.1 Loading :

An electrical resistance strain gauge dynamometer of 200 KN capacity has been designed for measuring the load. This consists of a hollow necked cylinder of 126 mm in height on which the strain gauges are placed. The strain gauge configuration is that of a full four arm bridge mounted on the dynamometer, which will produce high sensitivity and temperature compensation. The dynamometer is placed under the centre crosshead as it can be seen in Plate 3.3. The load is applied to the specimen by a screw-jack. The lifting screw of the jack passes through the lower crosshead and receives the hollow steel cylinder. The detailed calculations for the design of the dynamometer are given in Appendix Two.

The screw-jack used to transmit the compressive load is a Duff-Norton 200 KN screw-jack which is used due to its inherent high stiffness. A 1820 Duff-Norton jack model is selected for the load application. Its worm gear ratio is 24:1 and the diameter of the lifting screw is 65 mm. The screw-jack is driven electrically through a variable speed gear box. The drive-unit consists of an electric motor with a maximum speed of 1415 rpm, which is coupled with a reduction gear box to drive the screw-jack described above. The reduction gear box has a maximum input speed of 2000 rpm with a ratio of 15 to 1. The normal rating is 1.335 KW at 1440 rpm. The steel frame supporting the motor and the reduction gear box is shown in Plate 3.2 as a complete drive unit.

3.3.2 Temperature :

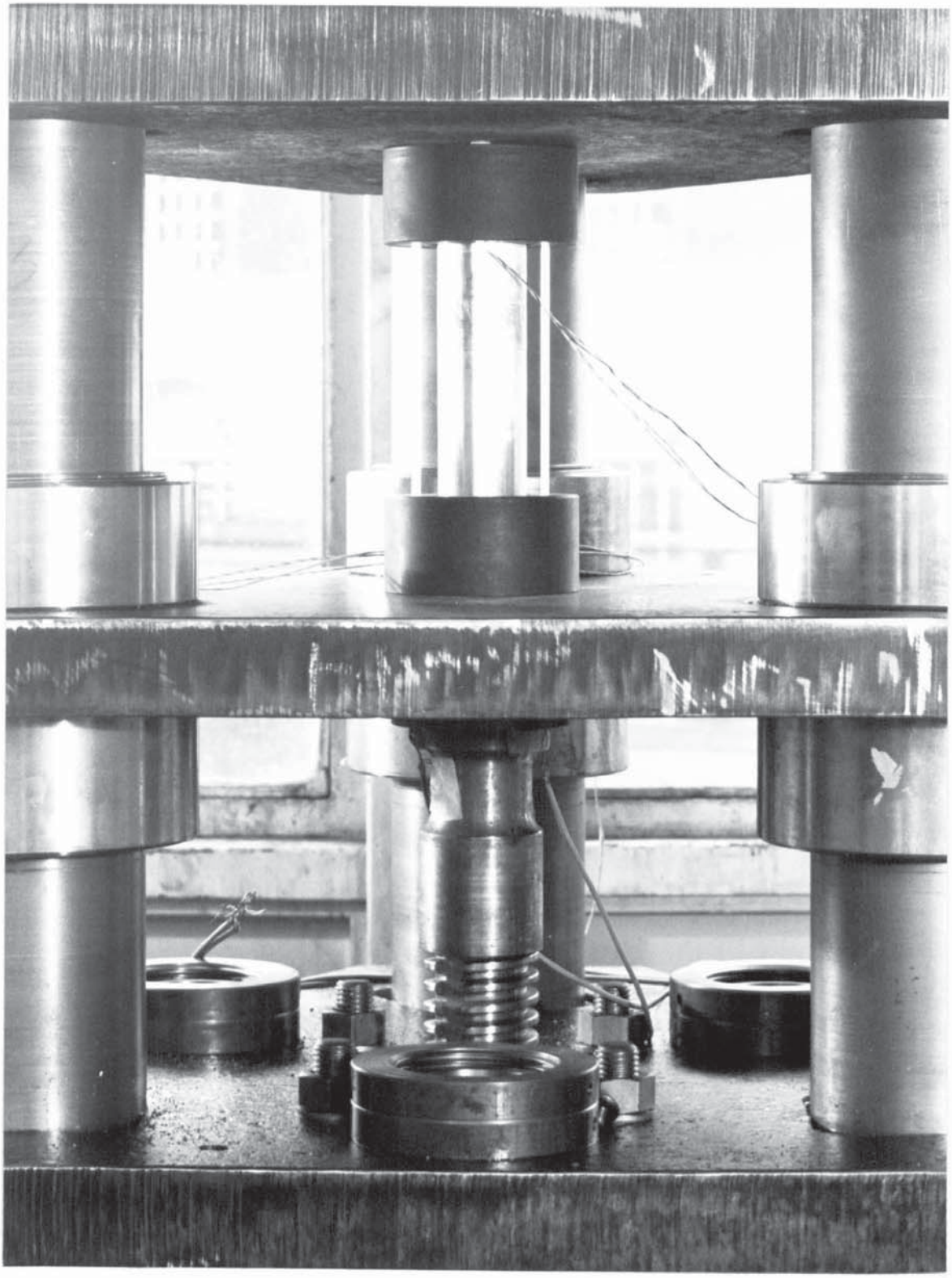

PLATE 3.3 LOAD APPLICATION (DYNAMOMETER)

The heating of specimen to the test temperature is accomplished by the use of an electric furnace designed especially for the experimental work. Plate 3.4 shows a general assembly of the furnace. A low heating rate furnace has been decided upon as the result of the difficulty to use the standard time-temperature curve as required by BS 476: Part 8: 1972.

The furnace was constructed in two halves enabling the specimen to be surrounded and heated. The split furnace is a cube whose edge is 230 mm with a 165 mm inside diameter. It was made of a refractory material consisting of Gibcrete 1300. Welded steel plates form a housing to the furnace.

Additional insulation of the furnace is obtained by inserting loose wool fibres between the welded steel plates and the refractory elements. The loose wool is manufactured by MacKechnie Refractory Fibres Limited. A detailed description of the fibres is given in Appendix Three. Plate 3.4 shows the insulation and the two parts of the furnace with the high temperature Nichrome alloy spirals inserted in quartz tubes forming the heating elements. The furnace was tested to a maximum temperature of 1100 ^{o}C.

The temperature of the furnace is controlled by a series of thermocouples connected to the Eurotherm temperature controllers with a temperature ranging from ambient to 950 ^{o}C, provided by Mand Precision Engineering Co. Ltd. The furnace, which is mounted on the centre crosshead, surrounds the specimen which can then be heated to the test temperature insitu. The thermocouples used consist basically

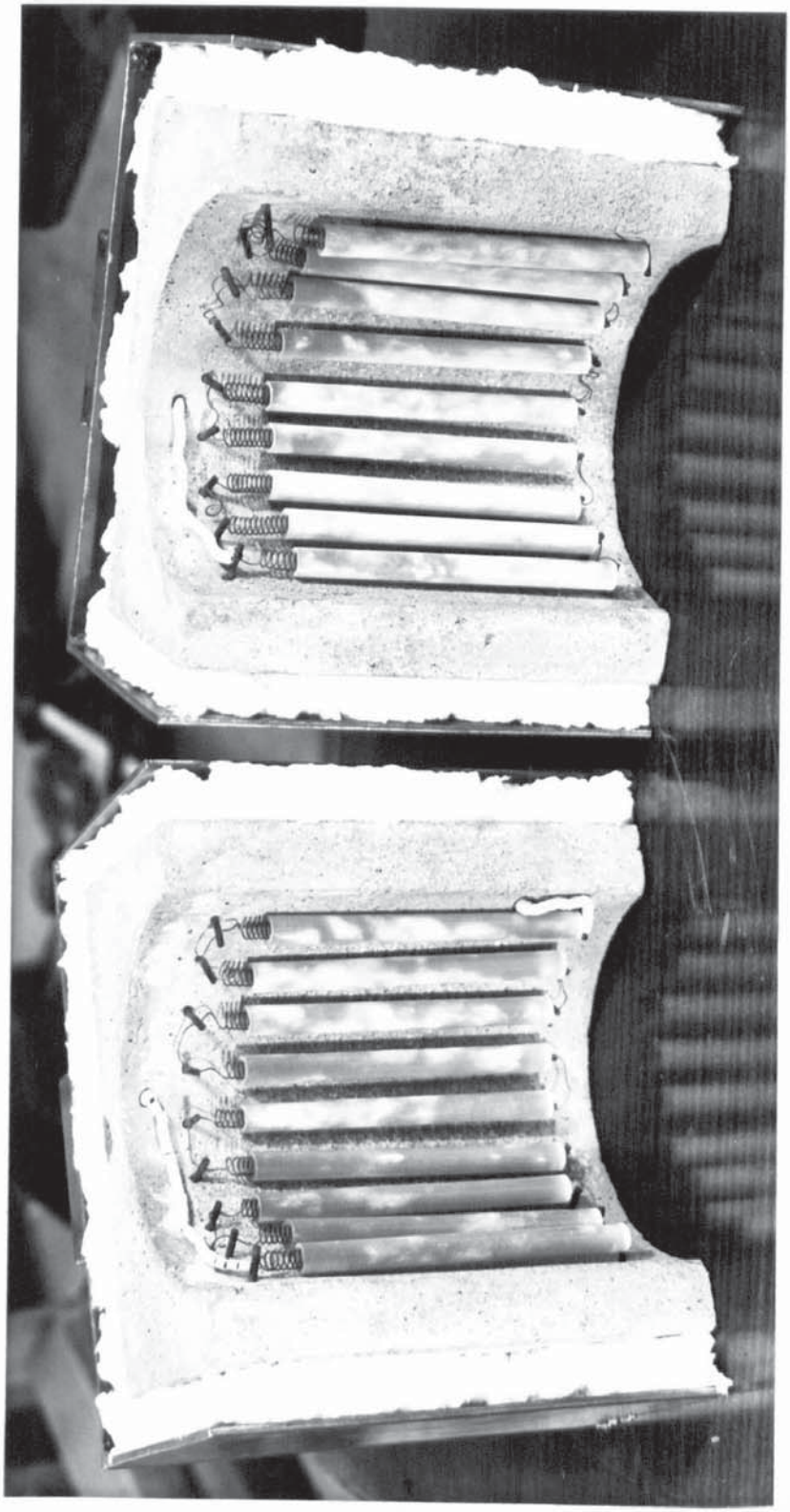

PLATE 3.4 GENERAL VIEW OF THE FURNACE

of wires of Chromel (Ni-Cr) and Alumel (Ni-Al) alloys, the ends of which are joined spot welded.

(Ni-Cr)/(Ni-Al) thermocouples are inserted in the furnace to monitor the temperature during testing, the output from which is input to a recording system. A digital thermometer was available to record the temperature as a reserve to the data logger during any malfunction.

3.3.3 Deformation Measurement :

Three linear variable differential transucers (LVDT) are used to measure the length changes of the specimen. They are mounted on the testing machine above the top crosshead with the aid of an insert made of brass as shown in Plate 3.5. They are aligned in order to record the movement of the platens, which is transmitted through a system of quartz rods and tubes with a very low coefficient of expansion of 0.54 $\times 10^{-6}$ deg.C^{-1}. The transducer core is fixed to a quartz rod which is inserted in the lower platen, whereas the upper platen is connected to the body of the transducer through a quartz tube. Figure 3.2 shows the disposition of the platens and the displacement measuring assembly. The LVDT type transducer selected is a D5/500A model which can be seen together with the quartz tubing in Plate 3.5 and 3.6.

The output from the transducers is fed to a recording system through an extensometer amplifier manufactured by Mand Precision Engineering Co. Ltd, which enables the mean of the three transducers

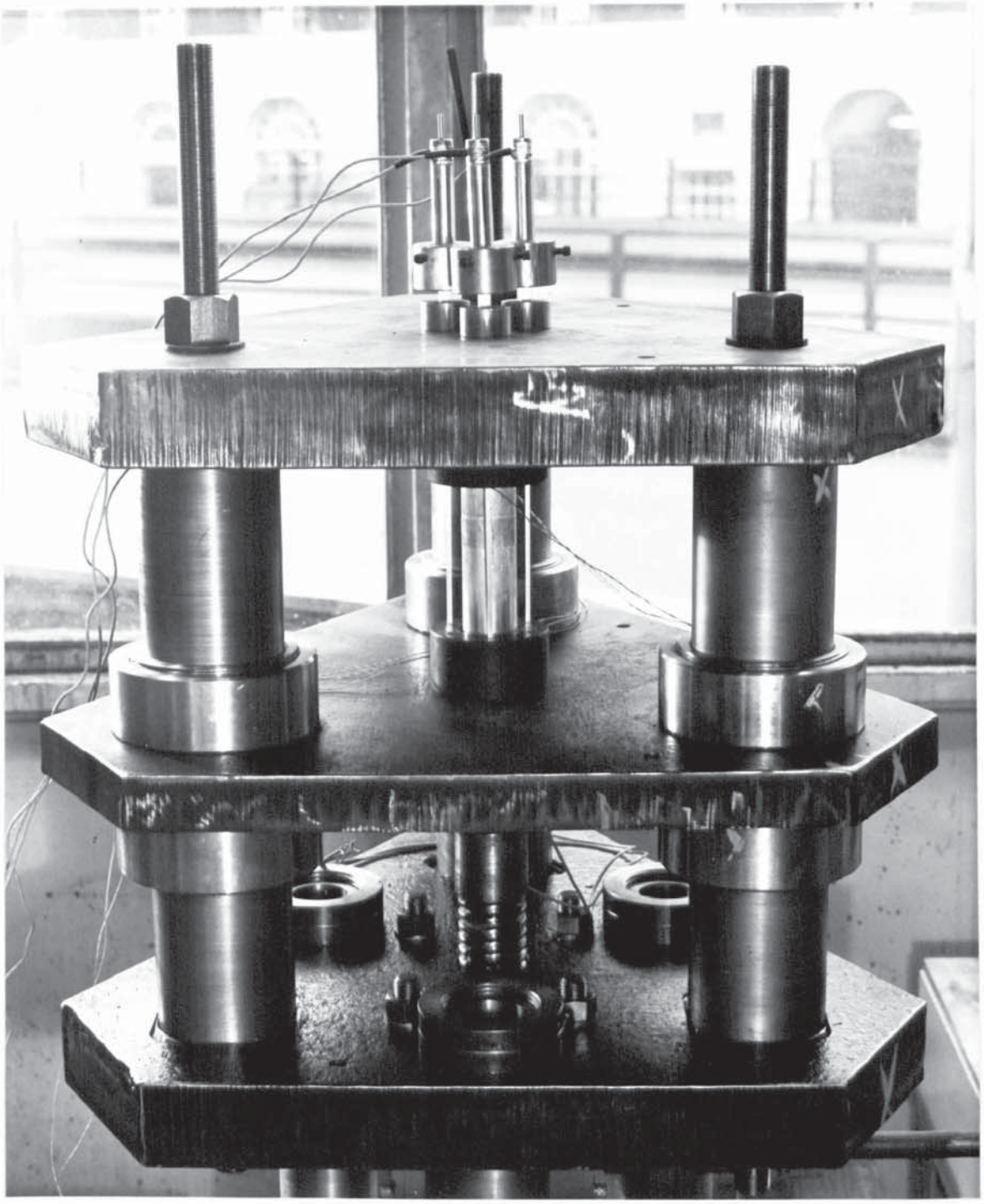

PLATE 3.5 DISPOSITION OF THE TRANSDUCERS

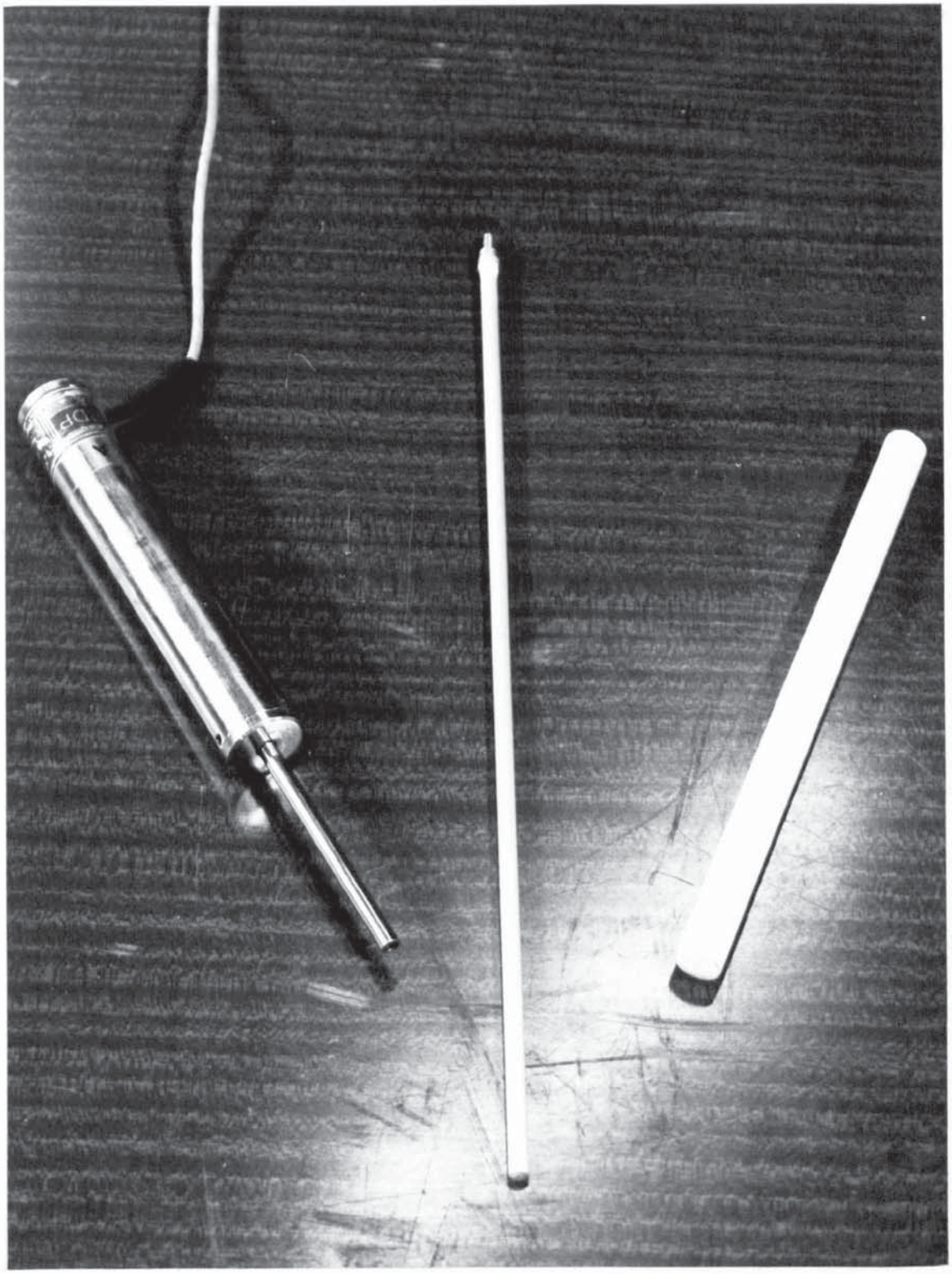

PLATE 3.6 TRANSDUCERS (LVDT) AND THE QUARTZ TUBING

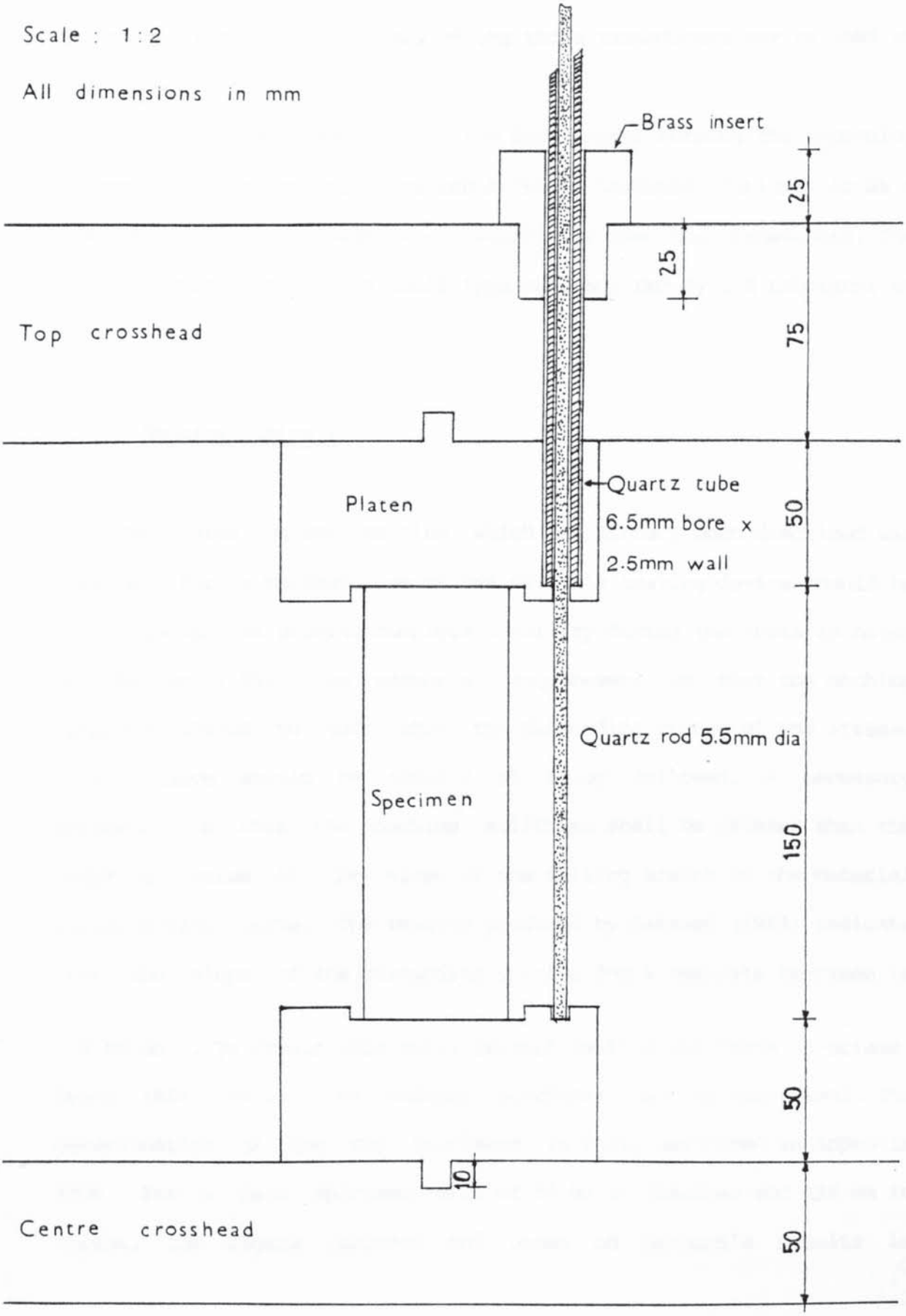

FIG. 3.2 PLATENS AND DISPLACEMENT MEASURING ASSEMBLY

to be monitored. However each of the three transducers may be read as individual units.

As mentioned previously, the data logger forming the recording system was not entirely reliable due to hardware problems. So as a reserve a digital voltmeter was available to read the transducers. The digital voltmeter is an SM211 type manufactured by S.E Laboratories Ltd.

3.3.4 Machine Design :

The three column machine which has already been described was designed for a maximum load of 200 KN. This testing device should be stiff enough to provide complete stability during the tests as noted by Chilver (1955). An essential requirement is that the machine response should be such that the descending branch of the stress-strain curve should be capable of being followed. A necessary criterion is that the machine stiffness shall be greater than the numerical value of the slope of the falling branch of the material stress-strain curve. The results produced by Barnard (1964) indicate that the slope of the descending portion for a concrete specimen is $6.6\ KN\ mm^{-2}$. To obtain this value Barnard carried out tests on prisms. Using this result, the machine stiffness can be determined. The determination of the rig stiffness is fully described in Appendix Four. For a test specimen size of 50 mm in diameter and 150 mm in height, the figure recorded and based on Barnard's results is

$90\ KN\ mm^{-1}$. The value obtained, however, for the machine stiffness is $355\ KN\ mm^{-1}$.

The machine, which was manufactured from mild steel, possesses an adequate margin of stiffness to prevent the buckling of the whole system. It has been shown that in compression testing machines, the main members are in tension as noted by Chilver, so the stability of such machines may be difficult to ensure. It is however possible to increase the stability of the apparatus designed by allowing the centre crosshead to slide freely along the vertical members. This has been achieved by using long close tolerance brass bushes bearing at their ends only to reduce friction between the cross members and the columns.

The general assembly of the machine may be seen in Plate 3.1. The centre crosshead also serves as a heat dissipator reducing the heat transfer to the dynamometer.

The complete testing machine is also used for conducting creep tests on concrete cylinder specimens subjected to different stress levels at temperatures up to $700^{\circ}C$.

3.4 CONTROL OF THE TEST RIG :

The testing equipment will be controlled using a data logger enabling the recording and storage of the results on a storage system disk. The next Chapter will deal with the recording facilities and includes the computer programs written to control the apparatus using a feed back loop.

3.5 PROVING TESTS :

Proving tests were conducted in order to determine the machine stiffness, the friction in the brass bushes and the output from the transducers.

The details of these tests are set out in Appendix Five. However the tests carried out on the machine were very successful. The rig was found to be stiff enough with an actual stiffness of 310 KN mm^{-1}. In addition to that the friction in the bushes was negligible and the transducers were reading correctly.

CHAPTER 4

MIX DESIGN & SPECIMEN PREPARATION

4.1 INTRODUCTION :

The testing machine, whose design has been set out in the previous chapter, has fixed platens and thus special requirements are imposed on the specimens, namely parallel and flat ends.

The cylindrical specimens used were 50 mm in diameter and 150 mm long. They were cast in split steel moulds, 50 mm inside diameter and 200 mm long, illustrated in Plate 4.1.

With fixed platens, it should be noted that if the end surfaces of the specimen be neither plane nor parallel, stress concentrations will be introduced and could possibly lead to premature failure. Neville (1981), reported that a loss of strength of concrete cylinders was caused by a lack of planeness of the end surface, when tested in compression. To avoid this reduction in strength ASTM standard C617-76 lays down that the end surfaces of a cylindrical specimen should be plane within 0.05 mm. Therefore it is essential that the end planes of a cylindrical specimen are normal to its axis.

The planeness of the lower end was obtained by casting against a machined steel plate. The as cast top surface was rough and so not truly plane. To overcome this, grinding techniques were employed since it is not possible to use normal capping materials at elevated temperatures.

4.2 MOULD DESIGN :

The moulds used were machined split steel moulds consisting of two vertical rectangular sections, 38 x 100 x 200 mm, with a 50 mm

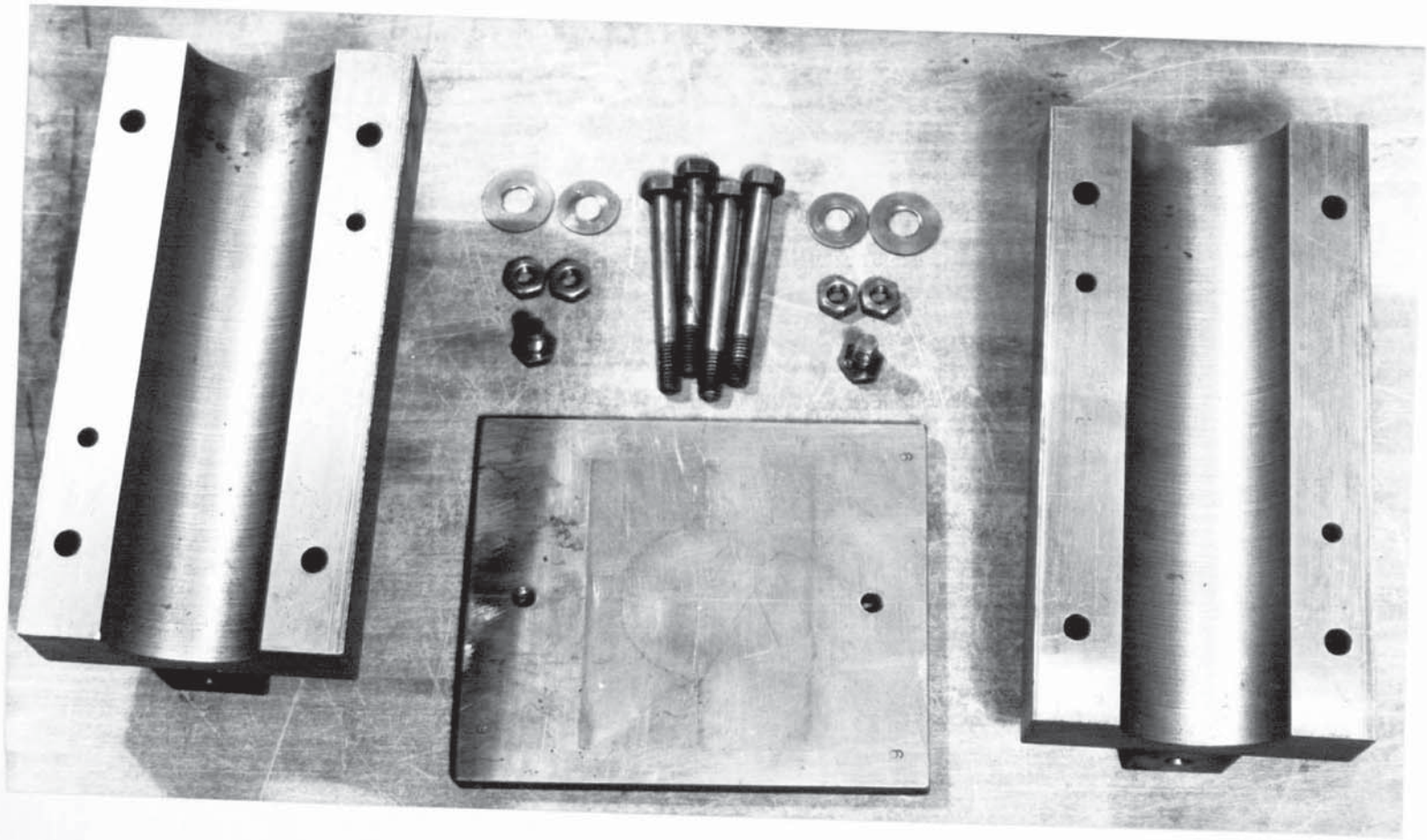

PLATE 4.1 GENERAL AND DETAILED VIEW OF A MOULD

diameter longitudinal centre hole, and a base plate. The upper part of the mould was clamped onto the base plate by means of small bolts. A detailed view of one of the moulds appears in Plate 4.1. One assembled mould together with one 100 x 100 mm standard cube mould used can be seen in Plate 4.2. A set of ten moulds was constructed for the purpose of the work.

4.3 MATERIALS :

The constituents of the concrete used in all the test specimens consisted of Ordinary Portland cement, Zone 2 sand, crushed siliceous aggregate of 10 mm maximum size, and water. The aggregate and sand were oven dried.

After several trial mixes were examined it was decided to use a mix with proportions of 1:2.5:3.5 with a water/cement ratio of 0.65.

This mix was designed to produce concrete having a target mean strength of 38 N/mm^2. The concrete mix was specified in terms of weight of the constituents. The batch weights for the mix proportions are given in Table 4.1.

Mix	Batch (m^3)	Cement (kg)	Sand (Kg)	Coarse aggregate (Kg)	Water (Kg)
1:2.5:3.5 w/c=0.65	0.00871	2.800	7.00	9.800	1.82

Table 4.1 Mix proportions

Each batch of concrete was sufficient to make ten 50 x 200 mm cylinders and three 100 x 100 mm cubes.

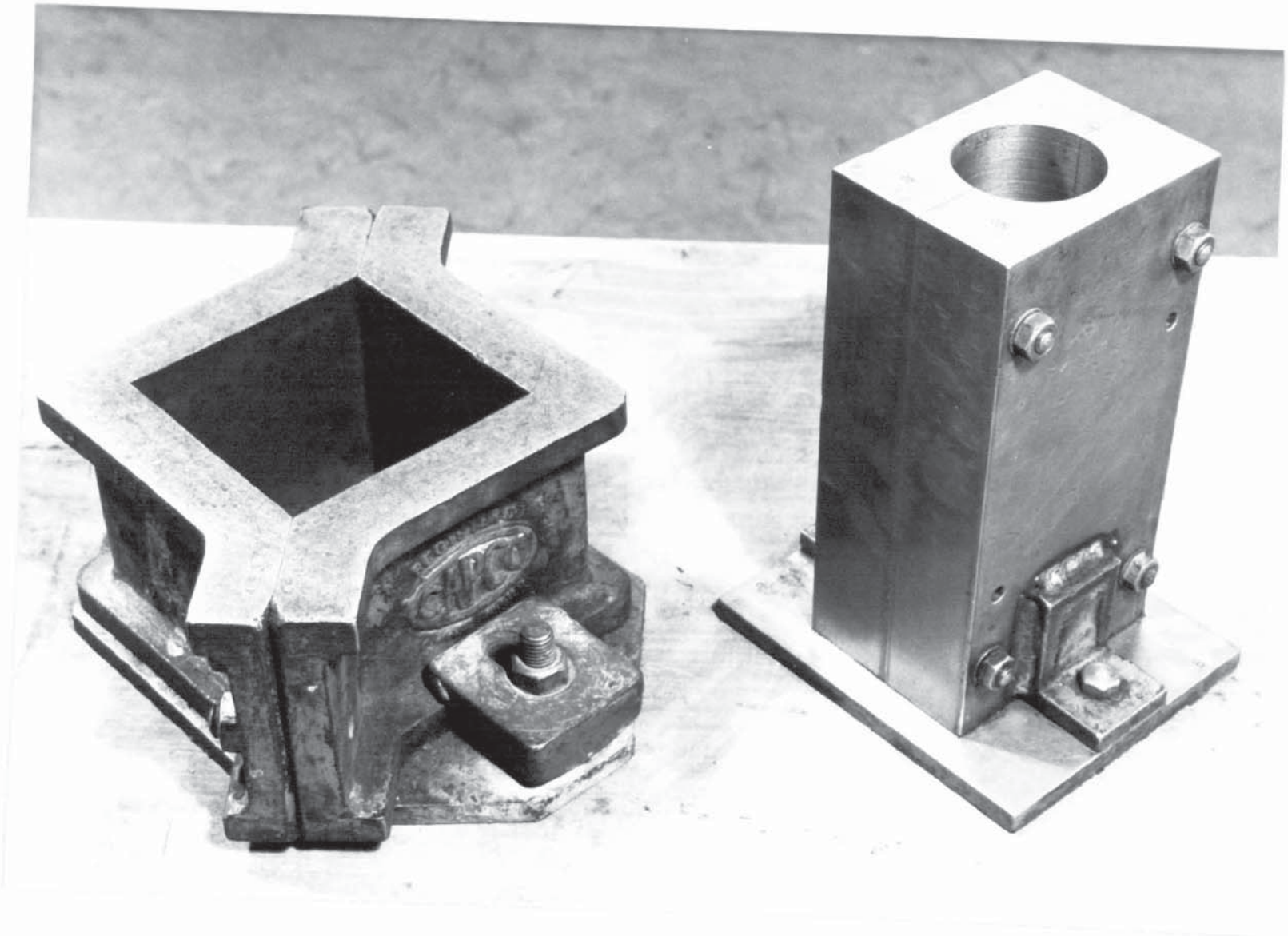

PLATE 4.2 CUBE AND CYLINDER MOULDS

4.4 CASTING METHOD :

The concrete was manufactured in a medium rotating mixer in small batches which have been given in Table 4.1.

The cylindrical specimens and the control cubes were cast in steel moulds and adequately compacted using a vibrating Table constructed by Triton Ltd.

4.5 CURING CONDITIONS AND CUBE STRENGTH :

All specimens were stored for twenty four hours at room temperature in the concrete laboratory. After being demoulded the specimens were cured in water at 19.5 + Ø.5 deg. C. The cubes were similarly cured until testing at twenty eight days as prescribed by BS 1881. The cylindrical specimens continued to mature under water until needed.

Water curing was used to ensure the full hydration of the cement and to remove age effects from the testing of the concrete as reported by Maréchal (197Ø). The cylindrical specimens were cured for a minimum of sixteen months.

Cubes were crushed in a grade A testing machine in accordance with BS 1881: Part 4: 197Ø. The results of the cube strength are shown in Table 4.2.

1Ø8 cubes of the same concrete were crushed corresponding to thirty six mixes cast.

Mix	Age (days)	No of Cubes (100 x 100mm)	Mean Strength (N/mm^2)	Standard Deviation (N/mm^2)	Coefficient of Variation (%)	Characteristic strength (N/mm^2)	Testing Machine
1:2.5:3.5 w/c = 0.65	28	108	40.1	2.20	5.5	36.5	300 Tons Avery-Denison (GRADE A)

Table 4.2 Crushing Strength

Table 4.3 summarises the results for the 100 cubes made from concrete mix (1:2.5:3.5, W/C = 0.65). The mean strength is 40.1 N/mm^2, the standard deviation 2.20 N/mm^2 and the coefficient of variation is 5.5%.

These values are plotted as shown in Fig. 4.1. It can be seen from the curve that a good representation of the normal distribution is obtained similar to that reported by Billig (1963) and Neville (1981). The mean strength corresponds to the centre line of the curve as shown.

The low value of the standard deviation indicates that a good control over the mix proportions and the water/cement ratio was exercised.

Range of strength (N/mm^2)	Number of Cubes	% of Cubes
32.4 - 34.5	3	2.78
34.6 - 36.7	4	3.70
36.8 - 38.9	26	24.07
39.0 - 41.1	45	41.67
41.2 - 43.3	21	19.44
43.3 - 45.3	9	8.33
	100	100

Table 4.3 Cube Strength Results

(Statistical Survey)

4.6 SPECIMEN PREPARATION :

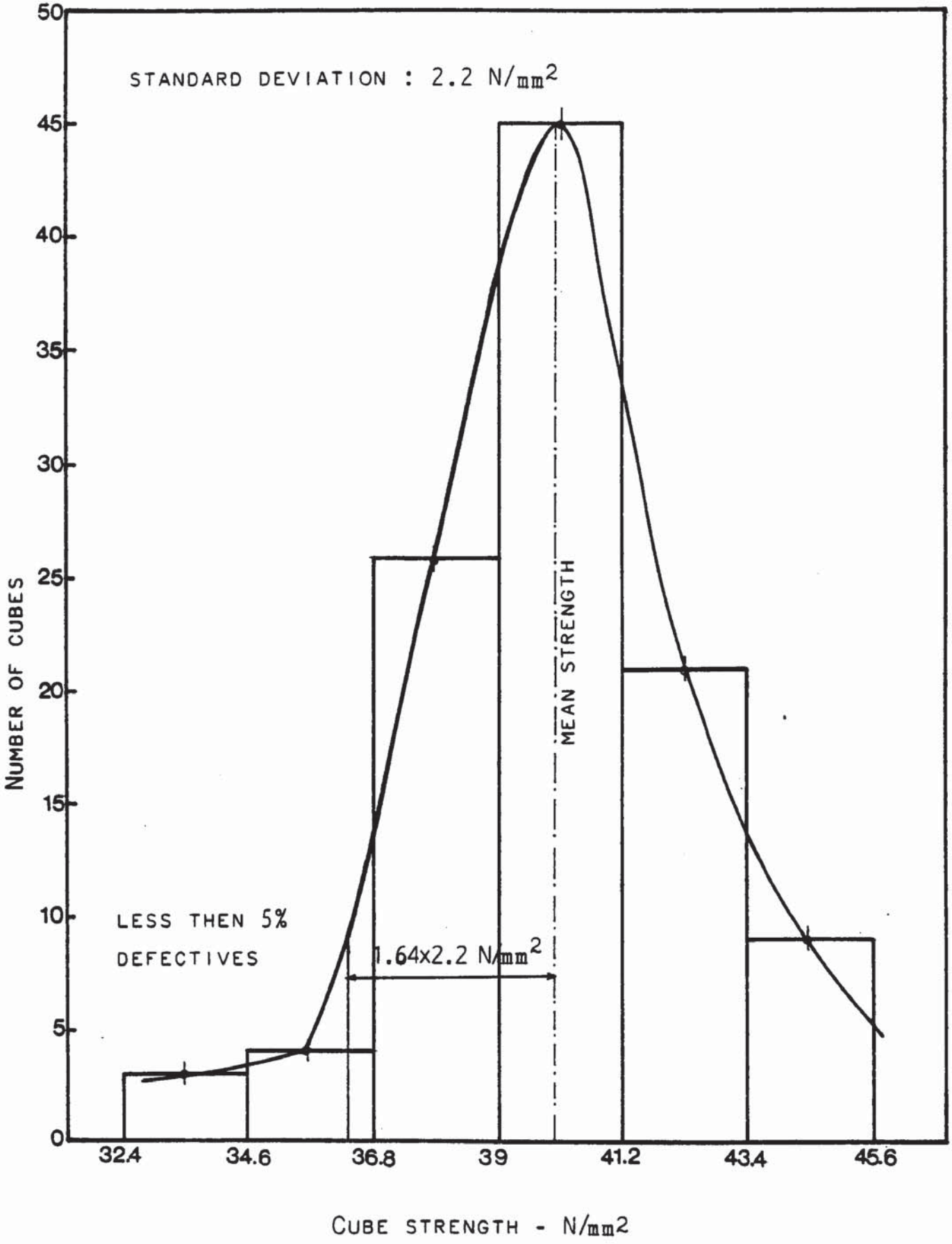

FIG. 4.1 DISTRIBUTION OF CONCRETE STRENGTH RESULTS.

The preparation of the cylindrical specimens consisted of two procedures :- cutting and grinding.

The concrete specimens when demoulded were approximately 200 mm in length and the required length of the test specimens was 150 mm. Therefore the specimens were cut down to the requisite length using a 'Clipper' saw. After cutting, the top end surface obtained was not truly plane as required for testing. It was therefore necessary to overcome the effect of the uneven end surface of the specimens. This was accomplished by using grinding techniques. Plate 4.3 shows a specimen at is original length and a finished specimen after being cut and ground.

A first batch of 40 specimens were ground flat, with the aid of a steel jig, by the author using a grinding machine of the Department of Geology. This proved slow and in order to accelerate the rate of specimen preparation, it was decided to use for the remainder another grinding machine. A second steel jig was made for this purpose, capable of holding ten specimens normal to the wheel. A general view of the jig can be seen in Plate 4.4.

To date 200 specimens have been ground using this method satisfactorily.

PLATE 4.3 SPECIMEN BEFORE AND AFTER PREPARATION

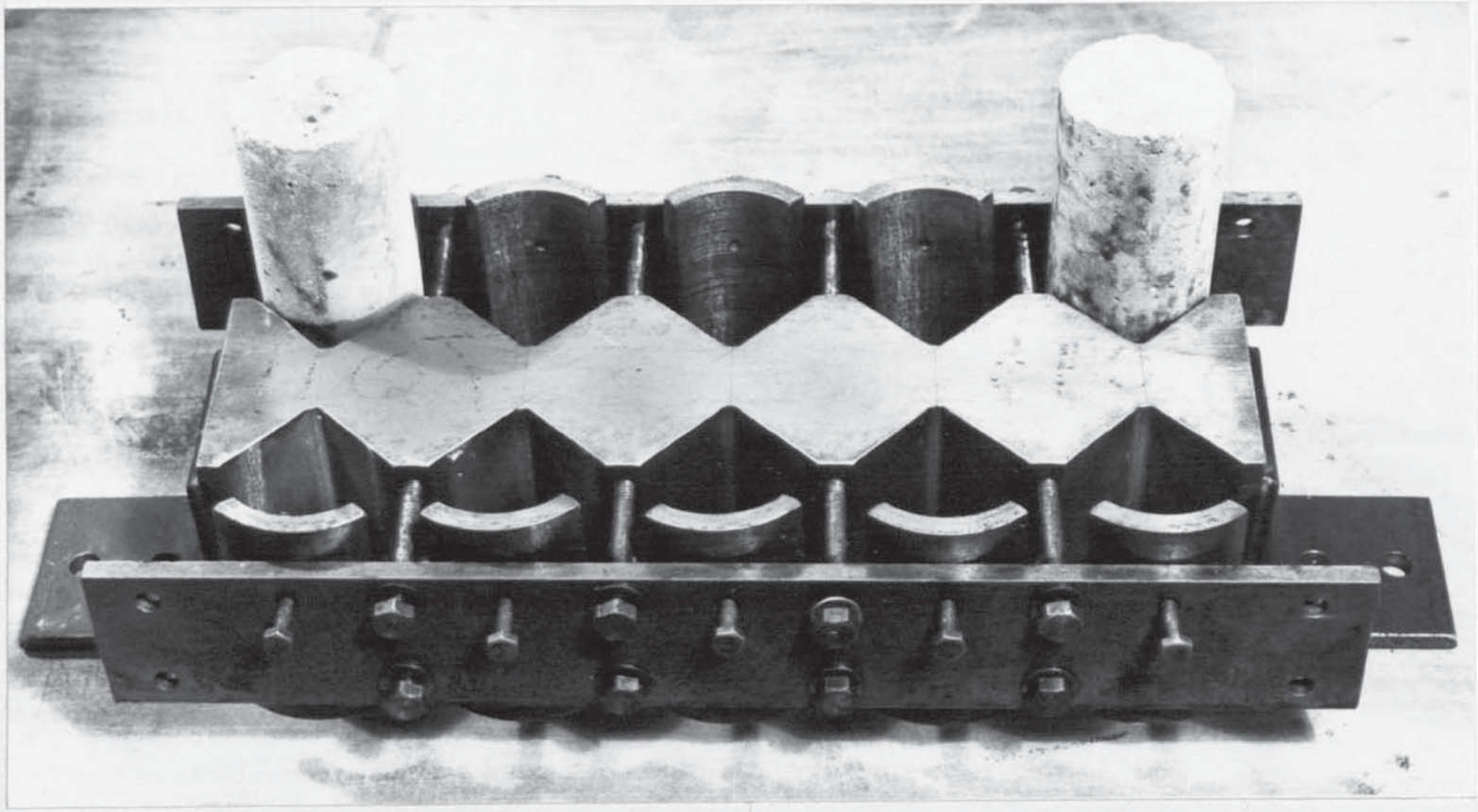

PLATE 4.4 GENERAL VIEW OF THE JIG

CHAPTER 5

COMPUTER CONTROL & LOGGING SYSTEM

5.1 INTRODUCTION :

This chapter deals with the overall control of the test rig which is achieved by using a logger/computer system.

The advantage of data logging equipment is that a large number of channels can be monitored continuously and economically. With such a system a high scanning speed of the channels is usual and high accuracy measurements of the analogue output signals are obtained and thus the stress, strain and temperature can be found to a known degree of accuracy. Data loggers are built to provide the user with a wide choice of facilities for monitoring, processing and controlling.

After outlining the need of a data logger for the purpose of the work, a description of the system used is given. The computer program and subprograms including the supplied standard subroutines are also presented in this chapter.

5.2 PURPOSE AND SPECIFICATIONS OF THE DATA LOGGER :

For the different tests envisaged in the experimental investigation, a data logger is needed to monitor the several readings from the channels allocated to the measuring devices which produce outputs in the form of voltage or currents. The other purpose of the data logging equipment is to provide the overall control of the testing apparatus during the whole period of test, enabling the load

to be held constant when conducting transient tests which form a part of the testing programme described in the next chapter.

The main specifications of the computer system consist of the ability to read the different devices on a defined time base, a control application and data storage/retrieval facilities. These outlined details are developed and examined separately.

5.2.1 Measuring devices :

Typical measurements which have to be made include the specimen deformation, the stress on the specimen and the temperature developed in the furnace and in the specimen. These quantities are measured using three major devices connected to the data logger, and these are

a) load cell

b) transducers and

c) thermocouples.

a) The load cell, consisting of a dynamometer on which strain gauges are mounted on a full arm bridge, allows the stress on the specimen as produced by the applied load (P), to be calculated by introducing the simplest form of direct stress, defined as :

$$\text{stress} = P/A_s \qquad (5\text{-}1)$$

where A_s is the area of the cross-section of the specimen. The signal produced by the load cell is known as analogue signal and is fed to the computer in its original form and then by means of conversion

circuitry implemented in the system, the voltages (or currents) are changed to digital form.

b) The specimen deformations at high temperatures are measured by the linear displacement transducers. The LVDTs, operating at a full scale range of Ø - ± 1Ø v, produce electrical output signals which are proportional to displacement. The calibration of the transducers and some other elements are discussed later in this chapter. Three transducers are used to monitor the specimen deformation. However the actual deformation is obtained by considering only the average reading of the three LVDT's, giving therefore :

$$\text{specimen deformation} = \frac{\text{mean displacement}}{\text{original specimen length}} \qquad (5\text{-}2)$$

Similarly the analogue signals are converted to digital form and by a simple program, the displacement can be obtained in mm.

c) The temperature in the furnace and in the specimen is measured by a series of Chromel/Alumel thermocouples which generate an e.m.f. The induced voltage signals recorded by computer are converted to digital form and through an appropriate software, the temperature in degrees centigrade is determined.

These three measuring devices are connected to the logging system via input channels and are monitored continuously for any period of time.

5.2.2 Control facility :

The entire testing equipment is controlled by the data logger by means of servo-loops. As mentioned earlier, this control is necessary so that the load can be maintained constant when creep and transient tests are carried out, allowing therefore accurate measurements to be recorded.

The control and the interconnections of the elements are illustrated in Fig. 5.1. The block diagram indicates how the whole system operates during a test and this can be explained as follows :-

The output from the transducers is fed to the data logger through an extensometer amplifier, whereas the dc output from the load cell is routed to the system through its allocated channel. The (Ni-Cr)/(Ni-Al) thermocouples with a dc output of 25 ^{o}C/mV are connected to the computer through the reserved channels. The furnace temperature is however controlled by a Eurotherm temperature controller.

5.2.3 Time base and specimen specification :

All the readings are monitored by the data logger on an interval basis by using a time variable. it is more convenient to set up a time base than choosing a stress or a strain increment in tests involving stress and displacement measurements. The time base which is a flexible dimension, enables the computer program to be used in all cases. When conducting creep tests, the time base is in fact the actual time at which the readings are taken.

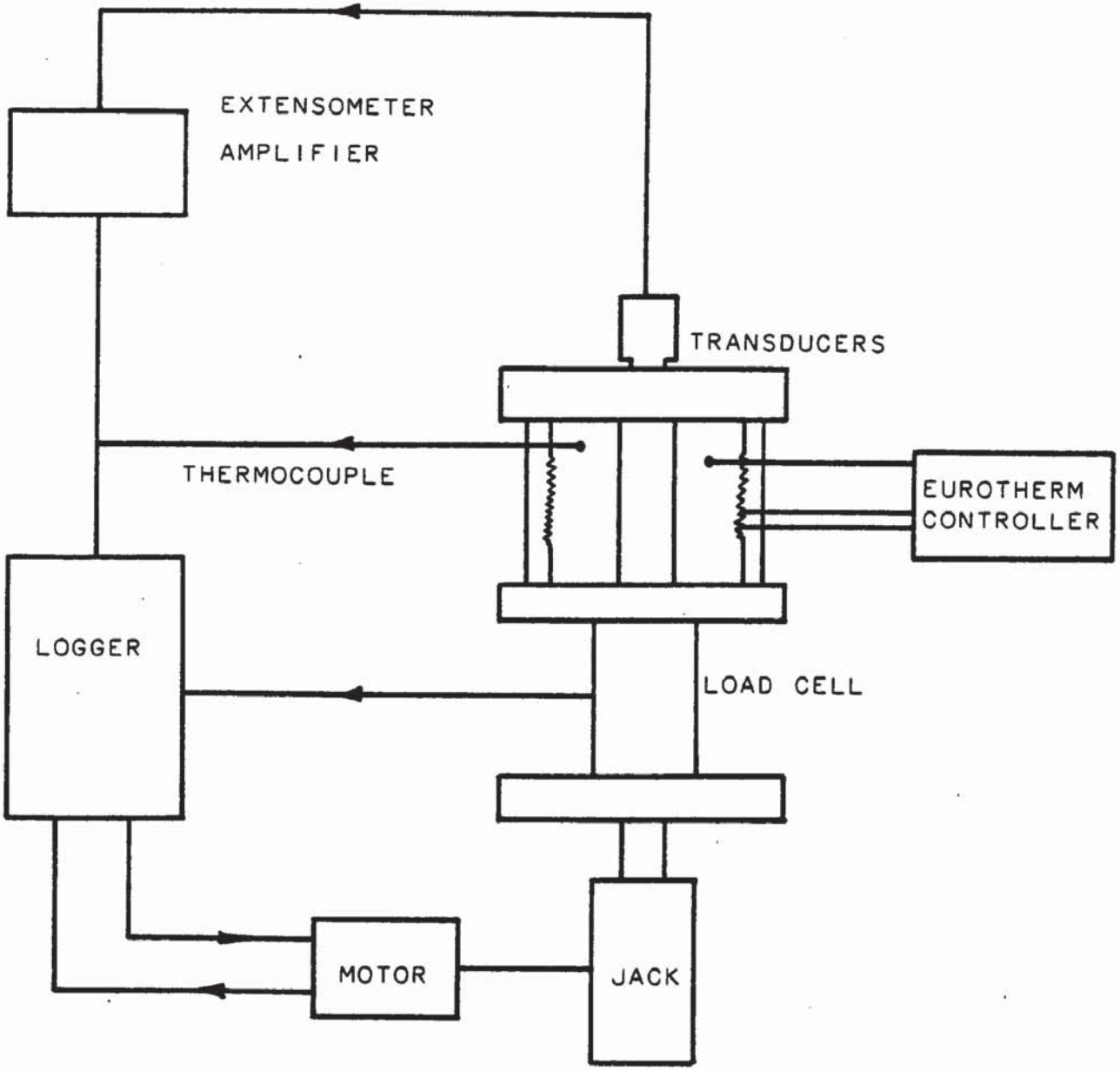

FIG. 5.1 BLOCK DIAGRAM OF THE TESTING EQUIPMENT.

Having introduced the time base, the test specifications are now examined together with the different parameters required from each of the tests.

When performing the proving tests of the rig, the following readings are continuously logged :

1) platen load : measured from the strain gauges on the duralumin specimen.

2) applied load : given by the load cell.

3) specimen displacement : measured from the transducers and the strain gauges.

The measurements are monitored using a time base (t).

In the preliminary test, the thermal gradient across a specimen is determined by measuring the temperatures from the thermocouples at the different locations on a time base (t), defined in the computer program.

From the free thermal expansion test, the following parameters are requied :- strain and temperature
which are measured from displacement transducers and thermocouples rspectively. The readings are monitored by the data logger on a time base (t).

The restrained tests consist of heating a specimen to failure under a constant stress ($\dot{\sigma} = 0$). The readings to be monitored by the computer are that of the strains given by the transducers and the temperature as measured by the thermocouples. During the whole test, the stress is maintained constant by the logger system which

continuously monitors the measurements on a regular basis by using a time variable.

The stress/strain curves are determined by stressing or straining a specimen to failure at a constant temperature ($\dot{T} = 0$). The parameters required from these tests are :

1) strain : measured from transducers.

2) stress ($\sigma = P/A_s$) : measured by the load cell.

The measuring devices are connected to the data logger which records on a regular time base all the corresponding readings.

The advantage in using the data logging system for conducting the creep tests is that the load as measured from the load cell is automatically maintained constant ($\dot{\sigma} = 0$) for the whole duration of test. The temperature is also kept constant ($\dot{T} = 0$) using the separate temperature control unit. The parameters needed from the tests are the strain, measured from the transducers and the time (t) given by the clock incorporated in the computer.

The logger/computer system with the appropriate software provides all the facilities for conducting accurately the different tests specified in this section.

5.2.4 Calibration and data storage/retrieval :

All the measuring devices produce voltage (or current) outputs. It is therefore necessary to calibrate the instruments in order to

allow the computer to convert the electric signals to the respective quantities such as load in (N), displacement in (mm) and temperature in (^{o}C). The calibration of the transducers produces a deformation/voltage curve. When the load cell and the duralumin specimen are calibrated in a grade A Denison machine, a load/voltage curve will result. The calibration test is carried out as follows :

At each increment of the load, the voltage signals produced from the strain gauges mounted on the load cell and the duralumin specimen are monitored by the data logger.

The logger/computer system provides a facility for data storage and data retrieval. When a test is being conducted, the data are safely stored in a file on a disc. However the data may be retrieved and presented graphically by incorporating a useful subroutine in the program available to operate the system.

All the voltage signals produced from the measuring devices are fed to the computer via the different input channels and these are :

Load cell : the strain gauge input connection is that of a full arm bridge with autobalance.

Duralumin specimen : the strain gauge input connection is that of a half arm bridge with autobalance.

Transducers : provide a dc output and operate on a full scale range Ø - $\pm$ 1Ø v. The input channel is via an extensometer amplifier.

Thermocouples : four Chromel/Alumel thermocoules connected to the logging system through the allocated input channels. They operate within a range of 0 - 39.35 mV corresponding to 0 - 950 ^{o}C.

The output signal is the last specification to be dealt with. The output to the motor is provided by an output interface board incorporated in the data logging system. The current (or voltage) output drive signals (+4 — + 20 milliamps) are directed to the relays implemented on the motor circuit. This allows the full control of the loading condition to be accomplished.

5.3 DATA LOGGER SYSTEM DESCRIPTION :

The data logging hardware is a Compulog System Four manufactured by Intercole Systems Limited (I.S.L). The system is described as a computer controlled data acquisition and control system which provides facilities for processing and evaluation of analogue and digital signals and data storage/retrieval. The different modules and sub-assemblies forming the 450 channel Compulog System are fully described in the instruction manuals provided by Intercole Systems Limited (1978). In order to have a good picture of the equipment, the system configuration is illustated in Fig. 5.2. A list of the modules and

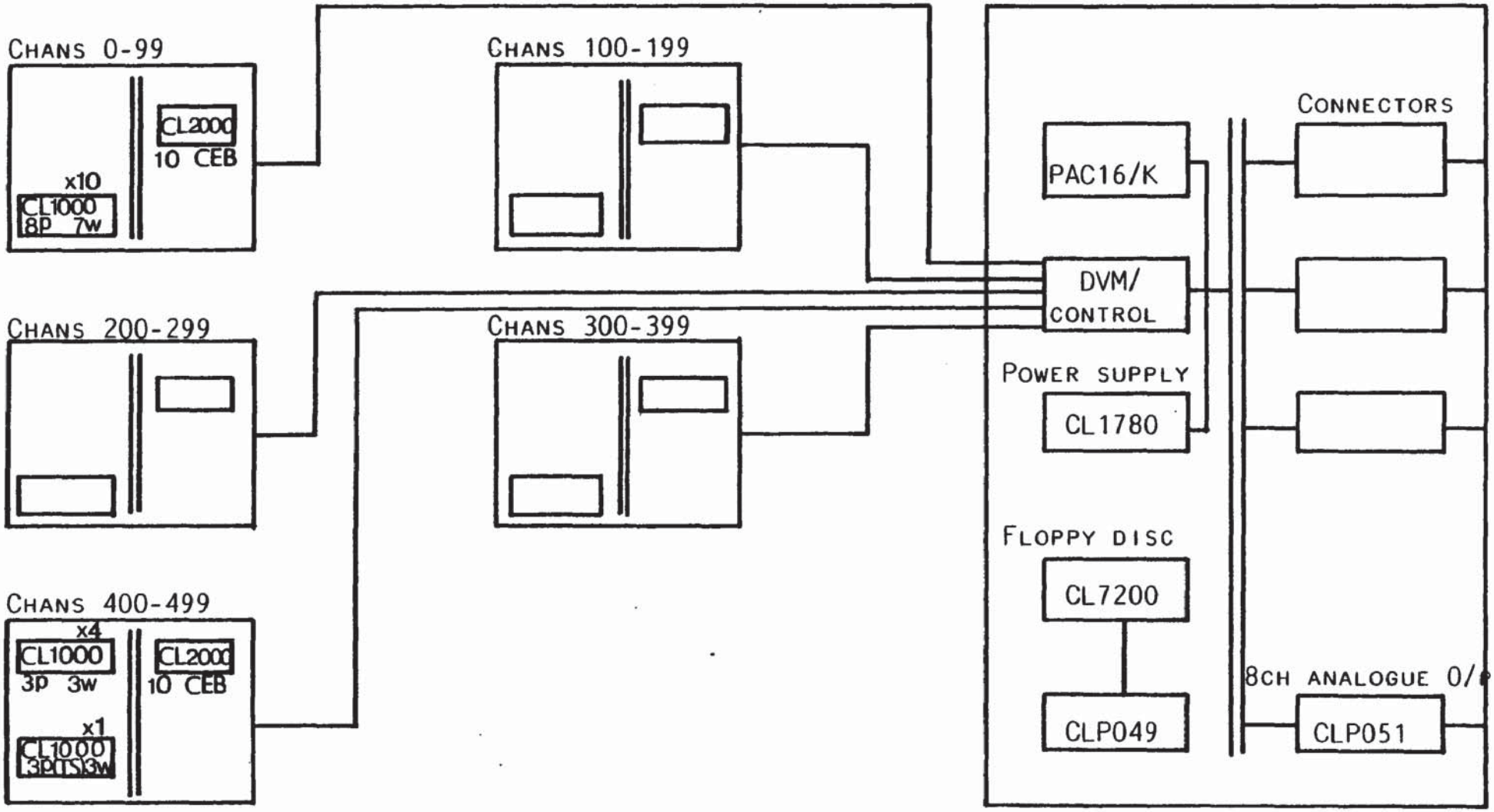

FIG. 5.2 SYSTEM CONFIGURATION.

assemblies is given in Table 5.1, to help understand the function of each element of the system.

The data logger includes a microcomputer (PAC 16/K) and a dual drive floppy disc system which is a high speed device enabling programming and data storage. The floppy disc system (CL7200) is connected to the computer by a single interface/controller board. The PAC 16/K is a 16 bit microcomputer with a 32K memory. This computer is used for supervising the data acquisition and control modules and analysing the data. Two high level languages can be used to generate the required software : BASIC and FORTRAN. With the latter faster program execution is obtained. Based on these two languages, software operating systems have been developed by Intercole Systems Limited. The options available at ASTON University are two disc operating systems :-

FODOS : FORTRAN disc operating system.

BASEDAC : standard BASIC disc system.

These two disc systems have been designed in order to provide simplicity and the amount of sophistication, speed and control required.

The function of the CL1780 power supply module is to provide independent dc power sources for the microcomputer (PAC 16/K). The system is protected against any power failure by the use of a built-in battery supply for a period of 15 hours, thus enabling the execution of the program to be completed. The batteries are automatically charged when the mains power is connected.

CABINET	MODULE SUB-ASSEMBLY	INTERFACE BOARD	REMARKS
MAIN	PAC16 K Digital Computer		For Contents see Manuals
	CL1780 Power Supply Module CL1790 Battery		AC DC supplies for PAC16 K
	Rear Connector Panel (Signal)	CLP051	Qty. 1 op for 8 channel Analogue Output
	Remote Cabinet Connector Panel		Qty. 5 input for Remote Cabinet
REMOTE 1	CL1000 Analogue Scanner Module 8 pole 7w CL2000 Analogue Data Amplifier & Autobal.		Qty. 10 for Chans 0 - 99 Qty. 1 for Chans 0 - 99
REMOTE 2	CL1000 Analogue Scanner Module 8 pole 7w CL2000 Analogue Data Amplifier & Autobal.		Qty. 10 for Chans 100-199 Qty. 1 for Chans 100-199
REMOTE 3	CL1000 Analogue Scanner Module 8 pole 7w CL2000 Analogue Data Amplifier & Autobal.		Qty. 10 for Chans 200-299 Qty. 1 for Chans 200-299
REMOTE 4	CL1000 Analoge Scanner Module 8 pole 7w CL2000 Analogue Data Amplifier & Autobal.		Qty. 10 for Chans 300-399 Qty. 1 for Chans 300-399
REMOTE 5	CL1000 Analogue Scanner Module 3 pole 7w CL2000 Analogue PRT (TS) Scanner Module 3 pole 3w CL2000 Analogue Data Amplifier & Autobal.		Qty. 4 for Chans 400-419, 430-449 Qty. 1 for Chans 420-429 Qty. 1 for Chans 400-449

TABLE 5.1 CABINETS AND MODULES

The other main element of the data logger is the measuring system which measures stress, strain, displacement, presure, temperature on each channel with high precision. The analogue measurement system consists of a digital voltmeter (DVM) incorporated in the microcomputer. The DVM comprises an analogue to digital converter (ADC), scanner modules and amplifiers. The input signal is first scanned via the remote scanner (CL1000) then is amplified through the CL2000 amplifier module before being applied directly to the analogue digital converter (ADC). Through these series of operations, the measurement signal is thus converted to a digital form by the ADC, and the conversion period is 1.5 milliseconds. The operation is relatively fast as a result of using the digital microcomputer which provides the speed and processing power.

The input signals generated by external transducers such as displacement transducers and strain gauges, are fed to the data logging system through the allocated channels which form the input section. in the Compulog System Four the input section is divided into three sectors according to the respective connected transducers. These subdivisions are the followings :

400	voltage/strain & autobalance	: 8 pole	7 ways	chs.	0-319
40	voltage/thermocouple	: 3 pole	3 ways	chs.	400-419
				& chs.	430-449
10	voltage/thermocouple	: 3 pole	3 ways	chs.	420-429

By using the autobalance facility, any configuration of the strain gauges is automatically balanced (i.e. the bridge is electrically balanced to zero).

Compulog System Four provides all the facilities required for conducting any series of tests necessary for the completion of this research. Software programs have been developed to operate the system and are dealt with in the next sections.

5.4 PRESENTATION OF THE COMPUTER PROGRAM :

5.4.1. Main Program :

Having briefly described the data logging system, the programs written for manipulating the equipment are now examined.

The computer program comprises a main progam (FRIGCONT) and subroutines for execution. The subprograms consist of standard and developed routines and are individually presented in the next paragraph.

The programming language used to write the software is FORDAC language (FORTRAN DATA Acquisition Compiler) designed especially for application to Compulog data logging and control systems. The language is in compliance with the standard FORTRAN. A typical FORDAC manual has been provided by Intercole Systems Limited (1978). All FORDAC statements are used in conjunction with FODOS Operating System.

The main task of the program "FRIGCONT" is to enable the control of the testing equipment and monitoring the results with the facility of storage on disc. It should also provide the capability of

maintaining the stress or strain during creep and transient tests. The sequence of procedures in "FRIGCONT" are clearly displayed in the flowchart of Fig. 5.3. A full listing of the program and the appropriate subroutines is however given in Appendix Seven. It can be seen that the main program can be divided into four sections, and each section has a specific function.

The first section consists of inputing the necessary information and the different constants. The date, the identifier code and the data file number are initially set in order to avoid any confusion in the final output of the results when needed. The access to the data file is gained using the subroutine CALL KOPEN. The next step is then to specify the constant fixing the time, time increments, specimen dimension (length) and the load required. It should be noted that, in this section, the program is protected from corruption if there is any mains failure. This protection is provided by CALL PFAIL subroutine. Having defined the duration of the test, the different time zones to be specified are shown in the following diagram of Fig. 5.4 :

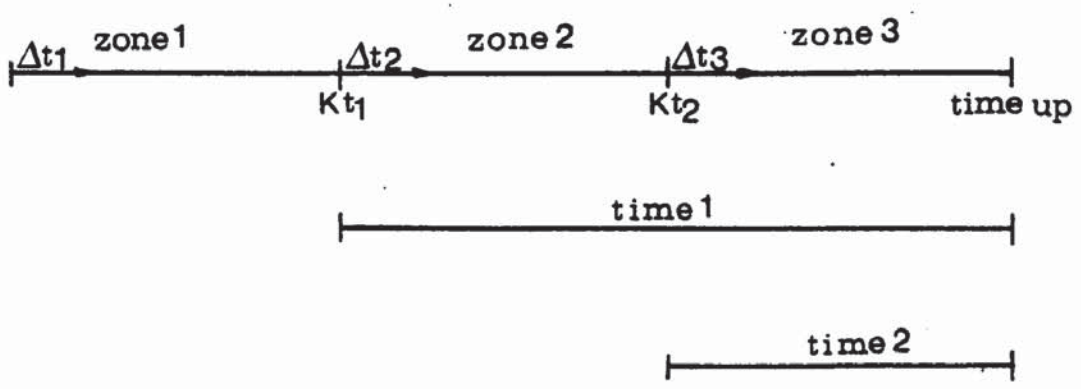

Fig. 5.4 : Time specifications

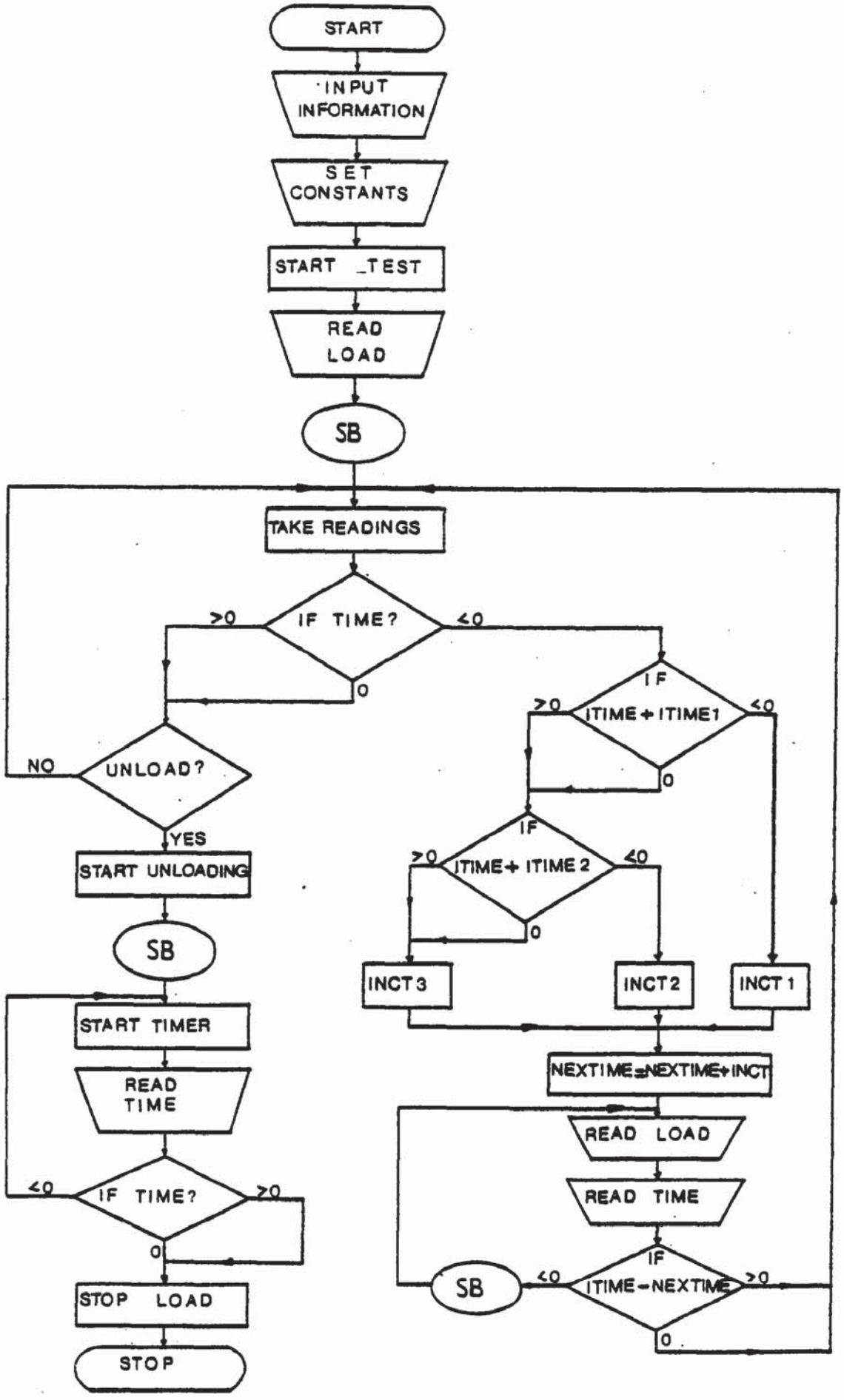

FIG. 5.3 FLOWCHART FOR "FRIGCONT" PROGRAM

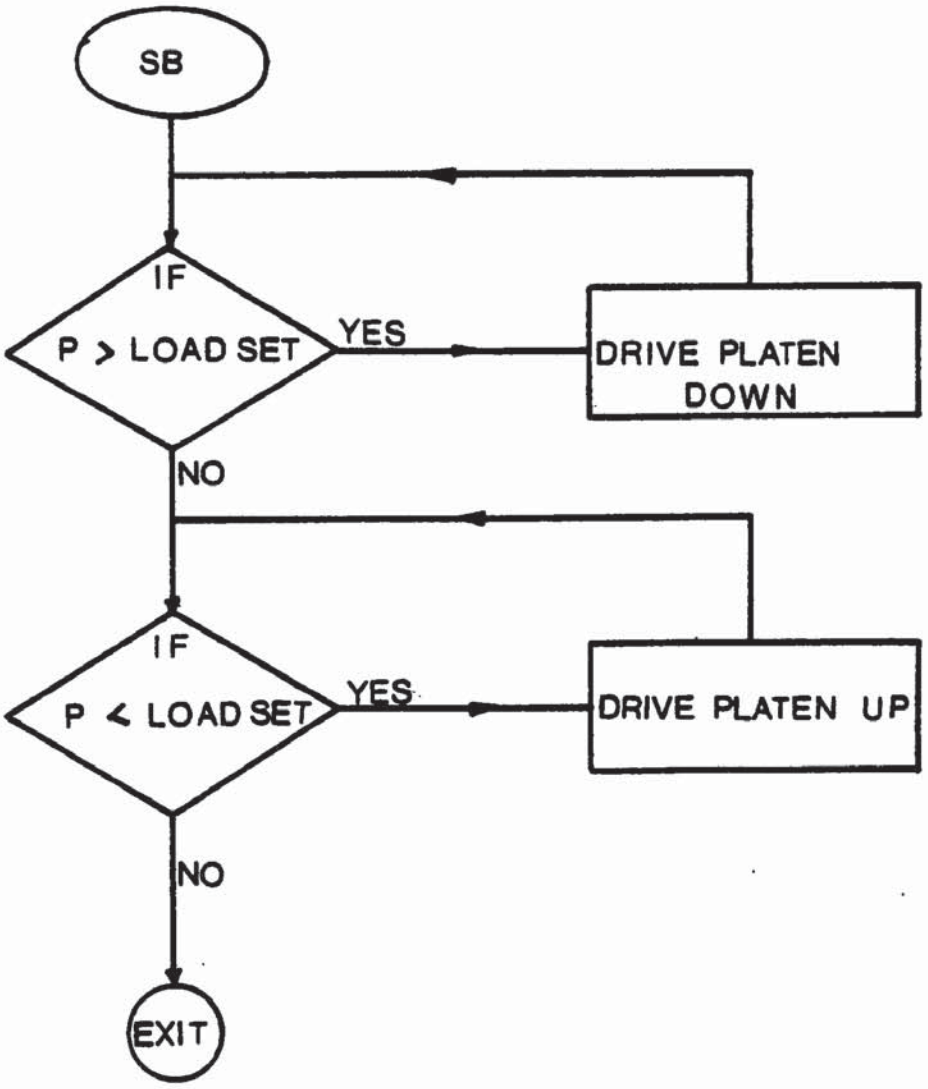

FIG. 5.5 FLOW CHART FOR THE SUBROUTINES ADDLD & REDLD RUN IN CONJUNCTION.

PAGE MISSING IN ORIGINAL

where Δt is the time increment and Kt the time for the zone considered. Once the constants are set, all the transducers including the thermocouples are checked in this section to ensure that they are reading correctly.

The second section deals with the start of the test. The computer is instructed to operate the equipment. The digital clock is first set using the subroutine CALL WCLOCK, and at the same time the motor drive is switched on by calling up the subroutine ADDLD, to add the load to the specimen. In fact, at this stage, the platens are not in contact with the specimen. However the motor will be functioning and the centre crosshead moving upwards until the contact is established and the count down starts subsequently through the subroutine CALL WSCANT. The load applied to the specimen is read and calculated by using the subprogram RLOAD. The full control of the test rig is attained by the computer which is capable of either increasing or maintaining the load constant.

The third section has been developed for recording and storing on disc the results while the test is being performed. The main calculations for time, stress, strain and temperature are also effectuated in this part of the program. The execution of these calculations has been possible only by using the subroutines RLOAD, DEFLTN and TEMP. The actual values of stress, strain and temperature are stored on a data file already opened for this purpose. A tabular form of the experimental results can be output on the Visual Display Unit (VDU).

The time and the load are countinuously checked. When the test is terminated, the motor is automatically stopped via STPLD subroutine whose function is to stop loading whenever called. The unloading is proceeded by REDLD routine which reduces the load by reversing the motor.

The last section concerns the detection of the errors during the program execution using the FORTRAN function KDS. When a data storage error has occured, a value different from zero is displayed on the VDU. this value indicates the type and the cause of the error. The details and the meanings of the errors are set out in the FODOS manuals (1978).

The output of the result can be obtained in the form of graphs. The recorded data are retrieved and then plotted by calling up the subroutine GRAPHS, and this completes the execution of the program.

5.4.2 Supplied and written subroutines :

The series of subroutines contained in the main program are either provided by Intercole System Limited for Compulog users or created using the FORDAC manual.

The eleven standard subroutines used can be listed as follows :

1) CALL RECUVA : is a statement enabling a return back to the program after a fatal error has occured. This subroutine can be called in the program as often as necessary.

2) CALL PFAIL : provides the computer with a protection against any power failure.

3) CALL KOPEN : a data file is opened via this statement.

4) CALL WCLOSE : this subroutine closes a file.

5) CALL WCLOCK : this statement presets the digital clock in days, hours, minutes and seconds.

6) CALL WSCANT : resets scan interval timer in seconds, in other words, it writes the interval time.

7) CALL RSCANT : this statement examines the scan timer or reads the interval time.

8) CALL JSENSE : this function checks the state of the sense switch.

9) CALL CHAN : this subroutine selects the channel and signal conditioning, including the conversion mode of the DVM and the data amplifier input configuration.

10) CALL DVM : this statement allows the analogue voltage input to be converted to a digital form and transfered as an integer to the program.

11) CALL ANOUT : this subroutine selects the device address, channel and output data. It is used for setting up output on an 8 channel CLP051 Analogue Interface.

The CALL statements have been listed with a brief description to allow the understanding of the logical operations used for the execution of the program. However more detailed definitions of these standard subroutines are given in the FORDAC manual (1978). It can be seen that these subroutines are very useful to develop the required communication between the computer and any particular unit in the data logging system.

The other set of subprogams designed as a part of the main program includes seven subroutines with specified roles.

The motor is switched on via an 8 channel analogue output interface board generating 8 analogue signals which are current outputs with a range of +4 to +20 milliamps. The following subroutines, ADDLD, REDLD and STLD have been created and use the facility provided by the CLP051 interface board which is used to control an external equipment through adopted relays. The major operations of the module (and the relays) include the starting and stopping of the motor. The role of each subprogram is now examined.

ADDLD : its main function is to switch the motor on and start the loading or just to add the load to the specimen.

REDLD : the motor can be reversed wether it is on or off, allowing therefore the unloading by gradually reducing the load.

These two routines are well described in the flowchart of Fig. 5.5

STPLD : the motor is stopped via this statement.

The combination of the three subroutines provides a full control of the loading section.

The subroutines RLOAD and DEFLTN are developed to calculate the laod and the displacement respectively. The signals produced from either the load cell or the transducers are voltage outputs which are dealt with by the DVM. It is necessary to introduce a method of converting the DVM output to voltage measurement since the DVM readings are in bits. The DVM maximum reading is +32,767 bits, the full scale, however, is 30,000 bits.

There are 10 scales labeled 0 to 9 with a full scale readings of between 10 mV to 10.0 V. Each scale has a resolution of

$$1 \text{ bit} = \frac{\text{Full Scale}}{30{,}000} \text{ (volts)} \qquad (5\text{-}3)$$

The resolution value is given with 7 significant digits in the FORDAC reference manual (1978) and are used in the computer program to convert the DVM readings to voltage.

The voltage measurement (V) is therefore obtained by multiplying the DVM output in bits by the resolution value (Vr) for the scale used.

$$\text{therefore :} \qquad V = DVM \cdot Vr \qquad (5\text{-}4)$$

Complete details of the conversion of the DVM readings are given in the FORDAC reference manual (section 9-4).

Once the voltage measurements are completed the actual load or displacement is calculated by using the appropriate equation to convert the voltage values to N or mm respectively. The conversion

equations are obtained from the calibration of the load cell and the transducers.

Consequently, the load is estimated by :

$$P = m_1 \cdot V \qquad (5\text{-}5)$$

where p : is the load in N.

m_1 : is the gradient in N/V and

V : the voltage as obtained by Eq. 5.4.

Similarly the displacement is calculated by DEFLTN using the relation :

$$\Delta 1 = c - m_2 V \qquad (5\text{-}6)$$

where $\Delta 1$: is the displacement in mm.

m : is the gradient in mm/V.

c : constant in mm.

The subroutine RLOAD and DEFLTN require channel number to be specified in order to enable the calculations to be performed. The channels are selected by the statement CALL CHAN which contains some necessary information as given in the following example :

CALL CHAN (X1, X2, X3, X4)

where X1 : is the channel number

X2 : is the scale (for the load, scale Ø has been selected, and for the displacement scale 9 due to the operational range of the transducers (Ø - ± 1Ø V)).

X3 : is the conversion mode of the DVM (1, for both the load and the displacement).

X4 : is the input configuration of the data amplifier, or the normalising code (5, for the load and 4 for the displacement).

More information about the different variables is reported in the FORDAC manual.

The other important subroutine is TEMP which determines the temperature in degrees centigrade for Chromel/Alumel thermocouples. This subprogram is a modified version of the FORDAC thermocouple measurment program developed by Intercole Systems Limited.

The temperature measurments are monitored by thermocouples which produce voltage signals. However the measured temperature includes the "Cold-Junction" e.m.f generated at the input connections, which should be compensated when calculating the actual temperature. This e.m.f can be taken as the temperature of the terminal mounting strip (see FORDAC manual).

The output obtained from the DVM is a linear function of temperature (FORDAC manual) and expressed as follows :

$$\text{DVM output } (\mu V) = A2.T_1 + B2 \qquad (5\text{-}7)$$

where A2 : is the slope of the thermocouple - $\mu V/^{\circ}C$

B2 : a constant - μV

and

$$T_1 = \frac{\text{DVM } (\mu v) - B2}{A2} \ (^{\circ}C) \qquad (5\text{-}8)$$

is the temperature as read by the thermocouple. Hence, the temperature of the strip (T_s) for any scale used is :

$$T_s = \frac{(\text{DVM readings} \cdot Vr) - B2}{A2} \quad {}^{o}C \qquad (5\text{-}9)$$

Where Vr is the resolution for the scale 5 used. Therefore for scale 5 the resolution value is 16.667 μV/bit

Considering T_s and T_1, the actual temperature (T_2) can be calculated by subtracting the "Cold-Junction" e.m.f from the output of the thermocouples.

Therefore : $T_2 = T_1 - T_s$ (relative) (5-10)

with T_s (relative) $= mT_s + c$ (5-11)

where m is the gradient of the curve - mV/^{o}C and c a constant - mV, and are refered in the program "TEMP" as A(13) and A(12).

The temperature T_2 is linearised by Horners method. The coefficients (Ai) are that of the polynomial required to linearise the thermocouple with a temperature ranging from ambient to 950 ^{o}C. The linearisation is needed because the output voltages from the thermocouples have a non-linear relationship with temperature.

The last subprogram included in the main program is GRAPHS with the capability of plotting the recorded data just after the test has been completed. As many graphs as necessary can be plotted with their

respective titles and identification code, avoiding thus any wastage of time.

The program provides then the user with facilities to operate the testing machine, and allows long tests to be performed without the assistance of any operator.

However, during the proving tests it was noticed that on random scans of the input channels spurious results were noticed. Attempts were made to isolate these as arising from the measuring devices used, but these attempts had no effect. It thus seemed apparent that these spurious results arose either from instabilities on the mains supply or a hardware fault in the system. The former was removed by the fitting of a mains stabilizing unit but to no effect. It was found that although the system was capable of generating a signal to control the movement of the jack, it was found that no signal was reaching the unit adjacent to the rig (it should be pointed out that the data logger and the rig are in separate laboratories some 150-200 m apart). The likelihood of the presence of a hardware fault is increased by the fact that other researchers within the Department of Civil Engineering have had very similar problems. Thus due to the uncertainty of producing a complete set of incorrupted readings (especially over the long 5 hour duration of a creep test), it was decided that it could be safer and more reliable to log the readings by hand, and thus it has, unfortunately, not been completely possible to test all the options in the control program and validate its complete operation.

The next chapter deals with the presentation of the testing programme, including the preliminary test carried out to determine the thermal gradient across a specimen.

I wish to thank Dr. S. Robinson, formerly a research student in the Department of Civil Engineering & Construction for his advice on the development of the computer program presented in this thesis.

CHAPTER 6

DETAILS OF THE TEST PROGRAMME

6.1 INTRODUCTION :

The scope of the investigation is to obtain a reasonable model for the overall behaviour of concrete at elevated temperatures. The experimental results will provide a basis for understanding the transient effect of the behaviour of concrete when subjected to high temperatures. Only few investigators have attempted to examine the complete mechanical behaviour of concrete under transient conditions. Very important work has, however, been carried out by Thelandersson & Anderberg (1976). Their objective was to establish a mathematical model for the behaviour of concrete subjected to compressive stress under transient conditions.

To understand the behaviour of concrete structures at elevated temperatures, it is important to examine the effect of heating on the properties of concrete. Malhotra (1982) divided the material properties into four categories, ie. mechanical, physical, chemical and thermal. He also considered six ways in which the determination of the mechanical properties could be carried out, as shown in Fig. 6.1. These tests fall into two distinct groups : steady state and transient tests.

The first group will therefore contain the following tests :-

1. stress-strain tests : stress rate controlled
2. stress-strain tests : strain rate controlled
3. creep tests : constant load and constant temperature.
4. relaxation tests : the initial load is applied, then the specimen is heated to the test temperature. The instantaneous strain is recorded and

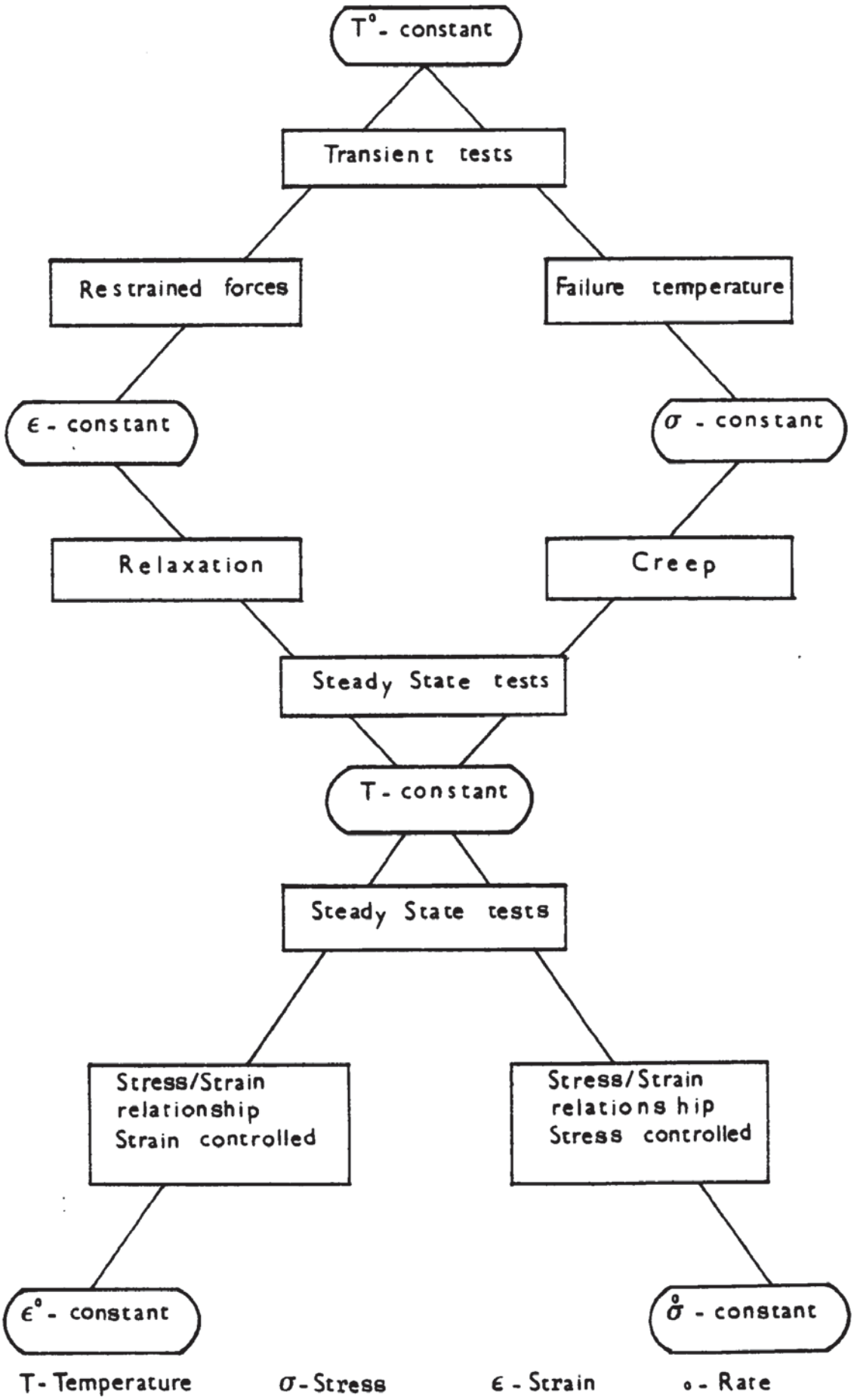

FIG. 6.1 DIFFERENT TESTING REGIMES FOR DETERMINING MECHANICAL PROPERTIES.

held constant by adjusting the load.

In the second group the following tests are considered :-

1. failure temperature tests : total strain is measured. Heating to failure under constant load
2. restraint forces : the load is applied. The initial strain is monitored and maintained constant during the the heating process until the load approaches zero.

Considering these methods of determining the mechanical properties of concrete described above, it was considered that the most relevant to producing adequate data to evaluate the response of concrete to elevated temperatures and loading could be covered by four test series as detailed in the next paragraphs.

The aim of the first two test series was to assess the stress-strain relationship of concrete at elevated temperatures for both specimens with and without a pre-load using the second steady state approach where the strain rate is controlled. The behaviour of restrained specimens was examined in the third series where the first system of transient tests was employed. Finally, creep tests were performed in the fourth series in accordance with the third approach to steady state testing.

The main test programme may thus be summarized as :-

series 1 : stress-strain behaviour of concrete at elevated temperatures (specimens heated with no load carried).

series 2 : stress-strain behaviour for "pre-loaded" specimens.

series 3 : restrained specimens (heating to failure under constant stress).

series 4 : time-dependence of concrete at elevated temperature and constant stress.

All of the test specimens were pre-dried for three days in an electric oven at 105 °C prior to the tests, in order to avoid explosive spalling of the specimen when heated at a high rate of heating. Thus no damage should be caused to the heating elements of the furnace by contact with small pieces of the specimen flying about.

Before conducting the main test programme, a preliminary test was performed to determine the thermal gradient across a specimen, so that the mean temperature within the section could be estimated.

6.2 THERMAL GRADIENT ACROSS A SPECIMEN :

To determine the transient temperature distribution in the specimen a test was conducted on a concrete specimen in which two thermocouples were cast, one in the centre and the other at a distance of 12.5 mm from the centre, and a third thermocouple was attached to its surface. The specimen temperatures thus measured at the three locations were recorded together with the furnace temperature during heating up to 750 °C and the subsequent cooling. The variation of the temperatures with time in both the furnace and the centre of the specimen are plotted in Fig. 6.2. Table 6.1 shows the temperatures monitored at the three points of the specimen together with the

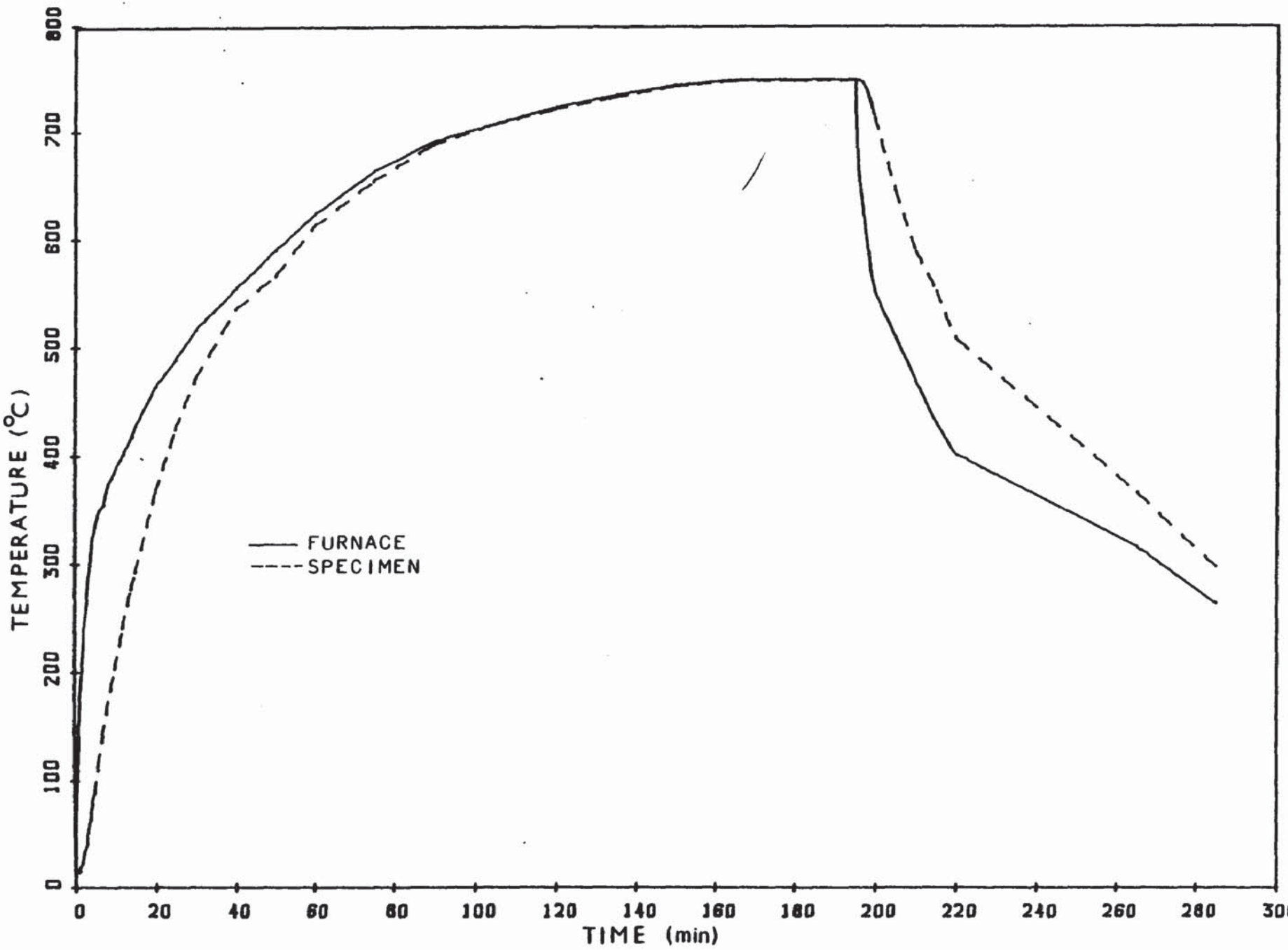

FIG. 6.2 TEMPERATURE VARIATION WITH TIME IN THE FURNACE AND THE CENTRE OF THE SPECIMEN

Time min	Furnace Temperature °C	Temperture Surface Specimen °C	Temperature Inside Specimen °C	Temperature Centre Specimen °C
0	14	14	14	14
0.30	68	41	15	14
1	120	49	19	15
1.30	170	69	26	18
2	210	88	35	23
2.30	237	109	47	31
3	263	126	60	40
3.30	283	139	74	51
4	305	156	88	63
4.30	323	166	102	75
5	335	177	116	88
6	351	207	143	114
7	355	225	169	140
8	372	245	192	162
9	381	265	215	185
10	388	283	236	203
12	402	313	275	241
14	418	346	312	277
15	428	362	329	293
20	465	420	400	367
25	490	468	453	425
30	518	505	495	472
40	555	551	549	536
50	591	590	588	567
60	624	624	623	613
75	664	663	662	655
90	692	692	691	689
105	709	708	709	708
120	724	722	724	722
135	736	734	734	734
150	745	744	744	744
165	750	748	748	749
180	750	748	748	749
195	750	748	748	749
196	665	696	740	749
197	631	669	719	746
198	600	652	702	739
199	570	634	685	727
200	551	622	669	713
205	510	573	606	645
210	470	531	559	589
215	430	499	524	552
220	400	471	494	507
265	315	325	330	365
285	262	285	289	296

Table 6-1 Temperature readings for the determination of the thermal gradient.

furnace temperature during heating, a 30 minute soaking period and the subsequent cooling period.

It can be seen from Table 6.1 that the temperature is varying from the heated surface to the centre of the specimen in a complex fashion. However this distribution may be assumed parabolic across the specimen during the early stages of heating, later this is not so as the temperatures are tending to equalize.

Thus the mean temperature may be obtained by calculating the shaded area of the diagram of Fig. 6.3.

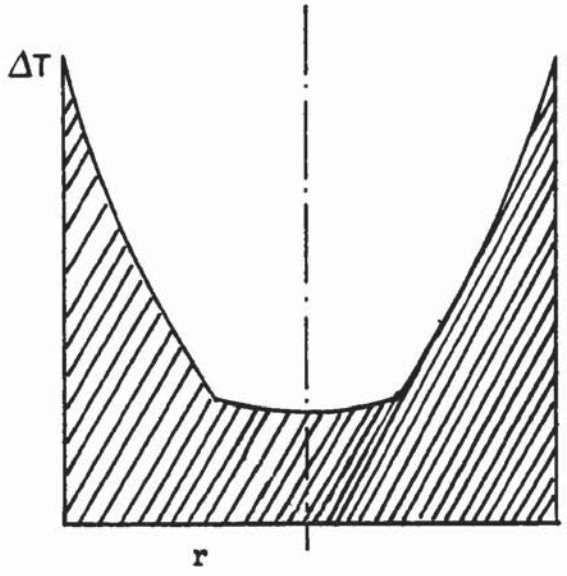

Figure 6.3 Temperature distribution across a specimen

The temperature difference ΔT in the specimen is related to the distance by the equation :

$$\Delta T = kr^2 \qquad (6.1)$$

where k is a constant and r the distance from the centre. Figure 6.4 shows the plot of the temperature differences against the position as obtained from Eq. 6.1.

Thus the specified specimen mean temperature is obtained by integration of Eq. 6.1.

$$\int_{T_c}^{T_m} dT = \int_{\emptyset}^{R} kr^2 \, dr \qquad (6.2)$$

Hence

$$T_m - T_c = k \frac{R^3}{3R} = k \frac{R^2}{3}$$

and finally

$$T_m = T_c + k \frac{R^2}{3} \qquad (6.3)$$

where T_c and T_m are the temperature in the centre and the mean specimen temperature respectively, and R is the radius of the specimen.

The results of the calculations of the mean temperature are set out in Table 6.2, where T_s refers to the temperature difference between the centre and the surface of the specimen, $T_{12.5}$ is the difference between the temperatures recorded at the centre and at 12.5 mm from the centre respectively, and T_{mean} is the mean specimen temperature whereas T_F represents the furnace temperature, and k is the constant derived from Eq. 6.1.

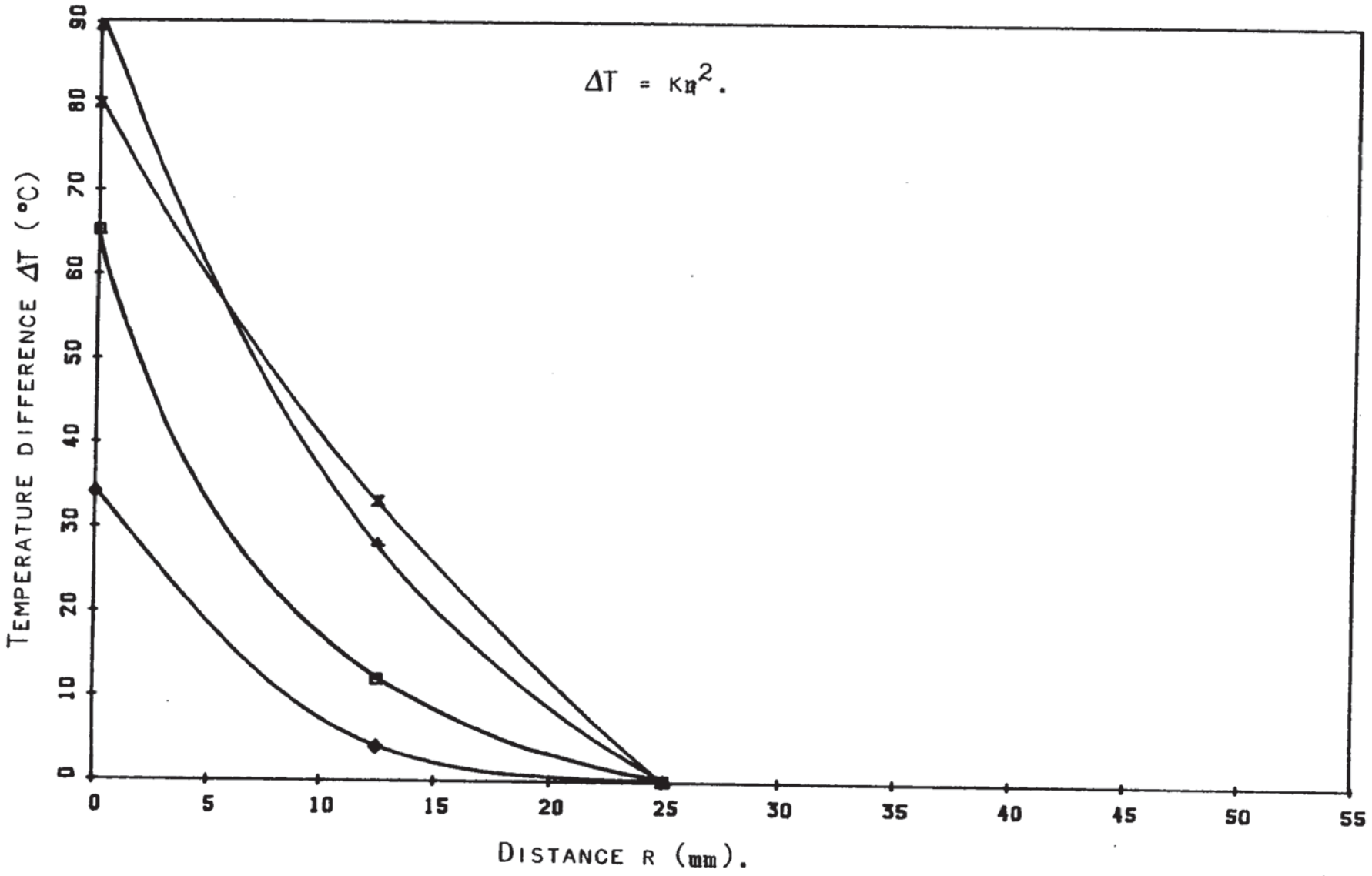

FIG. 6.4 TEMPERATURE VARIATION IN A CONCRETE SPECIMEN.

Time min	T_s °C	$T_{12.5}$ °C	T_{25} °C	K	T_{mean} °C	T_F °C
1	34	4	0	0.040	23	120
2	65	12	0	0.091	42	210
5	89	28	0	0.161	122	335
10	80	33	0	0.170	238	388
15	69	36	0	0.170	328	428
20	53	33	0	0.148	398	465
25	43	28	0	0.124	451	490
30	33	23	0	0.100	493	518
40	15	13	0	0.054	547	555
50	23	21	0	0.086	585	591
60	11	10	0	0.041	622	624
75	8	7	0	0.029	661	664

Table 6.2 Data for the determination of the mean specimen temperature

The furnace and the mean* specimen temperatures are connected by the line of equality as shown in Fig. 6.5, and from this information, all of the test results which are plotted to a base of temperature are therefore corrected using the new specified mean specimen temperature as defined by the above relation.

6.3 STRESS-STRAIN RELATIONSHIP AT ELEVATED TEMPERATURES :

6.3.1 Stress-strain characteristics of "un-loaded" specimens :

In this first test series the specimens were heated to the required temperature at a maximum rate of heating, were allowed to soak for 30 minutes and then strained to failure. At each increment of the displacement, the specimen load was recorded. The six temperature levels considered in these experiments were : 20 °C, 200 °C, 325 °C, 450 °C, 575 °C and 700 °C. For every temperature level three tests were performed. A total of eighteen tests were carried out. The details of the tests are given in Table 6.3. The specimens were tested at an age of 15-17 months.

The results from these tests are reported in Chapter 7 and analysed in Chapter 8.

6.3.2 Stress-Strain Characteristics of "pre-loaded" Specimens :

The "pre-load" is no doubt the main parameter in this set of tests. After the failure test results were examined, it was thus decided to conduct the tests of this series (2) using two stress

* This is not the true space average but is in general not significantly different

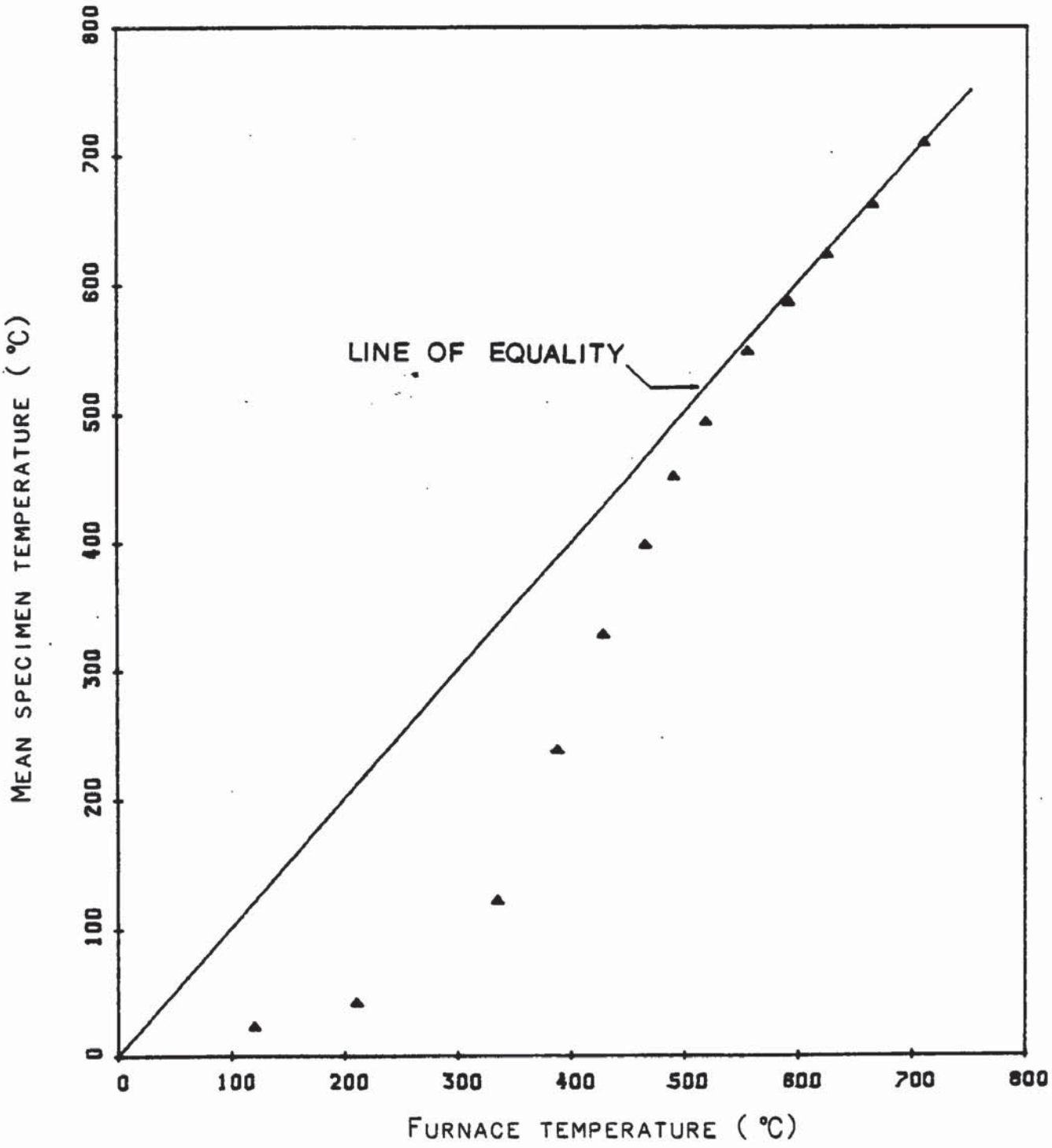

FIG. 6.5 MEAN SPECIMEN TEMPERATURE AGAINST FURNACE TEMPERATURE.

Test No.	Specimen No.	fcu N/mm^2	f'_c N/mm^2	Temperature °C
1	S35	38	30.4	
2	S36	37.9	30.3	20
3	S35	38	30.4	
1	S36	37.9	30.3	
2	S36	37.9	30.3	200
3	S35	38	30.4	
1	S20	41	32.8	
2	S20	41	32.8	325
3	S20	41	32.8	
1	S21	44.3	35.44	
2	S21	44.3	35.44	450
3	S21	44.3	35.44	
1	S25	41.9	33.52	
2	S25	41.9	33.52	575
3	S25	41.9	33.52	
1	S20	41	32.8	
2	S20	41	32.8	700
3	S20	41	32.8	

Table 6.3 Description of Test Series 1

Note the cylinder strength is given by $f'_c = 0.8 f_{cu}$ (f_{cu} = cube strength)

levels : 0.2 & 0.6 f'_c, where f'_c is the cylinder strength at 20 °C defined as a percentage of the cube strength, ie. $f'_c = 0.8\ f_{cu}$. The test procedure was as follows : the specimens were loaded then heated to the test temperature which ranged from 200 °C to 700°C in an increment of 175 °C and from 200 °C to 450 °C in an increment of 125 °C for the stress levels 0.2 and 0.6 f'_c respectively. After the heating cycle, which included a soaking period of 30 minutes, was terminated, the load was quickly removed and the specimens were then strained to failure. For each stress and temperature level, tests were performed three times. Thus 21 specimens were tested in order to investigate the influence of the pre-load on the stress-strain relationships.

The results obtained from tests conducted on pre-loaded specimens are compared with those from the first test series and presented in Chapters 7 and 8.

Table 6.4 gives details of the specimens tested at an average age of 22 months.

6.4 FAILURE TEMPERATURE TESTS :

The tests of this series were carried out to study the behaviour of concrete under thermal non-steady state conditions. The specimens were heated to failure under sustained stress.

The specimens were tested at each of the following stress levels : 0.2, 0.4, 0.6, 0.7 and 0.8 f'_c. The stress was first applied and the initial compressive strain was recorded. During the whole test, the

Test No.	Specimen No.	fcu N/mm^2	f'_c N/mm^2	Temperature °C	Pre-load % f'_c
1	S12	39	31.2		
2	S12	39	31.2	200	20
3	S18	43.5	34.8		
1	S16	35	28		
2	S16	35	28	375	20
3	S16	35	28		
1	S14	38.8	31.04		
2	S14	38.8	31.04	550	20
3	S14	38.8	31.04		
1	S19	42.8	34.24		
2	S19	42.8	34.24	700	20
3	S19	42.8	34.24		
1	S15	39.4	31.5		
2	S15	39.4	31.5	200	60
3	S15	39.4	31.5		
1	S 9	41.6	33.28		
2	S 9	41.6	33.28	325	60
3	S25	41.9	33.52		
1	S33	37.4	29.32		
2	S10	41.7	33.36	450	60
3	S10	41.7	33.36		

Table 6.4 Description of Test Series 2

stress was kept constant while heating the specimen to failure. The deformation of the specimen was monitored and the results are set out in Chapter 7.

Prior to the main tests of this series, an experiment to evaluate the free thermal expansion of concrete was performed. The test procedure was as follows : the specimen was heated to a temperature of 750 °C and during the heating period no load was applied. Thus the test cylinder was free to expand. The expansion was recorded and the results will be discussed in Chapter 7. When the test temperature was reached but before starting the cooling cycle, the specimen was permitted to soak for one hour.

Sixteen tests were conducted to complete this third test series. Table 6.5 gives information on the specimens used for the required experiments. The average age of the specimens was 19 months.

6.5 CREEP TESTS :

In these tests, the specimens were heated and held at the required constant temperature and were loaded in compression with a constant load one hour after the test temperature was reached.

The stress levels considered were : 0.2, 0.4 and 0.6 f'_c and the respective temperature levels ranged from 200°C to 700°C, from 200°C to 550 °C and from 200°C to 450°C. The details of the test procedure are reported in Table 6.6.

Test No.	Specimen No.	fcu N/mm^2	f'_c N/mm^2	Temperature °C	Stress % f'_c
1	S26	44.3	35.44	750	0
1	S26	44.3	35.44		
2	S26	44.3	35.44	heated to failure	20
3	S26	44.3	35.44		
1	S28	39.2	31.36		
2	S28	39.2	31.36	heated to failure	40
3	S28	39.2	31.36		
1	S29	39.4	31.52		
2	S29	39.4	31.52	heated to failure	60
3	S29	39.4	31.52		
1	S30	40.5	32.4		
2	S30	40.5	32.4	heated to failure	70
3	S30	40.5	32.4		
1	S 2	38	30.4		
2	S 2	38	30.4	heated to failure	80
3	S 2	38	30 4		

Table 6.5 Description of Test Series 3.

Test No.	Specimen No.	fcu N/mm^2	f'_c N/mm^2	Temperature °C	Stress % f'_c
1	S16	35	28		
2	S16	35	28	200	20
3	S16	35	28		
1	S31	39.7	31.8		
2	S31	39.7	31.8	375	20
3	S31	39.7	31.8		
1	S22	44.5	35.6		
2	S22	44.5	35.6	550	20
1	S21	44.3	35.4		
2	S21	44.3	35 4	700	20
1	S20	41	32.8		
2	S20	41	32.8	200	40
1	S25	41.9	33.5		
2	S25	41.9	33.5	375	40
1	S13	38.2	30.6		
2	S13	38.2	30.6	550	40
1	S7	39.7	31.8		
2	S7	39.7	31.8	200	60
1	S13	38.2	30.6		
2	S13	38.2	30.6	325	60
1	S18	43.5	34.8		
2	S18	43.5	34.8	450	60

Table 6.6 Description of Test Series 4

For each combination of stress and temperature level the tests were carried out twice. However for the stress level $0.2 f'_c$ three tests were performed at 200°C and 375°C respectively.

The creep tests were conducted over a period of five hours. When the load was applied, the instantaneous response was first recorded and then the creep strains were monitored every 10 minutes during the whole testing period.

The results obtained from the 22 tests will provide the required information on the time-dependent behaviour of concrete at elevated temperatures. They will be presented and discussed in the next two Chapters.

CHAPTER 7

DISCUSSION OF THE EXPERIMENTAL RESULTS

7.1 INTRODUCTION :

The results of the tests outlined in Chapter 6 are reported in this section. The data produced are analysed in Chapter 8.

The results obtained for the stress-strain behaviour are presented first, followed by those of tests conducted on restrained specimens and finally those recorded for the time-dependent behaviour.

The test series already described were performed for convenience in the following order :

- stress-strain tests on "unloaded" specimens.
- transient tests (failure temperature tests).
- creep tests.
- stress-strain tests on "pre-loaded" specimens.

The load recorded in the stress-strain tests on "pre-loaded" specimens is based on a recalibration of the dynamometer (reported in Appendix Two), which was needed because of the failure of the strain gauges on the load cell, which occured accidentally. The recalibration produced a load-strain characteristic which was not significantly different from the earlier one.

7.2 STRESS-STRAIN BEHAVIOUR :

7.2.1 Stress-strain result of "un-loaded" concrete specimens :

The Stress-strain curves from the tests conducted on concrete specimens bearing no load are shown in Fig. 7.1. These were determined under steady-state conditions. Although three tests were performed for each tempetature level, only one typical curve for every batch is

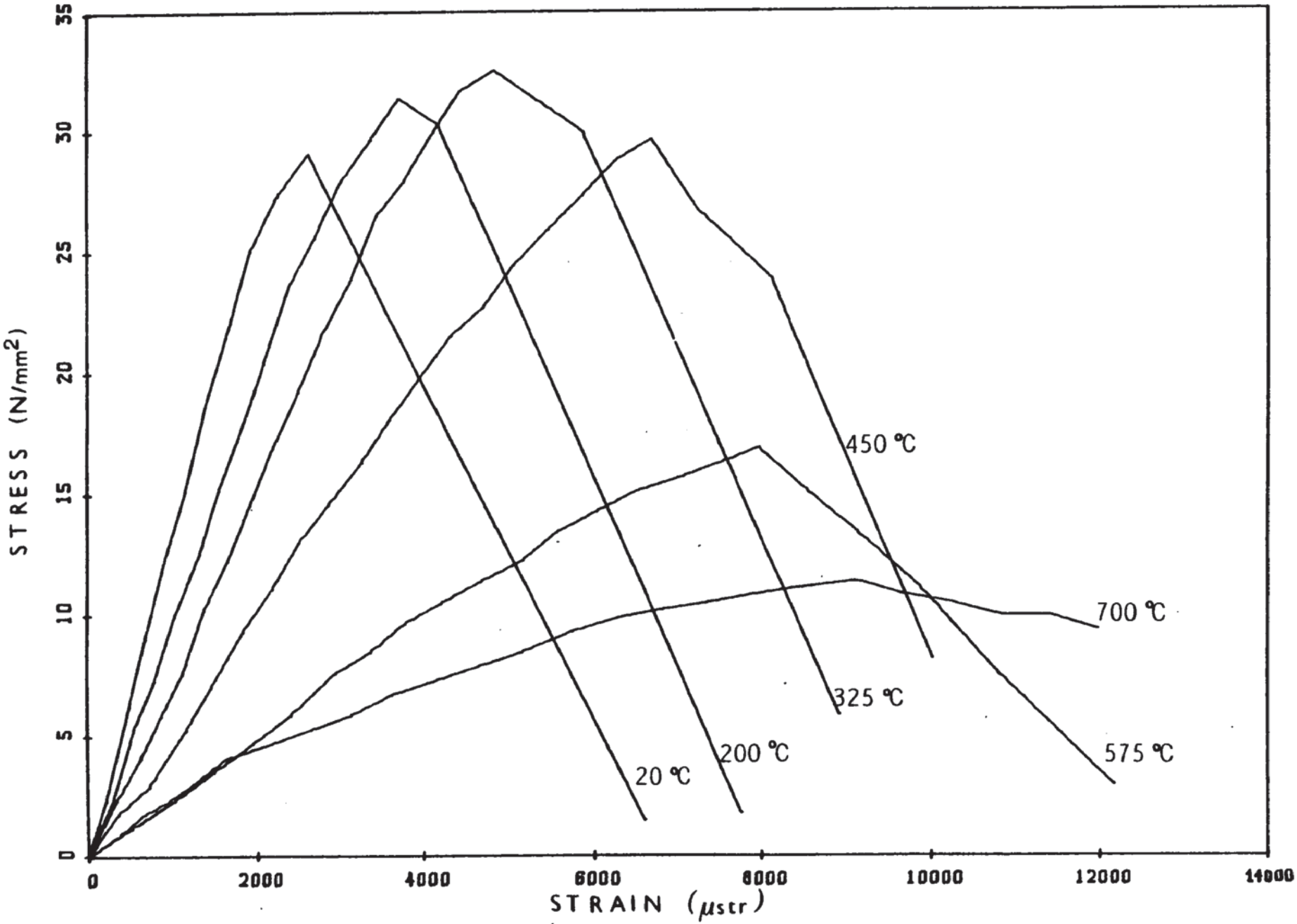

FIG. 7.1 STRESS/STRAIN CURVES FOR DIFFERENT TEMPERATURES (NO PRE-LOAD).

plotted. Table 7.1 shows, however, the average values of the characteristics of the curves. The Young's modulus was taken at a stress of 0.25 ultimate stress as suggested by Baldwin & North (1973).

The data obtained show the effect of temperature upon the mechanical properties of concrete subjected to uniaxial compression. The results in Fig. 7.1 indicate that the peak stress decreases with increasing temperature whereas the corresponding strain increases. One interesting aspect of these tests is that at a temperature of 200°C a slight increase in the ultimate strength rather than a decrease is observed. This can be attributed mainly to the water still held in the concrete in spite of predrying the specimens. Beyond this temperature the strength dropped as a result of the increasing degradation of the specimen due to the development of internal cracks from thermal incompatibility between the mortar matrix and the aggregate as reported by Dougill (1972) when examining the explosive spalling of concrete. The stress-strain curves show also significant reduction in the intial tangent modulus of elasticity as the temperature increases. At a temperature of 700°C Young's modulus was reduced to about 20% of its original value while the strength was equal to only half its value at 20°C. It can be noted that the elasticity of concrete when subjected to elevated temperatures is affected in a similar way as strength.

In general terms, the decrease in strength of concrete is due, in part, to the observed high thermal expansion of the siliceous aggregate used (see section 7.3) and in part to the physical changes in the crystalline structure which take place at high temperatures

Specimen Batch	Cylinder Strength N/mm^2	Mean Peak Stress N/mm^2	Mean Peak Strain 10^{-6}	Young's Modulus at $0.25\sigma_o$ KN/mm^2	Temperature °C
1	30.4	28.57	2622	13.2	20
2	30.32	30.98	3712	9.50	200
3	32.8	31.18	4957	6.70	325
4	35.44	29.04	5765	6.83	450
5	33.52	16.85	7656	2.30	575
6	32.8	11.62	9642	2.03	700

Table 7.1 Effect of Temperature on The Properties of Concrete

followed especially by an increase in volume, as outlined by Abrams (1968) and Fischer (1970). The specimens tested at 575 °C showed a pronounced drop in strength. Figures 7.4-7.6 show the effect of temperature upon the mean strength, the mean ultimate strain and the mean Young's modulus (β= 0 refers to results of tests on unstressed specimens). The analysis of the experiment results is set out in the next Chapter. The curves obtained, however, are similar to those produced by some investigators such as Anderberg & Thelandersson (1976), Cruz (1966), Purkiss (1972), Schneider (1976), Malhotra (1956) and Fischer (1970).

The results of this first test series showed that as the temperature increased the ductility of the material increased. Figure 7.1 shows clearly that at temperatures up to 575 °C and 700 °C the concrete appeared to be very ductile.

7.2.2 Stress-strain result of "pre-loaded" concrete specimens :

The purpose of the tests in this series is to determine the properties of concrete in more realistic conditions; since in a fire in a structure the concrete is loaded before exposure to heating.

The specimens were tested at two stress levels. The stress-strain curves from such tests are shown in Fig. 7.2 and Fig. 7.3 for 0.2f'_c and 0.6 f'_c respectively. The results of the mechanical properties are listed in Tables 7.2 and 7.3.

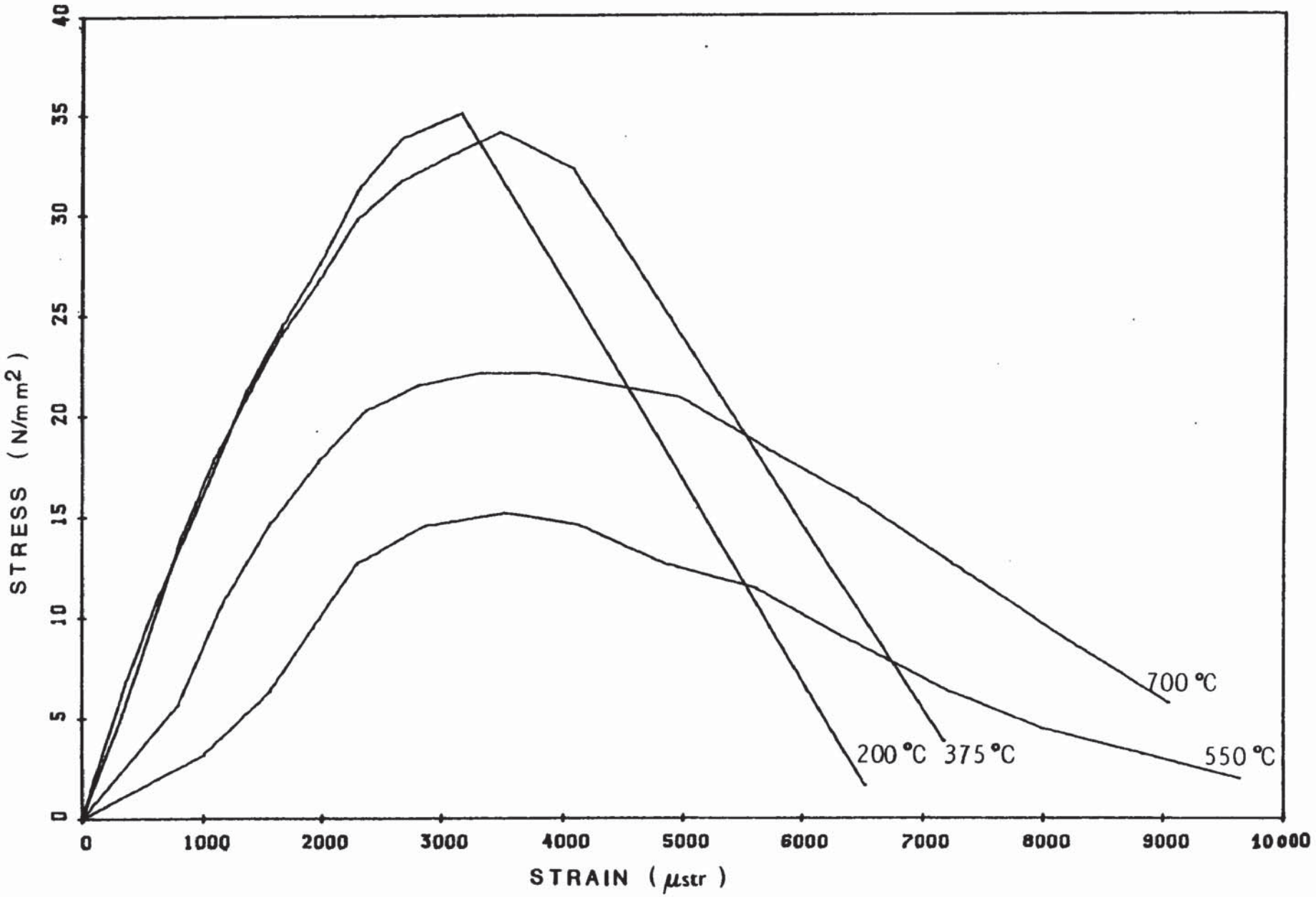

FIG. 7.2 STRESS/STRAIN CURVES FOR DIFFERENT TEMPERATURES (PRE-LOAD = 20%).

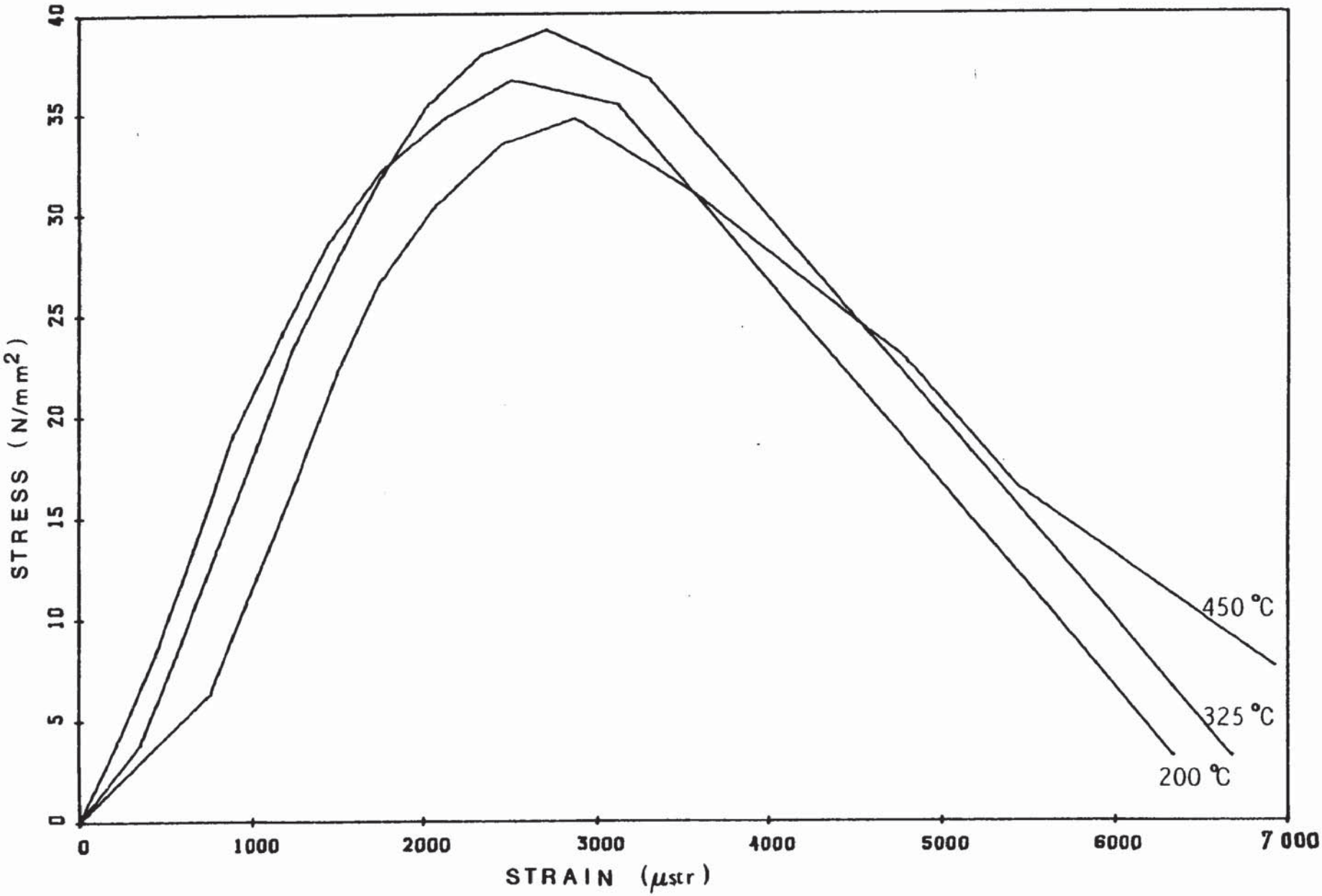

FIG. 7.3 STRESS/STRAIN CURVES FOR DIFFERENT TEMPERATURES (PRE-LOAD = 60%).

Specimen	f'_c N/mm^2	Mean Peak Stress N/mm^2	Mean Peak strain 10^{-6}	Mean E_c KN/mm^2	Temp °C
1	32.4	32.79	3148	14.16	200
2	28	31.40	3483	13.87	375
3	31.04	20.67	3043	8.20	550
4	34.24	15.3	3176	4.96	700

Table 7.2 Mechanical Properties of Concrete Specimens (with pre-load = 0.2 f'_c)

Specimen Batch	f'_c N/mm^2	Mean σ max N/mm^2	Mean ϵ max 10^{-6}	Mean E_c KN/mm^2	Temp °C
1	31.52	34.98	2503	14.99	200
2	33.36	38.15	2741	14.56	325
3	32.01	31.2	2746	10.32	450

Table 7.3 Mechanical Properties of Concrete Specimens (with pre-load = 0.6f'_c)

Note

The descending portions of the $\sigma - \epsilon$ curves (figs. 7.1 – 7.3) at lower temperatures may not give the true slope

The stress-strain curves obtained with specimens stressed to 0.2 f'_c show that the ultimate stress undergoes a reduction and the strains are increased as is expected at elevated temperatures. Up to a temperature of 375 °C the test cylinders showed an appreciable increase in strength (up to 12%). As the temperature increased the strength was significantly reduced and at 700 °C it was equal to only 45% of its unstressed initial value. This effect is shown in Fig. 7.4 (β= 0.2). Figure 7.5 (β= 0.2) shows that the strain is almost constant for the test temperatures.

The test specimens loaded to 0.6 f'_c exhibit a similar behaviour. From the stress-strain curves in Fig. 7.3 it can be seen that the concrete shows a higher strength at a temperature up to 325°C. However, at 450 °C, no increase was noticed, and the specimens even retained their original unstressed ambient strength. Young's modulus did not exhibit any significant change up to 325 °C.

The influence of temperature upon the strength, the strain at peak stress and the elastic modulus is shown in Figs. 7.4–7.6. The strain seemed to be constant as noticed with specimens stressed to 0.2 f'_c. The data plotted in these three figures represent the average values for each parameter at each temperature level.

The results in this section agree well with those obtained by Malhotra (1956), Abrams (1968) and Schneider (1976) when testing pre-loaded specimens.

The increase in concrete strength occurs since cracking due to the thermal incompatibility between the aggregate and the mortar

matrix is suppressed or reduced as suggested by Dougill (1972) and Malhotra (1982), and the matrix is in a state of compression during heating.

The three main parameters of concrete (strength, strain and elasticity) are influenced by the amount of the sustained load and this is confirmed by the results of both stress levels. A comparison between the two shows, for instance, that at 200°C an increase in strength of 11% was obtained with a load equal to 0.6 f'_c while the strength, for a load of 0.2 f'_c, rose only by about 2%.

Some important results appear when the stress-strain curves of "pre-loaded" concrete specimens are compared with the results obtained for "unloaded" specimens. First higher strength is obtained with "pre-loaded" specimens as shown in Fig. 7.4 where the curves are plotted for the three different stress levels (β=0, 0.2 & 0.6). Their ultimate strains, however, are lower and even decrease with increasing pre-load. Such influence is illustrated in Fig. 7.5. The other interesting observation is the higher values recorded for the modulus of elasticity with "pre-loaded" specimens, and this can be seen in Fig. 7.6.

The test results obtained show that the stress-strain curve of concrete at elevated temperatures is markedly influenced by the "pre-load". This results in a small strength loss and the strain being lower than those of unstressed specimens. The same observations were made by Fischer (1970) and the other investigators already mentioned. The presence of a load reduced the ductility of the concrete although heated to temperatures greater than 500°C.

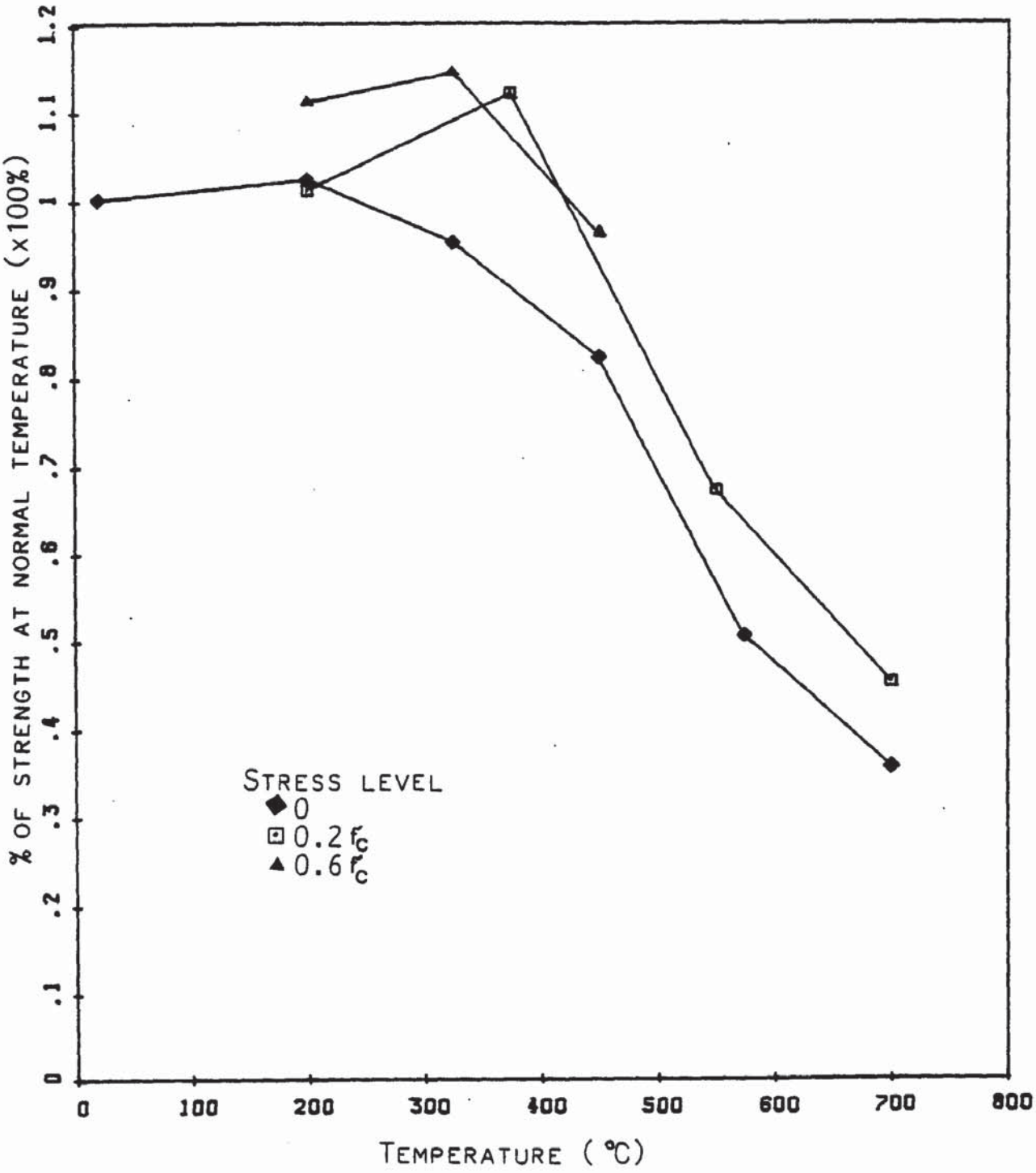

FIG. 7.4 THE INFLUENCE OF TEMPERATURE AND PRE-LOAD UPON COMPRESSIVE STRENGTH.

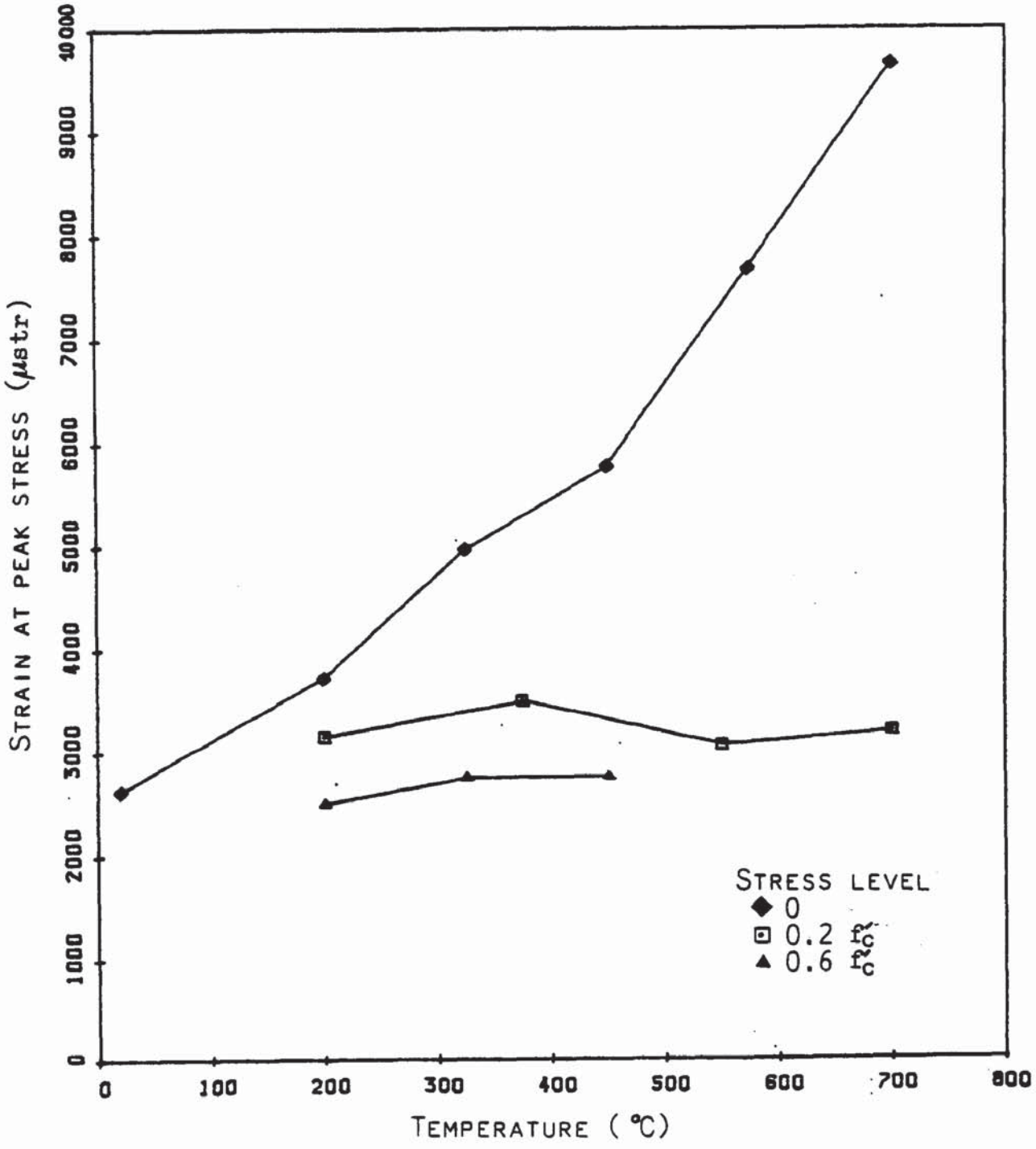

FIG. 7.5 THE INFLUENCE OF TEMPERATURE AND PRE-LOAD UPON THE PEAK STRAIN.

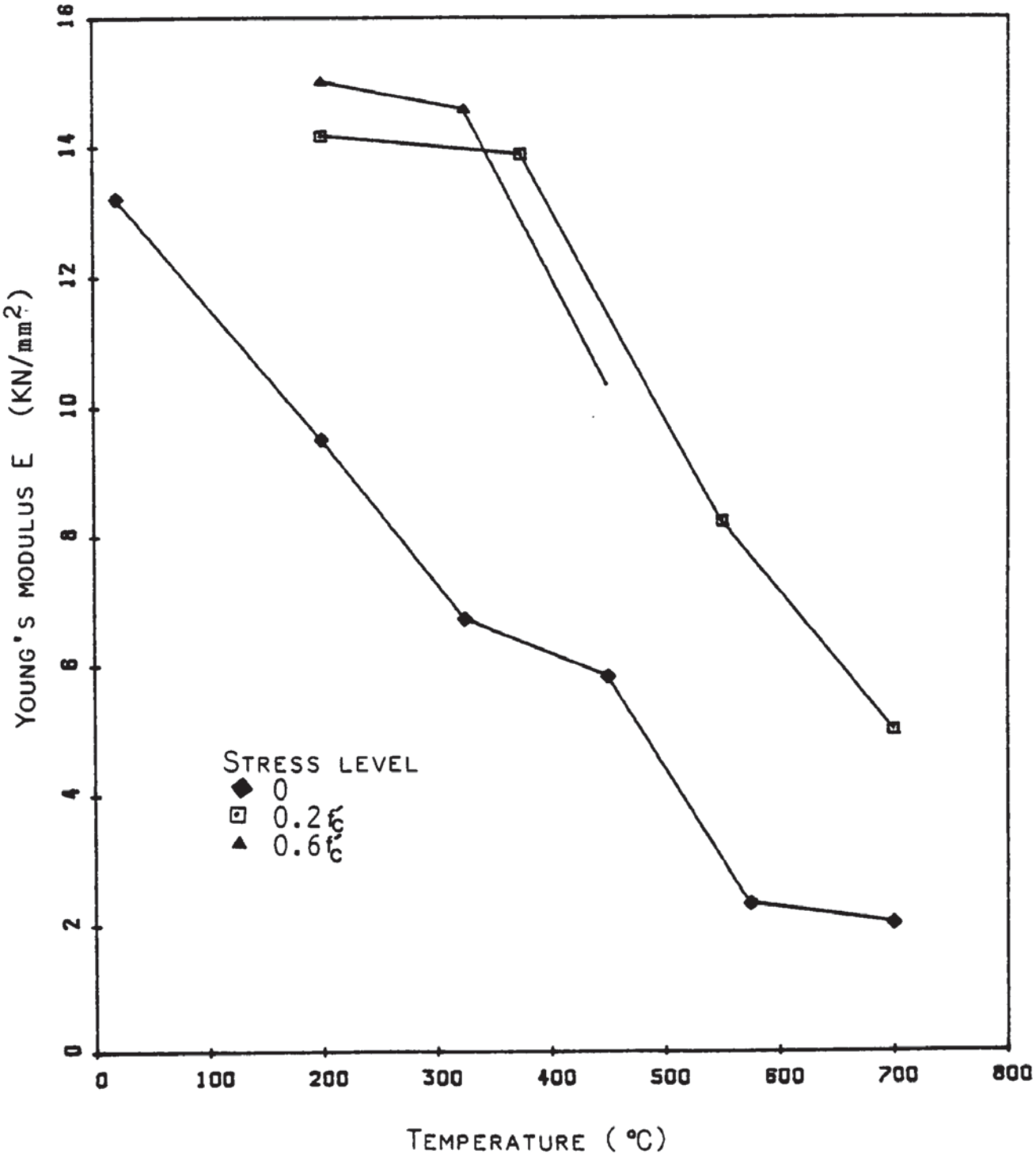

FIG. 7.6 THE INFLUENCE OF TEMPERATURE AND PRE-LOAD UPON YOUNG'S MODULUS.

Further discussion will be presented when the results are analysed in Chapter 8.

7.3 FAILURE TEMPERATURE TESTS RESULTS :

Figure 7.7 shows the behaviour of concrete specimens heated to failure under different stress levels. The objective of the tests performed was to obtain data on the deformation of concrete under transient conditions and preload which represent the real behaviour of a structure exposed to heating in case of a fire.

The results of the tests are presented without the initial strain caused by the application of the load and are plotted against mean specimen temperatures. Each curve represents the average of three tests. An exception is, however, made for the zero value curve where only one test was performed. For this particular test the strains were recorded during the heating period and the subsequent cooling. The complete results including the initial deformations for each test are contained in Appendix Six.

During the early stage of heating all specimens showed a negative deformation before the expansion began. This was probably due to shrinkage which normally occurs in the begining of the heating process. This can be explained by the water which continued to be driven out of the concrete although the specimens were pre-dried for three days at 105 °C.

As commonly observed, concrete expands as the temperature increases. This is confirmed by the test results of Fig. 7.7, which

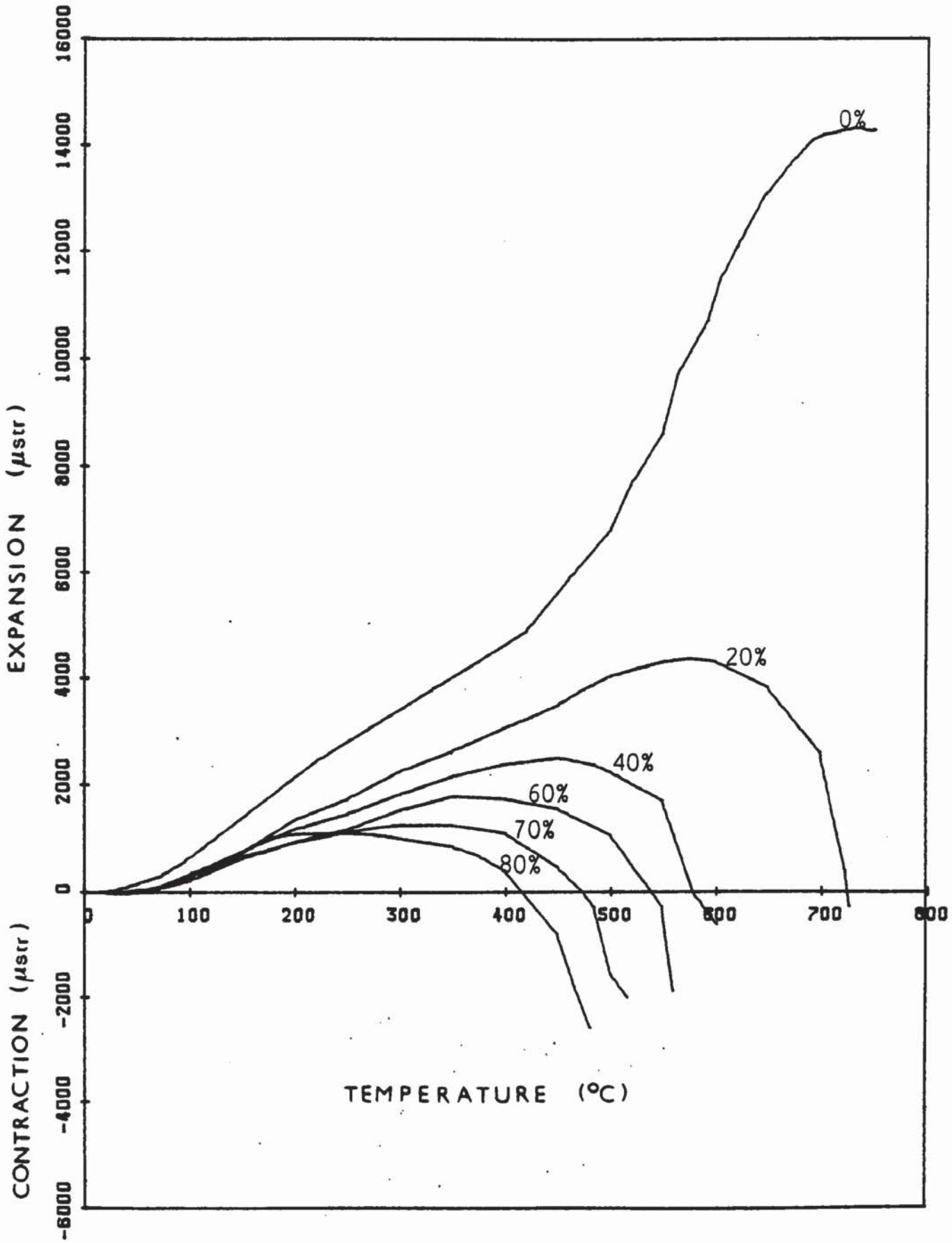

FIG. 7.7 THERMAL STRAIN UNDER DIFFERENT STRESS LEVELS.

shows the change in length of the specimens due to heating. The other effect illustrated is that of the applied load which varies from 0 to 0.8 f'_c. The curve at zero load represents the free thermal expansion. It can be seen that it undergoes a substantial increase above 550°C due mainly to the α-to-β quartz transformation and the absence of drying shrinkage. The expansion, however, decreases significantly under applied stress as reported in the literature particularly by Fischer (1970). Accordingly, the curves obtained at different stress levels show that the behaviour of concrete under transient heating is strongly influenced by the magnitude of the load. The other observation is that the temperatures at which the specimens failed also decreased as the load increased. As an indication, the critical temperature for specimens heated under a stress of 0.2 f'_c was about 730°C, whereas specimens tested under a stress of 0.6 f'_c failed at about 560°C.

Despite the large strains and the formation of cracks on its surface, the specimen used in the unstrained thermal expansion test did not fail. The cracks had developed during heating and were observed when the furnace was switched off and the cooling cycle had started.

The specimens tested at a stress equal to 0.7 and 0.8 f'_c, first expanded up to temperatures of 300°C and 250°C respectively, then their thermal expansion was stopped as the result of the compressive deformation produced by high stresses. The results of tests on specimens stressed to 67.5% obtained by Thelandersson & Anderberg

(1976) showed that the thermal expansion was fully compensated by the stress-induced strain. The reason is probably due to the small aggregate/cement ratio (1.92) used if compared with a ratio of 3.5 used for the purpose of this investigation.

The failure temperatures of the restrained specimens when compared with the unloaded stress-strain results show that no major difference appears between the two test procedures. The results plotted in Fig. 7.8 indicate that the two curves obtained are similar. The only difference, occuring at temperatures above 550 °C, is attributed to the physical changes and mainly to the quartz transformation which takes place at 575 °C. It should be noted that the specimens used in the two test methods are from different batches. A further source of error may be due to the method used to estimate the mean temperature in the specimen.

Although a better fit is obtained in this work, Thelandersson & Anderberg (1976) came up with similar conclusions.

7.4 CREEP RESULTS :

The results of the creep tests conducted on concrete specimens heated to a stabilized temperature, loaded for five hours under a constant uniaxial stress, are reported in this section.

Due to the fact that three different stress levels were used, and in order to show their influence, the results are presented in three groups.

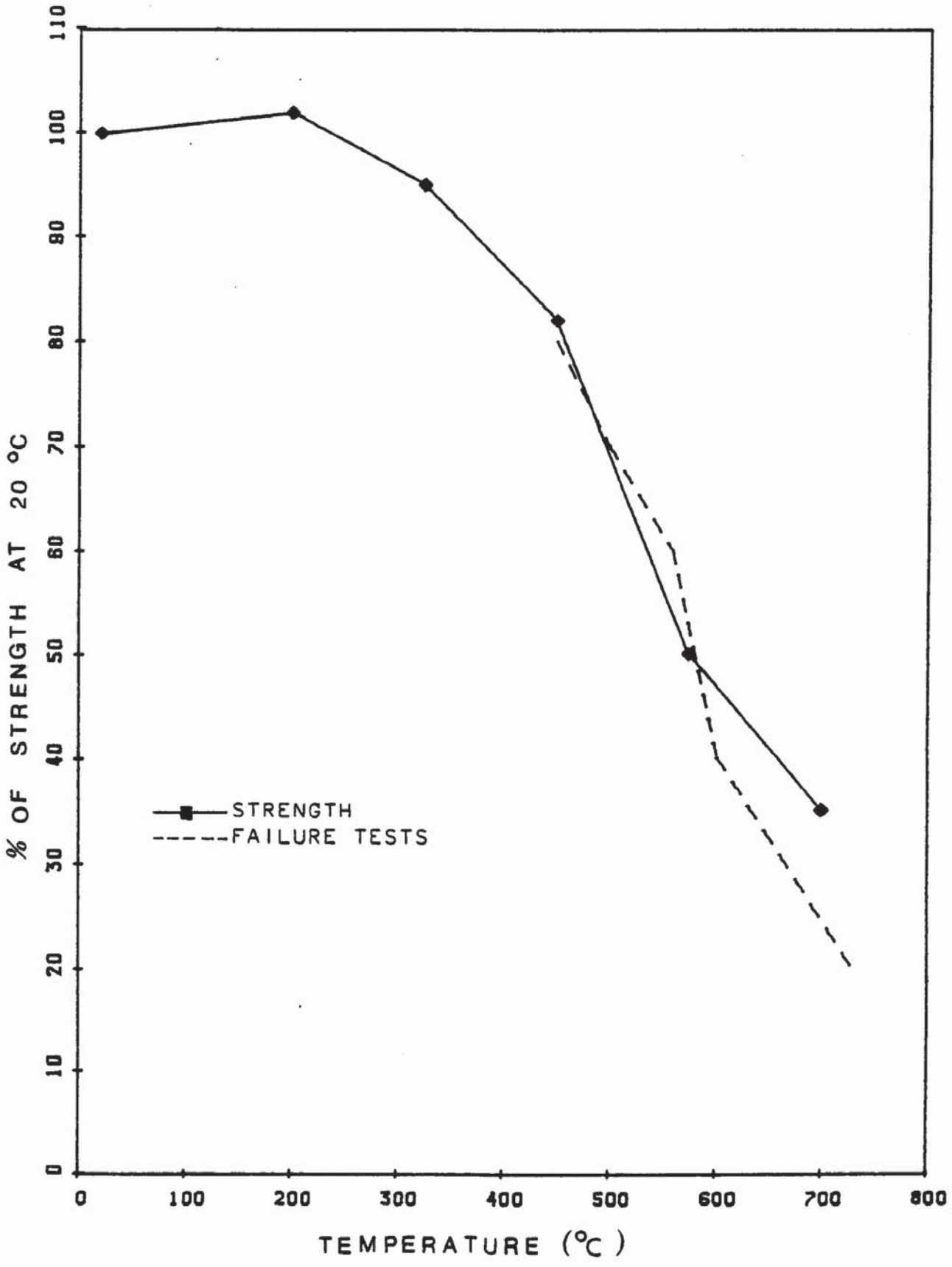

FIG. 7.8 COMPARISON BETWEEN COMPRESSIVE STRENGTH OF UNLOADED SPECIMENS AND DATA FROM FAILURE TEMPERATURE TESTS.

In the first group the specimens were heated to four temperature levels under a constant stress of 0.2 f'_c. The observed creep behaviour of such tests is shown in Fig. 7.9. The mean curves are plotted for the different temperature levels. The individual results are given in Appendix Six. When the load was applied, the heated specimen deformed elastically. The initial instantaneous strain due to the corresponding stress does not appear in results of Fig. 7.9. As the load was maintained constant, the strains increased with time. The specimen entered the primary creep region and then the secondary which was characterized by a sensibly constant strain rate. Tertiary creep appeared, however, to be reached with specimens tested at 550 °C and 700 °C. They did not fail despite the large deformations and the wide cracks which formed on their surfaces. These cracks were observed immediately after the test was completed. When the last reading was taken, the heating process was stopped and one section of the split furnace was removed, giving access to the specimen, which was still hot. The observed cracks are shown in Plate 7.1.

The temperature levels of the second group ranged from 200 °C to 550 °C at an increment of 175 °C and the applied stress was equal to 0.4 f'_c. Figure 7.10 shows the curves of creep strains against time for each temperature level, each curve being the average of two tests. A set of tables giving the entire data are included in Appendix Six. The results of tests at 200 °C and 375 °C show a similar creep behaviour as observed in the first group for the same temperature levels. The only

PLATE 7.1 TYPICAL CRACKS ON A SPECIMEN HEATED TO 700°C IN CREEP TESTS (β= 0.2)

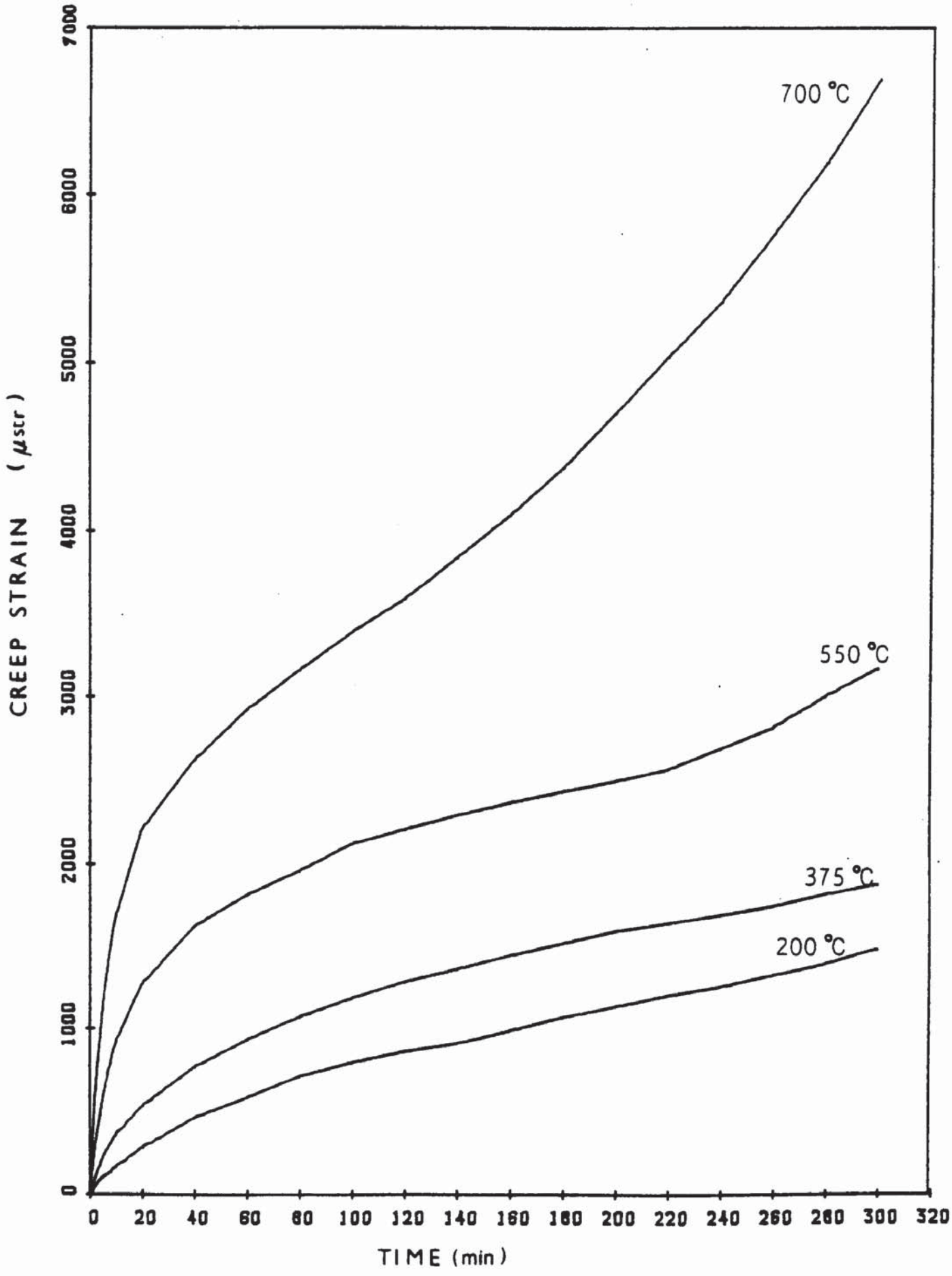

FIG. 7.9 CREEP CURVES FOR DIFFERENT TEMPERATURES (β = 0.2)

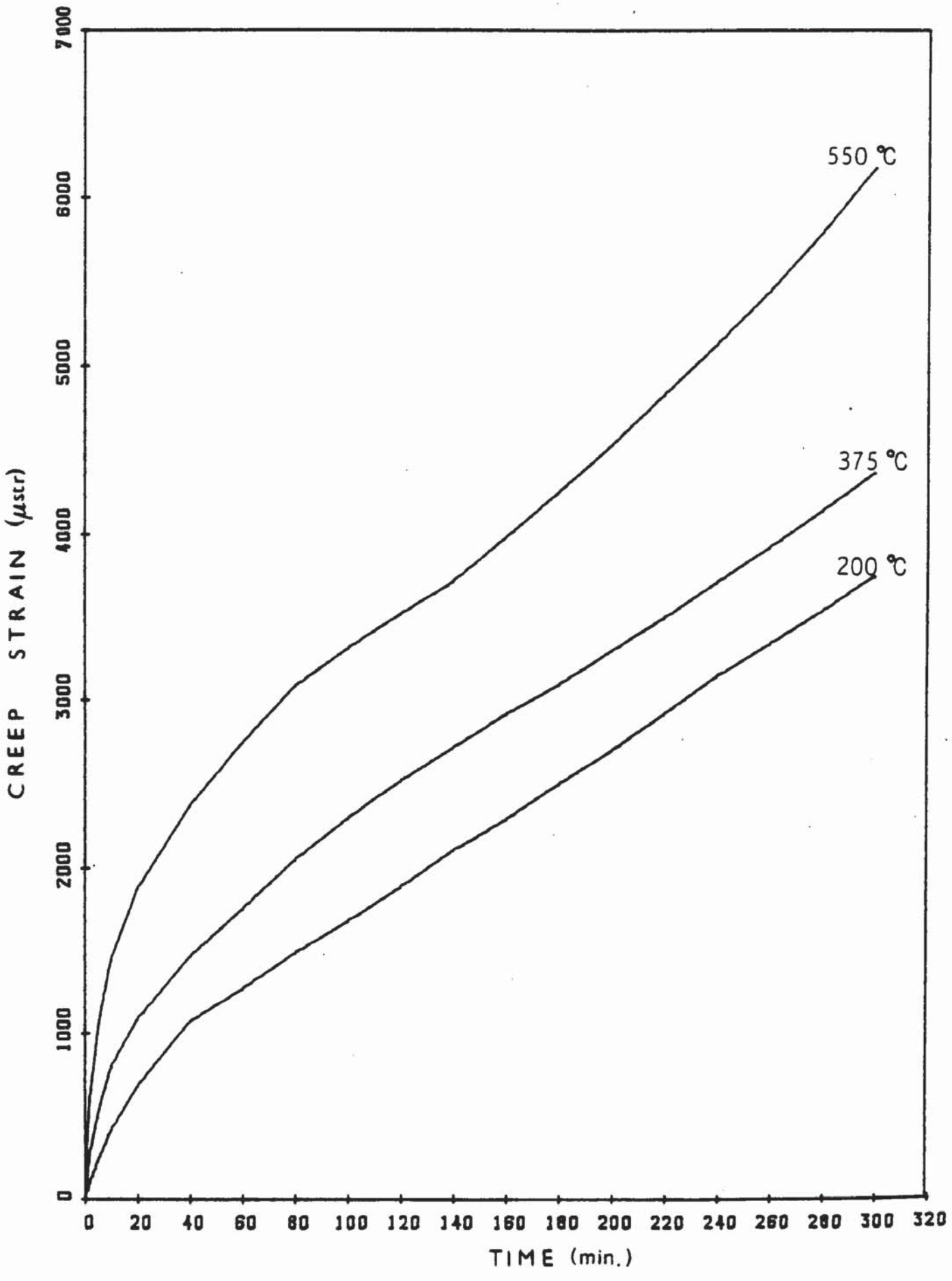

FIG. 7.10 CREEP CURVES FOR DIFFERENT TEMPERATURES ($\beta = 0.4$)

difference is that with a stress of 0.4 f'_c increased strains are recorded.

At a temperature of 550 °C, higher creep strains were obtained and the specimens did exhibit a tertiary region but did not fail. The time required for a creep rupture at this temperature is greater than five hours. Purkiss (1972) produced a similar trend of results when testing at a temperature of 570 °C and at a stress of 7.5 Nmm^{-2}.

In the last group are reported the results of tests conducted on specimens heated at 200 °C, 325 °C and 450 °C, and stressed to 60% of the cylinder strength. Figure 7.11 shows the creep results of such tests. The curves are similar in shape to those obtained in the previous groups. No creep rupture occured with all of the specimens tested. However, they exhibited higher strains and crack formation. When considering the secondary creep region of the curves in Fig. 7.11, it can be seen that the strains obtained at 450 °C are smaller than those recorded at 325 °C. The reason for this anomaly is not known. It could be, however, attributed to the amount of aggregate contained in the specimens which were from two different batches (see Chapter 6, section 6.5).

In general, the results of the creep tests illustrate the behaviour of concrete specimens subjected to a constant stress and held at a constant temperature.

For different stress levels up to 0.6 f'_c, the results in Fig. 7.9 to 7.11 agree with those obtained from former investigations made namely by Gillen (1981) and Cruz (1968).

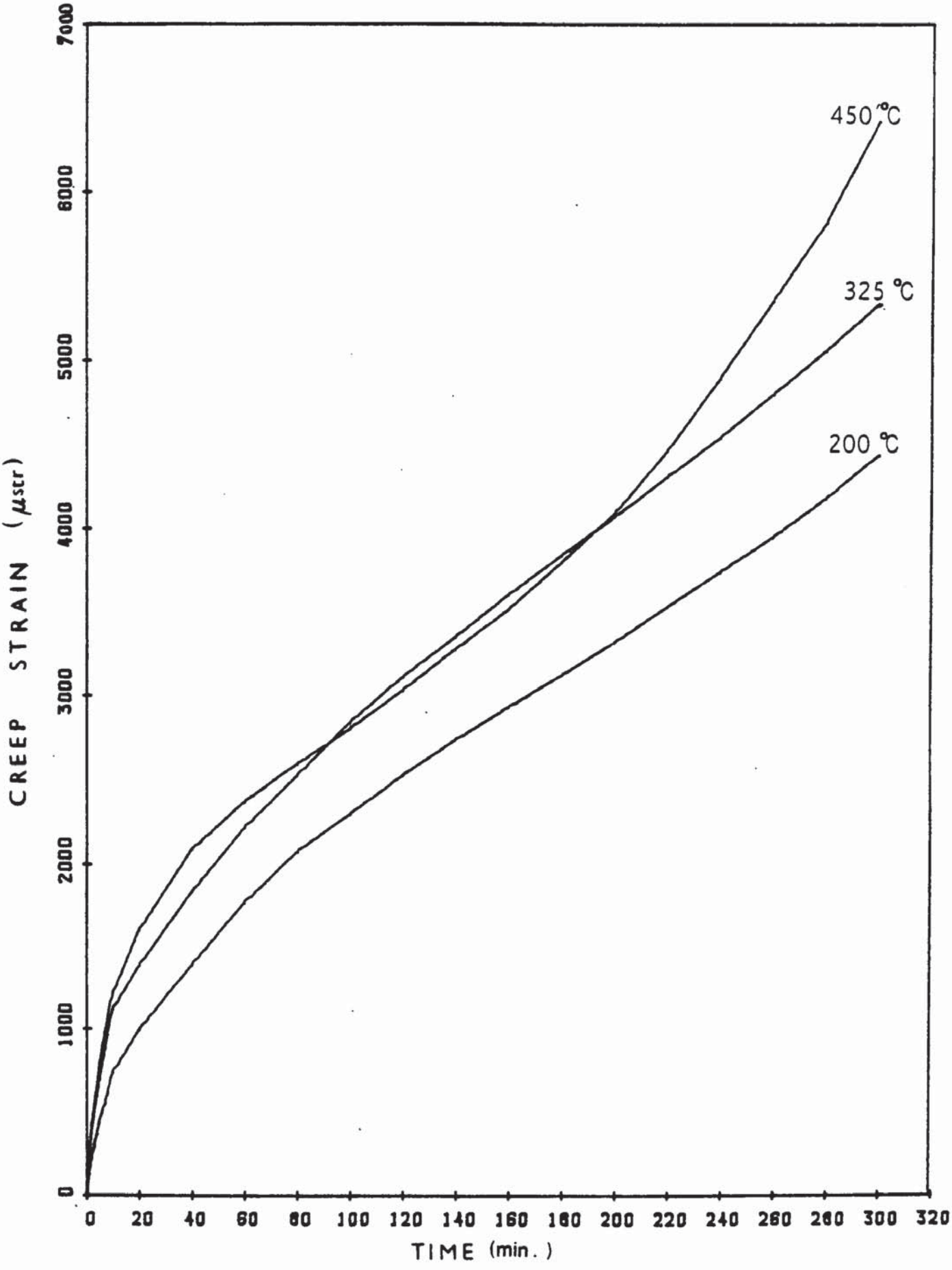

FIG. 7.11 CREEP CURVES FOR DIFFERENT TEMPERATURES (β = 0.6)

The series of curves of Fig. 7.9 - 7.11 show the effect of temperature and stress upon creep. Increasing either variable causes the strain to increase. The relative importance of each of these variables is difficult to assess qualitatively but a quantitative analysis such as that performed in the next Chapter will give some guidance. It is preceeded by an analysis of the stress-strain curves, after which a total strain model is evaluated for the concrete under test.

CHAPTER 8

ANALYSIS OF THE EXPERIMENTAL RESULTS

8.1 INTRODUCTION :

This chapter deals with the analysis of the test results already reported in the previous chapter (7). The analysis will be accompanied by a fuller discussion on the data.

The stress-strain behaviour of concrete is first examined followed by an analysis of the creep results. The total strain concept is studied and the transient strain is then calculated in accordance with the approach used by Thelandersson & Anderberg (1976).

8.2 STRESS/STRAIN BEHAVIOUR :

It has been already noted that as the temperature increases, the strain is related to the stress in a complex fashion. the stress/strain curves as obtained from the different tests, are linear over the early part of the curves and thereafter non-linearity of the relationship appears over the remainder of the range. Figures 7.1 - 7.3 distinctly illustrate this complicated relationship with temperature.

The analysis of the stress/strain results is based on that approach as introduced by Baldwin & North in 1969 and reported in the Magazine of Concrete Research in 1973 and later used by Purkiss (1972). The analysis consists of the normalization of the data obtained from tests. The non-dimensionalized curves are superimposed for "unloaded" and "pre-loaded" concrete specimens individually.

Furthermore, for comparison purposes, another approach introduced by Popovics (1973) is used to fit the experimentally obtained stress/strain data.

8.2.1 Stress/strain behaviour of "un-loaded" specimens :

The typical stress/strain curves obtained from tests on specimens bearing no load during heating are shown in Fig. 7.1. The transformation of these curves will result in a single stress/strain curve which will have the same shape at all temperatures (Purkiss (1972)). The normalization of the data is obtained for each curve by dividing the stress (σ) by the peak stress (σ_0) and the strain (ϵ) by the strain at peak stress (ϵ_0). The transformed data were used to plot σ/σ_0 against ϵ/ϵ_0. The superimposed curve was then obtained by fitting the normalized data by a polynomial. A standard computer program was available to calculate the coefficients of a polynomial of any degree. The polynomial as defined in the computer program can be written by letting P be (σ/σ_0) and X be (ϵ/ϵ_0), thus the polynomial expression is,

$$P_n(X) = a_0 + a_1X + a_2X^2 + \ldots + a_nX^n \qquad (8.1)$$

where a_0 to a_n are the coefficients of the polynomial and n is the degree of the polynomial.

In order to obtain a sufficiently accurate fit to the normalized data, the degree of the polynomial has been increased progressively. Consequently, three fits have been attempted using degree 10, 15 & 20.

Figure 8.1 to 8.3 show the normalized stress/strain data together with the superimposed curves obtained by using the polynomial of the 3 different degrees respectively. It can be seen that the three fits do not exhibit a major difference and produce almost the same curve for the three values of the degree of the polynomial. For this reason, it has been decided to use only a polynomial of degree 10 to fit the data for the "pre-loaded" specimens which will be dealt with later in this section.

As noted earlier, when plotting the normalized data a single curve will result. Figure 8.1 shows that the results lie along the same curve up to the peak and thereafter a large scatter is observed. Purkiss (1972) attributed this to the amount of cracking which affects the descending portion of the stress-strainstrain curve which is due to the small variations in the aggregate/cement ratio between the individual specimens. Before analysing the non-dimensionalized data, it was necessary to verify that the resulting normalized stress/strain curve would have the same shape at all temperatures, by examining the ratio of Young's modulus E to a stress-strain parameter defined as σ_0/ϵ_0. Figure 8.4 shows the plot of E against σ_0/ϵ_0 . The resulting curve is a straight line having a gradient of 1.16. This value agrees well with that obtained by Purkiss (1972) who used a similar aggregate type with the same aggregate size of 10 mm, but the a/c ratio was different (2.2 for Purkiss). On the other hand, the cement type and the curing conditions were also similar. Despite the scattered experimental data

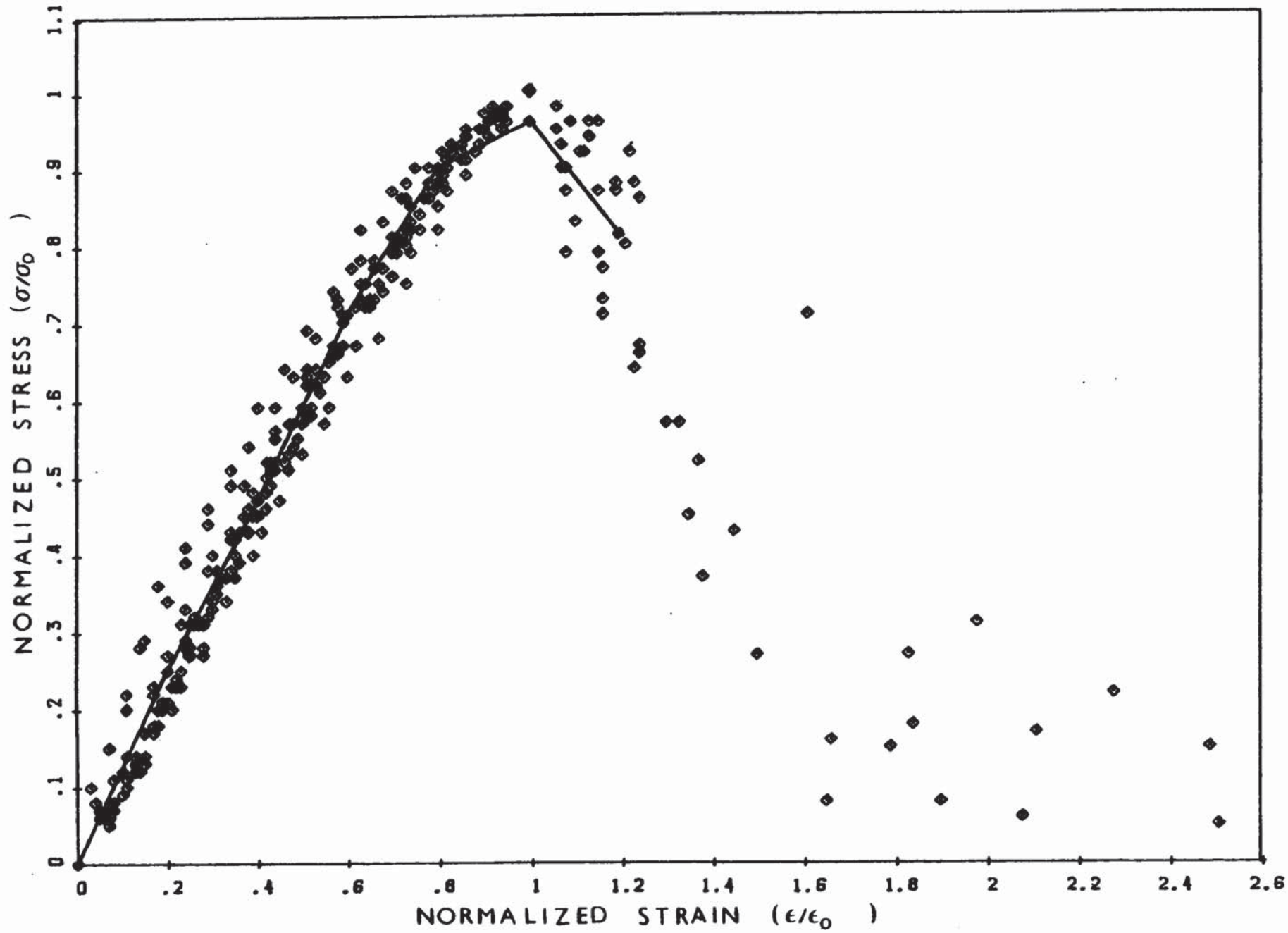

FIG. 8.1 NORMALIZED STRESS/STRAIN CURVES (NO PRE-LOAD) - POLYNOMIAL FIT : DEGREE 10

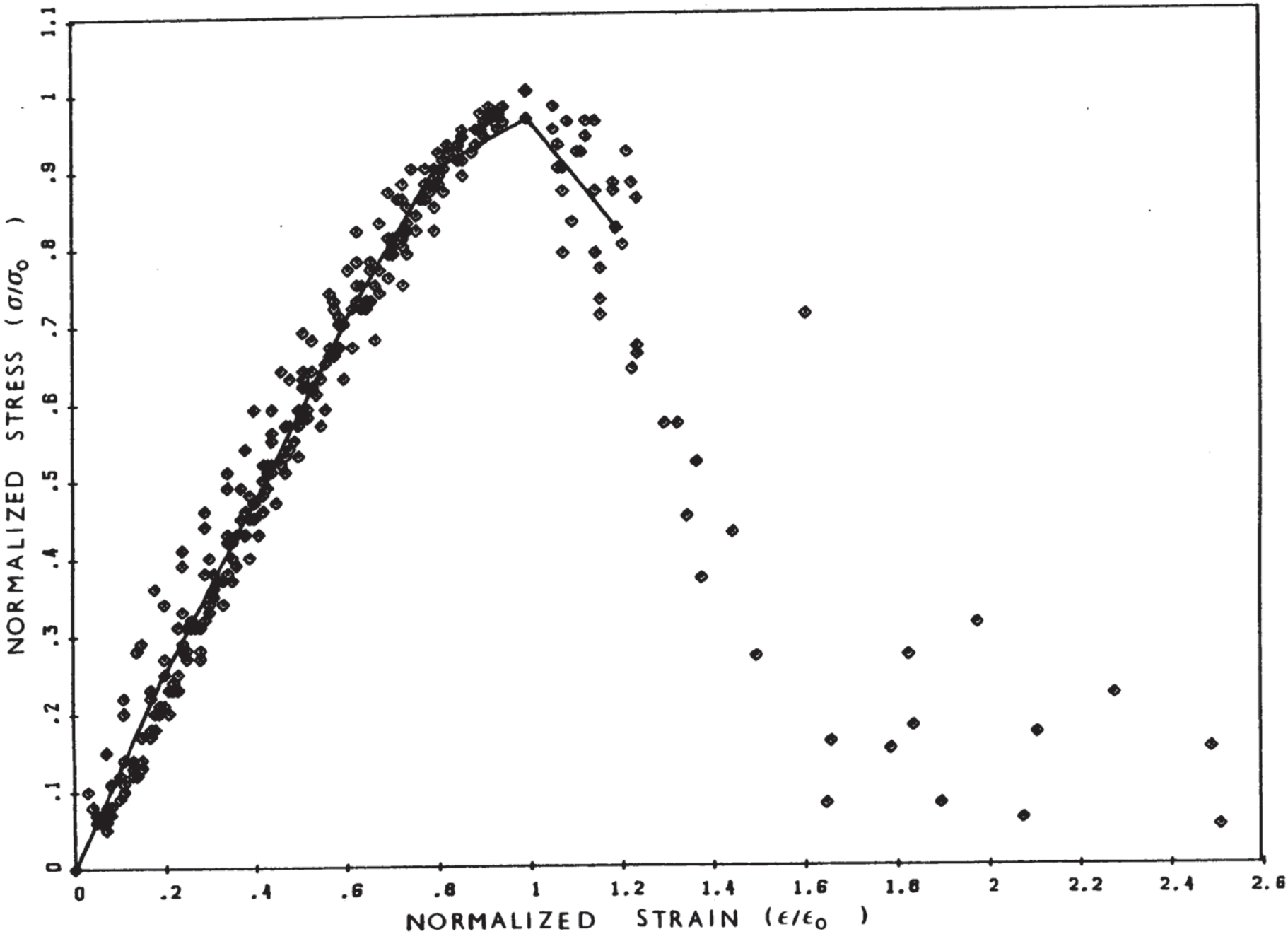

FIG. 8.2 NORMALIZED STRESS/STRAIN CURVES (NO PRE-LOAD) - POLYNOMIAL FIT : DEGREE 15

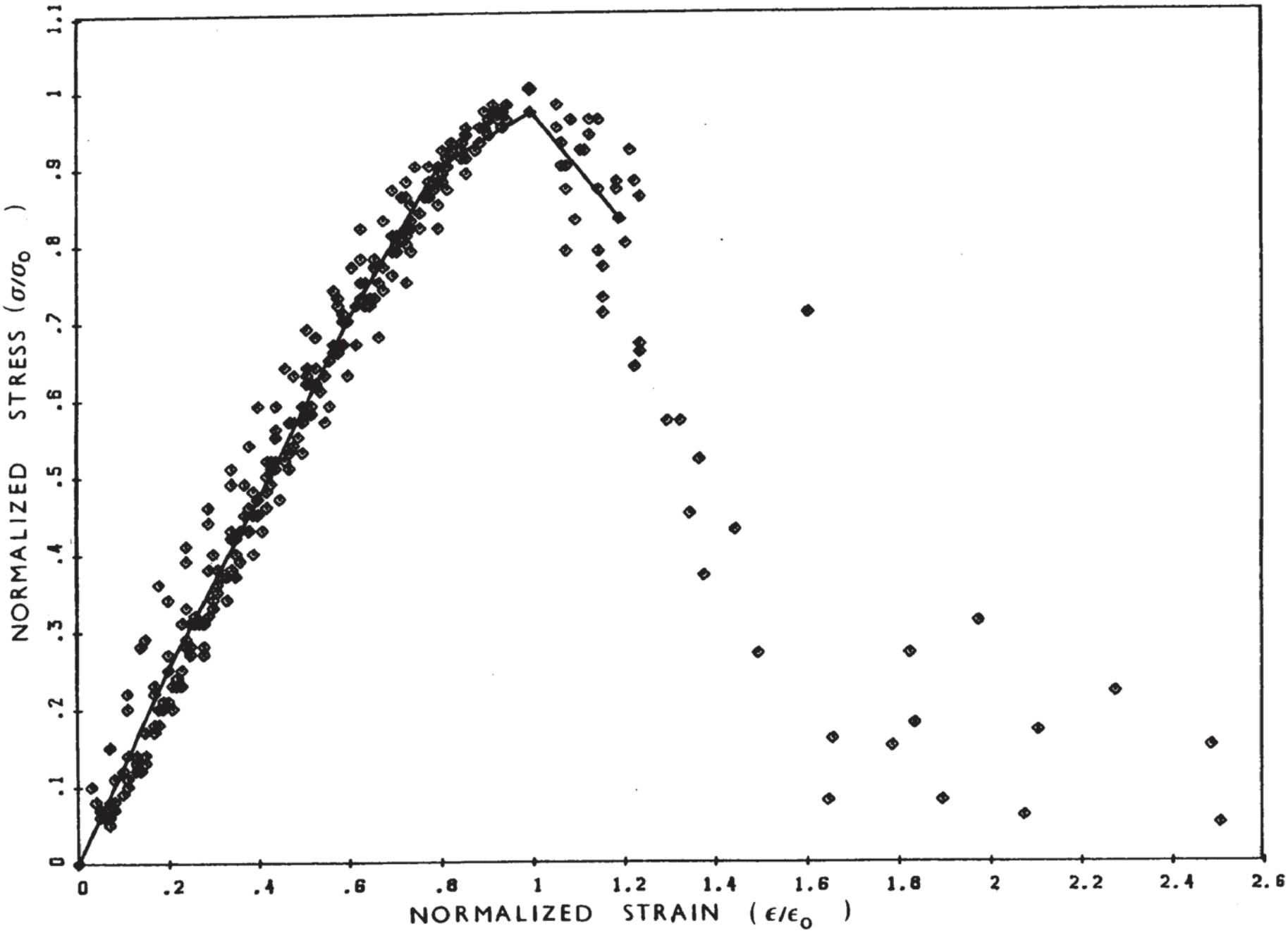

FIG. 8.3 NORMALIZED STRESS/STRAIN CURVES (NO PRE-LOAD) - POLYNOMIAL FIT : DEGREE 20

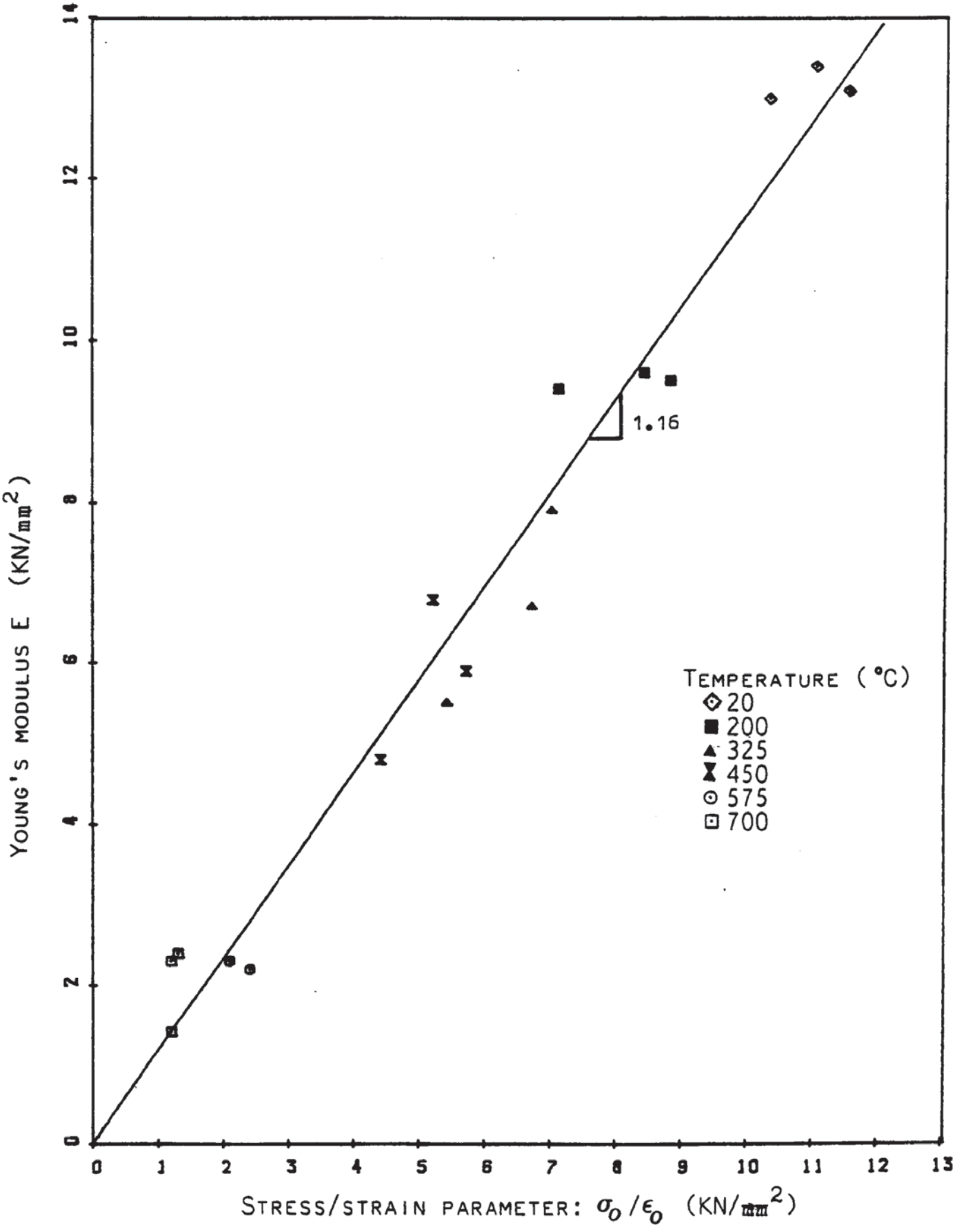

FIG. 8.4 YOUNG'S MODULUS AGAINST STRESS/STRAIN PARAMETER (NO PRE-LOAD).

shown in Fig. 8.4 a relationship between E and σ_o/ϵ_o exists and the coefficient of correlation is found as 0.98.

The superimposed curve is of the form $\sigma/\sigma_o = f(\epsilon/\epsilon_o)$. This indicates that all the curves for different temperatures are represented by a single curve, and that it is therefore possible to determine the stress/strain curve for concrete at elevated temperatures by only considering the stress/strain curve at room temperature. This conclusion had been already drawn by Baldwin & North in 1969 and reported in 1973 and was later confirmed by Purkiss (1972).

The characteristic parameters of the observed stress/strain behaviour are now examined. The effects of temperature upon the mechanical properties of concrete have been discussed in Chapter 7. The result obtained for each parameter are studied separately.

The peak stress at different temperatures and the strength as a percentage of the strength at normal temperature are plotted in Figs. 8.5 and 8.6 respectively. It can be seen from the two graphs that the peak stress and consequently the strength decreases significantly above a temperature of 300 °C. These results compare favourably with that obtained by other researchers.

The variation of the strain, ϵ_o, at peak stress with temperature is illustrated in Fig. 8.7. The curve obtained shows that ϵ_o increases with increasing temperature. This implies that the material attains a "quasi-ductile" state as the temperature rises.

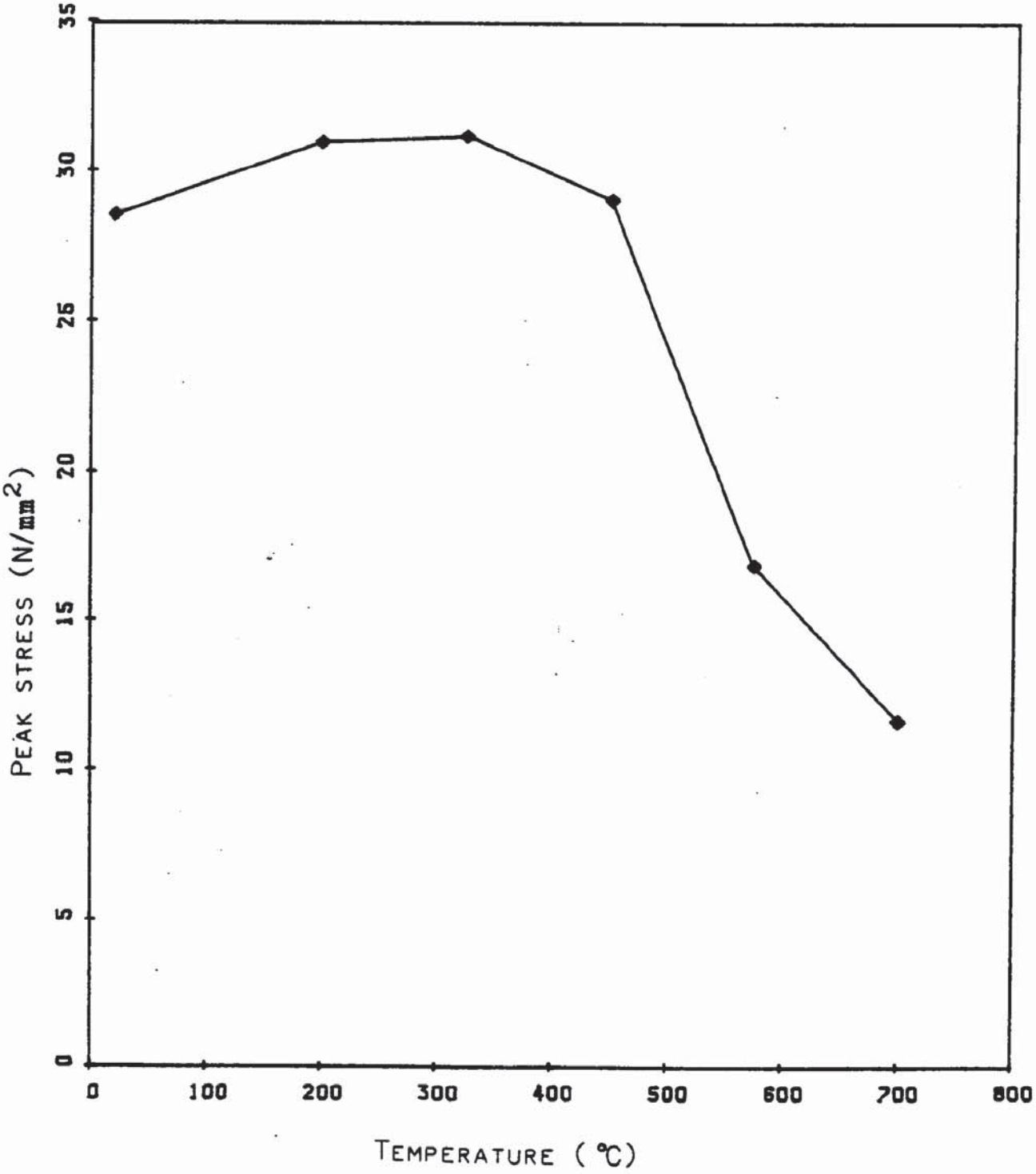

FIG. 8.5 VARIATION OF PEAK STRESS WITH TEMPERATURE (NO PRE-LOAD).

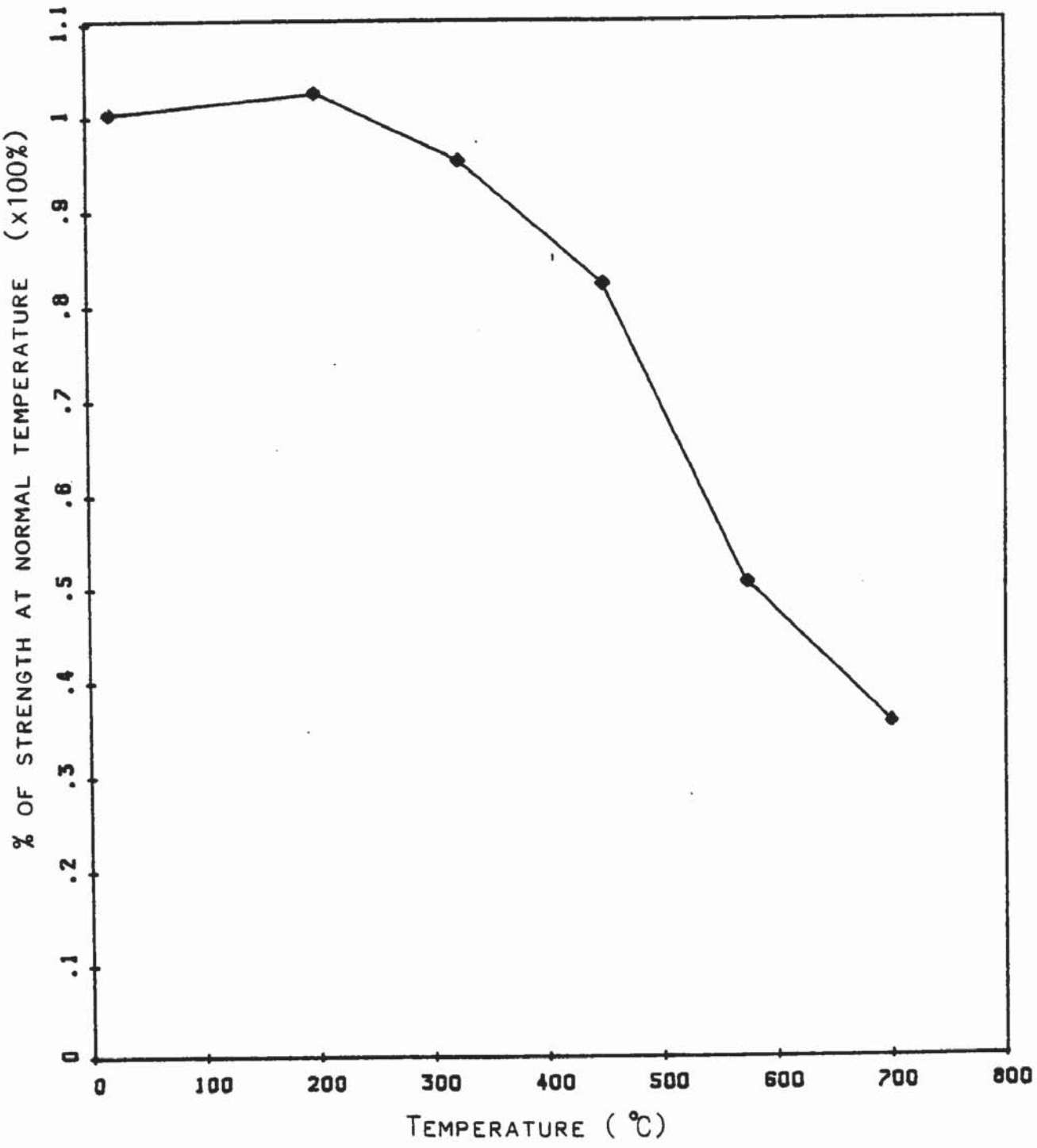

FIG. 8.6 NORMALIZED STRENGTH AT ELEVATED TEMPERATURES (NO PRE-LOAD).

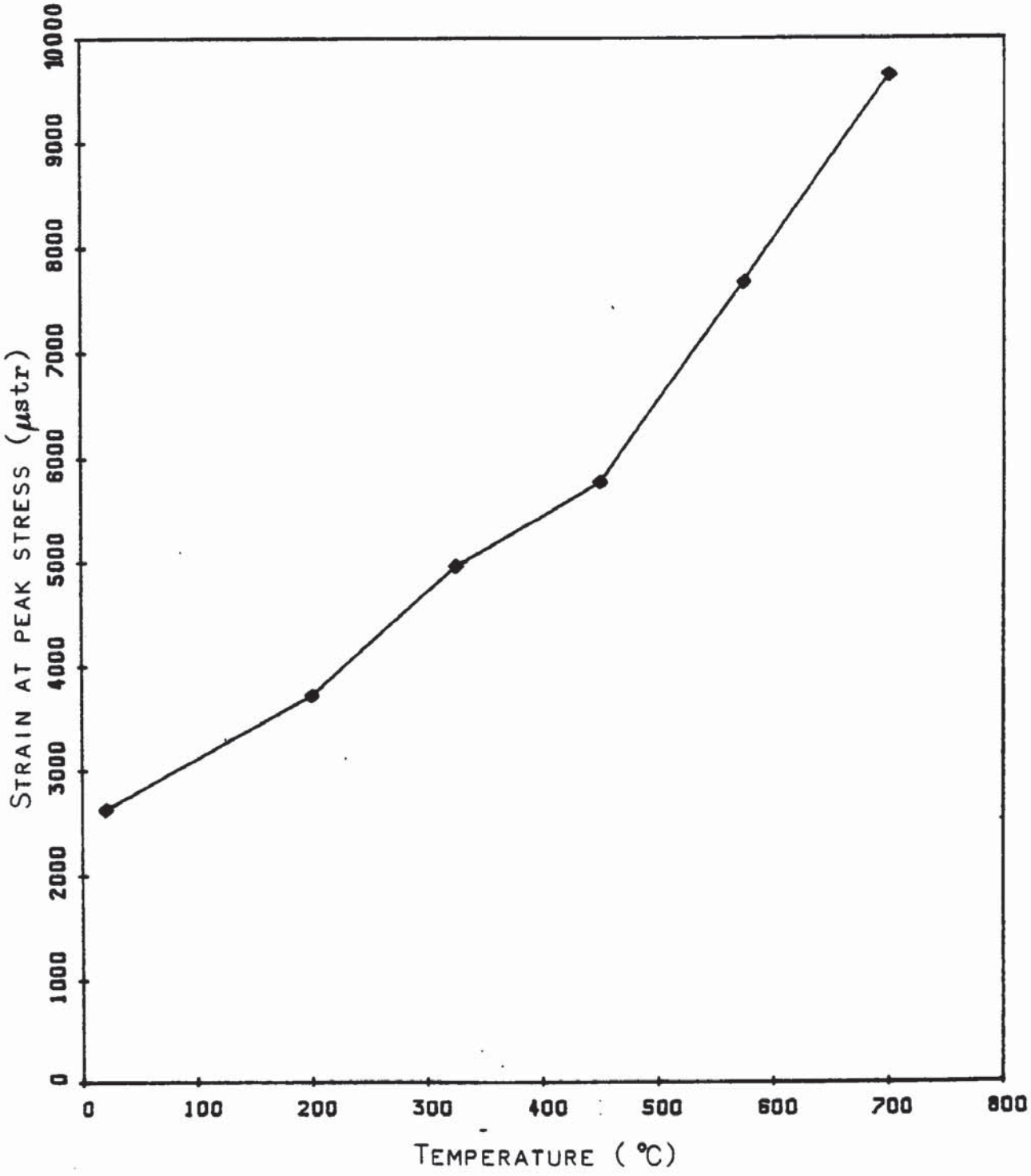

FIG. 8.7 VARIATION OF PEAK STRAIN WITH TEMPERATURE (NO PRE-LOAD).

The last parameter to be examined is the elastic modulus which is defined as the initial tangent modulus determined over the linear part of the stress/strain curve. Young's modulus at different temperatures is measured between Ø and Ø.25 peak stress of each curve as suggested by Baldwin & North (1973). Figure 8.8 shows the plot of E against temperature. The results indicate a significant reduction in Young's modulus with increasing temperature. Similar conclusions have been reported by Phillèo (1958), Cruz (1966) and Baldwin & North (1973) when analysing Furamura's results.

In the following the results are analysed using an approach introduced by Popovics (1973). The method consists of a formula developed to estimate theoretically the complete stress/strain curve of concrete at room temperature. This approach is very useful since it produces directly a non-dimensionalized form of the σ/ϵ diagram. For this reason, it has been decided to fit the experimentally obtained stress/strain curves at elevated temperatures by Popovics equation. Such an equation after rearrangement is of the form :

$$\sigma/\sigma_0 = \epsilon/\epsilon_0 \frac{n}{n - 1 + (\epsilon/\epsilon_0)^n} \qquad (8.2)$$

where the n power is defined by Popovics as an approximate function of the compressive strength.

Writing $s = \sigma/\sigma_0$ (8.3)

and $e = \epsilon/\epsilon_0$ (8.4)

Then the derivative of the rearranged equation (8.2), gives :

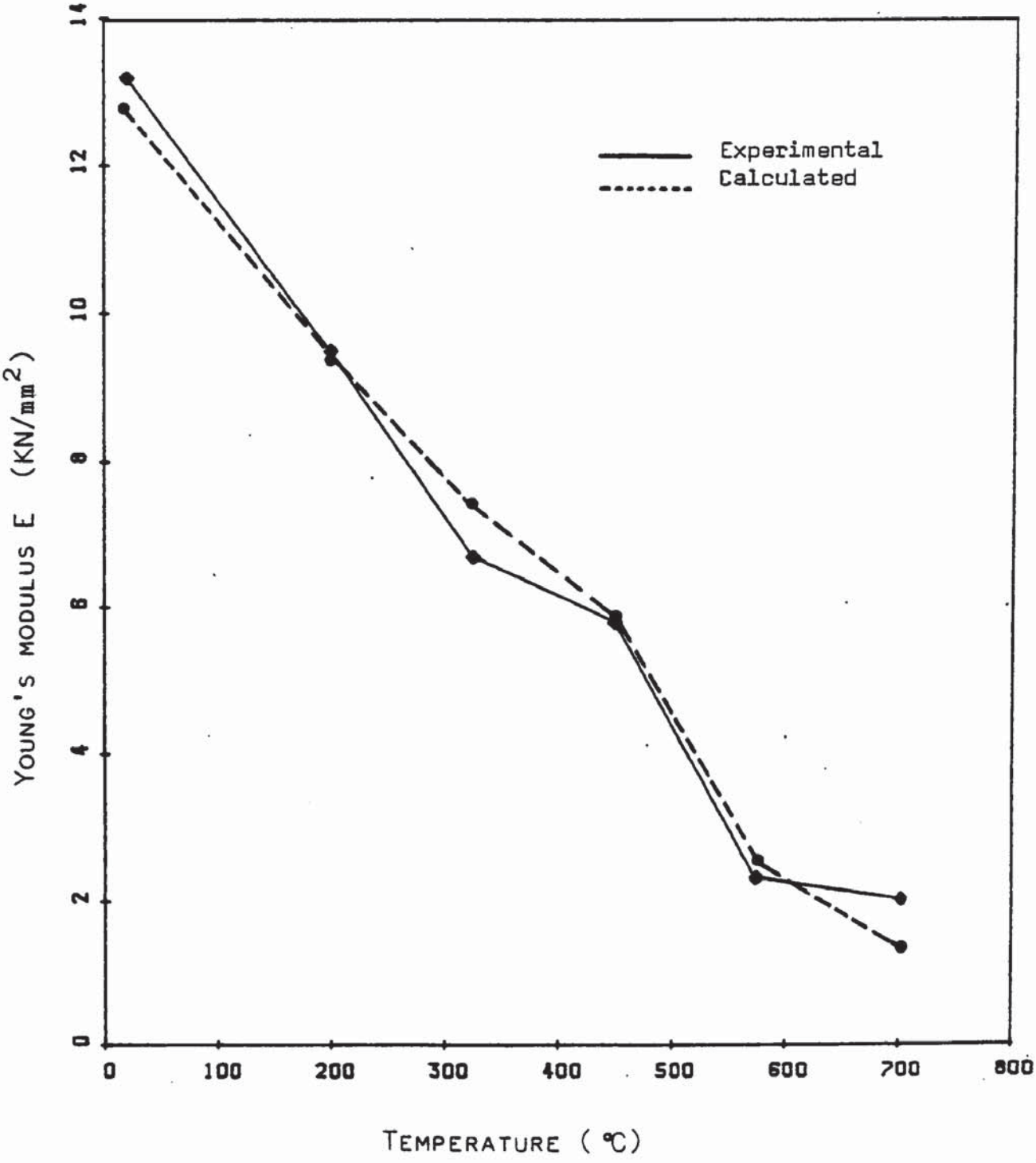

FIG. 8.8 VARIATION OF YOUNG'S MODULUS WITH TEMPERATURE (NO PRE-LOAD).

$$\frac{ds}{de} = \frac{n\,(n-1)\,(1-e^{n})}{[(n-1)+e^{n}]^{2}}$$

with the following boundary condition, e = ∅, leading to :

$$\left.\frac{ds}{de}\right|_{e=\emptyset} = \frac{n\,(n-1)}{(n-1)^{2}} = \frac{n}{n-1} \qquad (8.5)$$

Furthermore, the differentiations of equations 8.3 and 8.4 give

$$d\sigma = \sigma_{0}\,ds \qquad \text{and}$$

$$d\epsilon = \epsilon_{0}\,de$$

Hence, upon rearrangement Eq. 8.5 becomes :

$$\left.\frac{d\sigma}{d\epsilon}\right|_{\epsilon=\emptyset} = \frac{\sigma_{0}}{\epsilon_{0}}\left.\frac{ds}{de}\right|_{e=\emptyset} = \frac{\sigma_{0}}{\epsilon_{0}}\,\frac{n}{n-1} = E \qquad (8.6)$$

This is an expression to evaluate Young's modulus.

Introducing a dimensionless constant λ, Eq. 8.6 can be rewritten,

$$\frac{\sigma_{0}}{\epsilon_{0}E} = \frac{n-1}{n} = 1/\lambda \qquad (8.7)$$

Where λ is the slope of the straight line obtained when plotting the values of E at high temperatures against the stress/strain parameter σ_{0}/ϵ_{0} reported earlier in this section. The value of $\lambda = E / (\sigma_{0}/\epsilon_{0})$ was found as 1.16.

If Eq. 8.8 is rearranged it will yield an expression for the determination of n :

$$n = 1 / (1 - 1/\lambda) \qquad (8.8)$$

from which n = 7.25.

This value, however, is found to be high to fit the descending branch although a very good fit is obtained for the ascending portion. It has been therefore decided to use two different values of n to fit

the respective branches of the stress/strain curve of "un-loaded" specimens. For the ascending portion, the initial value $n_1 = 7.25$ is maintained, for the descending branch, however, a new value n_2 has been chosen after trying several values. This method of determining the second value of n was used in order to avoid undertaking a complicated optimization of n.

Let n_1 and n_2 be the values of n for the ascending and the descending portion respectively. By considering and rearranging Eq. 8.2, it follows :

$$s = \frac{e}{1 - 1 / n_1 + 1 / n_1 \, e^{n_1}} \qquad (8.9)$$

from which it can be seen that if n_1 is large $1/n_1 \, (e^{n_1} - 1)$ will be large, and a small value of stress will result for $e > 1$. Thus $1/n_1 \, . \, (e^{n_1}-1) + 1$ should decrease, and therefore n_1 should be reduced, consequently $n_2 < n_1$ where n_2 is the new value chosen.

Using the two values ($n_1 = 7.25$ and $n_2 = 5.5$) the complete stress/strain curve (Eq. 8.2) when superimposed on the experimental data produces a reasonable fit as shown in Fig. 8.9. When compared with the polynomial fit, it can be seen that a similar shape is obtained for the ascending portion and there is no significant difference between the values of stress determined by both methods.

According to Popovics, the long fraction of Eq. 8.2 represents the deviation from the linear elasticity. This result is now examined mathematically by using the diagram of Fig. 8.10 :

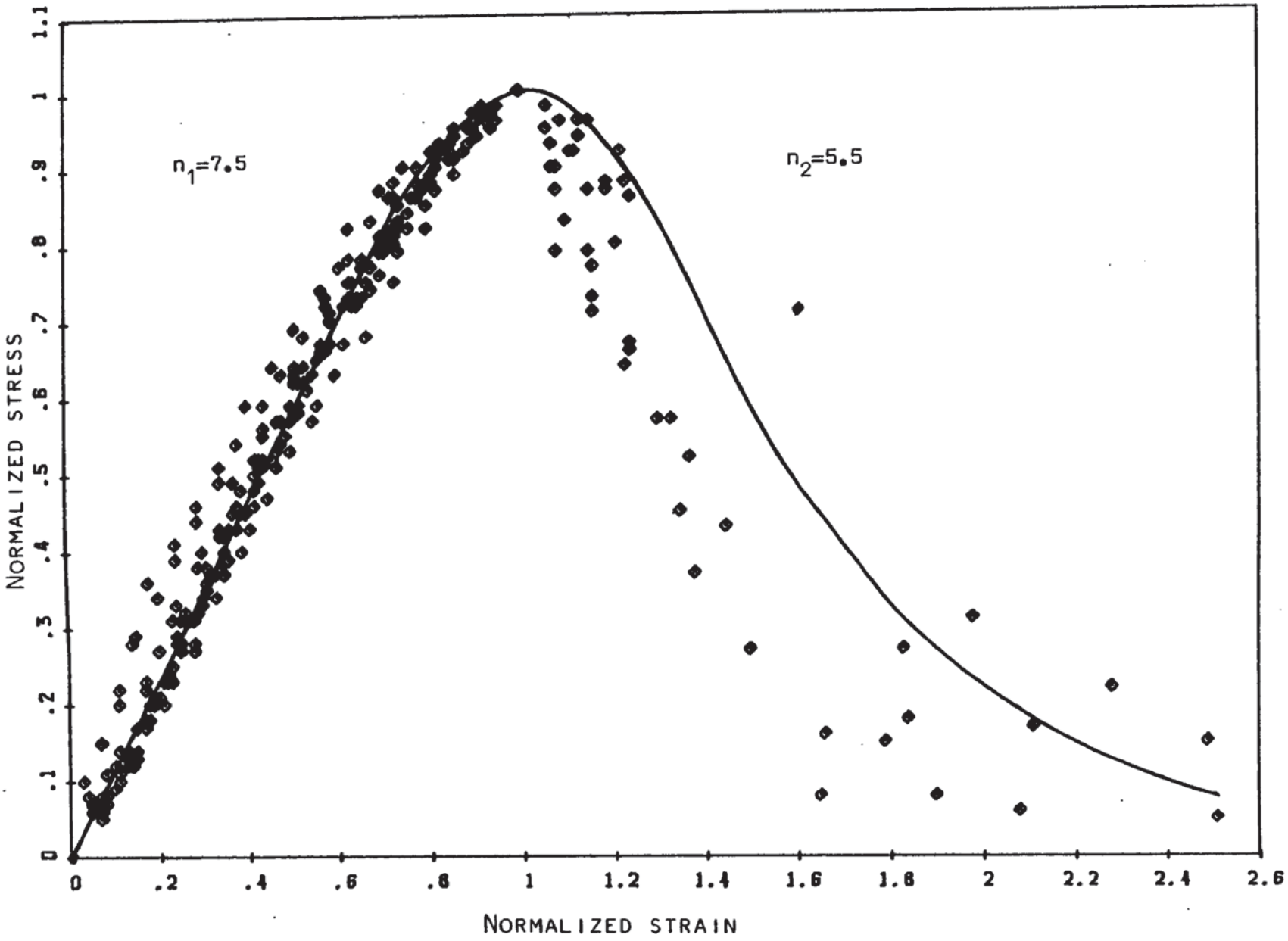

FIG. 8.9 NORMALIZED STRESS/STRAIN CURVES (NO PRE-LOAD) - POPOVIC'S EQUATION FIT.

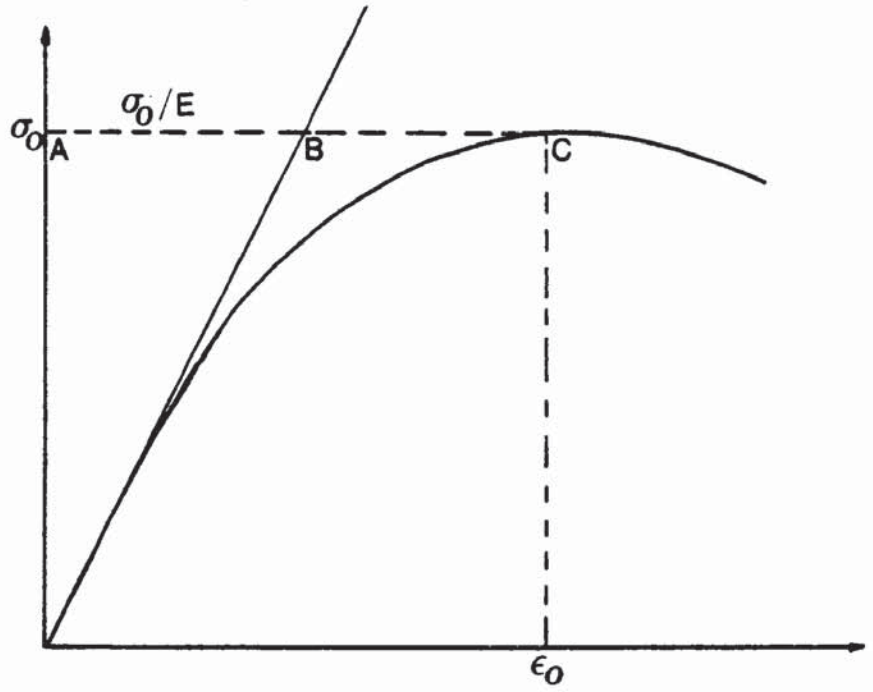

Fig. 8.1Ø : Stress/strain diagram

By using Eq. 8.7 and introducing the ratio AB / AC, it follows;

$$1/\lambda = \sigma_0/E\epsilon_0 = AB / AC \qquad (8.1Ø)$$

this is now substituted into Eq. 8.8 to give :

$$n = 1 / (1 - AB / AC) \qquad (8.11)$$

From which $n = 1 / ((AC - AB) / AC) = 1 / (BC / AC)$ (8.12)

This relation indicates a deviation of the curve from linearity. This can be expressed as :

$$n = \epsilon_0 / \text{error from linearity} = AC / BC \qquad (8.13)$$

It can be concluded that n is a measure of the lack of linearity of fit.

The elastic modulus can be expressed by a relation of the form

$$E = \sigma_0/\epsilon_0 \cdot n / (n - 1)$$

This is Eq. 8.6 repeated, where $n / (n - 1) = \lambda = 1.16$.

This expression of E is similar to that introduced by Baldwin & North (1973). The variation of Young's modulus with temperature as determined by the above equation is plotted in Fig. 8.8 and represented by the dashed line, whereas the solid line represents the experimental values of E measured between Ø and Ø.25σ_o for each stress/strain curve. It can be seen that although the two curves are similar in shape, however a slight difference, appears in the locations of some points. This is mainly due to two types of random errors which arise when estimating the elastic modulus measured between Ø and Ø.25σ_o , and when using λ = n / (n - 1) = 1.16 which is in fact an average value of those obtained at different temperatures. The slight variation between the two curves is therefore acceptable.

8.2.2 Stress-strain behaviour of "pre-loaded" concrete specimens :

The stress/strain results obtained for the two stress levels (Ø.2 and Ø.6 f'_c) are plotted in Figs. 7.2 and 7.3. Similarly, these data have been normalized and one curve has resulted for all temperatures. The normalized data have been fitted by a polynomial of degree 1Ø. Figures 8.11 and 8.12 show the plot of σ/σ_o against ϵ/ϵ_o for stress levels of Ø.2 and Ø.6 f'_c respectively. The superimposed curve for each stress level can be seen on the graphs of Figs. 8.11 and 8.12. The results as plotted are situated on the same curve up to the peak and thereafter the data on the descending portion are scattered. Although the cracking was reduced by keeping a constant load on the specimen

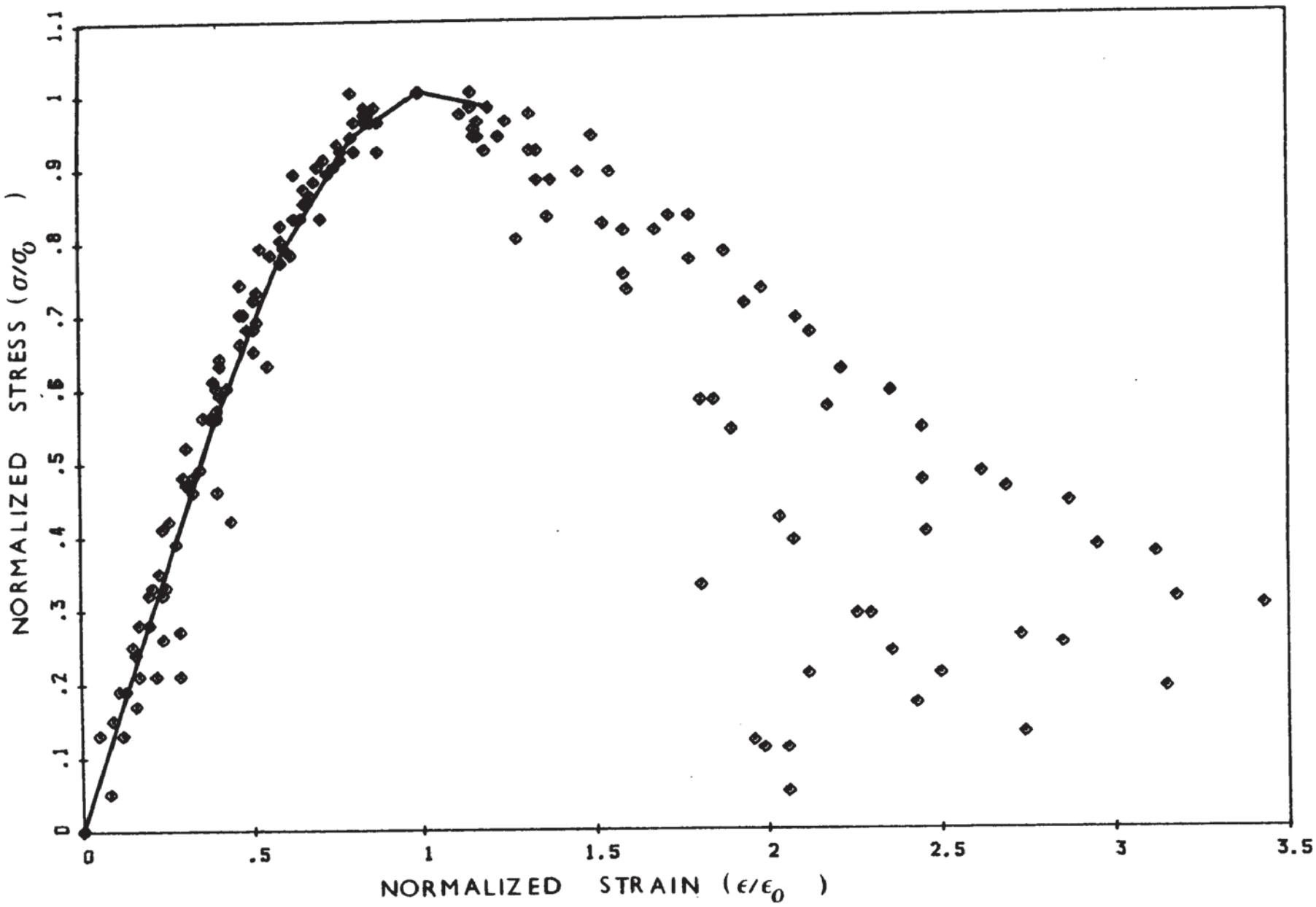

FIG. 8.11 NORMALIZED STRESS/STRAIN CURVES (PRE-LOAD=20%) - POLYNOMIAL FIT : DEGREE 10

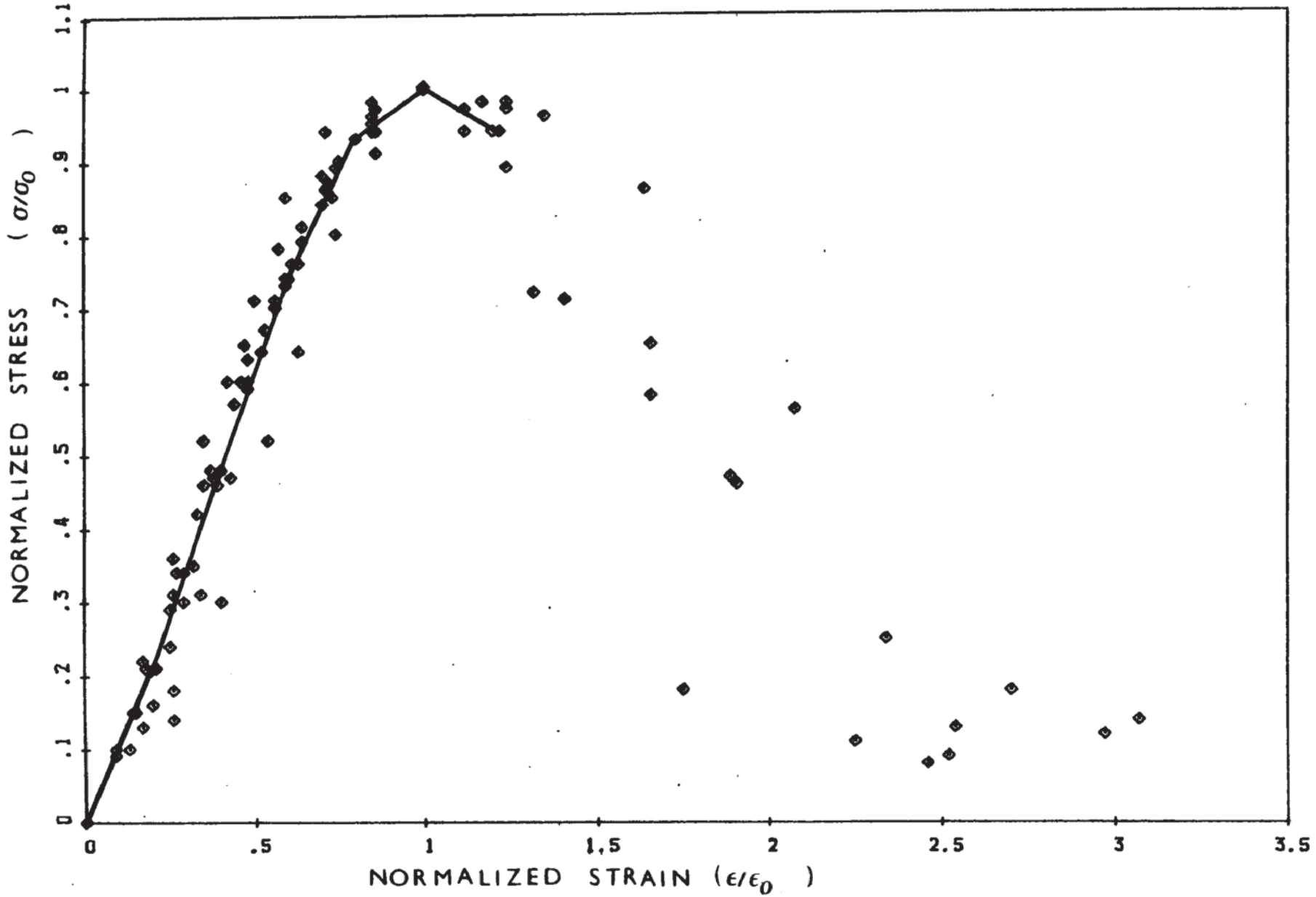

FIG. 8.12 NORMALIZED STRESS/STRAIN CURVES (PRE-LOAD=60%) - POLYNOMIAL FIT : DEGREE 10

during heating, this did not prevent the strain softening from being influenced by the cracking and the temperature, and thus resulting in the large scatter indicated.

The ratio of Young's modulus to a stress/strain parameter has been also examined for the two sets of curves obtained at Ø.2 and Ø.6 f'_c . Figures 8.13 and 8.14 show the plot of E against σ_o/ϵ_o . It can also be seen that the results are represented by straight lines having slopes of 1.34 and 1.Ø2 for the stress levels of Ø.2 and Ø.6 f' respectively. In both cases, the results at room temperature have been omitted. The results obtained by Schneider (1976) also show a similar trend and that the results from pre-loaded specimens can be normalized in this fashion.

The normalized stress/strain curves plotted are of the form $\sigma/\sigma_o = f(\epsilon/\epsilon_o)$ similar to those obtained at zero stress level. Analogous conclusions can be drawn, although the stress/strain relationships are affected by the magnitude of the pre-load. Thus all the curves for different temperatures and for the same pre-load are represented by a single curve.

The stress/strain curves obtained for the two stress levels (Ø.2 and Ø.6 f'_c) exhibit a similar shape as those of "un-loaded" specimens but with a steeper ascending slope as a result of the presence of a load during heating. In order to study the overall stress/strain behaviour, the main derived mechanical properties already discussed in Chapter 7 are now examined.

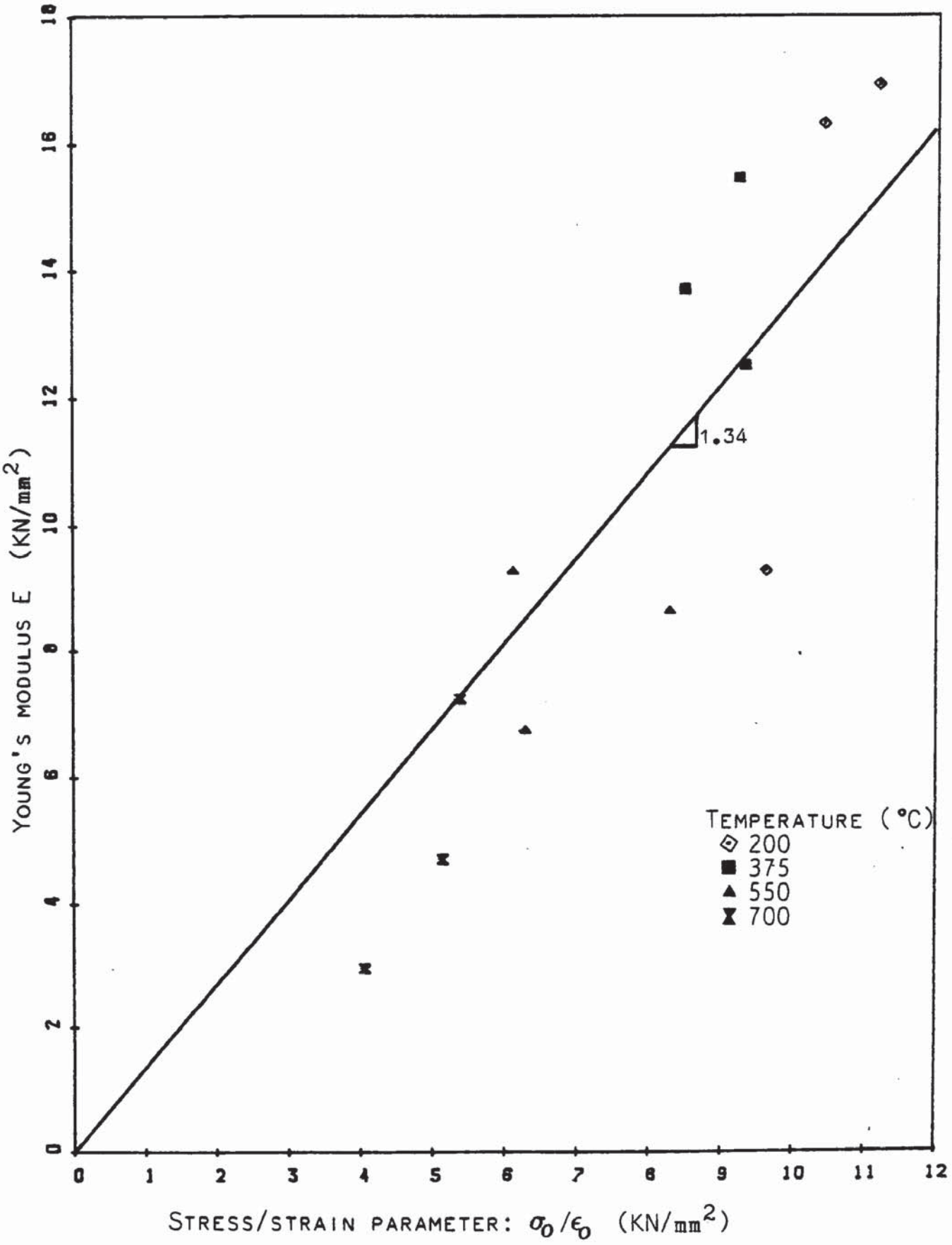

FIG. 8.13 YOUNG'S MODULUS AGAINST STRESS/STRAIN PARAMETER (PRE-LOAD = 20%).

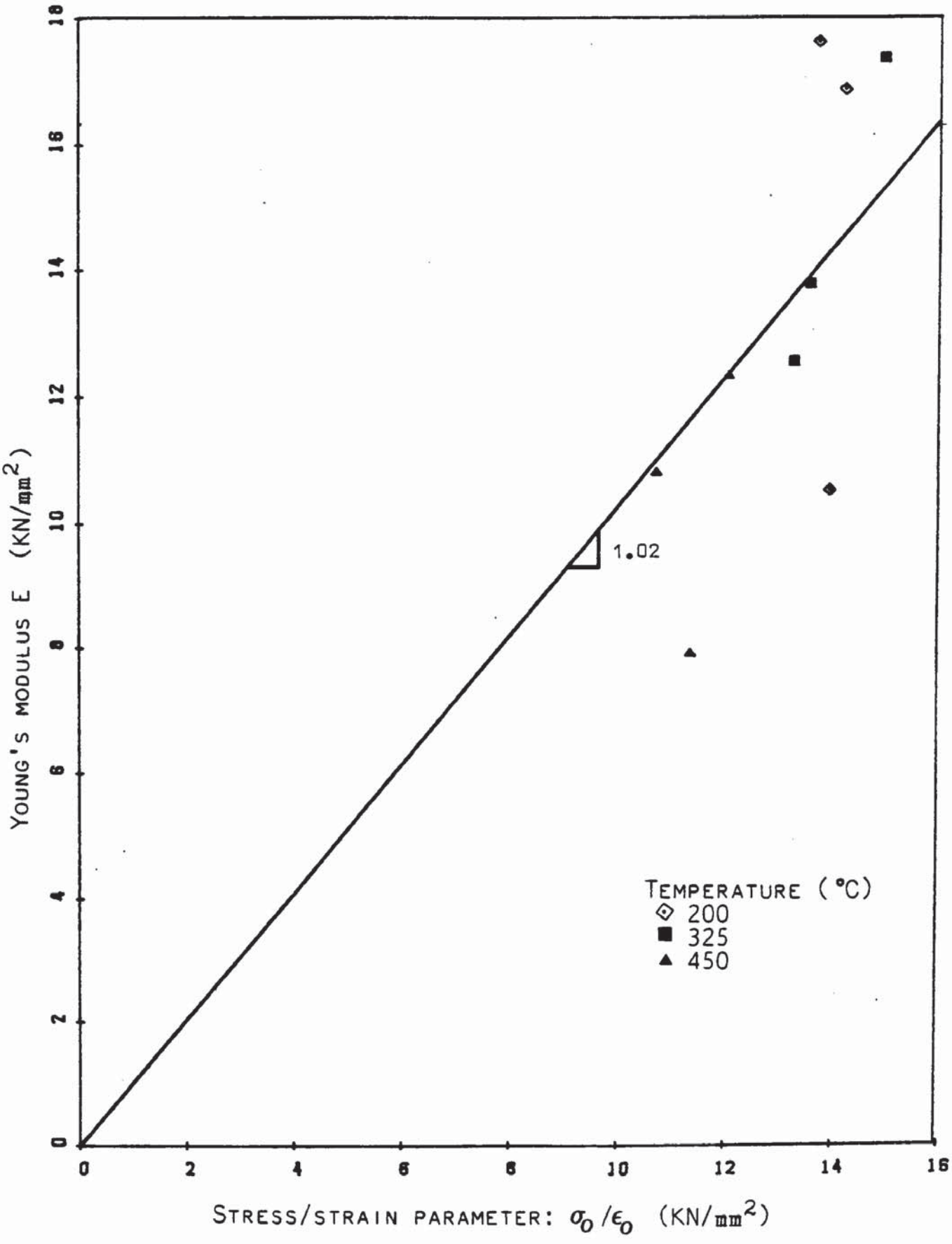

FIG. 8.14 YOUNG'S MODULUS AGAINST STRESS/STRAIN PARAMETER (PRE-LOAD = 60%).

The strength of concrete is dependent on its microstructure. The presence of a load while heating delays the formation of cracks and therefore prevents the microstructure from rupture (splitting). Figures 8.15 to 8.18 show for the two stress levels considered, the effect of temperature upon the peak stress and the strength of concrete as a percentage of the strength at 20 °C. The results show essentially that the concrete specimens heated under load maintained their strength up to 400 °C and 450 °C for 0.2 and 0.6 f'_c respectively. At a temperature of 375 °C the strength, for 0.2 f'_c , increased by 12% whereas at 325 °C the strength, for 0.6 f'_c , rose by 14.5%. However the specimens stressed to 0.2 f'_c began to show an appreciable loss of strength at 500 °C.

The pre-loaded specimens retain more strength at high temperatures than the un-loaded ones. Malhotra (1956) and Abrams (1969) reported similar trends of results.

The other major parameter to be considered is the strain at peak stress. A plot of ϵ_0 against temperature (T) is shown in Figs. 8.19 and 8.20 for the corresponding stress level. The information provided by these graphs indicates that the peak strain is very much influenced by the sustained load during heating. The results show that the presence of a pre-load reduces considerably the ductility gained at high temperatures. This has also been reported by Fischer (1970), Schneider (1976) and by Sullivan & Dougill (1983).

The variation curves of the elastic modulus with temperature shown in Figs. 8.21 and 8.22 are drawn for 0.2 and 0.6 f'_c

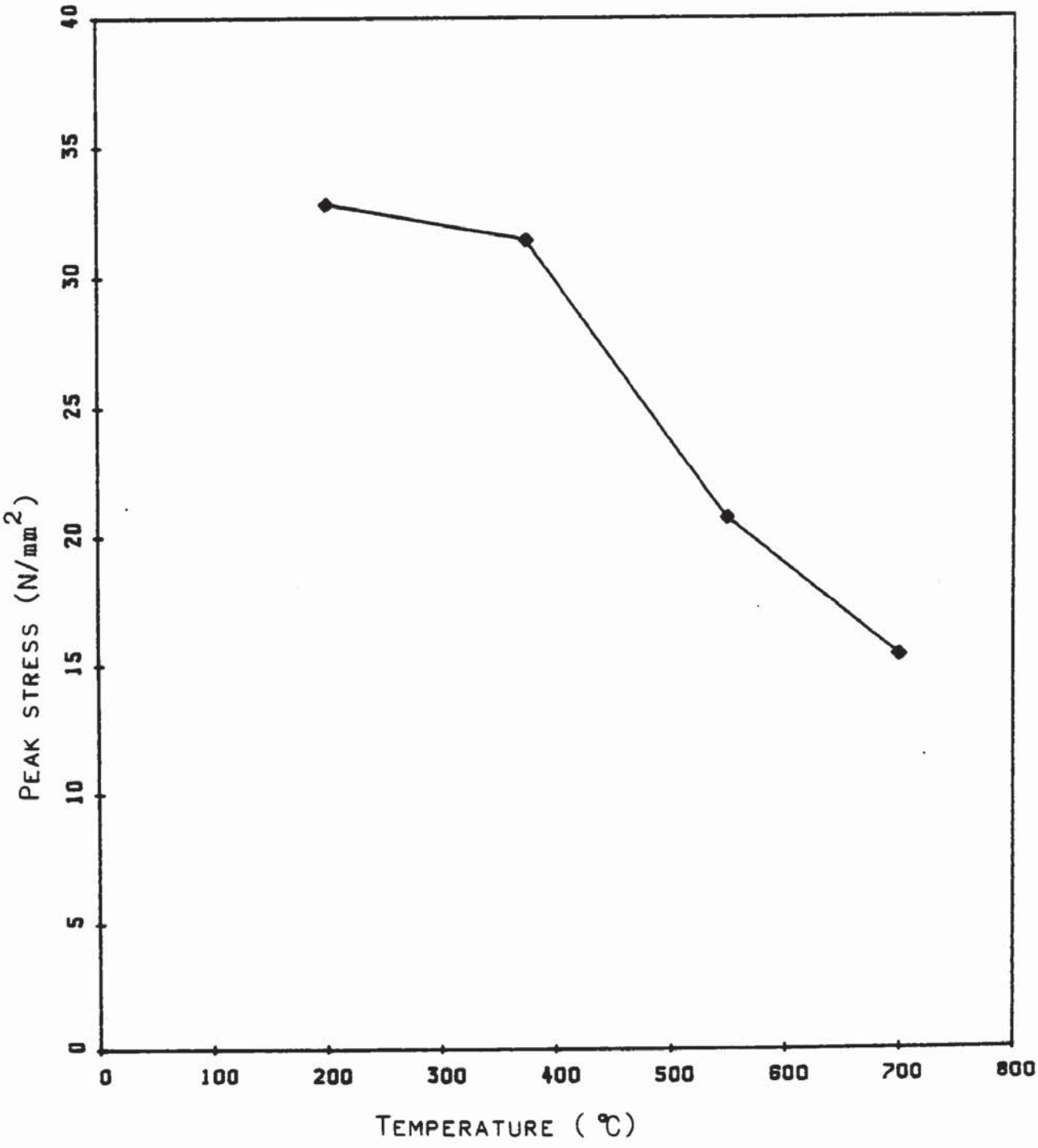

FIG. 8.15 VARIATION OF PEAK STRESS WITH TEMPERATURE (PRE-LOAD = 20%).

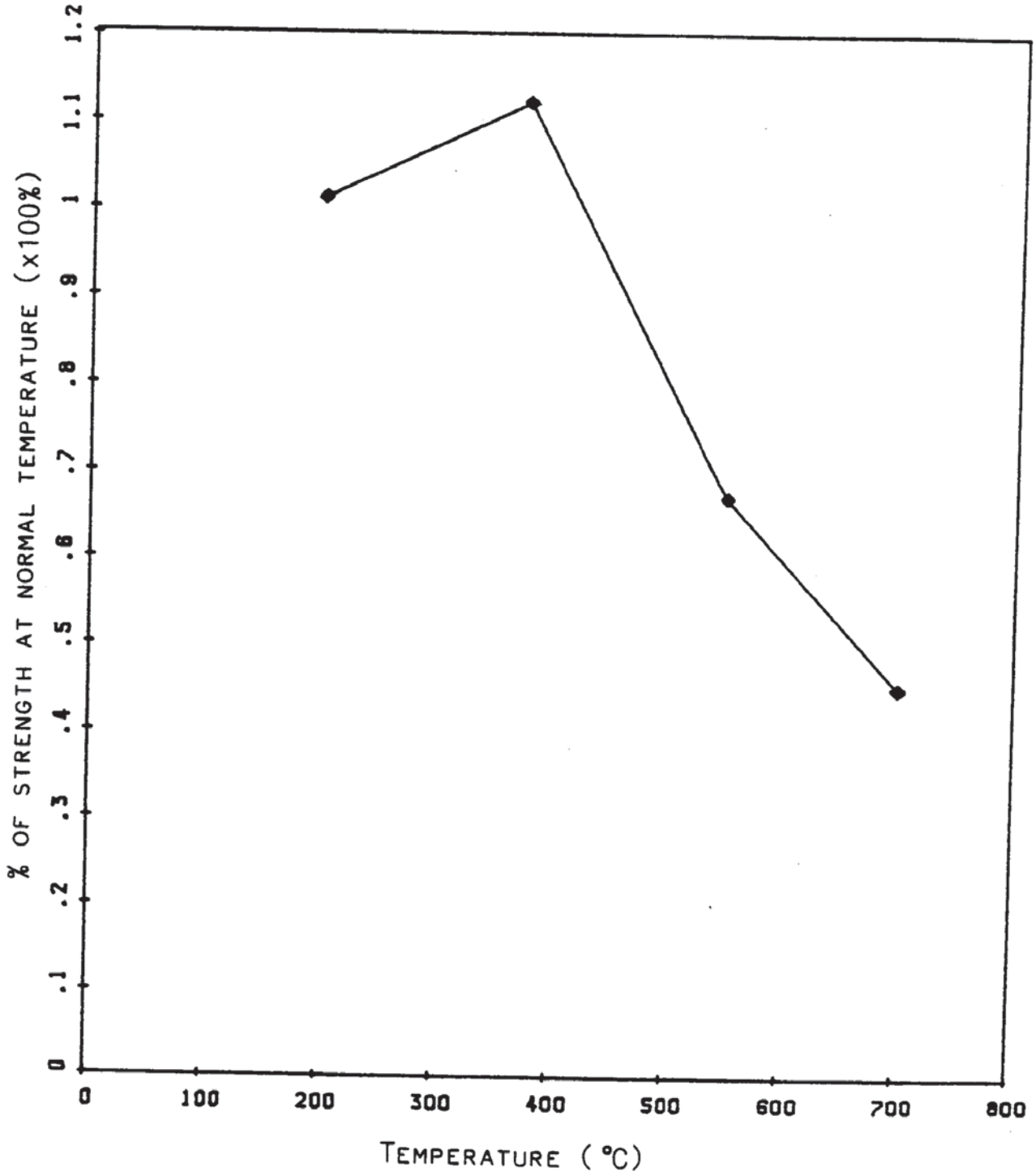

FIG. 8.16 NORMALIZED STRENGTH AT ELEVATED TEMPERATURES (PRE-LOAD = 20%).

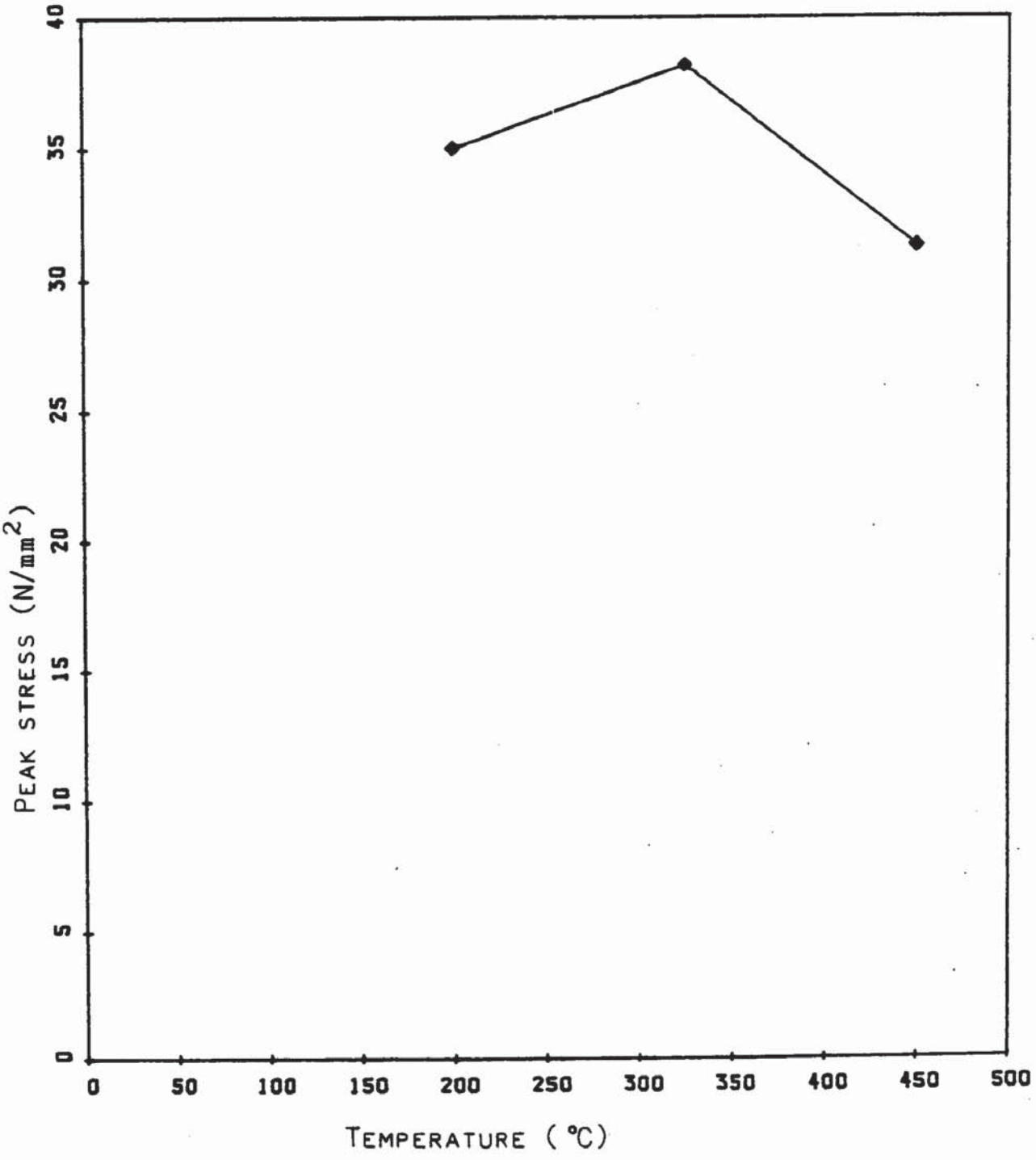

FIG. 8.17 VARIATION OF PEAK STRESS WITH TEMPERATURE (PRE-LOAD = 60%).

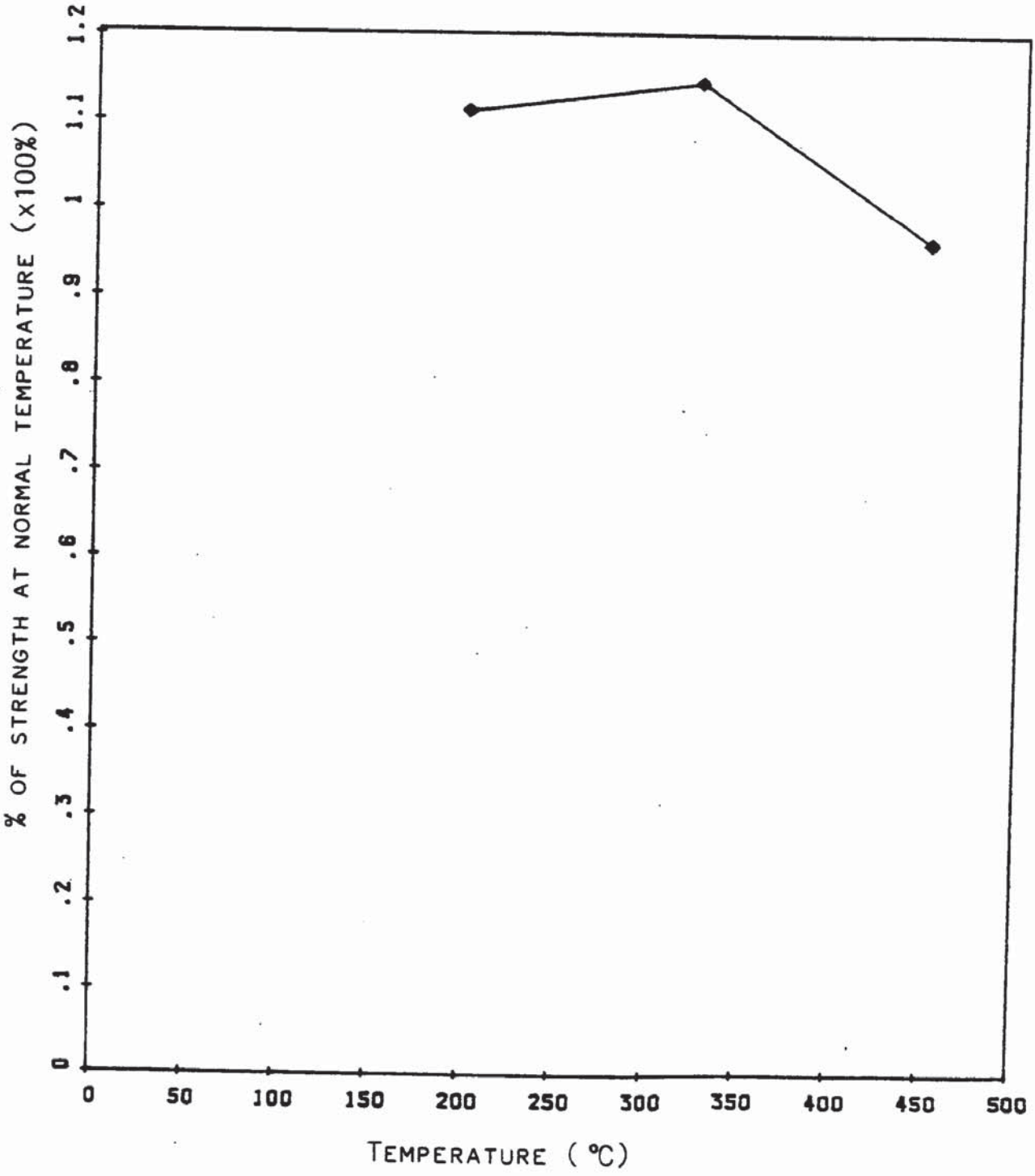

FIG. 8.18 NORMALIZED STRENGTH AT ELEVATED TEMPERATURES (PRE-LOAD = 60%).

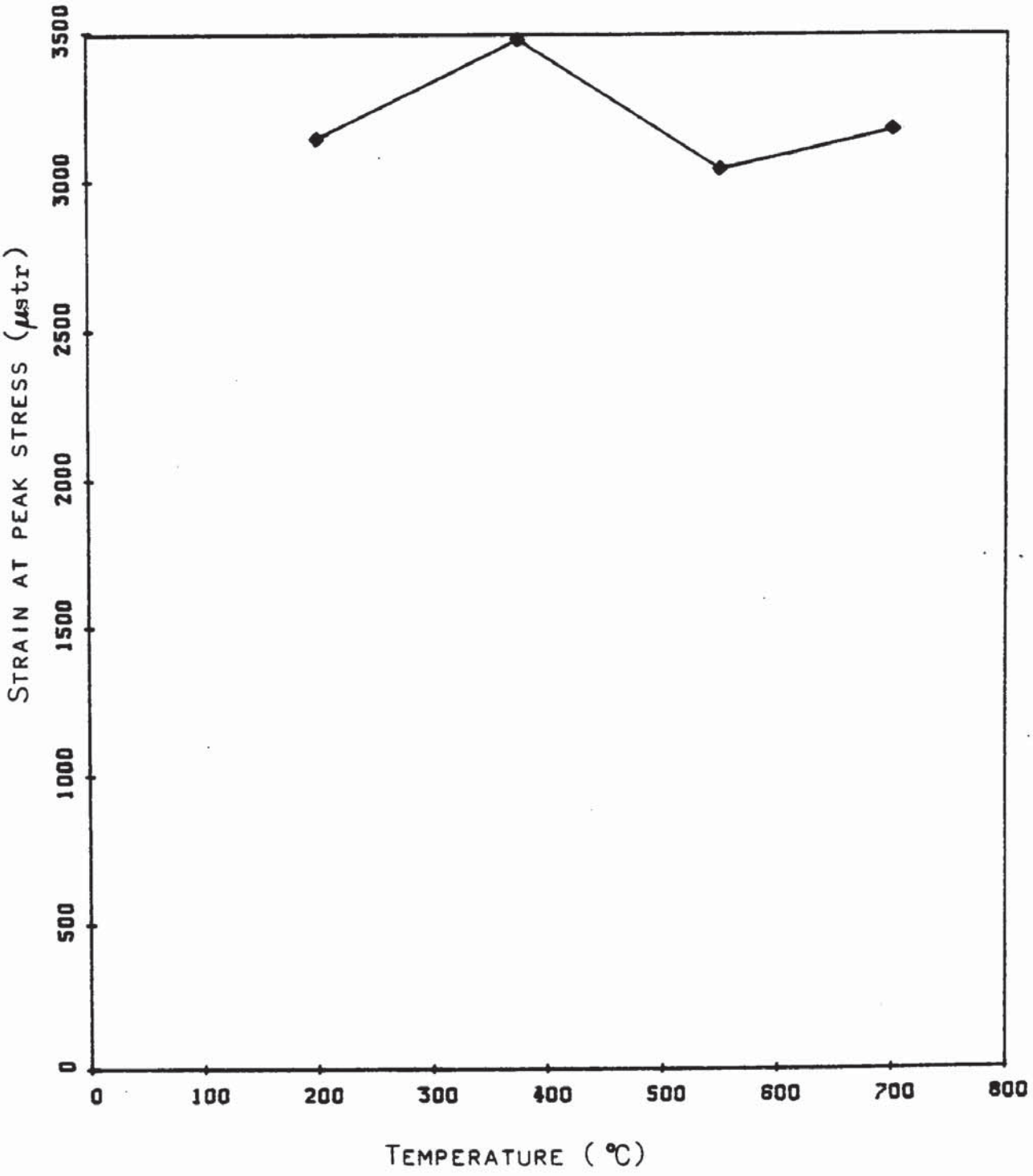

FIG. 8.19 VARIATION OF PEAK STRAIN WITH TEMPERATURE (PRE-LOAD = 20%).

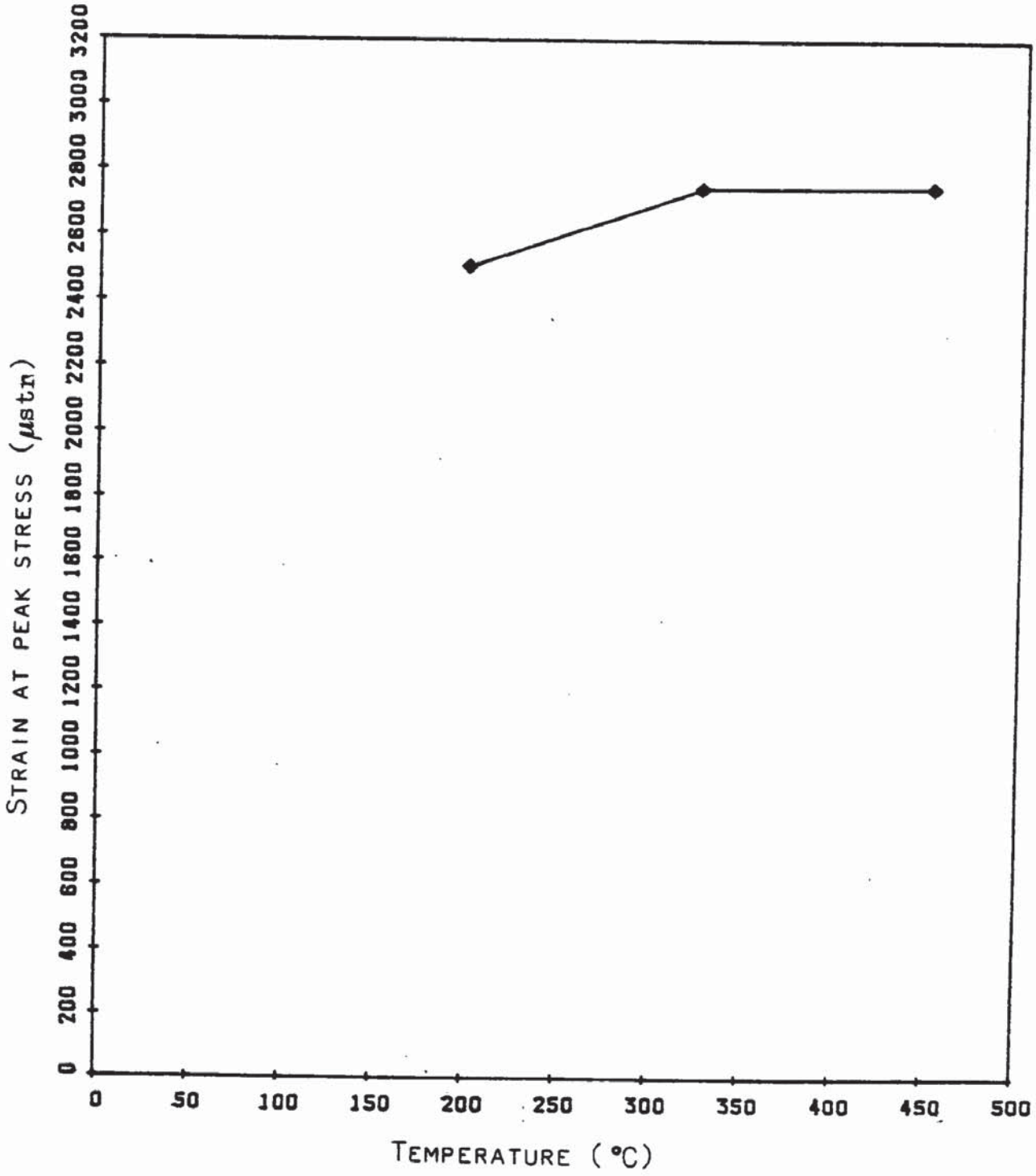

FIG. 8.20 VARIATION OF PEAK STRAIN WITH TEMPERATURE (PRE-LOAD = 60%).

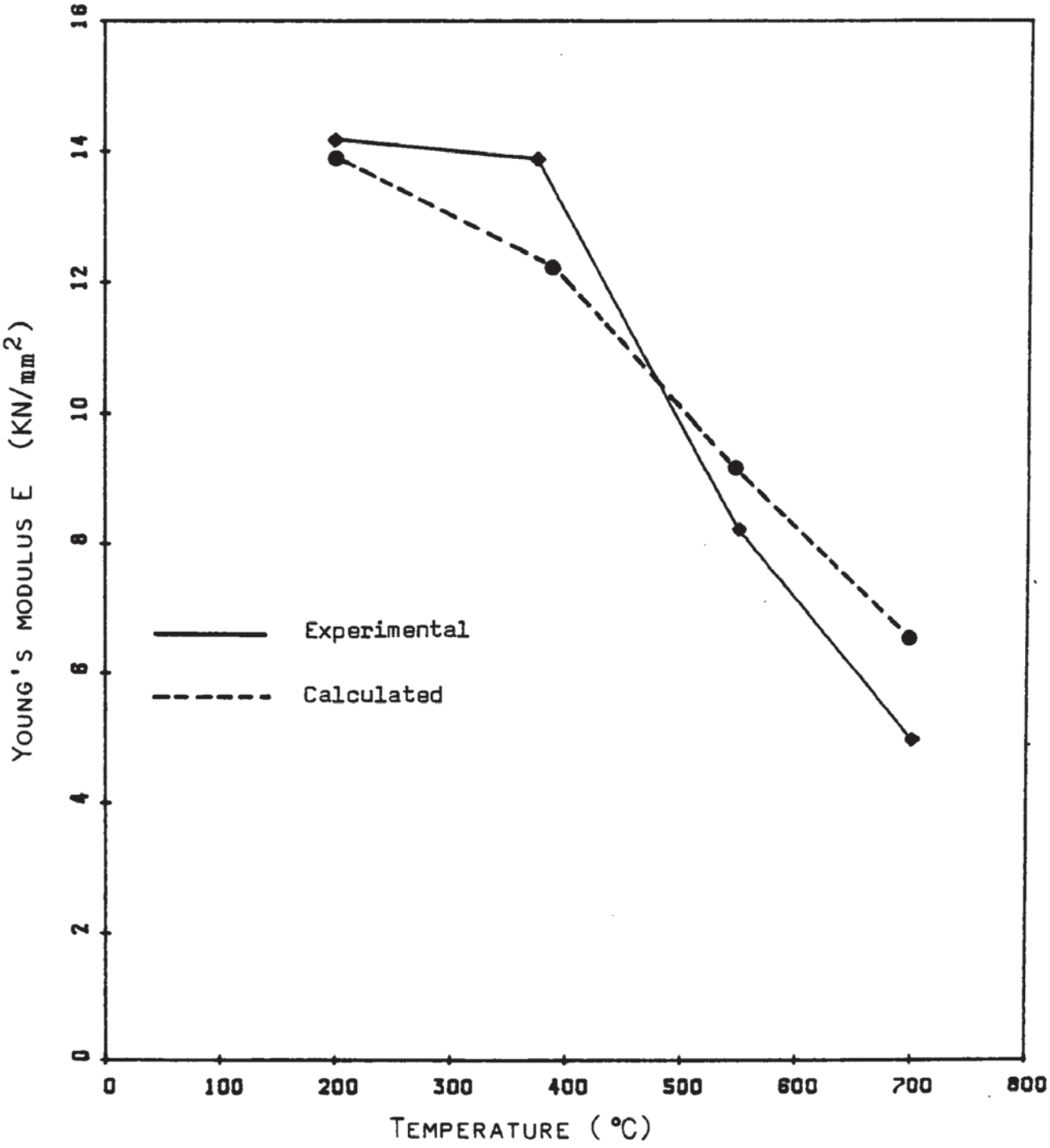

FIG. 8.21 VARIATION OF YOUNG'S MODULUS WITH TEMPERATURE (PRE-LOAD = 20%).

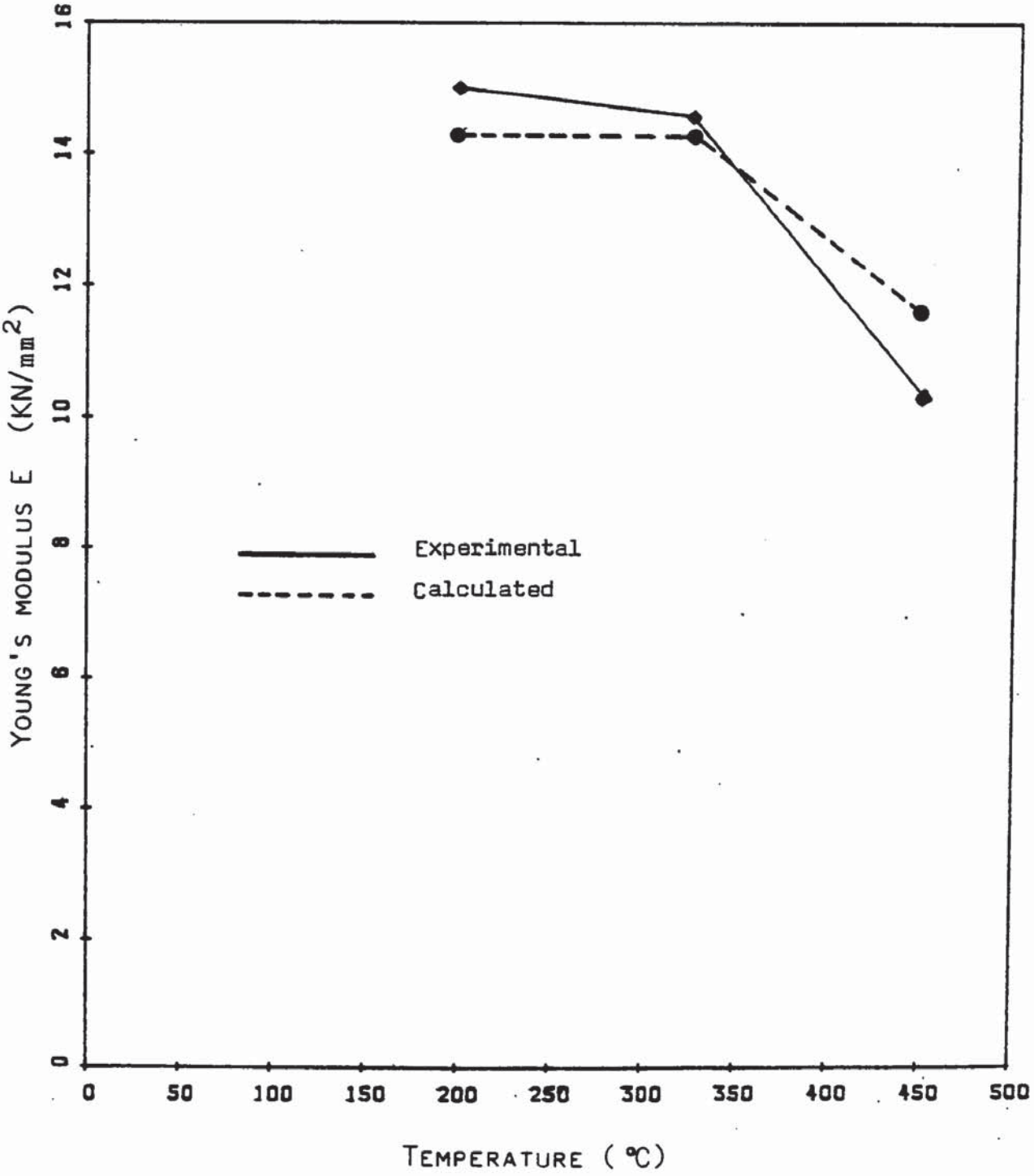

FIG. 8.22 VARIATION OF YOUNG'S MODULUS WITH TEMPERATURE (PRE-LOAD = 60%).

respectively. The values of E are estimated from the initial slope of the stress/strain curves between Ø and Ø.25 the maximum stress at each temperature. The results indicate that Young's modulus of concrete heated under load undergoes a less reduction in the early stages of heating and then decreases rapidly and mainly at 575 °C when the phase changes in the quartz take place. The plot of E against T for Ø.2 and Ø.6 f'_c shows, however, that the elastic modulus is either constant or slightly increased particularly for T < 4ØØ °C and then decreases linearly. The discussion cannot be further extended because of the relatively small amount of data obtained.

For comparison purposes, the data obtained from tests on pre-loaded specimens, are now analysed using Popovics approach. Here again, two values of n have to be determined for each set of data corresponding to the stress levels Ø.2 and Ø.6 f'_c respectively. The same rearranged equation (Eq. 8.2) introduced earlier is used, and the same method is applied to find the values of the power n. It has been found, however, that for Ø.2 f'_c the actual value of n obtained best fits the ascending as well as the descending branch of the normalized stress-strain curve. This value is calculated using Eq. 8.8 which gives $n_3 = 3.78$. The superimposed curve determined by Eq. 8.2 is then plotted in Fig. 8.23. On the other hand, the second set of data needed two values of n to be determined. The first estimation $n_4 = 51$ is obtained by Eq. 8.8, the second one, however, is chosen after trying several values of n as indicated in the previous section (8.21). This resulted in a new estimation $n_5 = 4.5$. The stress/strain curve then

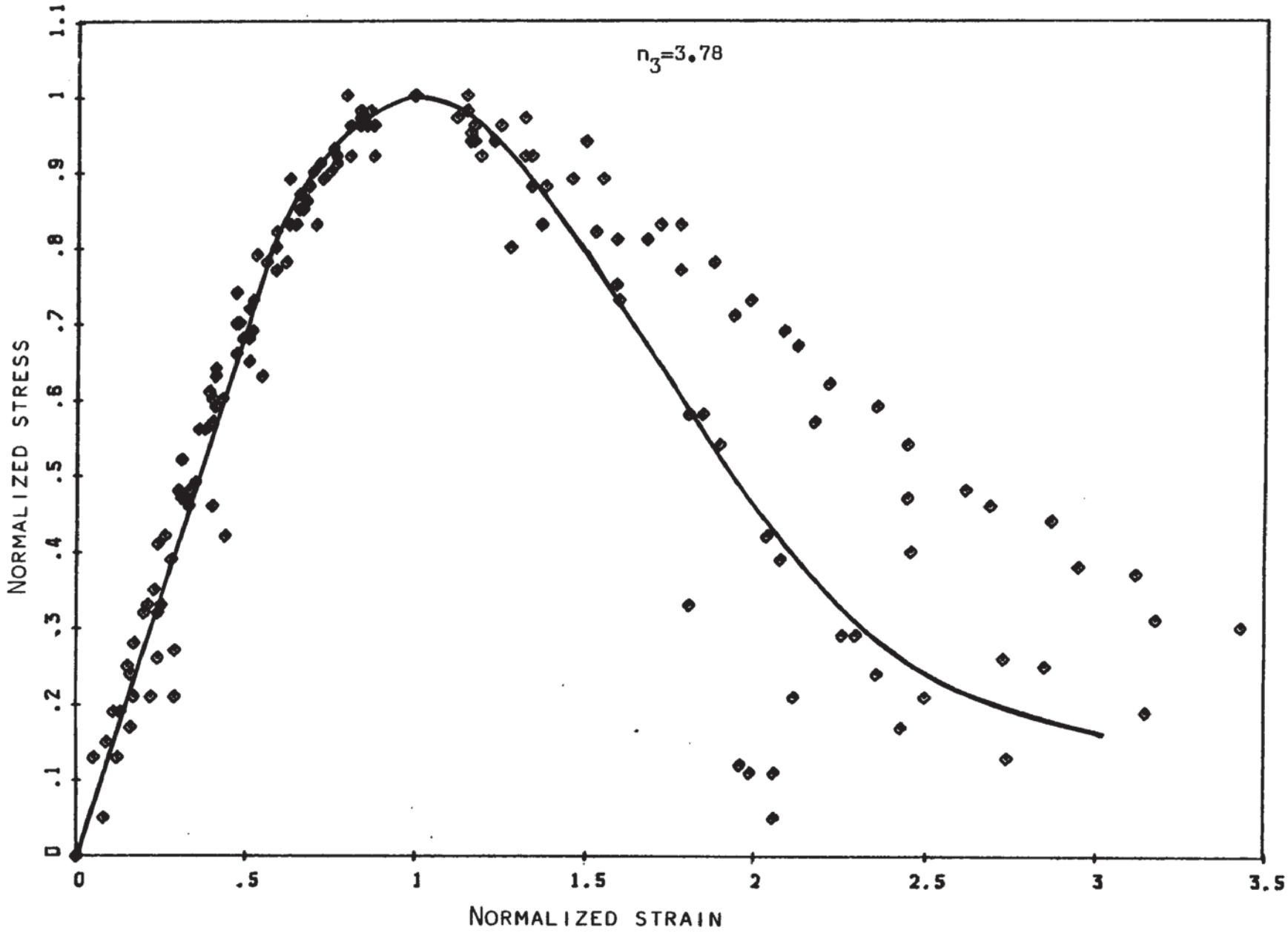

FIG. 8.23 NORMALIZED STRESS/STRAIN CURVES (PRE-LOAD = 20%) - POPOVIC'S EQUATION FIT.

determined fit well the experimental data and is plotted in Fig. 8.24. The curve drawn in this graph represents the results obtained for a stress level of Ø.6 f'_c.

It can be seen that there is no difference between the values obtained for the ascending portion of the stress/strain curve by either the polynomial or Popovic's equation.

Similarly, the elastic modulus for both stress levels can be expressed by the following equation :

$$E = \sigma_0/\epsilon_0 \cdot n / (n - 1)$$

The measurement of E as obtained by the above relation for Ø.2 and Ø.6 f'_c are plotted in Figs. 8.21 and 8.22 respectively. The resulting curves are identified by the dashed lines in both graphs. Here again, the slight variation observed between the experimental and the calculated values of E are due to errors occuring in the estimation of the initial tangent modulus and the value of $\lambda = n / n-1$ which in fact represents an average value.

8.3 CREEP BEHAVIOUR :

8.3.1 Introduction :

In this section, the time-dependent behaviour of concrete is examined. In Chapter 7, creep results obtained over a 5 hour period test have been presented. The observed inelastic deformation of concrete specimens is typically a function of stress, temperature and time. Typical creep curves are shown in Figs. 7.9 - 7.11,

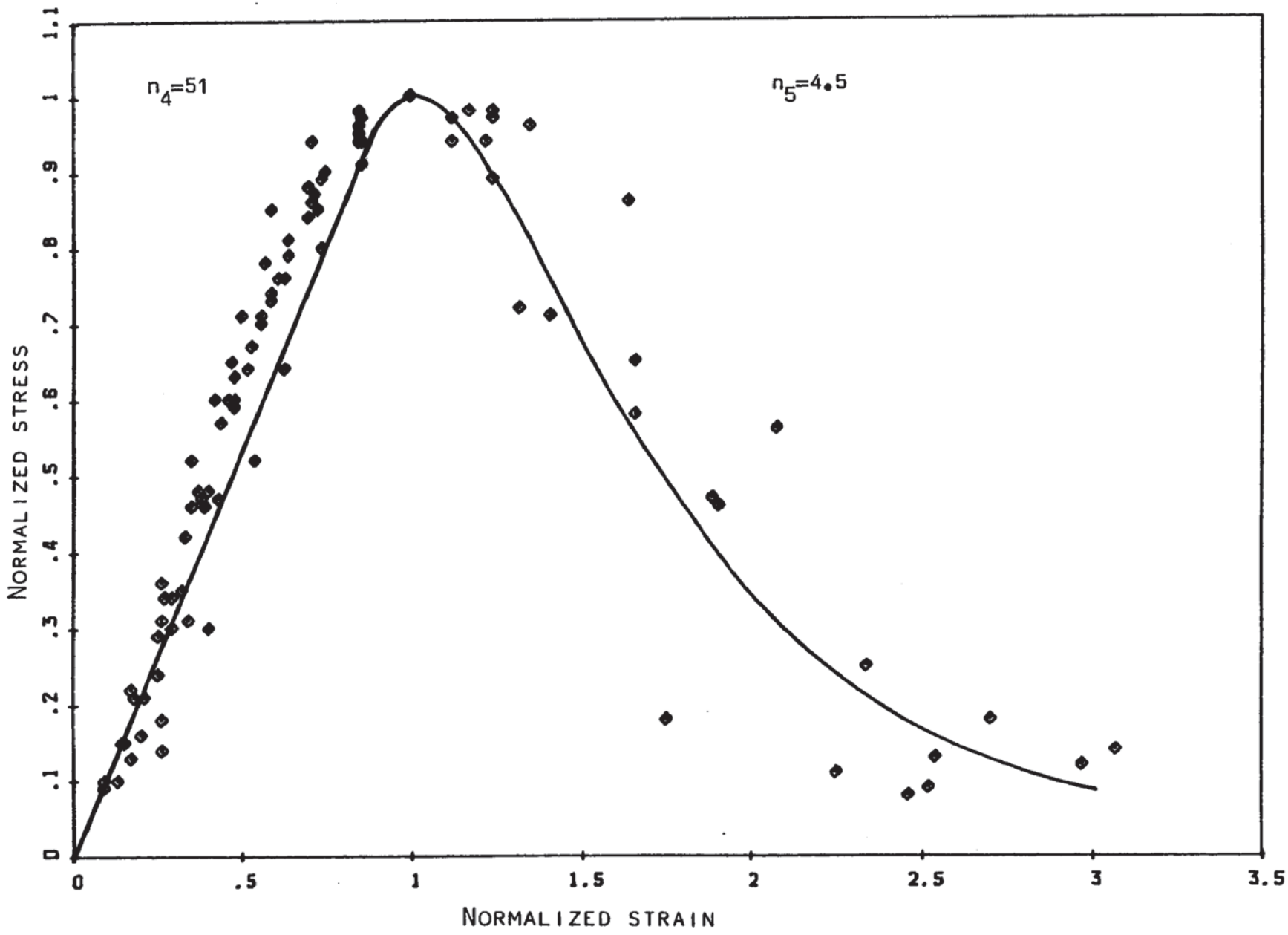

FIG. 8.24 NORMALIZED STRESS/STRAIN CURVES (PRE-LOAD = 60%) - POPOVIC'S EQUATION FIT.

corresponding to three stress levels (Ø.2, Ø.4 and Ø.6 f'_c) for different temperature levels.

it is to be noted that time-dependent deformations occur under constant stress and temperature. In order to explain the increase in strain with time under the above conditions, extensive work on creep of materials in general has been carried out by several researchers. It is now mostly accepted that creep is a thermally activated process. This result has been introduced by many authors such as Dorn & Mote (1963) and those reported in Dorn (1961). However the work undertaken by these researchers was mainly concerned with metals. It is admitted that their findings can apply to concrete, and some investigators have attempted successfully to formulate creep models for concrete using the approach involving the activation energy (Maréchal (1969)) and Wittmann (1982)).

The analysis of the experimental data consists of two sections:-

1) evaluation of the time dependence of creep as described by Thelandersson & Anderberg (1976).
2) the temperature dependence of creep is determined using the approach presented by Wittmann (1982) and reported in Bazant & Wittmann (1982).

8.3.2 Creep analysis :

8.3.2.1 Time dependence of creep :

The formulation of models enables creep results to be predicted. It is thus required to use a mathematical approach to analyse the obtained experimental data.

The uniaxial creep can be modelled by an expression of the form :

$$\epsilon_c = F\ (\sigma, T\ , t) \tag{8.14}$$

where ϵ_c is the creep strain and F a function of the stress, the temperature and time. This expression is widely used in the literature such as Kraus (1980).

To examine the time dependence, it can be assumed that

$$\epsilon_c = g\ (\sigma,\ T)\ f(t) \tag{8.15}$$

which indicates that the effects of the variables are separable. In general a power law now seems to be accepted (Wittmann (1982)).

Thus $$f(t) = (t\ /\ t_3)^n \tag{8.16}$$

This is a relation introduced by Thelandersson & Anderberg (1976) where t_3 = 3 hours. This equation is only applied to primary and secondary creep. Therefore on a given curve $(t\ /\ t_3)^n = 1$ when $t = t_3$

Or $$\epsilon_c|_{t=t_3} = g\ (\sigma,\ T) = \epsilon_{c3} \tag{8.17}$$

By letting $\tau = (t\ /\ t_3)$, Eq. 8.15 becomes :

$$\epsilon_c = \epsilon_{c3} \cdot \tau^n \tag{8.18}$$

from which $$e_c = \tau^n \tag{8.19}$$

where $e_c = \epsilon_c / \epsilon_{c3}$

It can be seen that Eq. 8.19 is independent of the stress and temperature. All curves should therefore superimpose to fit this equation.

By taking the logarithm of Eq. 8.19, the n power can be estimated,

$$\log e_c = n \log \tau \qquad (8.20)$$

This equation shows that a plot of $\log e_c$ vs. $\log \tau$ yields a straight line having a slope of n. The values of e_c and τ have been determined for all creep curves obtained from the different tests. Then a graph is plotted as shown in Fig. 8.25. A total of 704 were used to perform a regression analysis to calculate the power n of the time function. The resulting value of n was 0.56 which compares favourably with that obtained by Thelandersson & Anderberg (1976) and which was equal to 0.50. The value produced however, by Gillen (1981) was 0.40 and was found to be dependent on σ and T.

8.3.2.2 Temperature dependence of creep :

The stress dependence is also dealt with in this section. But the influence of temperature is first examined.

Since creep is thermally activated, the creep rate can be represented by the following relation :

$$\dot{\epsilon}_c = A' \exp(-Q / RT) \sinh(V / RT \cdot \sigma) \qquad (8.21)$$

which is in fact a type of Arrhenius equation where,

A' = a constant determined at $t = t_3$.

Q = activation energy, J / mole.

R = universal gas constant.

T = absolute temperature.

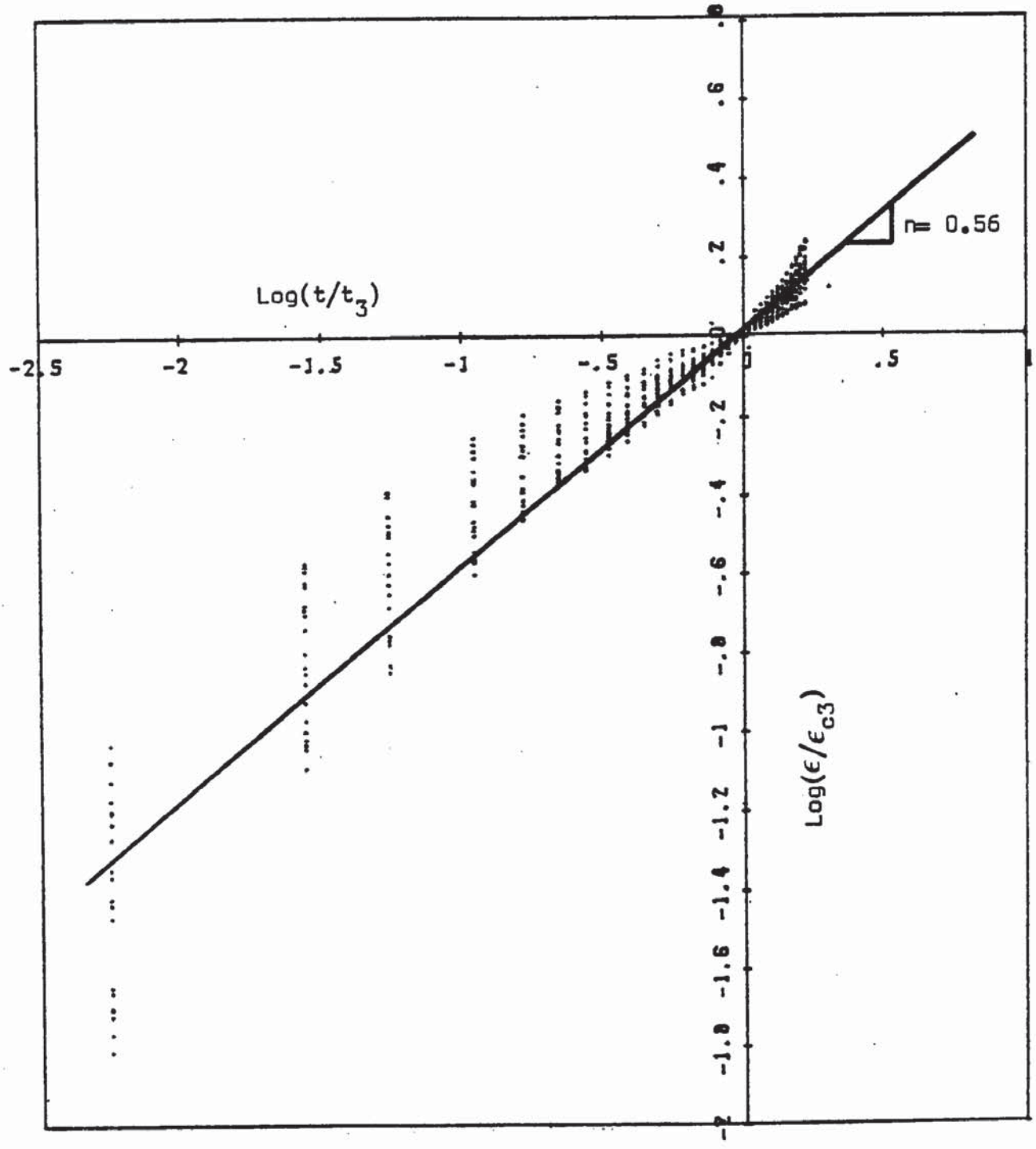

FIG. 8.25 DETERMINATION OF THE POWER n

σ = applied stress, N / mm^2.

V = creep activation volume.

Eq. 8.21 describes the influence of temperature and stress on creep. This expression is similar to that derived by Wittmann (1982).

In order to evaluate the activation energy, the temperature dependence of creep is considered. It is admitted that creep rate increases with temperature probably due to thermally activated processes (vacancy motions) as reported in the literature (Eisenstadt (1971)).

Upon rearrangement Eq. 8.21 becomes :

$$\dot{\epsilon}_c = B \exp(-U / T) \qquad (8.22)$$

where $B = A' \sinh(V / RT.\sigma)$ and $U = Q / R$.

It should be noted that the creep rate is examined in the secondary creep region only where $\dot{\epsilon}_c$ is generally called steady-state creep (Eisenstadt (1971)).

Taking the natural logarithm of Eq. 8.22,

$$\text{Ln } \dot{\epsilon}_c = \text{Ln } B - U / T \qquad (8.23)$$

The graph of the logarithm of the creep rate against the reciprocal of the temperature (1/T) for the different stress levels is illustrated in Fig. 8.26. It can be seen that the plot yields a straight line which indicates that creep is a thermally activated process as suggested by some authors in Dorn (1961) when they studied the mechanical behavior of materials at elevated temperatures.

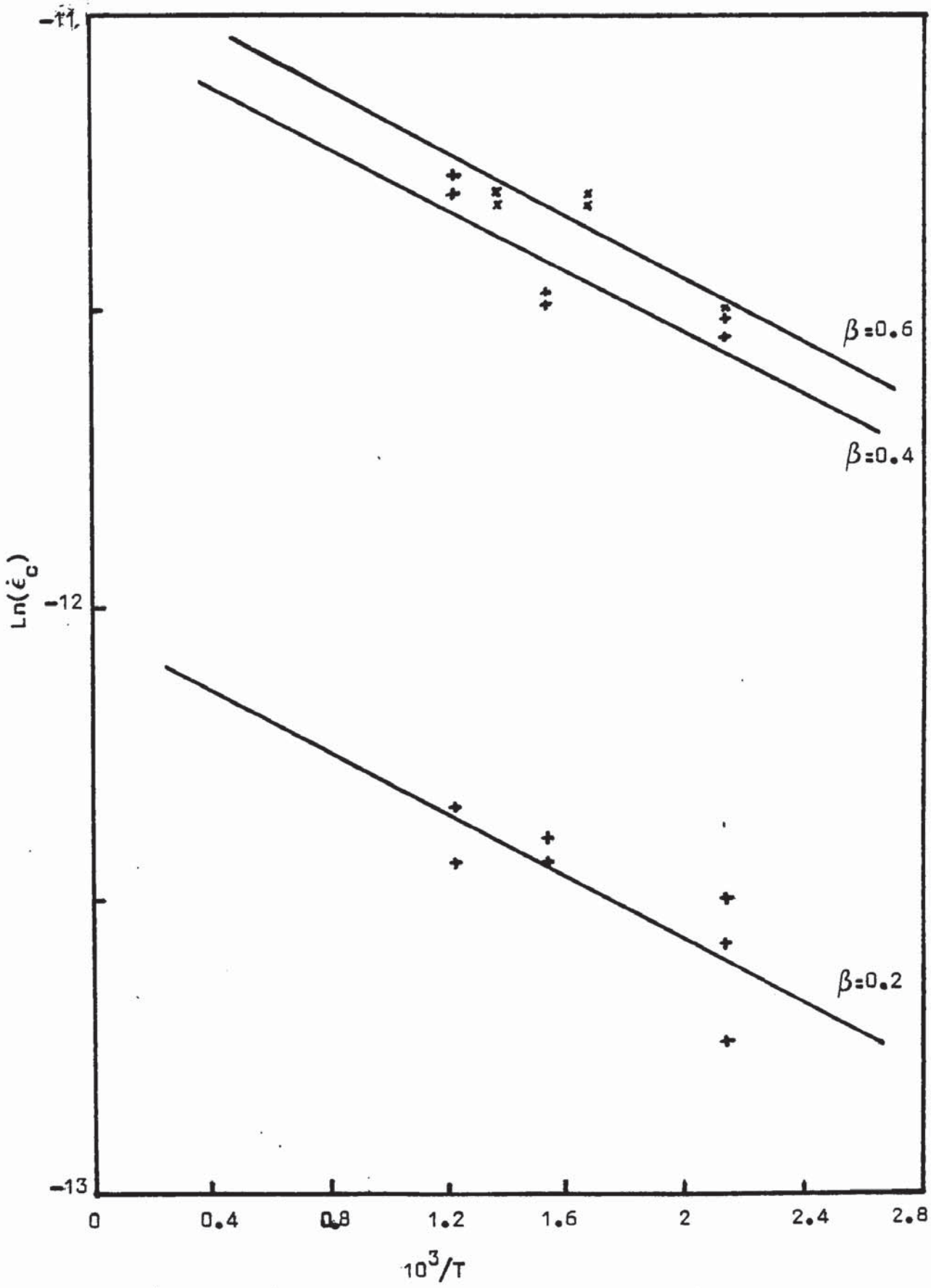

FIG.8.26 CREEP RATE AS A FUNCTION OF 1/T.

Furthermore the activation energy resulting from the three straight lines corresponding to the three stress levels, has been found to be constant and stress independent. However, the test results obtained at 700 °C were omitted because they produced a very high value of the activation energy. This can be explained by the α-to-β quartz transformation that occurs at 575 °C, thus leading to vacancies caused by high motion of the particles , resulting therefore in an increased activation energy. The constant B as determined from the graph of Fig. 8.26, has been found to be stress dependent. The summary of the results is given in table 8.1 :

β	σ N/mm^2	Q J/mole	B μstr/min
0.2	6.42	2167	5.9
0.4	12.83	2137	16.5
0.6	19.25	2220	18.3

Table 8.1 : Values of Q and B.

The stress dependence of creep is now examined by exploiting the values of B. It has been assumed earlier that :

$$B = A' \sinh (V / RT.\sigma) \qquad (8.24)$$

It can be seen that the second term sinh (V / RT.σ) of the equation describes the stress dependence of creep although it contains the temperature T, but in practice, it has usually been assumed that the

creep activation volume, V is proportional to the product RT. This simplification has been made in this analysis. It can be therefore assumed that V / RT is a constant and it is evident then that V varies as T. Wittmann (1982) defined the activation volume as the cross section of the moving particle multiplied by the distance of one jump. This motion is temperature dependence therefore so is V.

It follows that Eq. 8.24 reduces to :

$$B = A' \sinh (C\sigma) \qquad (8.25)$$

Furthermore sinh $(C\sigma)$ will reduce to $(C\sigma)$ if Sinh $(C\sigma)/C\sigma \rightarrow 1$. This will indicate that the creep is a linear function of the stress. Since the activation energy is sensibly constant over the stress range $\emptyset.2 - \emptyset.6\ f_c'$ for the concrete under test it is likely that the concept of specific creep may be used. Furthermore it seems likely that the non-linearity of creep will depend on the shape on the stress/strain curve as illustrated in Fig. 8.27. By considering the following equation :

$$\lambda = \dot{\epsilon}_o / (\sigma_o / E) \qquad (8.26)$$

where λ is the slope of the straight line obtained when plotting E vs. σ_o/ϵ_o (See section 8.2).

It is suggested that creep will be linear if both the activation energy is stress independent and the stress/strain curve is sensibly linear in the stress range considered. It is unfortunate that most of the creep results reported do not include full stress/strain data whereby a full examination of this hypothesis could be made.

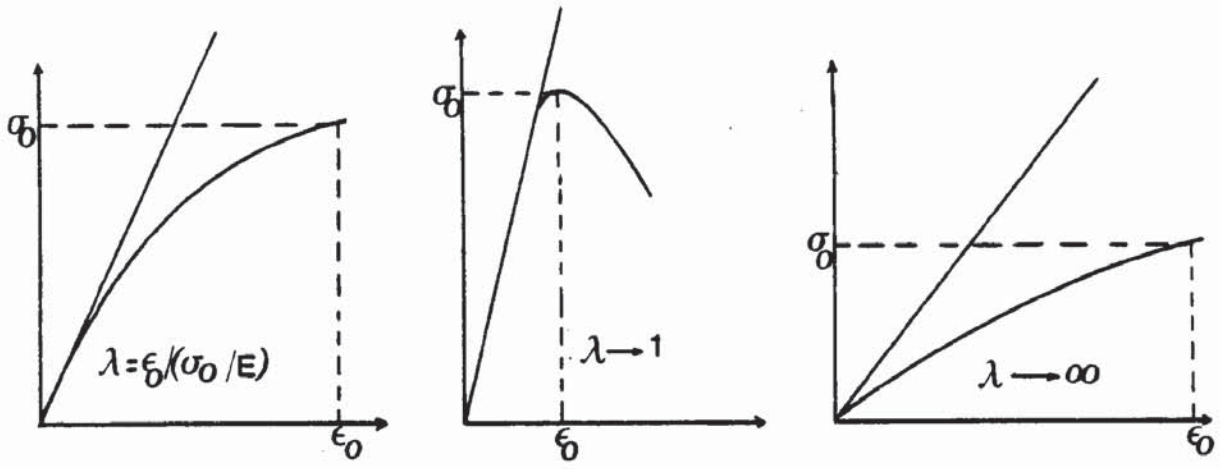

Fig. 8.27 : Stress-strain diagram for different values of λ .

The different values of $(1/\lambda)$ or (λ) yield the following observations :

1) if $1/\lambda \to 1$: creep will be linear to applied stress as little cracking occurs until the maximum stress is reached.

2) if $1/\lambda \to 0$: creep will be non linear because much early cracking occurs.

For the experimental data reported in this thesis, the value of λ obtained is 1.16 from which $1/\lambda = 0.9$. Thus it can be assumed that creep is linear to applied stress to a fairly high value. Upon rearrangement, Eq. 8.25 can then be written as :

$$B = m\sigma \qquad (8.27)$$

Where m = constant which includes A' and C.

σ = applied stress.

The plot of B against the applied stress, is shown in Fig. 8.28. The resulting straight line has a slope of m = 1.044 x 10^{-6} / (min.N mm^2).

To obtain a complete expression of the creep model, some additional factors have to be considered when estimating the creep rate. Rearrangement of Eq. 8.15 yields a new relation of the form :

$$\epsilon_c = K\ (t / t_3)^n \qquad (8.28)$$

Where K is the function of the stress and temperature. Since the creep rate is measured at t = t_3 = 3 hours, therefore :

at t = t_3 Therefore $\dot{\epsilon}_c = n\ K\ t_3^{n-1} / t_3^n = n\ K / t_3$ (8.29)

Comparison of Eqs. 8.21 and 8.29 reveals that the function K can be expressed as :

$$K = (t_3 / n) A' \exp(-Q / RT) \sinh (V / RT \cdot \sigma) \qquad (8.30)$$

Which represents the function $g(\sigma, T)$. Therefore the expression of the creep model is obtained by substituting K in Eq.(8.28) with the linearity of creep accounted for,

Therefore : $\epsilon_c = (t_3 / n)\, m\sigma \exp(-Q / RT)\ (t / t_3)^n$ (8.31)

Where ϵ_c = creep strain.

m = 1.044 X 10^{-6} / (min. N mm^2).

σ = applied stress - N / mm^2 .

Q = activation energy - J / mole.

R = gas constant (8.314 J / mole K).

T = absolute temperature.

t = time.

t_3 = 3 hours or (180 min.).

n = dimensionless constant = 0.56.

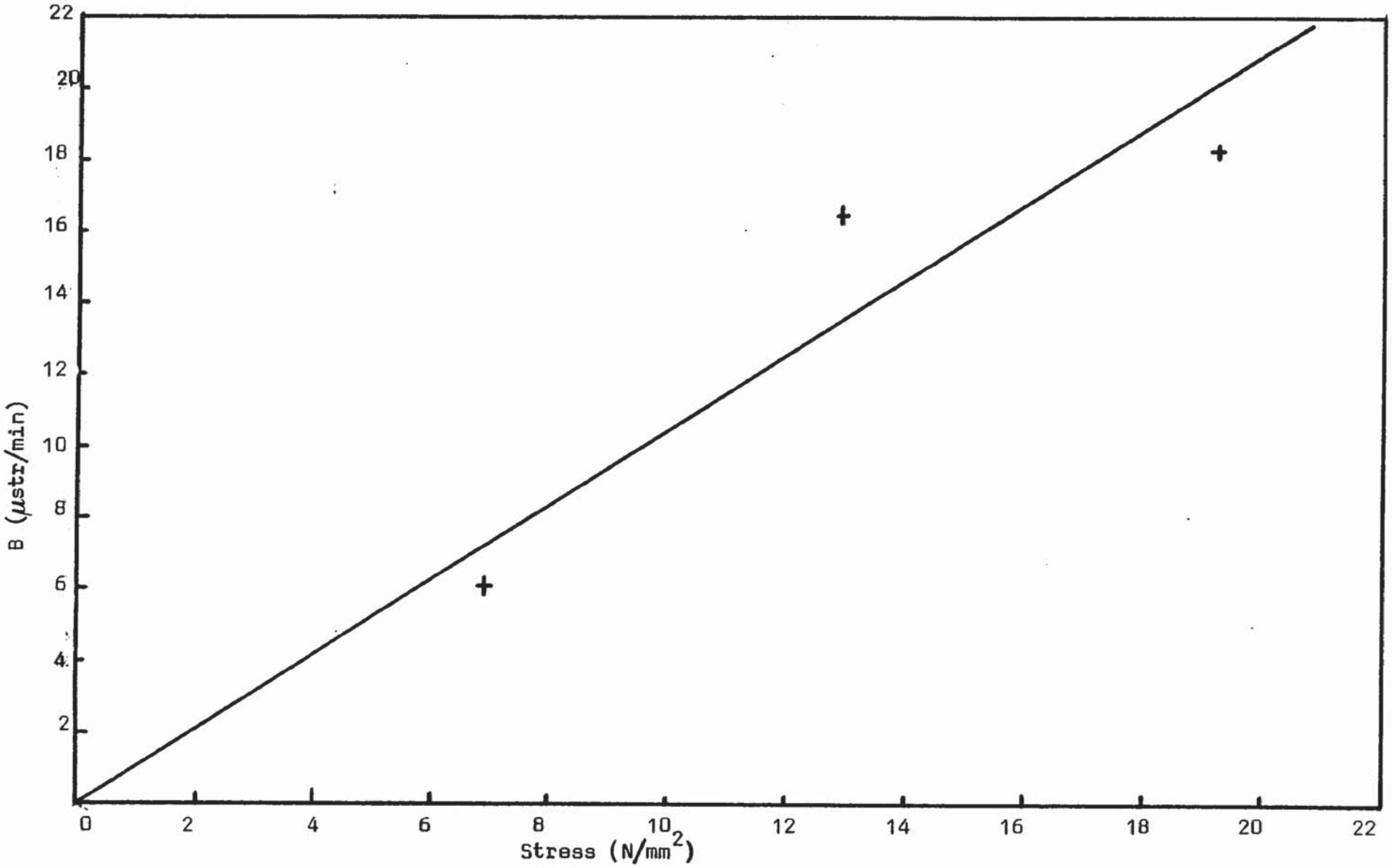

FIG.8.28 PLOT OF B AGAINST THE APPLIED STRESS

This equation is used to fit the data from a uniaxial creep test. The creep strains used in the determination of the transient strains are calculated using Eq. 8.31.

The analysis of the creep results has shown that creep is linear with the applied stress. This same conclusion has been reported by Gross (1973). It is confirmed that creep is a thermally activated process and the resulting activation energy has been found to be constant and stress independent. This result agrees well with Maréchal's conclusion (1969-1970). However at a temperature of 700 °C an increased value of the activation energy was obtained. This is probably attributed to the phase changes in the quartz which take place at 575 °C, thus leading to a high energy of dislocation of the gel particles.

For comparison purposes some data obtained using the creep model (Eq. 8.31) are plotted together with selected experimental results and are shown in Fig. 8.29. It can be seen that significant differences between the calculated and the experimental creep strains appear at temperatures above 500 °C. This is mainly due to the phase change in the quartz at high temperatures and which is not accounted for in the model. Thelandersson & Anderberg (1976) reported similar problems with their creep model.

8.4 TRANSIENT STRAIN :

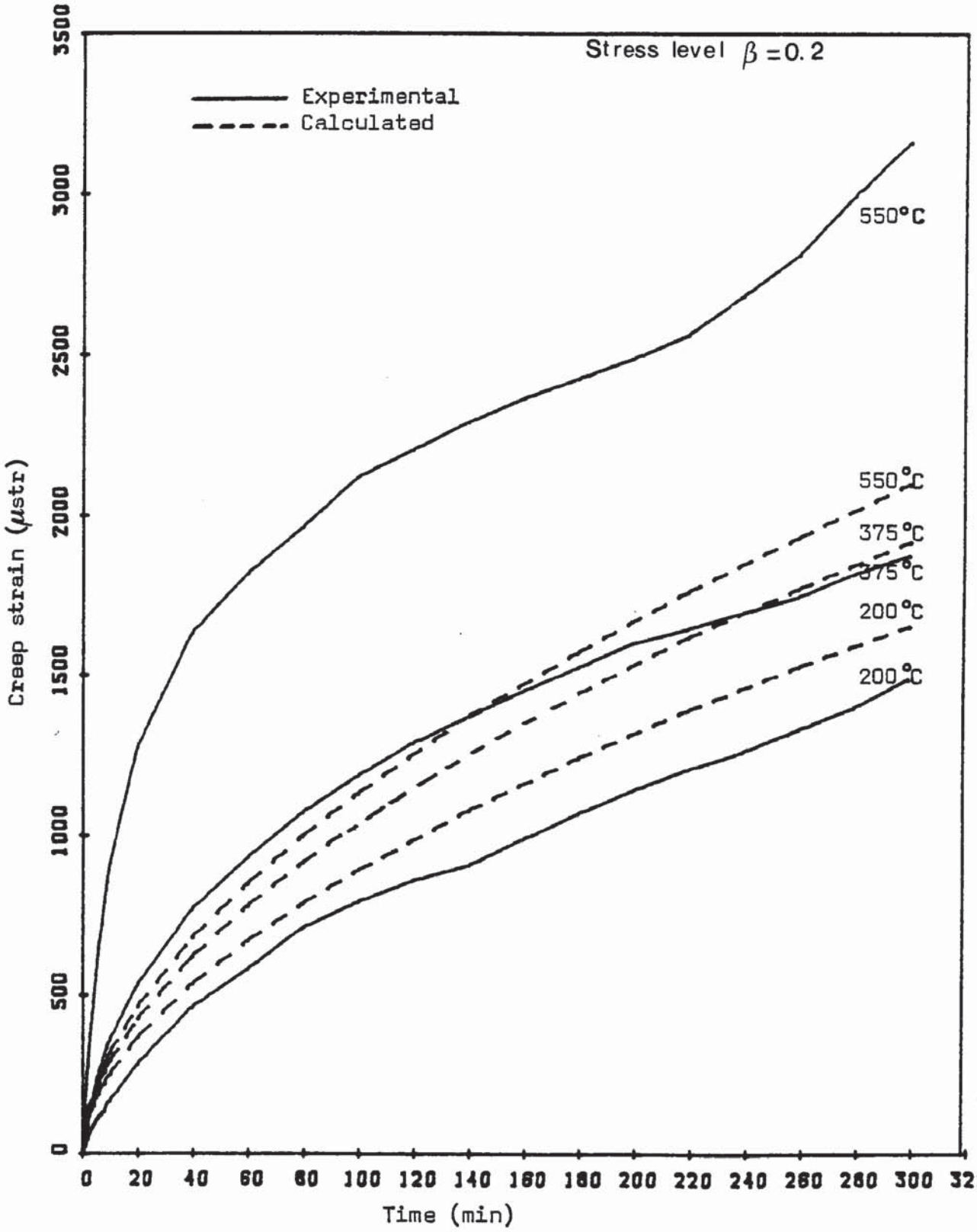

FIG.8.29 COMPARISON BETWEEN THE MEASURED & CALCULATED CREEP STRAINS.

The transient strains are caused by heating under compressive stresses and they are due to chemical transformation in the cement paste and thermal incompatibilities. Transient strains which are temperature dependent are found to be irrecoverable and as reported by Thelandersson & Anderberg (1976) only occur under first heating. They also argued that the transient strains are estimated from the failure tests, since it is impractical to measure directly ϵ_{tr}. Accuracy in the strain measurement is therefore required mainly because of the difficulty in controlling the transient conditions. Recently Sullivan et al (1983) designed an apparatus for measuring accurately the strain under transient thermal states, which is automatically controlled by a data-logging system.

The evaluation of ϵ_{tr} is obtained by considering the model based on the concept of total strain expressed by the relation of the form :

$$\epsilon = \epsilon_{th} + \epsilon_{\sigma} + \epsilon_{c} + \epsilon_{tr} \qquad (8.32)$$

From which

$$\epsilon_{tr} = \epsilon - \epsilon_{th} - \epsilon_{\sigma} - \epsilon_{c} \qquad (8.33)$$

Where ϵ = total strain

ϵ_{tr} = transient strain

ϵ_{th} = thermal strain

ϵ_{σ} = instantaneous, stress-related strain

ϵ_{c} = creep strain

The components of Eq. 8.33 are determined as follows :-

- The thermal strain is taken from the measured thermal expansion of specimens under variable temperature (See Fig. 7.7).

- The instantaneous stress-related strain is calculated using the following expression since the section of the stress/strain curve used is the initial portion which may be considered linear

$$\epsilon_\sigma = \sigma / E_T \qquad (8.34)$$

Where σ = stress

E_T = Young's modulus at current temperature.

The initial elastic strain on loading is deducted in this equation.

- The creep strain is calculated according to the principle of strain hardening as used by Thelandersson & Anderberg (1976), and this consists of the determination of the cumulative creep, since it is needed to express the creep strains on a temperature basis. The stress is considered constant and the method is therefore reduced to two variables (T and t) as shown in Fig. 8.30.

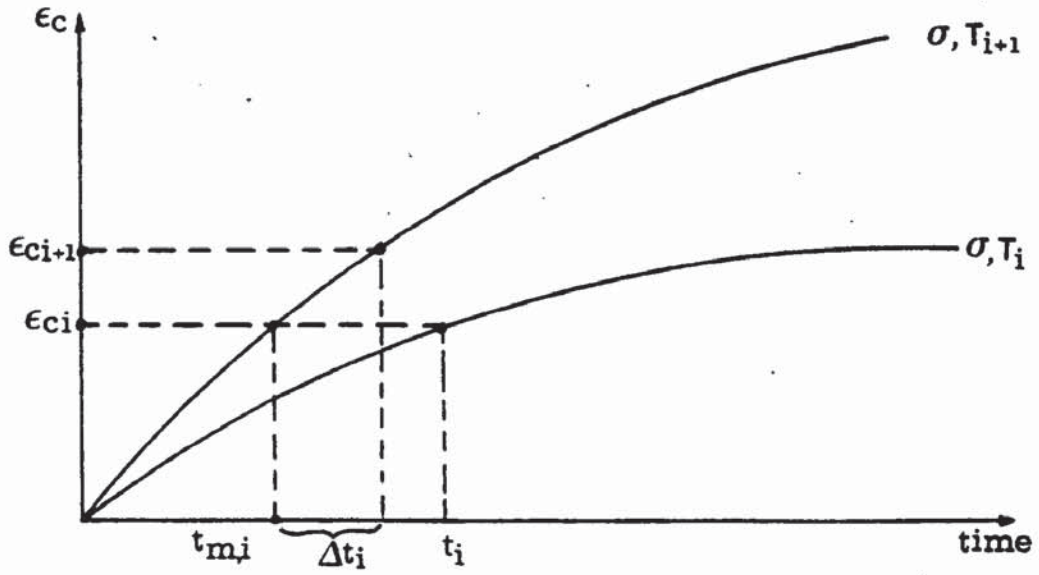

Fig. 8.30 Principle of strain hardening for creep.

The procedure consists of the evaluation of creep strains using Eq. 8.31, in time sequence values. The accumulated creep ϵ_{ci+1} at the temperature Ti+1 can be therefore determined by assuming that ϵ_{ci} and the temperature Ti are known at the time ti. The material time tm,i is then calculated by considering the creep ϵ_{ci} on the curve(σ, Ti+1) and using the following expression :

$$t_{m,i} = \left[\frac{\epsilon_{ci}}{A\sigma \cdot \exp(-Q/RT)}\right]^{1/n} \cdot t_3 \qquad (8.35)$$

Where $A = (t_3/n) \cdot m$

Hence the subsequent time $t_{i+1} = t_{m,i} + \Delta t_i$ is substituted in Eq. 8.31 to calculate the accumulated creep ϵ_{ci+1}. The stress is considered constant and for the analysis of the transient strain, the same procedure have been used for 5 stress levels (Ø.2, Ø.4, Ø.6, Ø.7 & Ø.8 f'_c). The results of these components are given in Tables 8.2-8.6.

With the values of the components as calculated, the transient strain is then evaluated. Using Thelandersson's approach, the plot of (ϵ_{tr}/β) against temperature as shown in Fig. 8.31 does not indicate a linear relationship between ϵ_{tr} and the stress σ. Furthermore, in Fig. 8.32, the plot of (ϵ_{tr}/β) against ϵ_{th} does not yield a straight line. A regression analysis of all the data plotted in Fig. 8.32 gives a value of the gradient K = 1.42. However, when omitting the results at temperatures above 55Ø °C, the new value of the gradient was K = Ø.56. The data producing this value are plotted in Fig. 8.33. It can be seen that the results are very scattered and do not produce a linear relationship between ϵ_{tr} and ϵ_{th}. The regression

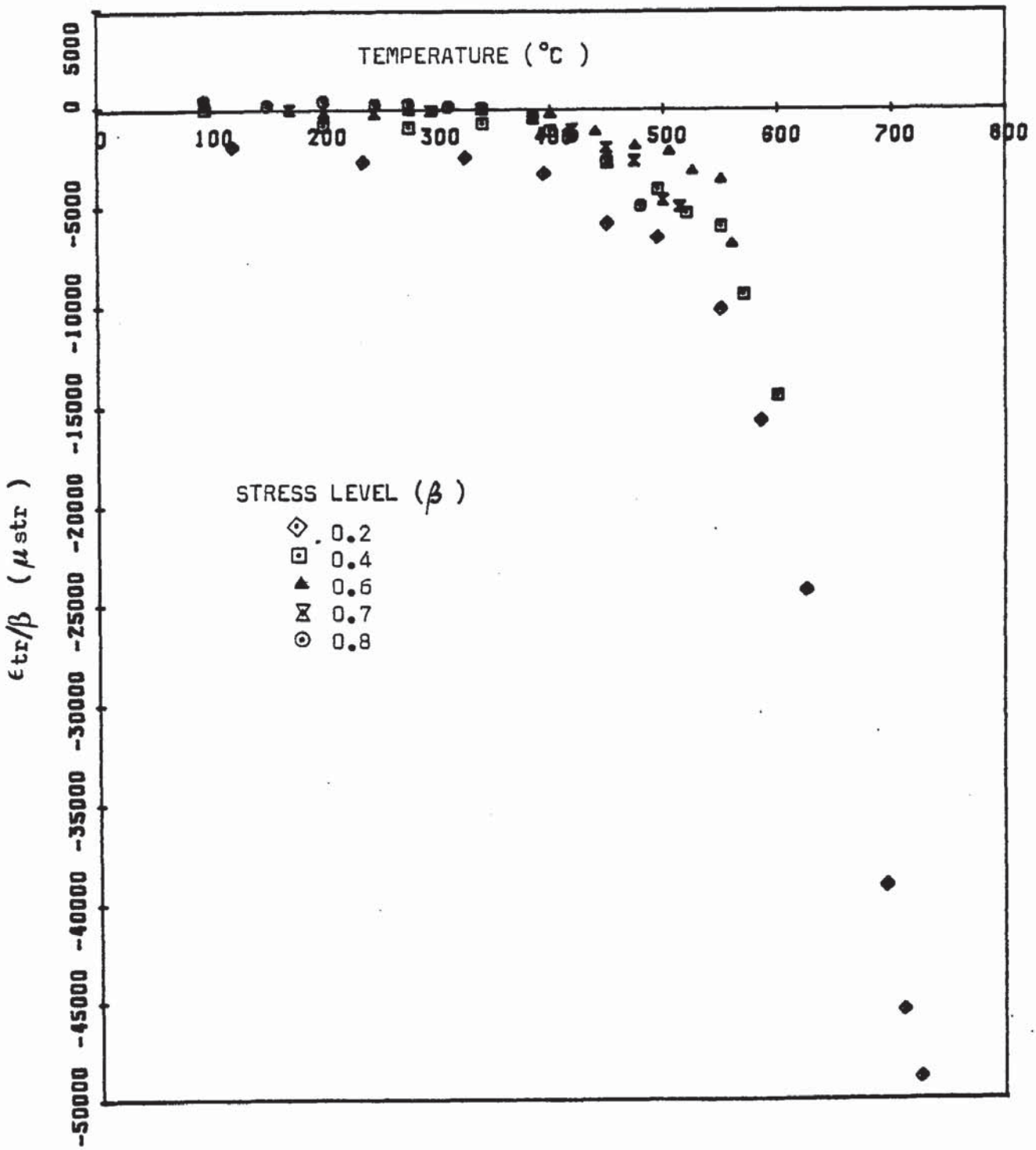

FIG. 8.31 PLOT OF ϵ_{tr}/β AGAINST TEMPERATURE.

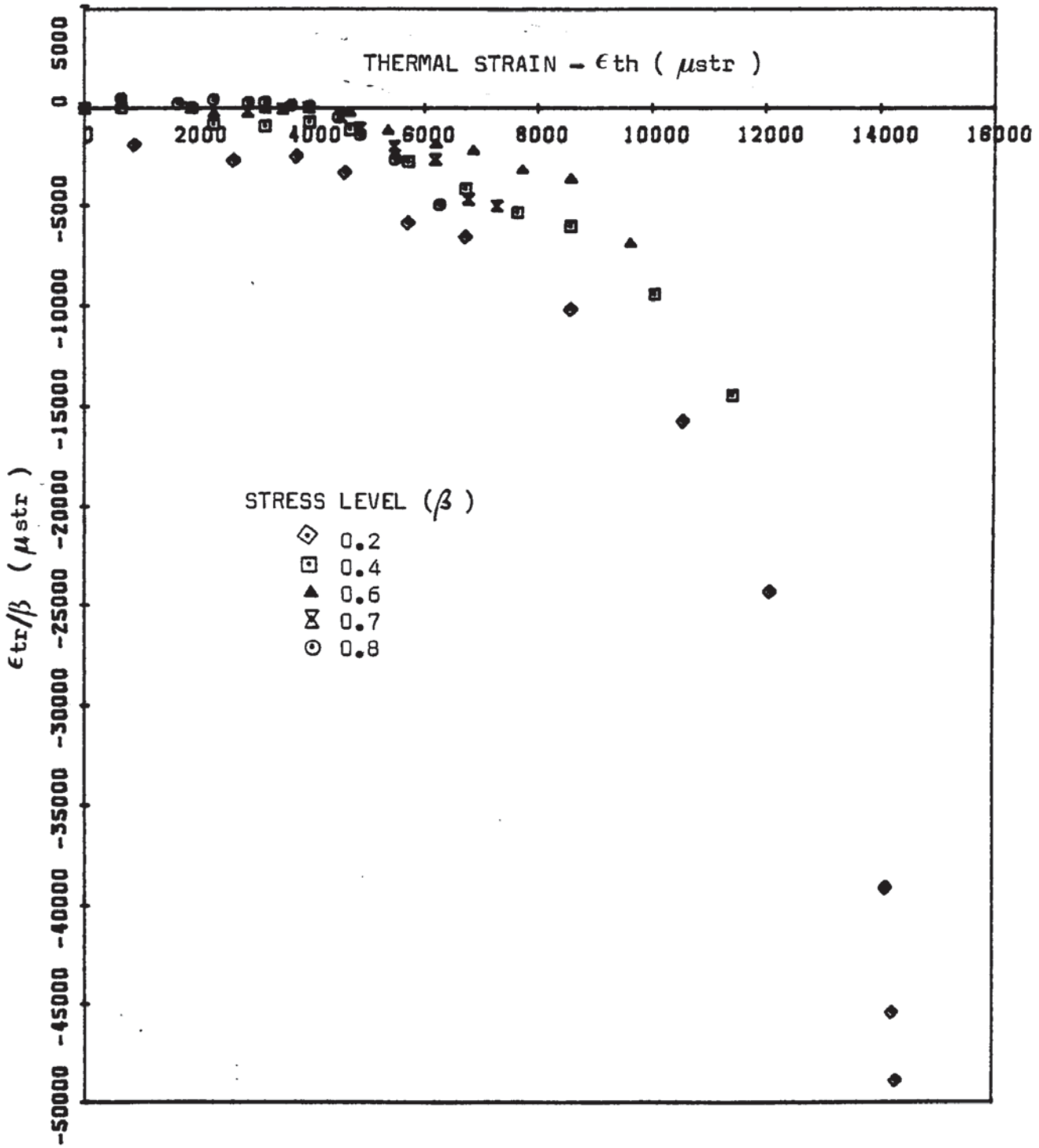

FIG. 8.32 PLOT OF ϵ_{tr}/β AGAINST ϵ_{th} (ALL POINTS INCLUDED).

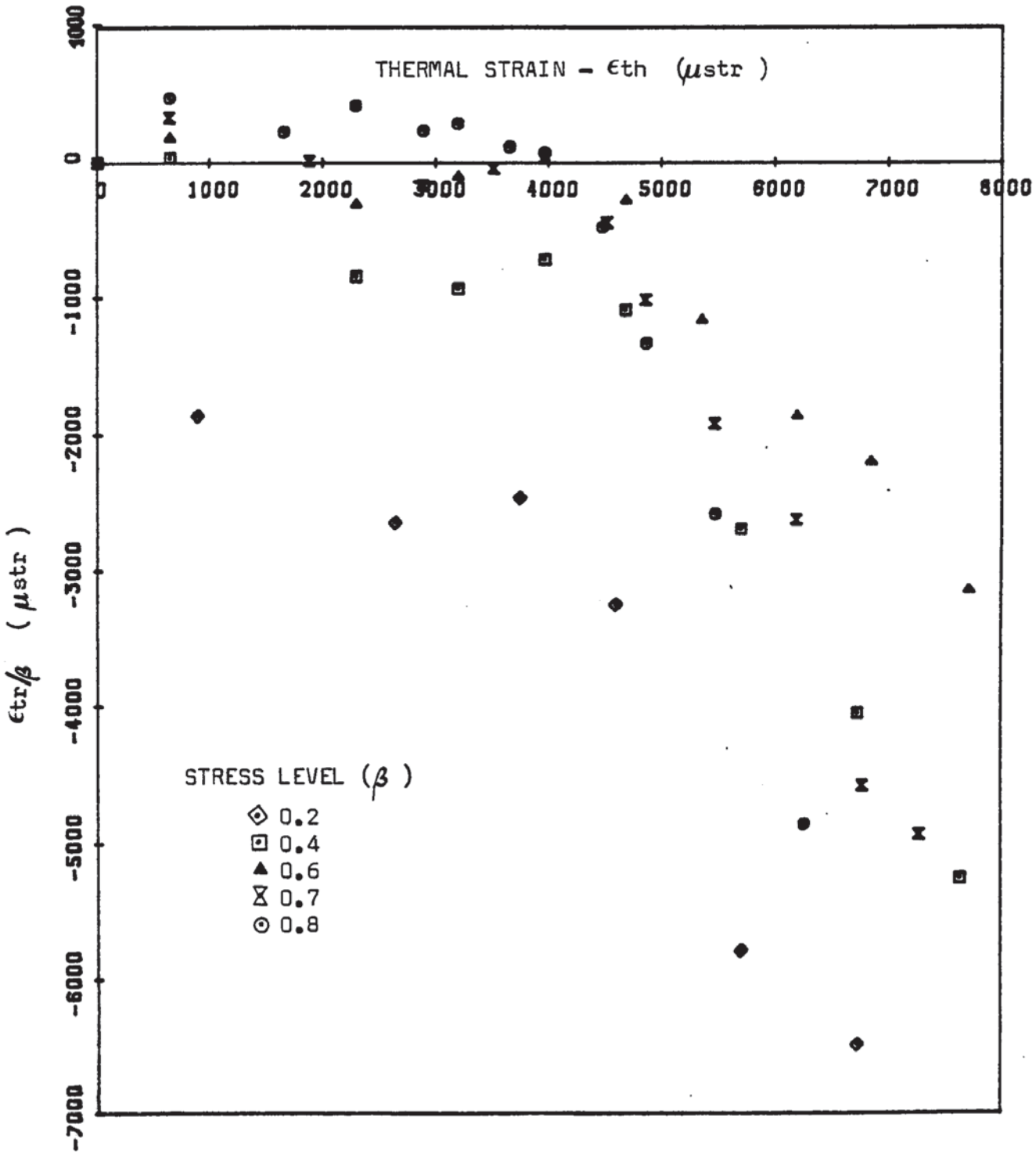

FIG. 8.33 PLOT OF $\epsilon tr/\beta$ AGAINST ϵth (RESULTS FOR 550-720 °C NOT INCLUDED).

analysis performed by Thelandersson & Anderberg (1976) gave K = 2.35. The difference between the value of K obtained in this work and that reported by Thelandersson is mainly attached to the variations in the transient behaviour of concrete examined. It should be noted that in this investigation, positive values of the total strain were monitored

Temp. °C	ϵ_σ μstr	ϵ_c μstr	ϵ_{th} μstr	ϵ μstr
120	- 93	- 149	894	468
235	- 256	- 273	2638	1617
325	- 472	- 314	3745	2468
395	- 539	- 383	4596	3025
450	- 621	- 446	5702	3478
495	- 920	- 505	6723	4000
550	-1654	- 616	8576	4285
585	-2409	- 711	10553	4298
625	-2467	- 802	12085	3958
695	-2656	-1043	14120	2595
710	-2795	-1153	14225	1192
725	-2870	-1252	14296	392

Table 8.2 Values of the components for the determinaton of the transient strain (β = 0.2).

Temp. °C	ϵ_σ μstr	ϵ_c μstr	ϵ_{th} μstr	ϵ μstr
95	- 125	- 251	647	284
200	- 379	- 403	2290	1174
275	- 658	- 533	3192	1613
340	- 943	- 651	3965	2086
400	-1105	- 760	4681	2382
450	-1240	- 887	5702	2499
495	-1840	-1005	6723	2258
520	-2418	-1115	7636	2000
550	-3308	-1219	8576	1681
570	-4393	-1337	10043	570
600	-4811	-1468	11420	- 620

Table 8.3 Values of the components for the determinaton of the transient strain (β = 0.4).

Temp. °C	ϵ_σ μstr	ϵ_c μstr	ϵ_{th} μstr	ϵ μstr
95	- 188	- 377	647	189
200	- 568	- 604	2290	934
275	- 988	- 799	3192	1343
340	-1415	- 975	3965	1619
400	-1658	-1139	4681	1717
440	-1796	-1291	5353	1569
475	-2357	-1434	6192	1285
505	-3012	-1569	6847	952
525	-3748	-1697	7710	380
550	-4864	-1820	8576	- 281
560	-5457	-1938	9606	-1893

Table 8.4 Values of the components for the determinaton of the transient strain (β = 0.6).

Temp. °C	ϵ_σ μstr	ϵ_c μstr	ϵ_{th} μstr	ϵ μstr
95	- 200	- 440	647	240
170	- 487	- 634	1883	770
245	- 914	- 812	2894	1050
295	-1299	- 975	3513	1203
340	-1622	-1126	3965	1239
385	-1841	-1269	4520	1102
420	-1995	-1405	4866	759
450	-2152	-1534	5475	449
475	-2731	-1658	6192	- 29
500	-3392	-1777	6779	-1597
515	-3954	-1891	7279	-2024

Table 8.5 Values of the components for the determinaton of the transient strain (β = 0.7).

Temp. °C	ϵ_σ μstr	ϵ_c μstr	ϵ_{th} μstr	ϵ μstr
95	- 236	- 503	647	280
150	- 474	- 650	1656	710
200	- 757	- 788	2290	1078
245	-1066	- 919	2894	1097
275	-1315	-1042	3192	1062
310	-1675	-1160	3657	911
340	-1886	-1273	3965	860
385	-2124	-1438	4480	541
420	-2300	-1594	4866	- 91
450	-2480	-1743	5475	- 808
480	-3086	-1886	6258	-2616

Table 8.6 Values of the components for the determinaton of the transient strain (β= 0.8).

at high stresses (Ø.6, Ø.7 & Ø.8 f'_c) due to the apparent expansion of the concrete specimen under test. Similar result had already been published by Kordina (1977) and reported in the FIP/CEB report (1978). Thelandersson & Anderberg, however, recorded no further expansion of the specimens at these stresses. They even reported that at Ø.4 f'_c, the thermal expansion was already stopped and the specimens contracted under the applied stress. Their total strain at high stresses was found to be entirely compressive.

It appears that the reason for the variations in behaviour between the two investigations may be attributed to the variations in the test conditions as welll as the concrete tested where different aggregate/cement ratios were used (4.8Ø for Thelandersson and 6 in the work described in this thesis). This suggestion is supported by the different values obtained for K when performing Thelandersson's approach on data from the literature. As an example, Thelandersson & Anderberg (1976) verified their analysis on Schneider's results (1973) (FIP/CEB report (1978)), and obtained a value of K = 1.8. It is noted that Schneider used an aggregate/cement ratio of 5.4 to make his concrete specimens. Similar procedure was also carried out on data produced by Fischer (197Ø) who tested specimens with an aggregate/cement ratio of 5.1, and Thelandersson & Anderberg obtained a value of K = 2. It can be seen that the value of K decreases as the aggregate/cement ratio increases.

Considering these results, it appears that the major factor influencing the transient behaviour of concrete is the

aggregate/cement ratio (a/c). It can therefore be suggested that the total strain tends to be positive (in tension) as the a/c ratio increases. This may explain the results obtained by the author who used an a/c ratio of 6. It is, thus, apparent that the transient strain, as a result, will be affected by the amount of aggregate contained in the concrete tested, since ϵ_{tr} is the difference between the total strain and the other components.

It can be concluded that the procedure for calculating the transient strain as introduced by Thelandersson & Anderberg (1976) does not hold for the data reported in this thesis.

In the next Chapter, the main conclusions and recommendations for further work are presented.

CHAPTER 9

CONCLUSIONS & RECOMMENDATIONS FOR FUTURE WORK.

9.1 Main conclusions :

9.1.1 Introduction :

It was suggested from previous work that, the effects of high temperatures on the behaviour of the material properties under transient thermal conditions were needed to be extensively studied. The aims of this investigation were therefore to provide comprehensive data of such behaviour. Due to a lack of consistent creep data, a study was undertaken to examine more extensively the effect of high temperature on the time-dependent behaviour.

The main conclusions arising from the different sections of the work are presented below.

9.1.2 Equipment :

1. Specimen preparation (Chapter 4):

The specimens with the ends ground performed satisfactorily, the end effects were to a certain extent eliminated avoiding therefore a premature failure to take place during the test.

2. Instrumentation (Chapter 3) :

The furnace performed well and an overall good control of the temperature was exercised.

The load was measured from the strain gauges mounted on the dynamometer. Despite the accidental failure of the first set of the strain gauges, a satisfactory performance of the load cell was achieved with a new set of gauges similar to the first ones. the dynamometer was not affected by the temperature transmitted to it through the centre crosshead.

The displacement transducers were found to read correctly the deformations. The expansion of the connecting quartz rods was not taken into account in the strain measurements. This was acceptable due to the low coefficient of thermal expansion of the quartz tubing used.

3. Testing machine (Chapter 3) :

The apparatus performed all the tests, and was found to be stiff enough to allow the complete stress/strain curve to be obtained. The expansion of the rig at high temperatures, might have affected some of the results. the friction in the bushes was negligible.

4. Data-logging system (Chapter 5):

It was very unfortunate that the computarized data-logging system did not function due to a hardware fault in the system. It was therefore not possible to perform tests to check all the options of the program and validate its complete operation.

9.1.3 Test results : (Chapters 7 & 8)

1. The stress/strain curves obtained for specimens bearing no load during heating, were affected by high temperatures as expected. The strain softening was found to be dependent on the temperature level. Therefore as the temperature increased, the following observations were made :

The strength and Young's modulus of concrete underwent a significant reduction. At temperatures above 500 °C the values of E decreased more than those of the strength. The strain at peak stress increased and the concrete reached a "quasi-ductile" state.

2. The stress-strain curves obtained with pre-loaded specimens exhibited a similar shape as expected at elevated temperatures, but with a steeper ascending and descending slope. With increasing temperature, the pre-loaded specimens retained more strength than the "un-loaded" ones. It was found, however, that the strength, the strain at peak stress and Young's modulus, were very much influenced by the magnitude of the load during heating. The presence of a load retarded the cracking due to thermal incompatibility between the cement paste and the aggregate.

The other observation is that the ductility of the concrete was considerably reduced.

3. The creep curves obtained were similar in shape to those reported in the literature. The test specimens experienced large creep strains at elevated temperatures. It was shown that the plot of the

logarithm of the creep rate against the reciprocal of the temperature yielded a straight line. The resulting linear curve indicated that creep could thus be described by an Arrhenius equation type, which was in accord with activated processes as presented by many authors reported in Dorn (1961). Furthermore creep was found to be linear with the applied stress and the activation energy was sensibly constant for the different stress and temperature levels.

The creep model developed did not hold for the test data at temperatues higher than 500 °C, due to the α-to-β quartz transformation occuring at 575 °C.

4. The results obtained from tests on specimens heated to failure under constant stress showed that the expansion of concrete is significantly reduced by the sustained load, but the total strain at high stresses was found to be positive in the early stages of heating then turned negative as the temperature increased. Similar results had been reported by Kordina et al (1977). This behaviour could be attributed to the aggregate/cement ratio used in the concrete in test.

5. Following this results, an attempt was made to evaluate the transient strain using Thelandersson's approach, which proved unsatisfactory. This was mainly due to the variation in the behaviour obtained when measuring the total strain. It can also be suggested that the significance of this result was related to the different aggregate/cement ratio used in both investigations. It was thus not possible to use the analysis of the transient strain as introduced by Thelandersson & Anderberg (1976).

9.2 Recommendations for future work :

1. In order to formulate validated models for the prediction of structural behaviour in a fire, more data on the effects of high temperatures on the material properties under transient conditions are needed.

2. Extensive work should be undertaken on the effect of high temperature on creep of "pre-loaded" specimens. The creep strains could be reduced as expected in the stress-strain tests of "pre-loaded" specimens. More work should be done on the development of consistent mathematical models to predict the creep behaviour at very high temperatures with the phase changes in the quartzite aggregate accounted for.

3. The results obtained on the total deformations showed clearly that the concept of total strain as introduced by Thelandersson & Anderberg (1976) needs to be extended so that higher aggregate/cement ratios could be used. For this reason more exprimental verifications of the analysis should be undertaken.

APPENDICES

APPENDIX ONE

Details of prestressing bars

The main columns of the testing machine are prestressed using "Macalloy" bars having the following specifications :-

- diameter	:	32 mm
- sectional area	:	804.3 mm^2
- weight/m	:	6.314 Kg
- minimum breaking load	:	800 KN

The bars were prestressed to 70% ultimate.

The prestressing force for a 32 mm diameter bar is

- initial prestress	:	500 KN
- after 15% losses	:	476 KN.

APPENDIX TWO

Design of the dynamometer

The dynamometer consists of a hollow shouldered steel cylinder. The maximum load to be monitored is 200 KN. Taking a minimum guaranteed yield strength of mild steel as 250 $N.mm^{-2}$, using a load factor of 1.5 then the core area can be obtained as follow :

$$A = \frac{200 \times 103 \times 1.5}{250} = 1200 \text{ mm}^2$$

The core area A may be expressed as

$$A = (D^2 - 41^2) \frac{\pi}{4}$$

giving a core diameter D of 57 mm. The wall thickness is 8 mm. A cross section of the dynamometer can be seen in Fig. A2-1. Plate A2-1 shows the dynamometer with the gauges mounted on the section of minmum thickness. The gauge configuration is that of a full four arm bridge. The calibration chart is given in Fig. A2-2. The sensitivity

Scale : 1:1

All dimensions in mm

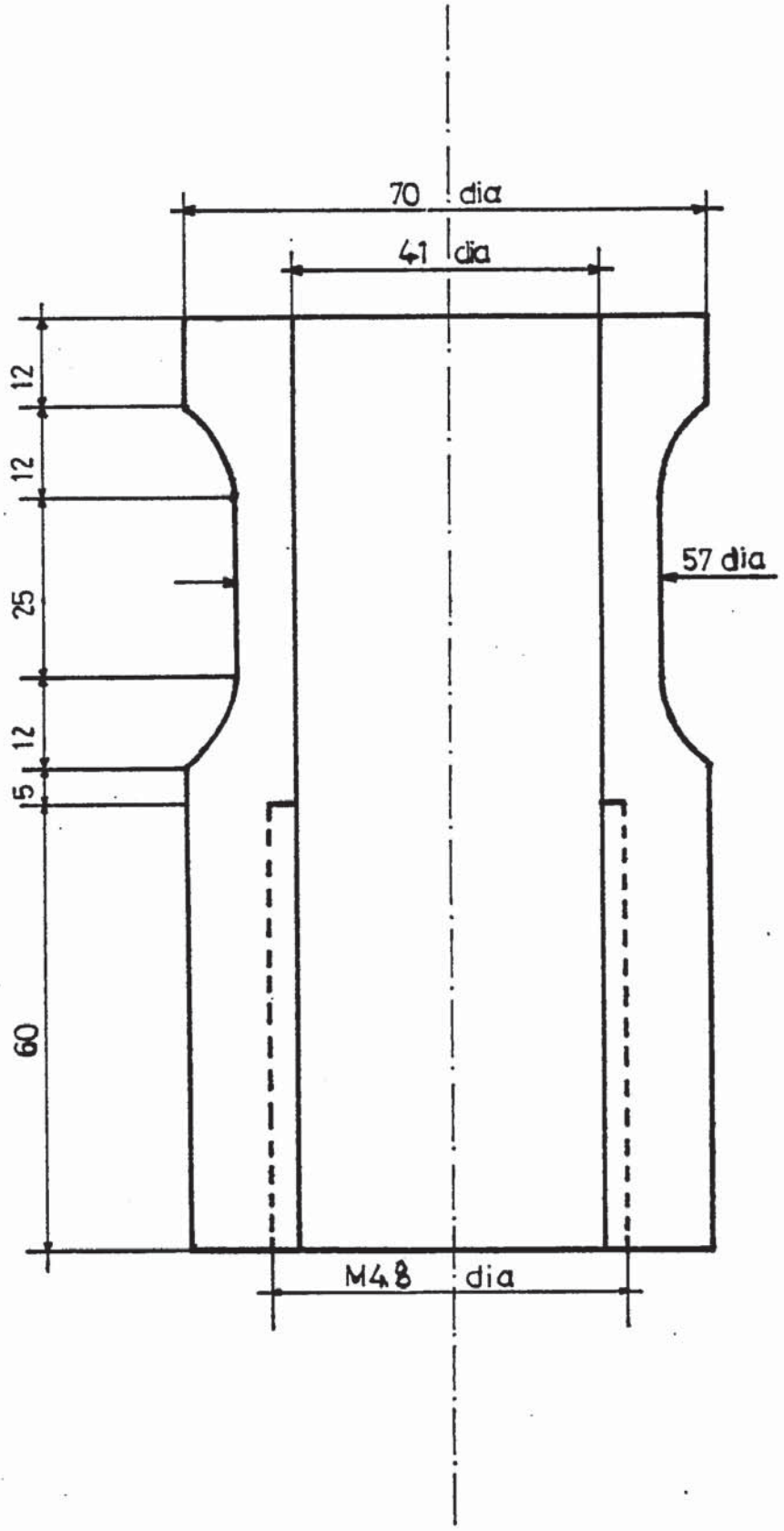

FIG. A2.1 CROSS SECTION OF THE DYNAMOMETER.

PLATE A2.1 THE DYNAMOMETER WITH THE GAUGE CONFIGURATION

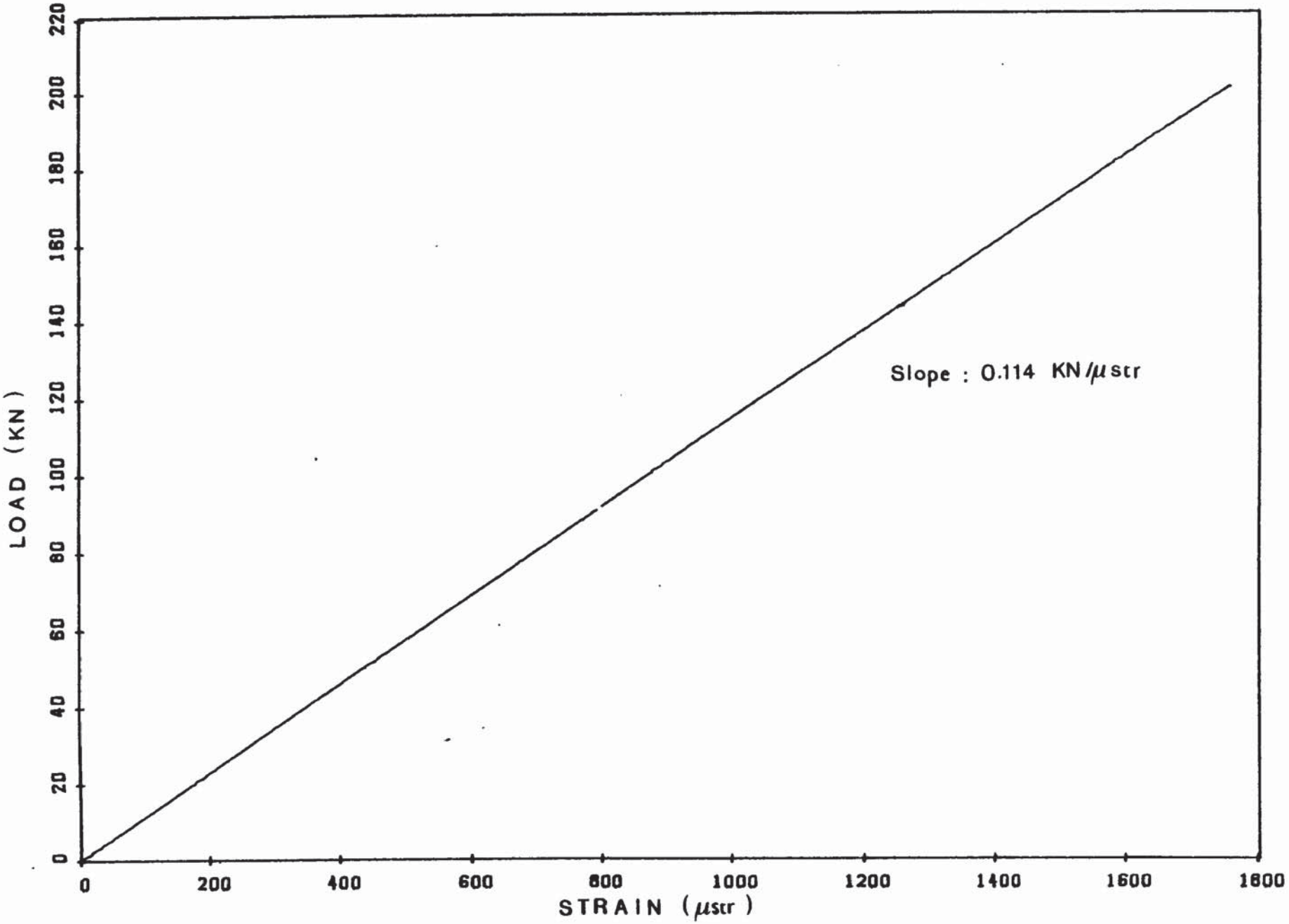

FIG. A2.2 CALIBRATION CHART FOR THE DYNAMOMETER.

recorded for the load cell is 114 $N.\mu str^{-1}$.

Before conducting the tests on "pre-loaded" specimens (test series 2), the strain gauges mounted on the dynamometer failed. New strain gauges of the same type as the previous ones (TML PC-10-11) were bonded on the load cell which was recalibrated in a grade A 50 tons Avery-Denison machine. The dynamometer was loaded and unloaded three times and thereafter the readings of the applied load and the strains as given by the strain gauges were taken. The results are plotted in Fig. A2-3 and a calibration curve is obtained having a gradient of 117 $N.\mu str^{-1}$, which compares favourably with the previous value of 114 $N/\mu str$ (as reported in this Appendix) and indicates that the dynamometer had suffered no undue distress in use due to temperature effects caused by the furnace being sited on the centre crosshead.

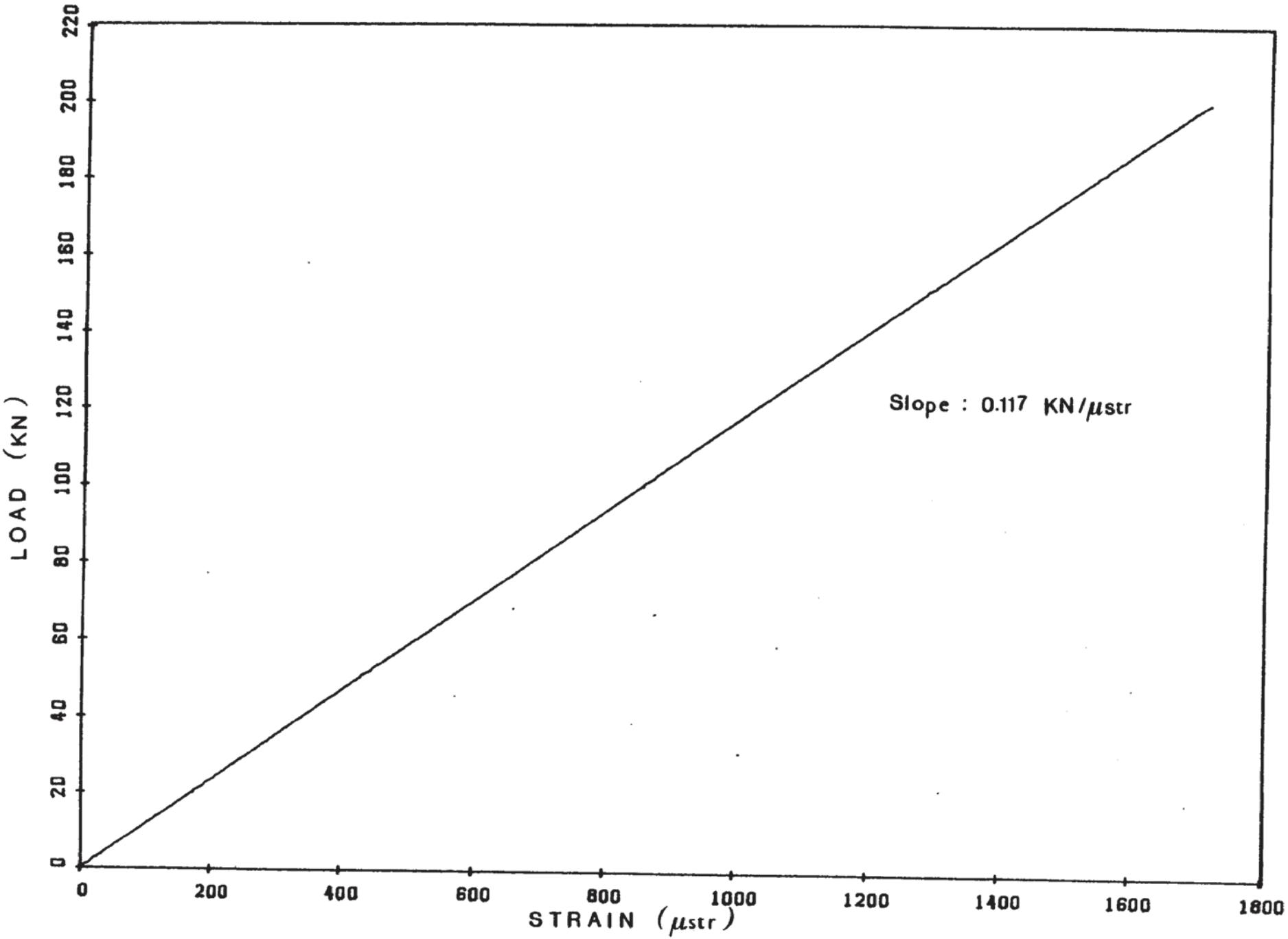

FIG. A2.3. RECALIBRATION GRAPH FOR THE DYNAMOMETER.

APPENDIX THREE

Additional insulation

In this section a general description of the Mackechnie loose wool is given together with the technical properties.

The information is reproduced from the Mackechnie Catalogue.

APPENDIX FOUR

Design of the test rig

A detailed description of the design of the test rig was reported by Purkiss (1972). The main assumptions made in the development of the analysis for the determination of the machine stiffness are that the members undergo only axial deformation for the columns and bending in the crossheads, the stiffness of the machine is not affected by temperature and the columns undergo no relative rotation to the plane of the crossheads.

Given these assumptions and using the concept of strain energy, the total energy can then be expressed as follows :

$$U^*_T = (A1.L1)\frac{\sigma^2}{2E_s} + (A2.L2)\frac{\sigma^2}{2E_s} + 3(A3.L3)\frac{(\sigma/3)^2}{2E_s} + \text{crosshead term} \quad (A1)$$

To express the strain energy in terms of load and dimensions, the value $\sigma = P/A$ is substituted, giving :

$$U^*_T = \frac{P^2 L1}{2E_s A1} + \frac{P^2 L2}{2E_s A2} + 3\left(\frac{P}{3}\right)^2 \frac{L3}{2E_s A3} + \text{crosshead term} \quad (A2)$$

where : P = the load applied to the specimen

E_s = Young's modulus for steel

L1 = length of the jack

A1 = the area of the core of the jack thread

L2 = the length of the platen

A2 = the area of the platen

L3 = the length of the column

A3 = the area of the column

since $\delta = \partial U^{*}_{T} / \partial P$ and using Eq. A2, the stiffness of the rig is :

$$E_s \delta/P = \left(\frac{L1}{A1}\right) + \left(\frac{L2}{A2}\right) + \left(\frac{L3}{A3}\right) + \text{crosshead term} \qquad (A3)$$

To determine the crosshead term, the crosshead has been idealised as a circular plate loaded in the centre by a point load and supported at three point supports 120^{o} apart. It should be noted that the load is distributed and there will be an element of fixity at the supports thus reducing the deflection. This however is counter balanced by the likelihood of shear deformation as the radius to plate thickness is low (275/75 = 3.67). The deflection of a circular plate supported at three points and loaded centrally is fully described by Timoshenko & Woinowsky-Krieger (1959). Figure A4.1 shows the idealised plate.

The deflection for a such plate is given by the relation

$$\delta = 0.067 \times \frac{Pa^{2}}{D} \qquad (A4)$$

where P = load

Scale : 1:5

All dimensions in mm

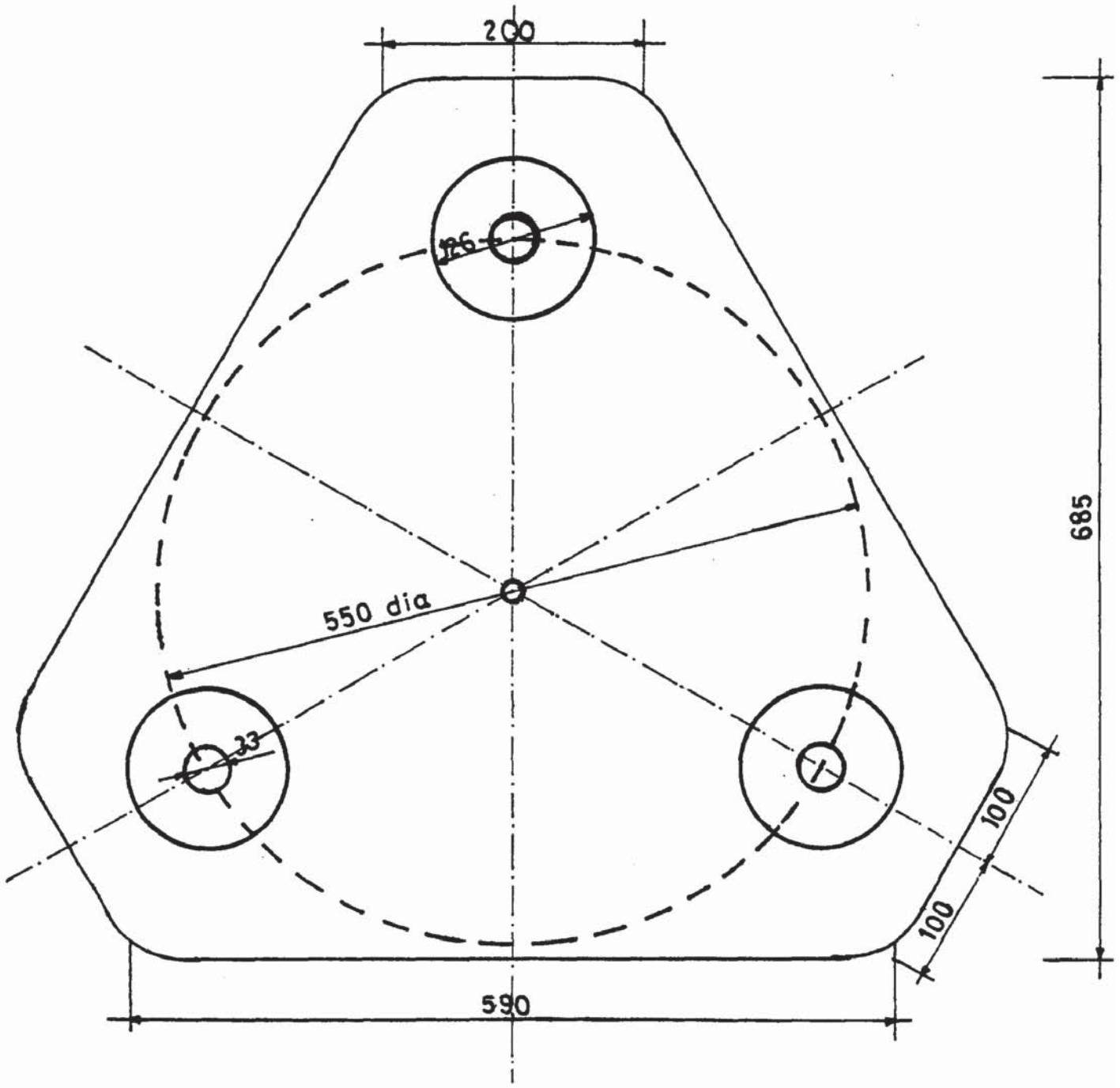

FIG. A4.1 IDEALIZED PLATE FOR ESTIMATING THE STIFFNESS OF THE TOP AND LOWER CROSSHEADS.

a = the radius of the plate

D = the flexural rigidity for a plate, which is defined as

$$E_s h^3 / 12 (1 - \nu^2) \qquad \text{(A5)}$$

where h = thickness of the plate

E_s = Young's modulus for steel

ν = Poisson's ratio which may be taken as Ø.3

from Eq. A4 and Eq. A5, the crosshead term is :

$$E_s \delta / P = Ø.Ø67 \times \frac{a^2 \times 12 (1 - \nu^2)}{h^3} \qquad \text{(A6)}$$

The value of the crosshead term is obtained by considering two crossheads and including a term again to allow for some measure of shear deformation.

Using Eq. A3 and Eq. A6, the stiffness of the rig is :

$$E_s \delta/P = \left(\frac{L1}{A1}\right)+\left(\frac{L2}{A2}\right)+\left(\frac{L3}{A3}\right)+\left(3 \times Ø.Ø67 \times \frac{a^2 \times 12(1-\nu^2)}{h^3}\right) \qquad \text{(A7)}$$

The components of Eq. A7 are given in Table A4.1. The overall stiffness is then calculated.

From Table A4.1 $E_s \delta/P$ is given as Ø.56Ø mm^{-1}, so the theoretical stiffness is found as 355 KN mm^{-1} and the proving tests described later give a value of 26Ø-31Ø KN mm^{-1}.

Member	Length mm	Area mm^2	No	$E_s\delta/P(mm^{-1})$
Dynamometer	50	1200		0.042
	17	2530		0.007
	25	2590		0.010
Jack (core dia: 65mm)	150	3310		0.046
Platens	100	2820	2	0.036
Columns	533	7850	3	0.024
Crosshead	plate a = 275mm		3	0.393
TOTAL				0.558

Table A4.1 Components of Eq.A7

It will be seen from Table A4.1 that allowance has been made for both crossheads although the lower one is to some extent stiffened by the body of the screw-jack and that any error in the estimation of the stiffness of the crosshead will affect the calculation of the overall stiffness of the rig to a large degree. However the result is seen to be reasonable by comparing the experimental and theoretical results for the stiffness of the rig.

APPENDIX FIVE

Proving Tests

This section deals with the performance of the machine which needs to be checked experimentally. The proving tests, consist of the determination of the stiffness of the rig and friction in the bushes and also a check on the accuracy of the transducers.

5.1 Stiffness of the rig :

This has been evaluated by recording the platen load and the platen movement.

The dynamometer which has already been described in Appendix Two, is used to measure the applied load. The load cell was gauged up and calibrated in a grade A 50 tons Avery-Denison machine. The calibration curve is shown in Figure A2-2. The platen load is given by the duralumin specimen 150 x 50 φ mm, which was also gauged up and calibrated in the same machine as the load cell. The calibration chart for the duralumin specimen is plotted in Figure A5-1.

To determine the stiffness, the platen load was recorded at each increment of the applied load. This was done by measuring the strains on the duralumin specimen and

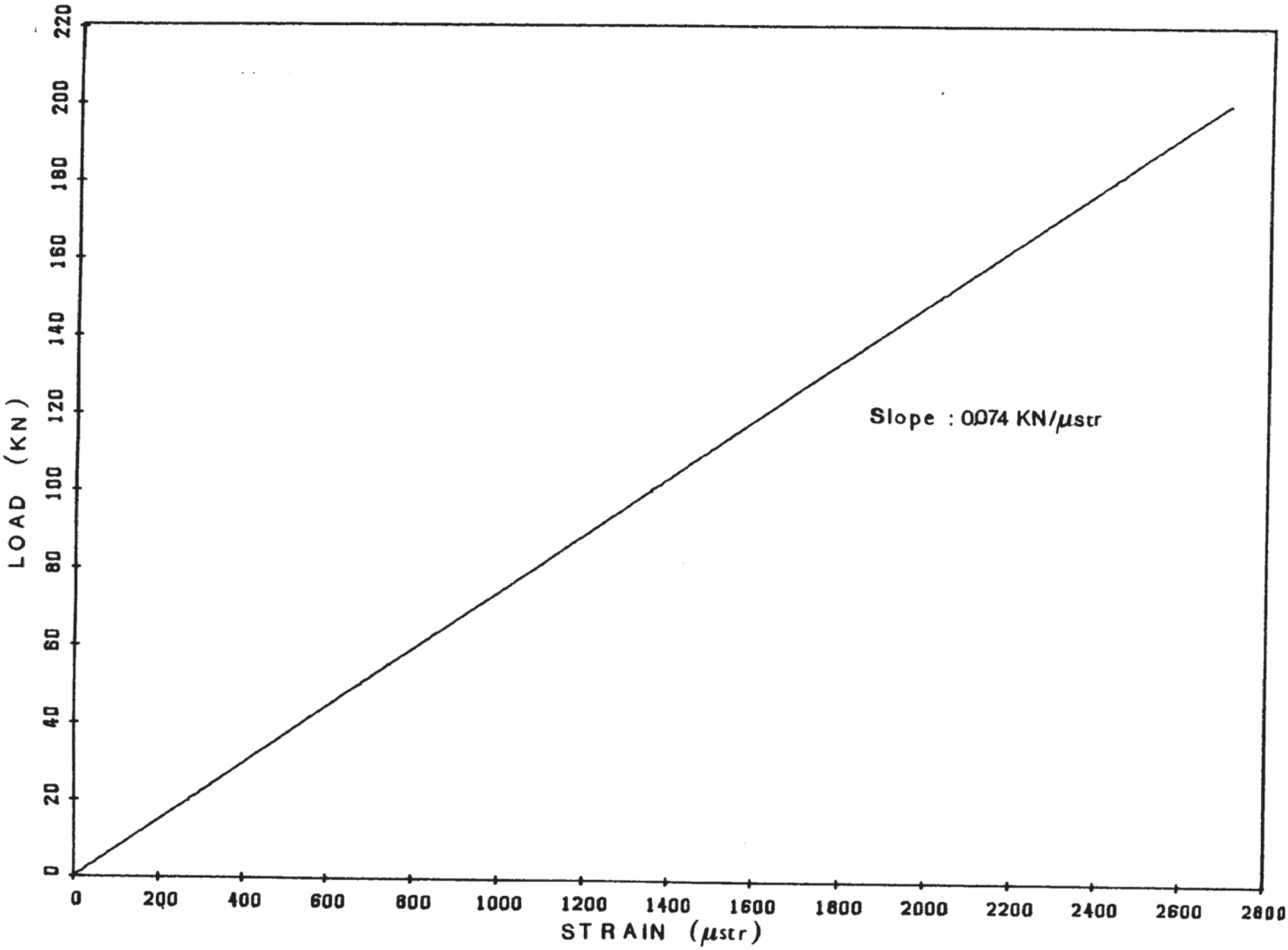

FIG. A5.1 CALIBRATION GRAPH FOR THE DURALUMIN SPECIMEN.

using the calibration chart in Fig. A5.1 to find the load. The values of the strains obtained were also used to calculate the shortening of the specimen which subtracted from the jack movement give the platen movement. The jack raise was determined by measuring the rotation of the input shaft. The data for the stiffness are plotted in Fig. A5.2. The curve obtained is non-linear at low loads. However the machine stiffness at high loads is about 260-310 KN mm^{-1} which compares favourably with the calculated value of 355 KN mm^{-1}.

5.2 Friction test :

This test was carried out at the same time as the stiffness calibration as the same readings are needed for both tests. The friction in the bushes may be taken as the difference between the forces in the duralumin specimen and the dynamometer after due allowance has been made for the weight of the centre crosshead. The results are plotted in Fig. A5.3. The line of equality obtained is at an angle of 45^{o}. This indicates that the crosshead travels without any significant friction in the bushes. Another test on the friction was conducted using three dial gauges fixed on the centre crosshead at three points 120^{o} apart. At each

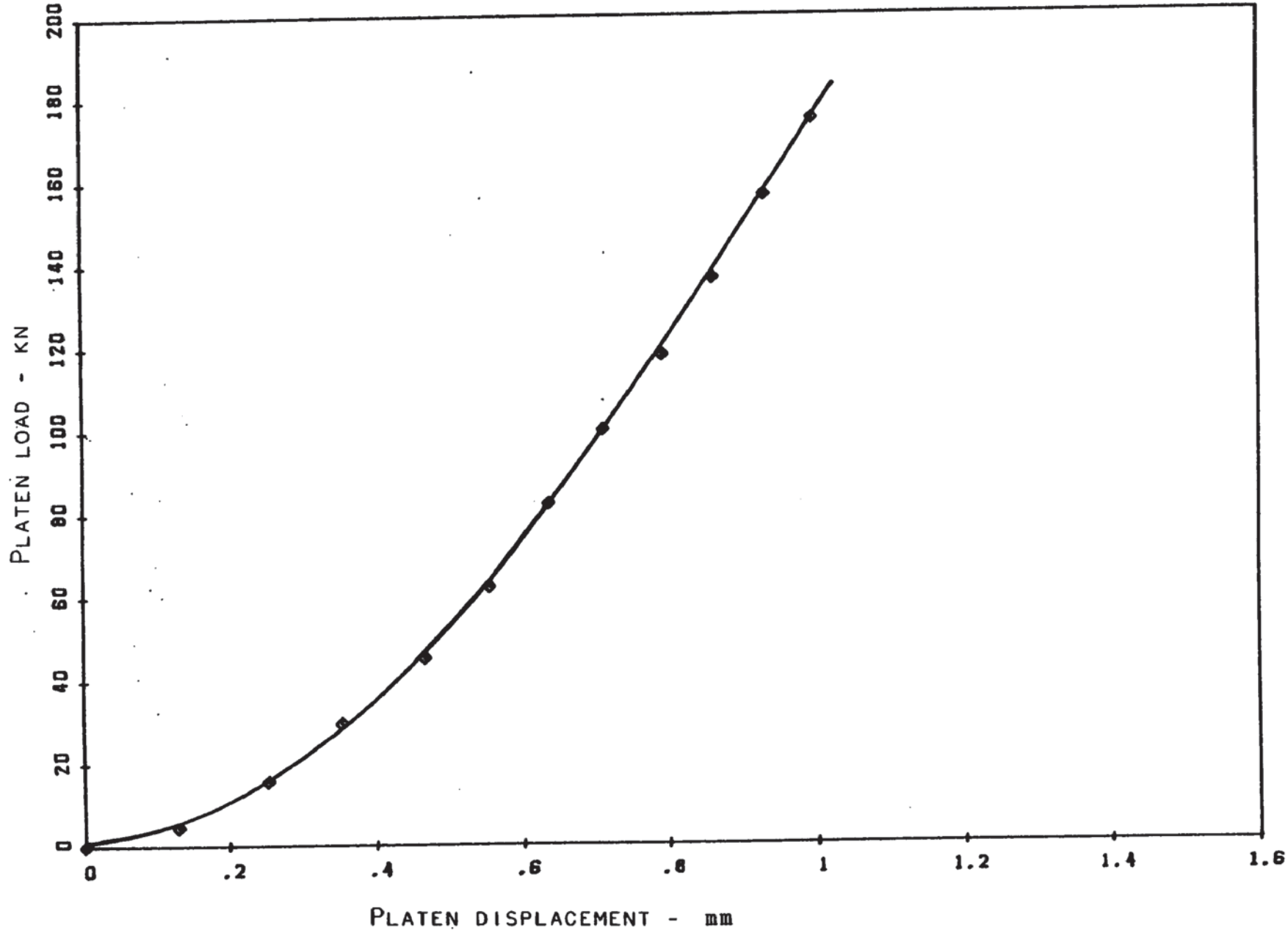

FIG. A5.2 STIFFNESS OF THE TEST RIG.

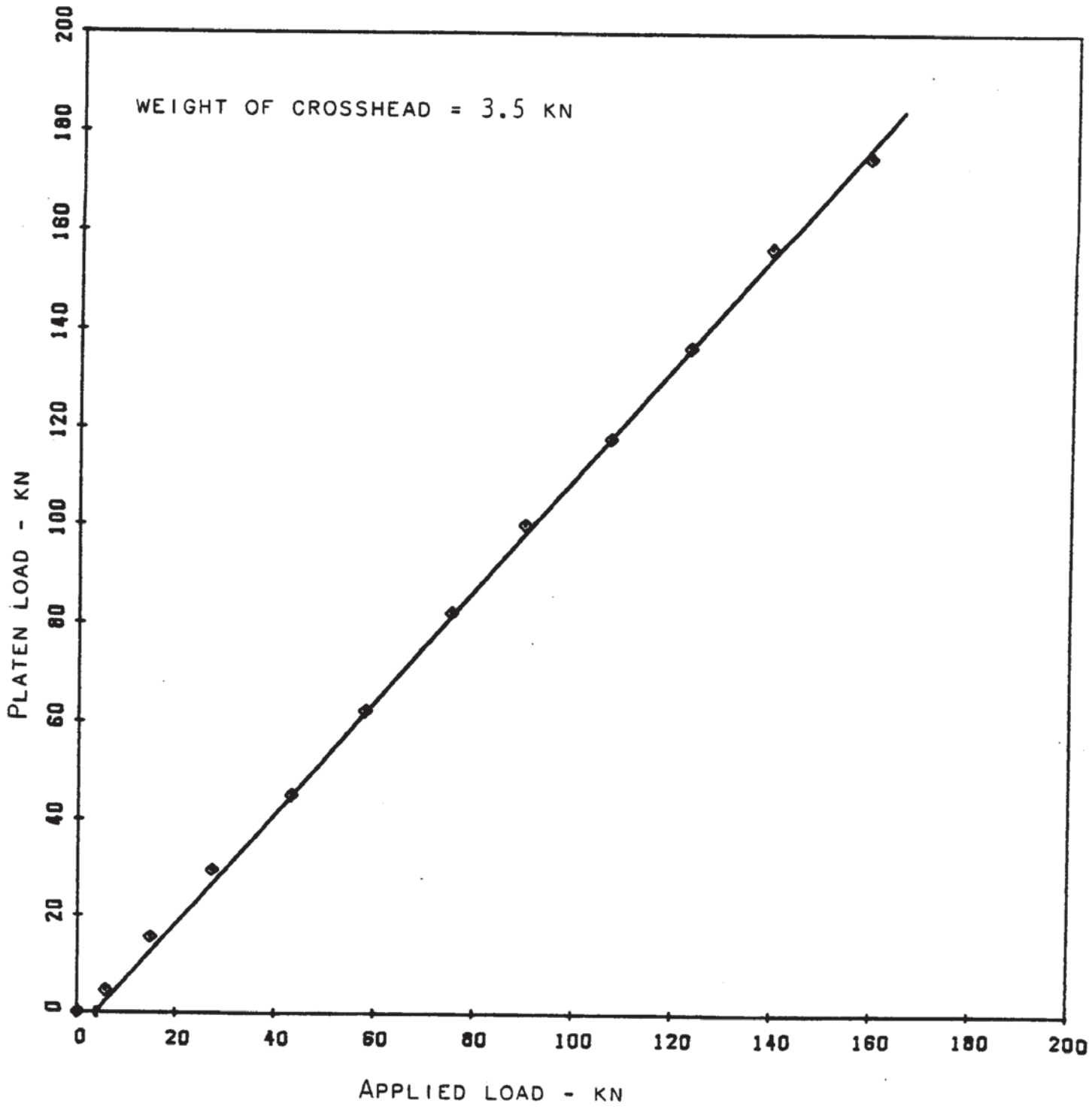

FIG. A5.3 FRICTION TEST RESULTS.

increment of the jack raise the readings of the dial gauges were taken. The results reported in Table A5.1 show again that the centre crosshead slides freely. The friction is therefore found to be negligable.

5.3 Check on the instrumentation :

Due to intermittent random errors apparently in the hardware of the data logger, a digital voltmeter was used at this stage to read the transducers. Figure A5.4 shows the calibration of the transducers obtained from a test using a dial gauge and the digital voltmeter.

Whilst carrying out the stiffness test and the friction test, the readings given by displacement transducers were monitored. Also the deformation of the duralumin specimen was calculated assuming the strains were constant along the specimen and were equal to those given by the strain gauges. A comparison between the two is shown in Fig. A5.5. It can be seen that the transducers are reading 10% high compared to the calculated values from the duralumin specimen. This is satisfactory, considering the assumption made in calculating the specimen contraction using the strain gauges. As a further check on the transducers, a test was carried out on a "Nimonic 105" specimen 50 mm in diameter and 150 mm in height. The specimen was heated to a

Position of the Centre crosshead	Dial gauge 1 mm	Dial gauge 2 mm	Dial gauge 3 mm
0	0.00	0.00	0.00
1	0.49	0.49	0.48
2	0.98	0.98	0.98
3	1.31	1.32	1.31
4	1.79	1.80	1.80
5	2.25	2.26	2.25
6	2.76	2.77	2.77
7	3.26	3.27	3.27
8	3.77	3.77	3.77
9	4.30	4.31	4.31
10	4.80	4.81	4.81
11	5.29	5.30	5.29
12	5.77	5.78	5.78
13	6.28	6.28	6.29
14	6.78	6.78	6.79
15	7.33	7.33	7.34
16	7.78	7.78	7.78
17	8.31	8.30	8.32
18	8.78	8.78	8.79
19	9.29	9.29	9.29
20	9.79	9.80	9.80
21	10.26	10.26	10.27
22	10.82	10.81	10.82
23	11.27	11.27	11.27
24	11.77	11.77	11.77
25	12.26	12.27	12.26
26	13.27	13.28	13.28
27	14.28	14.29	14.28
28	15.27	15.28	15.27
29	16.24	16.24	16.24
30	17.27	17.27	17.27

Table A5.1 Movement of the Centre Crosshead

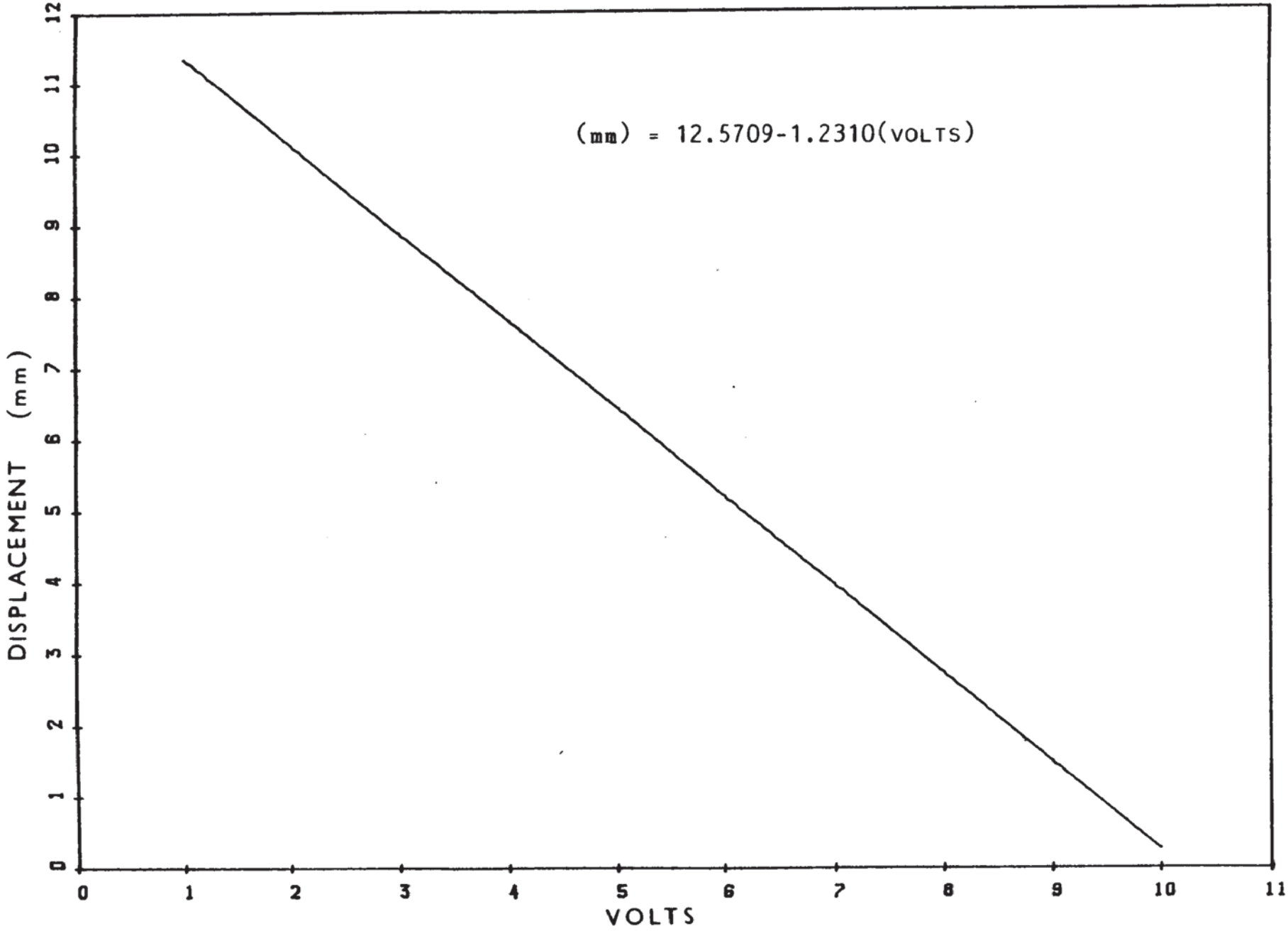

FIG. A5.4 CALIBRATION CHART FOR THE TRANSDUCERS.

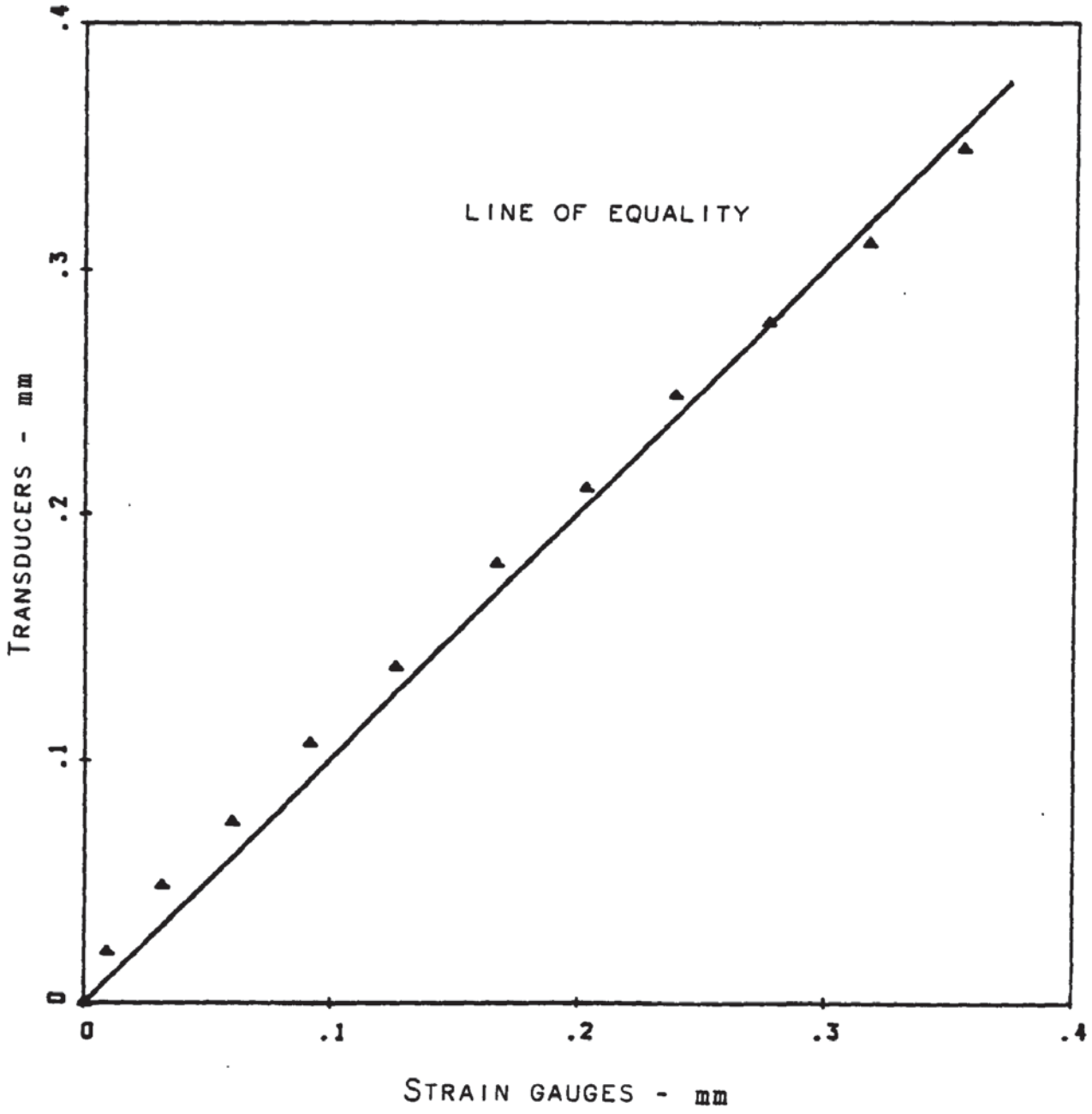

FIG. A5.5 COMPARISON BETWEEN STRAIN GAUGES AND TRANSDUCERS READINGS.

temperature of 500 °C and Young's modulus and the mean coefficient of expansion were determined. Figure A5.6 shows the graph of strain against furnace temperature. By comparison with the temperature distribution curves for concrete (Fig. 6.1), it is likely that in the latter stages of the test the furnace and the specimen temperatures are sensibly equal since steel has a higher thermal conductivity than concrete. Hence the value of the mean thermal expansion is found as 14.6×10^{-6} / deg. C. This figure is around 10% higher than the one recorded for the same temperature by Nimonic Alloys (1970) and which is equal to 13.3×10^{-6} / deg. C.

The values obtained for the elastic modulus were 187.5 KN mm^{-2} at 500 °C and 217.4 KN mm^{-2} at room temperature giving a 13.8% reduction, whilst the handbook values are respectively 193.1 KN mm^{-2} and 223.1 KN mm^{-2} giving a 13.4% reduction.

This would seem to indicate that although the transducers may be reading slightly high (up to 10%), the relative values are such that this possible error will be acceptable. Part of the error at elevated temperature under transient tests may be due to the relative expansion of the quartz rods, although this should be small.

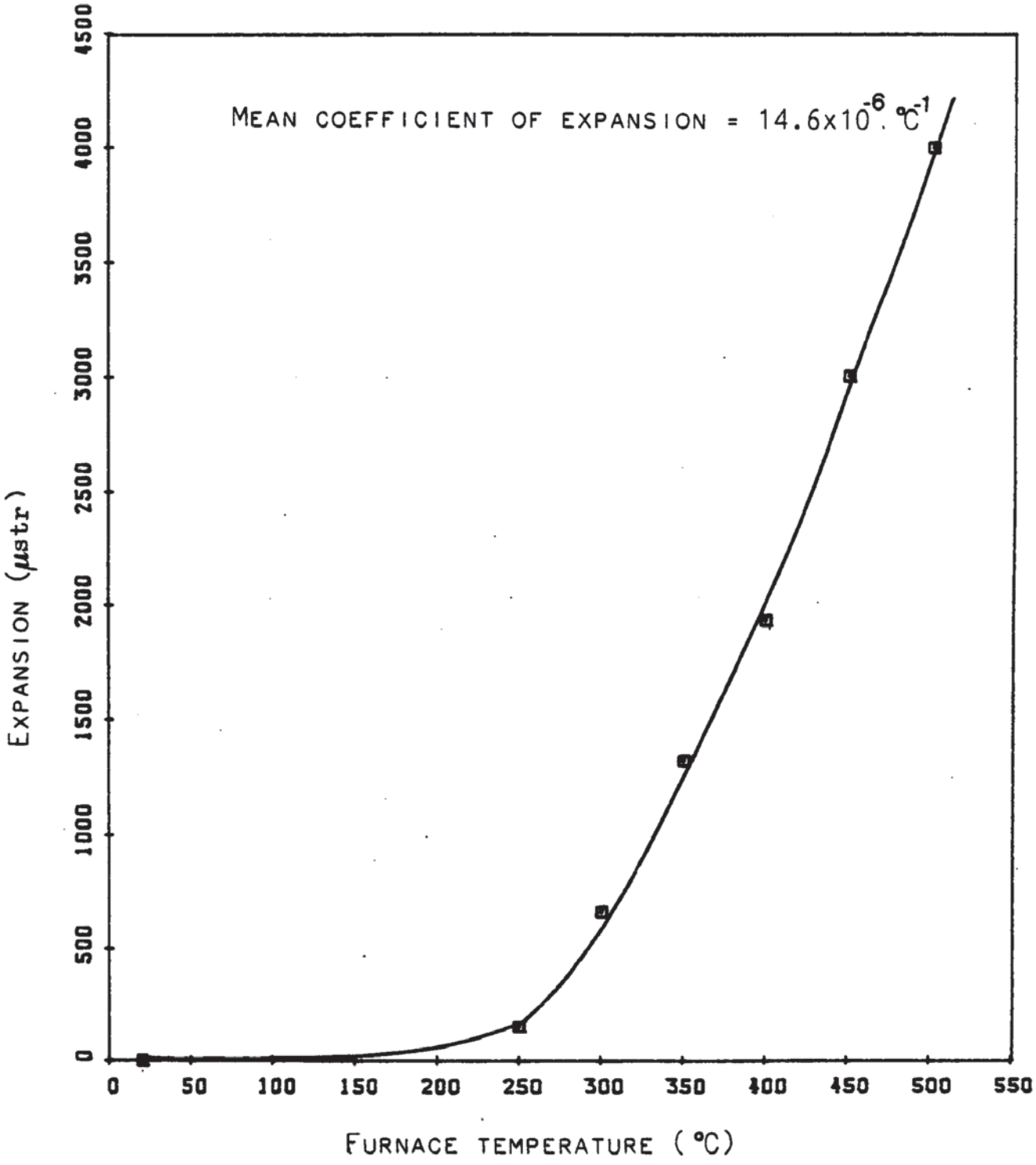

FIG. A5.6 THERMAL EXPANSION OF THE "NIMONIC 105" SPECIMEN.

APPENDIX SIX

Experimental Results

In this section the test results, obtained in the test series 3 and 4 are reported.

Tables A6.1 - A6.16 give the test results for heating to failure under constant stress at different stress levels. At a time zero, two values are reported corresponding to before and after loading. In these Tables T_F refers to furnace temperature whereas T_{mean} is the mean specimen temperature.

Tables A6.17 - A6.26 give the complete creep test results.

In both series of Tables, the initial deformation is reported.

The sign convention adopted is as follows :-

- : indicates compression and,

+ : tension.

Time min	T_F °C	T_{mean} °C	Strain 10^{-6}
0	17	17	0
1	122	20	8
2	202	40	92
3	273	72	291
4	305	95	557
5	326	115	857
10	385	220	2437
15	430	330	3768
20	468	420	4866
25	494	460	5839
30	520	500	6779
35	532	520	7636
40	556	550	8576
45	570	565	9691
50	593	593	10697
55	604	604	11438
60	621	621	12070
70	644	644	12976
80	670	670	13617
90	690	690	14083
100	701	701	14183
110	717	717	14257
120	729	729	14316
130	738	738	14299
140	742	742	14257
150	747	747	14249
160	750	750	14282
180	750	750	14257
200	750	750	14116
220	750	750	13950
222	658	748	13933
223	638	746	13916
224	621	730	13867
225	605	711	13808
230	558	656	13176
235	525	617	12120
240	500	588	10140
245	476	560	8925
250	455	535	8160
255	439	516	7611
260	422	496	7162

Table A6.1 Thermal Expansion Results

Time min	T_F °C	T_{mean} °C	Strain 10^{-6}
0	15	15	0
0	15	15	- 599
1	139	30	- 632
2	225	50	- 591
3	279	80	- 441
4	310	100	- 241
5	346	145	8
6	360	160	275
7	372	182	524
8	382	210	774
9	390	240	1031
10	402	265	1273
15	440	355	2204
20	474	425	2853
25	494	460	3227
30	516	490	3569
35	542	535	3760
40	560	555	3835
45	574	574	3826
50	588	588	3768
55	600	600	3735
60	619	619	3693
65	632	632	3593
70	656	656	3494
74	672	672	3336
80	681	681	3094
86	692	692	2845
90	701	701	2703
96	706	706	2471
100	709	709	2296
106	713	713	2046
110	715	715	1880
120	718	718	1388
130	723	723	940
140	729	729	516
145	731	731	141
146	731	731	58
150	732	732	- 308
153	733	733	- 731
154	734	734	- 907
155	734	734	- 1140
156	736	736	- 1464
157	736	736	- 1938
158	737	737	- 2753

Table A6.2 Experimental Results (failure Test)
Stress level: $0.2f'_c$ (Test 1)

Time min	T_F °C	T_{mean} °C	Strain 10^{-6}
0	17	17	0
0	18	18	- 823
1	118	20	- 839
2	207	40	- 791
3	276	75	- 648
4	318	110	- 424
5	347	145	- 176
6	363	165	88
7	377	195	352
8	386	220	616
9	394	245	847
10	402	265	1055
15	440	355	1936
20	481	440	2550
25	508	480	2998
30	532	520	3318
35	554	550	3493
40	565	562	3581
45	581	580	3613
50	599	599	3597
55	610	610	3517
60	617	617	3445
65	632	632	3366
70	644	644	3238
75	656	656	2910
80	666	666	2694
85	672	672	2502
90	681	681	2302
95	689	689	1895
100	697	697	1567
105	703	703	1271
110	706	706	1007
115	709	709	715
120	712	712	296
125	719	719	- 168
130	723	723	- 831
132	724	724	- 1343
133	725	725	- 2174

Table A6.3 Experimental Results (failure Test)
Stress level: $0.2f'_c$ (Test 2)

Time min	T_F °C	T_{mean} °C	Strain 10^{-6}
0	16	16	0
0	16	16	- 903
1	124	21	- 952
2	223	50	- 911
3	283	80	- 796
4	316	105	- 607
5	336	125	- 386
6	348	145	- 148
7	356	160	98
8	368	180	353
9	375	193	575
10	396	250	796
15	451	380	1666
20	479	440	2265
25	503	475	2700
30	524	510	2996
35	537	530	3160
40	555	550	3242
45	570	570	3291
50	590	590	3267
55	602	602	3143
60	612	612	3070
65	625	625	2971
70	641	641	2848
75	650	650	2700
80	659	659	2495
85	668	668	2290
90	676	676	2117
95	680	680	1920
100	688	688	1638
105	696	696	1477
110	699	699	1248
115	703	703	1034
120	709	709	813
125	712	712	591
130	716	716	304
135	719	719	33
140	722	722	- 197
145	725	725	- 558
150	728	728	- 1018
155	729	729	- 1921
157	729	729	- 2602

Table A6.4 Experimental Results (failure Test)
Stress level: $0.2f'_c$ (Test 3)

Time min	T_F °C	T_{mean} °C	Strain 10^{-6}
0	15	15	0
0	15	15	- 919
1	129	24	- 943
2	208	45	- 911
3	262	65	- 783
4	301	92	- 592
5	329	120	- 368
6	350	145	- 136
7	363	160	96
8	371	175	296
9	380	200	488
10	393	250	640
15	435	345	1255
20	466	410	1687
25	487	450	1911
30	511	485	1951
35	535	505	1839
40	565	560	1615
45	572	570	1279
50	583	583	831
55	591	591	320
60	602	602	- 224
65	616	616	- 1279
66	617	617	- 2254

Table A6.5 Experimental Results (failure Test)
Stress level: $0.4f'_c$ (Test 1)

Time min	T_F °C	T_{mean} °C	Strain 10^{-6}
0	17	17	0
0	17	17	- 974
1	134	26	- 1006
2	220	50	- 958
3	269	70	- 829
4	312	100	- 620
5	342	135	- 386
6	360	160	- 129
7	372	180	97
8	384	220	322
9	393	250	499
10	406	272	636
15	432	340	1143
20	461	400	1336
25	482	440	1304
30	498	470	1086
35	522	500	644
40	553	550	- 24
45	568	565	- 917
50	581	581	- 2575
51	581	581	- 3557

Table A.6.6 Experimental Results (failure Test)
Stress level $0.4f'_c$ (Test 2)

Time min	T_F °C	T_{mean} °C	Strain 10^{-6}
0	16	16	0
0	16	16	- 847
1	140	25	- 887
2	232	52	- 879
3	279	75	- 759
4	310	100	- 592
5	349	145	- 392
6	356	152	- 176
7	377	200	80
8	383	220	232
9	390	240	408
10	402	265	560
15	428	330	1111
20	454	400	1447
25	478	440	1559
30	495	462	1583
35	516	495	1447
40	534	520	1151
45	550	545	807
50	569	566	240
55	586	586	- 248
60	595	595	- 783
64	602	602	- 2782

Table A6.7 Experimental Results (failure Test)
Stress level $0.4f'_c$ (Test 3)

Time min	T_F °C	T_{mean} °C	Strain 10^{-6}
0	16	16	0
0	16	16	- 1320
1	127	22	- 1344
2	212	42	- 1336
3	268	70	- 1255
4	298	90	- 1127
5	321	110	- 942
6	349	145	- 732
7	361	160	- 531
8	375	190	- 346
9	386	224	- 185
10	397	250	- 64
15	426	320	290
20	463	410	338
25	493	460	121
30	525	510	- 370
32	530	515	- 676
34	540	530	- 1062
35	543	535	- 1287
37	553	550	- 1835
39	560	558	- 2615
40	561	560	- 3170
41	561	560	- 4184

Table A6.8 Experimental Results (failure Test)
Stress level: $0.6f'_c$ (Test 1)

Time min	T_F °C	T_{mean} °C	Strain 10^{-6}
0	17	17	0
0	17	17	- 1159
1	128	22	- 1191
2	209	40	- 1191
3	267	69	- 1103
4	303	95	- 935
5	335	125	- 711
6	350	145	- 520
7	368	173	- 320
8	383	210	- 128
9	392	240	16
10	403	264	152
15	428	330	512
20	457	398	616
25	485	447	488
30	519	500	176
32	526	510	- 40
34	536	522	- 272
36	546	540	- 560
38	554	552	- 927
40	560	559	- 1391
42	566	565	- 1999
43	570	569	- 3535

Table A6.9 Experimental Results (failure Test)
Stress level: 0.6 f'_c (Test 2)

Time min	T_F °C	T_{mean} °C	Strain 10^{-6}
0	22	22	0
0	22	22	- 1157
1	150	30	- 1174
2	218	47	- 1165
3	270	70	- 1083
4	310	100	- 968
5	329	120	- 771
6	353	147	- 575
7	390	205	- 345
8	393	240	- 172
9	401	260	- 8
10	409	280	123
15	430	330	517
20	455	392	566
25	480	440	443
30	512	490	- 148
32	520	500	- 427
34	529	516	- 681
36	538	532	- 1026
38	549	547	- 1461
40	554	552	- 1986
42	563	562	- 3710

Table A6.10 Experimental Results (failure Test)
Stress level: $0.6f'_c$ (Test 3)

Time min	T_F °C	T_{mean} °C	Strain 10^{-6}
0	19	19	0
0	19	19	- 2253
1	150	28	- 2277
2	240	55	- 2301
3	279	75	- 2229
4	302	92	- 2092
5	324	115	- 1915
6	365	170	- 1746
7	382	210	- 1577
8	394	250	- 1424
9	400	260	- 1304
10	406	273	- 1263
12	428	330	- 1207
14	436	350	- 1247
16	446	372	- 1336
20	467	412	- 1633
22	475	430	- 1883
24	488	450	- 2221
26	494	465	- 2696
28	509	485	- 3275
30	518	495	- 4297
31	521	502	- 5697

Table A6.11 Experimental Results (failure Test)
Stress level $0.7f'_c$ (Test 1)

Time min	T_F °C	T_{mean} °C	Strain 10^{-6}
0	20	20	0
0	20	20	- 1481
1	121	22	- 1521
2	213	45	- 1513
3	266	70	- 1424
4	302	92	- 1263
5	328	120	- 1054
6	350	145	- 853
7	367	173	- 660
8	379	200	- 491
9	391	231	- 346
10	398	252	- 257
12	414	290	- 161
14	428	326	- 161
16	445	370	- 193
18	460	400	- 290
20	466	414	- 426
22	476	430	- 628
24	481	440	- 893
26	494	460	- 1223
28	504	480	- 1625
30	516	492	- 2148
32	523	505	- 2921
34	530	517	- 4699
35	531	518	- 5576

Table A6.12 Experimental Results (failure Test)
Stress level $0.7f'_c$ (Test 2)

Time min	T_F °C	T_{mean} °C	Strain 10^{-6}
0	22	22	0
0	22	22	- 1372
1	133	25	- 1405
2	207	42	- 1388
3	258	65	- 1289
4	293	90	- 1124
5	314	105	- 909
6	339	130	- 702
7	348	143	- 521
8	366	173	- 347
9	378	200	- 215
10	389	230	- 132
12	406	270	- 25
14	426	325	33
16	444	370	41
18	460	400	- 25
20	473	430	- 124
22	482	440	- 264
24	490	450	- 479
26	506	482	- 735
28	514	490	- 1099
30	523	505	- 1545
32	530	517	- 2140
34	535	520	- 2958
36	538	530	- 4751
37	538	530	- 4999

Table A6.13 Experimental Results (failure Test)
Stress level: $0.7f'_c$ (Test 3)

Time min	T_F °C	T_{mean} °C	Strain 10^{-6}
0	21	21	0
0	21	21	- 1749
1	121	22	- 1790
2	207	42	- 1798
3	262	66	- 1709
4	303	92	- 1531
5	322	110	- 1304
6	348	145	- 1085
7	359	160	- 875
8	368	173	- 721
9	378	200	- 632
10	386	225	- 599
12	407	270	- 616
14	419	306	- 640
16	438	350	- 786
18	452	384	- 940
20	462	402	- 1166
22	472	430	- 1474
23	475	435	- 1668
24	482	440	- 1879
25	490	450	- 2114
26	493	455	- 2406
27	498	467	- 2721
28	500	470	- 3159
29	506	482	- 3944
30	510	486	- 5329

Table A6.14 Experimental Results (failure Test)
Stress level: 0.8 f'_c (Test 1)

Time min	T_F °C	T_{mean} °C	Strain 10^{-6}
0	18	18	0
0	18	18	- 1871
1	124	23	- 1911
2	202	40	- 1919
3	259	65	- 1831
4	292	85	- 1679
5	320	110	- 1503
6	336	126	- 1303
7	348	145	- 1135
8	359	160	- 983
9	370	175	- 879
10	379	200	- 839
12	395	250	- 855
14	409	280	- 943
16	428	330	- 1039
18	439	350	- 1223
20	450	382	- 1439
22	461	402	- 1759
24	473	430	- 2182
26	481	440	- 2694
28	493	455	- 3501
29	498	467	- 4653

Table A6.15 Experimental Results (failure Test)
Stress level: $0.8f'_c$ (Test 2)

Time min	T_F °C	T_{mean} °C	Strain 10^{-6}
0	22	22	0
0	22	22	- 1725
1	120	22	- 1741
2	212	45	- 1741
3	256	65	- 1644
4	300	90	- 1474
5	325	115	- 1272
6	340	130	- 1093
7	360	160	- 899
8	368	173	- 737
9	380	200	- 640
10	391	240	- 599
12	400	265	- 575
14	412	285	- 648
16	432	345	- 761
18	444	365	- 931
20	454	385	- 1174
22	467	420	- 1506
24	478	438	- 1911
26	490	450	- 2422
28	496	465	- 3240
30	506	482	- 4762

Table A6.16 Experimental Results (failure Test)
Stress level: 0.8 f'_c (Test 3)

Time min	Test 1	Test 2	Test 3
	Creep Strain 10^{-6}	Creep Strain 10^{-6}	Creep Strain 10^{-6}
0	0	0	0
0	499	676	716
1	515	700	740
2	539	732	756
3	555	756	781
4	571	772	797
5	587	789	813
6	595	805	829
7	603	821	837
8	612	829	845
9	628	853	869
10	636	861	885
20	748	966	1014
30	821	1054	1126
40	893	1151	1223
50	925	1215	1287
60	982	1287	1368
70	1038	1352	1440
80	1086	1416	1521
90	1118	1472	1569
100	1135	1513	1625
110	1159	1545	1674
120	1183	1577	1714
130	1199	1601	1754
140	1223	1625	1770
150	1279	1650	1818
160	1328	1682	1843
170	1384	1698	1883
180	1432	1738	1915
190	1481	1770	1955
200	1521	1794	1987
210	1545	1835	2028
220	1593	1859	2052
230	1625	1899	2084
240	1650	1915	2100
250	1698	1931	2132
260	1746	1979	2148
270	1794	2004	2164
280	1875	2020	2181
290	1955	2044	2213
300	2020	2084	2245

Table A6.17 Creep Results
Stress level: 0.2 f'_c , T= 200°C

Time min	Test 1	Test 2	Test 3
	Creep Strain 10^{-6}	Creep Strain 10^{-6}	Creep Strain 10^{-6}
0	0	0	0
0	1339	1181	1071
1	1397	1206	1095
2	1481	1239	1135
3	1547	1264	1183
4	1614	1289	1215
5	1672	1314	1255
6	1722	1347	1279
7	1763	1363	1303
8	1797	1372	1343
9	1830	1388	1367
10	1863	1405	1391
20	2071	1553	1559
30	2213	1669	1711
40	2312	1768	1815
50	2404	1851	1911
60	2479	1918	1991
70	2545	1991	2070
80	2604	2049	2150
90	2654	2107	2222
100	2703	2165	2278
110	2753	2206	2350
120	2803	2247	2406
130	2836	2297	2446
140	2870	2347	2478
150	2920	2388	2518
160	2953	2421	2566
170	2995	2454	2590
180	3036	2495	2630
190	3078	2528	2654
200	3111	2570	2702
210	3144	2578	2726
220	3169	2611	2742
230	3186	2660	2742
240	3211	2694	2766
250	3236	2760	2782
260	3252	2760	2814
270	3277	2801	2862
280	3294	2851	2894
290	3319	2892	2902
300	3344	2958	2918

Table A6.18 Creep Results
Stress level: $0.2f'_c$, T= 375°C

Time min	Test 1	Test 2
	Creep Strain 10^{-6}	Creep Strain 10^{-6}
0	0	0
0	2094	1907
1	2254	2044
2	2406	2132
3	2526	2221
4	2630	2317
5	2734	2390
6	2838	2462
7	2910	2535
8	2982	2599
9	3046	2663
10	3110	2720
20	3493	3050
30	3693	3251
40	3821	3436
50	3917	3540
60	4005	3629
70	4085	3701
80	4157	3766
90	4261	3838
100	4341	3903
110	4389	3967
120	4405	4007
130	4445	4055
140	4485	4096
150	4525	4128
160	4557	4168
170	4589	4200
180	4621	4232
190	4653	4265
200	4677	4297
210	4709	4337
220	4741	4377
230	4781	4450
240	4844	4514
250	4900	4570
260	4956	4659
270	5044	4739
280	5148	4836
290	5244	4908
300	5324	4997

Table A.6.19 Creep Results
Stress level: $0.2f'_c$, T=550°C

Time min	Test 1	Test 2
	Creep Strain 10^{-6}	Creep Strain 10^{-6}
0	0	0
0	3134	2823
1	3418	3143
2	3661	3373
3	3888	3595
4	4074	3767
5	4244	3931
6	4390	4079
7	4519	4202
8	4641	4325
9	4738	4416
10	4827	4498
20	5362	5006
30	5645	5212
40	5815	5376
50	5961	5540
60	6107	5688
70	6220	5835
80	6317	5950
90	6431	6065
100	6536	6188
110	6641	6303
120	6714	6410
130	6828	6549
140	6925	6697
150	7038	6829
160	7144	6993
170	7241	7140
180	7403	7296
190	7540	7460
200	7670	7674
210	7832	7854
220	7978	8035
230	8140	8216
240	8286	8380
250	8480	8593
260	8674	8806
270	8861	9036
280	9055	9291
290	9306	9512
300	9582	9759

Table A6.20 Creep Results
Stress level: $0.2f'_c$, T=700°C

Time min	Test 1	Test 2
	Creep Strain 10^{-6}	Creep Strain 10^{-6}
0	0	0
0	1047	1311
1	1095	1367
2	1135	1415
3	1183	1455
4	1223	1503
5	1271	1543
6	1311	1575
7	1351	1615
8	1383	1655
9	1415	1695
10	1447	1735
20	1703	2007
30	1903	2230
40	2078	2414
50	2166	2526
60	2254	2638
70	2358	2750
80	2478	2854
90	2574	2958
100	2662	3054
110	2758	3166
120	2846	3278
130	2958	3390
140	3070	3493
150	3174	3581
160	3270	3661
170	3374	3765
180	3469	3877
190	3557	3997
200	3637	4110
210	3749	4213
220	3861	4317
230	3973	4421
240	4093	4533
250	4173	4645
260	4261	4749
270	4357	4852
280	4453	4956
290	4557	5068
300	4677	5164

Table A6.21 Creep Results
Stress level: 0.4 f'_c, T=200°C

Time min	Test 1	Test 2
	Creep Strain 10^{-6}	Creep Strain 10^{-6}
0	0	0
0	1843	1965
1	2004	2087
2	2140	2193
3	2221	2275
4	2309	2348
5	2382	2413
6	2462	2479
7	2527	2552
8	2575	2601
9	2623	2658
10	2679	2715
20	2953	3017
30	3154	3253
40	3323	3416
50	3484	3530
60	3589	3726
70	3717	3930
80	3814	4085
90	3911	4231
100	4023	4370
110	4152	4476
120	4232	4598
130	4329	4704
140	4434	4802
150	4522	4900
160	4635	4998
170	4723	5079
180	4820	5161
190	4908	5267
200	5005	5381
210	5101	5479
220	5198	5585
230	5311	5691
240	5415	5789
250	5520	5878
260	5632	5992
270	5745	6098
280	5866	6204
290	5978	6302
300	6099	6416

Table A6.22 Creep Results
Stress level: $0.4f'_c$, T=375°C

Time min	Test 1	Test 2
	Creep Strain 10^{-6}	Creep Strain 10^{-6}
0	0	0
0	3878	4021
1	4232	4421
2	4434	4629
3	4585	4788
4	4723	4916
5	4852	5036
6	4949	5172
7	5037	5276
8	5126	5356
9	5198	5444
10	5270	5524
20	5673	5972
30	5962	6291
40	6131	6499
50	6316	6715
60	6501	6875
70	6662	7083
80	6807	7243
90	6952	7323
100	7089	7419
110	7226	7515
120	7322	7602
130	7419	7706
140	7531	7786
150	7660	7914
160	7805	8050
170	7934	8186
180	8079	8314
190	8199	8474
200	8312	8626
210	8473	8770
220	8610	8921
230	8771	9081
240	8940	9193
250	9125	9321
260	9302	9465
270	9519	9593
280	9728	9745
290	9905	10000
300	10090	10160

Table A6.23 Creep Results
Stress level: $0.4f'_c$, T=550°C

Time min	Test 1	Test 2
	Creep Strain 10^{-6}	Creep Strain 10^{-6}
0	0	0
0	1830	1746
1	1944	1883
2	2025	1971
3	2098	2060
4	2171	2140
5	2235	2205
6	2292	2277
7	2349	2325
8	2406	2406
9	2454	2470
10	2511	2535
20	2786	2768
30	2997	2961
40	3175	3170
50	3369	3363
60	3564	3540
70	3726	3701
80	3863	3854
90	3969	3975
100	4082	4080
110	4212	4184
120	4317	4297
130	4430	4393
140	4536	4506
150	4649	4603
160	4730	4699
170	4811	4796
180	4900	4908
190	4997	5005
200	5103	5101
210	5192	5206
220	5289	5335
230	5402	5439
240	5508	5536
250	5597	5657
260	5694	5769
270	5791	5906
280	5904	6027
290	6010	6172
300	6131	6308

Table A6.24 Creep Results
Stress level: $0.6f'_c$, T=200°C

Time min	Test 1	Test 2
	Creep Strain 10^{-6}	Creep Strain 10^{-6}
0	0	0
0	2357	2323
1	2527	2552
2	2657	2758
3	2770	2897
4	2851	3020
5	2948	3111
6	3062	3193
7	3143	3291
8	3215	3390
9	3296	3463
10	3361	3546
20	3637	3800
30	3871	4038
40	4074	4268
50	4268	4473
60	4455	4645
70	4617	4809
80	4762	4949
90	4924	5113
100	5086	5261
110	5256	5384
120	5378	5515
130	5491	5630
140	5653	5737
150	5783	5868
160	5896	5983
170	6026	6098
180	6131	6221
190	6253	6336
200	6366	6443
210	6479	6558
220	6609	6681
230	6714	6796
240	6836	6919
250	6949	7050
260	7087	7173
270	7208	7313
280	7330	7444
290	7459	7592
300	7597	7731

Table A6.25 Creep Results
Stress level: $0.6f'_c$, T=325°C

Time min	Test 1	Test 2
	Creep Strain 10^{-6}	Creep Strain 10^{-6}
0	0	0
0	3222	3070
1	3453	3316
2	3613	3472
3	3741	3611
4	3853	3743
5	3973	3874
6	4085	3981
7	4181	4071
8	4261	4161
9	4341	4227
10	4413	4292
20	4788	4695
30	5068	4982
40	5260	5195
50	5388	5392
60	5500	5524
70	5604	5638
80	5708	5753
90	5828	5868
100	5908	5975
110	6028	6098
120	6132	6213
130	6243	6344
140	6379	6459
150	6499	6566
160	6619	6689
170	6779	6804
180	6939	6935
190	7091	7083
200	7243	7222
210	7443	7387
220	7626	7575
230	7802	7822
240	8002	8051
250	8218	8289
260	8426	8511
270	8642	8749
280	8897	9012
290	9177	9381
300	9457	9676

Table A.26 Creep Results
Stress level: $0.6f'_c$, T=450°C

APPENDIX SEVEN

Listing of the program

This appendix deals with the listing of the programs written to control the test rig.

The language used is FORTRAN, as presented in the Fordac manual provided by Intercole Systems Limited. The main program "FRIGCONT" is first listed, followed by the appropriate subroutines.

The standard subroutines are not included.

```
0001 C      FRIGCONT IS A PROGRAM FOR CONTROLING THE TEST RIG.
0002 C      IT PROVIDES FACILITIES FOR DATA STORAGE/RETRIEVAL.
0003 C      THE DATA FROM THIS PROGRAM IS STORED IN DATA FILE ON DRIVE "1".
0004 C      THE STRESS OR THE STRAIN CAN BE MAINTAINED CONSTANT DURING TEST.
0005 C
0006        DIMENSION NTEMP(4)
0007        CALL PFAIL
0008 C      INPUT INFORMATION
0009 C
0010        CALL RECUVA
0011 5      FORMAT(X/)
0012        WRITE(1,10)
0013 10     FORMAT(/19HENTER:- DAY & MONTH)
0014        READ(1,30)IDAY,MNTH
0015 30     FORMAT(2I3)
0016 C
0017        CALL RECUVA
0018        WRITE(1,20)
0019 20     FORMAT(/52HENTER:-DATA FILE NUMBER FOR OUTPUT & IDENTIFIER CODE)
0020        READ(1,30)IDFILE,IDENT
0021 C
0022 C      OPEN DATA FILE ON DISC IN DRIVE "1"
0023        CALL KOPEN(1,IDFILE,8)
0024        IF(KDS(M))500,35,500
0025 35     WRITE(25,5)0,NDATA,IDAY,MNTH,IDENT,DUM,DUM
0026        IF(KDS(M))500,36,500
0027 36     NDATA=0
0028 C
0029        CALL RECUVA
0030        WRITE(1,40)
0031 40     FORMAT(/44HENTER:- DURATION OF TEST IN HRS, MINS & SECS)
0032        READ(1,50)IHRS,MINS,ISECS
0033 50     FORMAT(3I3)
0034        ITIMEUP=(IHRS*60+MINS)*60+ISECS
0035 51     FORMAT(/58HENTER:-END OF FIRST & SECOND TIME ZONES IN HRS,MINS &
0036       /SECS)
0037 53     FORMAT(/71HENTER:-TIME INCREMENTS AT WHICH READINGS ARE TO BE
0038       /TAKEN FOR THE FIRST,/53HSECOND & THIRD TIME ZONES RESPECTIVELY IN
0039       /MINS & SECS)
0040 C
0041 C---- SETTING OF TIME CONSTANTS ----
0042 C      SETTING OF TIME ZONES
0043        CALL RECUVA
0044        WRITE(1,51)
0045        READ(1,52)IHRS1,MINS1,ISECS1,IHRS2,MINS2,ISECS2
0046 52     FORMAT(6I3)
0047        KT1=(IHRS1*60+MINS1)*60+ISECS1
0048        KT2=(IHRS2*60+MINS2)*60+ISECS2
0049        ITIME1=ITIMEUP-KT1
0050        ITIME2=ITIMEUP-KT2
0051 C
0052 C      SETTING OF TIME INCREMENTS
0053        CALL RECUVA
0054        WRITE(1,53)
0055        READ(1,52)IMIN1,ISEC1,IMIN2,ISEC2,IMIN3,ISEC3
```

```
0056        INCT1=IMIN1*60+ISEC1
0057        INCT2=IMIN2*60+ISEC2
0058        INCT3=IMIN3*60+ISEC3
0059 C
0060        CALL RECUVA
0061        WRITE(1,55)
0062 55     FORMAT(/25HENTER:- LOAD REQUIRED (N))
0063        READ(1,70)SMAXLD
0064 C
0065        CALL RECUVA
0066        WRITE(1,60)
0067 60     FORMAT(/36HENTER:- LENGTH OF THE SPECIMEN IN MM)
0068        READ(1,70)SLENGTH
0069 70     FORMAT(F7.3)
0070 C
0071        WRITE(1,80)
0072 80     FORMAT(/62HCHANNEL NUMBERS 400, 401, 402 & 403 ARE USED FOR
0073       /THERMOCOUPLES/28HHOW MANY DO YOU WISH TO USE?)
0074        READ(1,30)NTHERM
0075 C
0076        CALL RECUVA
0077        WRITE(1,90)
0078 90     FORMAT(/50HENTER:- CHANNEL NUMBERS USED FOR LOAD & DEFLECTION)
0079        READ(1,30)ICHANLOAD,ICHANDEF
0080 C
0081 C----- SETTING OF CONSTANTS ----
0082 C      OTHER CONSTANTS
0083 C      SPECIMEN DIAMETER IN (MM)
0084        DIAM=50.0
0085        AREA=3.141593*DIAM*DIAM/4.0
0086 C
0087 C----- TESTING OF TRANSDUCERS BEFORE START OF TEST ----
0088 C      TESTING OF LOAD TRANSDUCER
0089 C      TAKING THE ZERO-LOAD READING IN VOLTS
0090 97     CALL RLOAD(ICHANLOAD,PLOAD,-1,VOLTS0)
0091        CALL RLOAD(ICHANLOAD,PLOAD,0,VOLTS0)
0092        IF(PLOAD)97,6,97
0093 6      CONTINUE
0094        CALL RLOAD(ICHANLOAD,PLOAD,0,VOLTS0)
0095        PLOUT=PLOAD/1.0E3
0096        WRITE(1,91)ICHANLOAD,PLOUT
0097 91     FORMAT(/12HCHANNEL NO.=,I3,12H LOAD (KN) =,F7.3)
0098 C
0099 C      TESTING OF DEFLECTION TRANSDUCER
0100        CALL DEFLTN(ICHANDEF,DLENGTH,0)
0101        WRITE(1,92)ICHANDEF,DLENGTH
0102 92     FORMAT(/12HCHANNEL NO.=,I3,18H DEFLECTION (MM) =,F7.3)
0103 C
0104 C      TESTING OF THERMOCOUPLES
0105        DO 93 I=1,NTHERM
0106        ICHAN=399+I
0107        CALL TEMP(ICHAN,ITEMP)
0108        WRITE(1,94)ICHAN,ITEMP
0109 94     FORMAT(/12HCHANNEL NO.=,I3,7H TEMP =,I4)
0110 93     CONTINUE
```

```
0111 C
0112 C      IS RE-TESTING REQUIRED?
0113 99     WRITE(1,95)
0114 95     FORMAT(/54HDO YOU WISH TO RE-TEST TRANSDUCERS? (ANS. 1=YES, 0=NO))
0115        READ(1,96)NOYES
0116 96     FORMAT(I3)
0117        IF(NOYES)99,98,97
0118 98     CONTINUE
0119 C
0120 C----- START OF TEST ----
0121        CALL RECUVA
0122        WRITE(1,100)
0123 100    FORMAT(/45HWHEN READY TO START TEST TYPE 'C' AFTER PAUSE)
0124 C       PLATEN DOES NOT HAVE TO BE IN CONTACT WITH SPECIMEN.
0125        PAUSE:-
0126 C      START CLOCK
0127        CALL WCLOCK(0,0,0,0)
0128 C
0129 C----- ADVANCING PLATEN ONTO SPECIMEN ----
0130 110    CONTINUE
0131 C      CALLING SUBROUTINE RLOAD TO READ LOAD
0132        CALL RLOAD(ICHANLOAD,PLOAD,1,VOLTS0)
0133        IF(PLOAD)120,120,130
0134 C
0135 C      CALLING SUBROUTINE ADDLD TO ADD LOAD
0136 120    CALL ADDLD(MOTOR)
0137        GOTO 110
0138 C
0139 C----- START OF LOADING ----
0140 C      PLATEN IN CONTACT WHITH SPECIMEN SO START COUNTDOWN TIMER
0141 130    CALL WSCANT(ITIMEUP)
0142        ITIME=-ITIMEUP
0143        NEXTIME=-ITIMEUP
0144 C
0145 C----- SECTION FOR TAKING THE READINGS AND RECORDING ONTO DISC ----
0146 135    CONTINUE
0147 C      TIME CALCULATIONS
0148        NTIME=ITIMEUP+ITIME
0149 C      STRESS CALCULATIONS
0150        STRESS=PLOAD/AREA
0151 C      STRAIN CALCULATIONS
0152        CALL DEFLTN(ICHANDEF,DLENGTH,1)
0153        NSTRAIN=DLENGTH/SLENGTH*1.E6-FLOAT(NSTRNO)
0154        IF(NTIME)136,136,137
0155 136    NSTRNO=NSTRAIN
0156 137    CONTINUE
0157 C      TEMPERATURE CALCULATIONS
0158        DO 140 I=1,NTHERM
0159        ICHAN=399+I
0160        CALL TEMP(ICHAN,ITEMP)
0161 140    NTEMP(I)=ITEMP
0162 C
0163 C      WRITE INFORMATION TO DATA FILE ON DISC IN DRIVE '1'
0164        NDATA=NDATA+1
0165        WRITE(25,5)NDATA,NTIME,STRESS,NSTRAIN,NTEMP(1)
```

```
0166        IF(KBS(M))500,150,500
0167 150    CONTINUE
0168 C
0169 C      OUTPUT TO VDU
0170 C
0171        IF(JSENSE(I))151,151,155
0172 151    IPT=IPT+1
0173        IF(IPT-15)154,152,152
0174 152    IPT=0
0175        WRITE(1,153)
0176 153    FORMAT(/68HREADING  LOAD      STRESS      STRAIN                TEMP.
0177       /C              /68H  NO.      KN       N/MME2        E-6      400
0178       /401      402      403  /)
0179 154    PLOUT=PLOAD/1.0E3
0180        WRITE(1,155)NDATA,PLOUT,STRESS,NSTRAIN,(NTEMP(I),I=1,4)
0181 155    FORMAT(I5,4X,F7.3,4X,I5,4(4X,I4))
0182 C
0183 C---- TESTING FOR TIME INCREMENTS & TIMEUP ----
0184 C      TIMEUP TEST
0185        IF(ITIME)160,2000,2000
0186 C      TIME INCREMENT TESTS
0187 160    IF(ITIME+ITIME1)200,170,170
0188 170    IF(ITIME+ITIME2)190,180,180
0189 180    INCTIME=INCT3
0190        GOTO 210
0191 190    INCTIME=INCT2
0192        GOTO 210
0193 200    INCTIME=INCT1
0194 210    NEXTIME=NEXTIME+INCTIME
0195 C
0196 C---- TESTING FOR LOAD & READING TIME ----
0197 C      READ LOAD
0198 215    CALL RLOAD(ICHANLOAD,PLOAD,1,VOLTS0)
0199 C      READ TIME
0200        CALL RSCANT(ITIME)
0201 C      TEST IF READINGS REQUIRED
0202        IF(ITIME-NEXTIME)220,135,135
0203 C
0204 C      TESTING OF LOAD
0205 220    IF(SMAXLD-PLOAD)230,240,250
0206 C      SUBROUTINE TO REDUCE LOAD
0207 230    CALL REDLD(MOTOR)
0208        GOTO 215
0209 C      SUBROUTINE TO STOP LOAD
0210 240    CALL STPLD(MOTOR)
0211        GOTO 215
0212 C      SUBROUTINE TO ADD LOAD
0213 250    CALL ADDLD(MOTOR)
0214        GOTO 215
0215 C
0216 C      END OF MAIN SECTION
0217 C
0218 C---- END OF TEST SECTION ----
0219 C      STOP LOAD
0220 2000   CALL STPLD(MOTOR)
```

```
0221 C
0222 C      WRITE NO. OF DATA STORED TO FIRST RECORD OF DATA FILE & CLOSE DATA
0223 C      FILE
0224        WRITE(25,5)0,NDATA,IDAY,MNTH,IDENT,DUM,DUM
0225        IF(KDS(M))500,260,500
0226 260    CALL KCLOSE
0227 C
0228        CALL RECUVA
0229 265    WRITE(1,270)
0230 270    FORMAT(/41HDO YOU WISH TO UNLOAD ?(ANS. 1=YES, 0=NO))
0231        READ(1,30)NOYES
0232        IF(NOYES)265,4000,280
0233 C
0234 C      UNLOADING
0235 280    CALL REDLD(MOTOR)
0236 C      READ LOAD
0237 290    CALL RLOAD(ICHANLOAD,PLOAD,1,VOLTS0)
0238        IF(PLOAD)300,300,290
0239 C
0240 C      TIME DELAY BEFORE STOPPING MOTOR
0241 C      REQUIRED TIME DELAY=IDELAY-SECS
0242 300    IDELAY=2
0243        CALL WSCANT(IDELAY)
0244 310    CALL RSCANT(ITIME)
0245        IF(ITIME)310,320,320
0246 C      STOP UNLOADING
0247 320    CALL STPLD(MOTOR)
0248 C
0249        CALL RECUVA
0250 4000   WRITE(1,330)
0251 330    FORMAT(/46HWHEN READY TO PLOT GRAPHS TYPE "C" AFTER PAUSE)
0252        PAUSE:-
0253 C
0254 C----- CALL UP GRAPH PLOTTING ROUTINES TO PLOT RECORDED DATA ----
0255        NGRAPH=NTHERM+2
0256        CALL GRAPHS(IDFILE,NGRAPH)
0257        GOTO 3000
0258 C
0259 C      DATA DISC ERROR OUTPUT
0260 500    M=KDS(M)
0261        WRITE(1,501)M,IDFILE
0262 501    FORMAT(/51HDATA STORAGE ERROR. SEE FODOS OPERATING MANUAL. KDSI6/
0263       /16HDATA FILE NUMBER,I6)
0264 3000   STOP
0265        END
```

```
  COMP DEFLTN,1


0001 C---- SUBROUTINE TO CALCULATE THE DEFLECTION IN "MM" FROM TRANSDUCERS
0002 C
0003       SUBROUTINE DEFLTN(ICHANDEF,DLENGTH,ITEST)
0004       RPT=0
0005 15    A=0
0006       DO 12 I=1,3
0007       CALL CHAN(ICHANDEF,9,1,4)
0008       CALL DVM(IDATA,IE)
0009       IF(IE)11,9,11
0010 11    WRITE(1,2)ICHANDEF
0011 2     FORMAT(/45HOPEN CIRCUIT ON DEFLECTION TRANSDUCER CHANNEL,I6)
0012       IF(ITEST)18,10,18
0013 9     A=A+FLOAT(IDATA)
0014 12    CONTINUE
0015       IF(IABS(IDATA)-32000)34,15,15
0016 34    IF((ABS(3.0/A*FLOAT(IDATA)-1.0)*100.0)-20.0)13,13,14
0017 14    RPT=RPT+1.0
0018       IF(RPT-5.0)15,16,16
0019 16    WRITE(1,17)ICHANDEF
0020 17    FORMAT(/42HINCONSISTENT DEFLECTION READING OF CHANNEL,I6)
0021       GOTO 18
0022 13    VOLTS=FLOAT(IDATA)*333.333E-6
0023 C     EQUATION TO CONVERT FROM VOLTS TO "MM"
0024       DLENGTH=24.70543-1.286555*(VOLTS+10.0)
0025 10    RETURN
0026 18    CALL STPLD(MOTOR)
0027       WRITE(1,20)
0028 20    FORMAT(/25HPROGRAM & TEST TERMINATED)
0029       STOP
0030       END
A          000E
I          0010
IE         0011
RPT        0012
IDATA      0014
MOTOR      0015
VOLTS      0016
COMPILED
```

RLOAD

```
0001 C---- SUBROUTINE TO CALCULATE THE LOAD IN "N" FROM LOAD CELL ----
0002 C
0003       SUBROUTINE RLOAD(ICHANLOAD,PLOAD,ITEST,VOLTS0)
0004       RPT=0.
0005 15    A=0.
0006       DO 12 I=1,3
0007       CALL CHAN(ICHANLOAD,0,1,5)
0008       CALL DVM(IDATA,IE)
0009       IF(IE)11,9,11
0010 11    WRITE(1,2)ICHANLOAD
0011 2     FORMAT(/39HOPEN CIRCUIT ON LOAD TRANSDUCER CHANNEL,I6)
0012       IF(ITEST)10,10,18
0013 9     A=A+FLOAT(IDATA)
0014 12    CONTINUE
0015       IF (IABS(IDATA)-32000)34,15,15
0016 34    IF((ABS(3.0/A*FLOAT(IDATA)-1.0)*100.0)-10.0)13,13,14
0017 14    RPT=RPT+1.0
0018       IF(RPT-5.0)15,16,16
0019 16    WRITE(1,17)ICHANLOAD
0020 17    FORMAT(/36HINCONSISTENT LOAD READING OF CHANNEL,I6)
0021       GOTO 18
0022 C     CALCULATIONS MICROVOLTS
0023 13    VOLTSM=FLOAT(IDATA)*.3333333
0024       IF(ITEST)19,21,21
0025 19    VOLTS0=VOLTSM
0026 21    CONTINUE
0027 C     EQUATION TO CONVERT FROM MICROVOLTS TO LOAD "N"
0028       PLOAD=297.6057*(VOLTSM-VOLTS0)
0029 10    RETURN
0030 18    CALL STPLD(MOTOR)
0031       WRITE(1,20)
0032 20    FORMAT(/25HPROGRAM & TEST TERMINATED)
0033       STOP
0034       END
```

ADDLD

```
0001 C      SUBROUTINE TO ADD LOAD TO SPECIMEN.
0002 C      SWITCHING VIA 8 CHANNEL CLP051 ANALOGUE OUTPUT INTERFACE
0003 C      POWER ON VIA CHANNEL 1  20 MILLIAMPS
0004 C      POWER OFF VIA CHANNEL 1   4 MILLIAMPS
0005 C      FORWARD VIA CHANNEL 2  20 MILLIAMPS
0006 C      REVERSE VIA CHANNEL 2   4 MILLIAMPS
0007 C
0008        SUBROUTINE ADDLD(MOTOR)
0009        IF(MOTOR)3,3,4
0010 C      SWITCH FORWARD
0011 3      CALL ANOUT(0,2,255)
0012 C      SWITCH ON
0013        CALL ANOUT(0,1,255)
0014        MOTOR=1
0015 4      RETURN
0016        END
COMPILED
```

REDLD

```
0001 C---- SUBROUTINE TO REDUCE LOAD TO SPECIMEN ----
0002 C      SWITCHING VIA 8 CHANNELS CLP051 ANALOGUE OUTPUT INTERFACE
0003 C      POWER ON VIA CHANNEL 1  20 MILLIAMPS
0004 C      POWER OFF VIA CHANNEL 1   4 MILLIAMPS
0005 C      FORWARD VIA CHANNEL 2  20 MILLIAMPS
0006 C      REVERSE VIA CHANNEL 2  4 MILLIAMPS
0007 C
0008        SUBROUTINE REDLD(MOTOR)
0009        IF(MOTOR)4,3,3
0010 C      SWITCH REVERSE
0011 3      CALL ANOUT(0,2,0)
0012 C      SWITCH ON
0013        CALL ANOUT(0,1,255)
0014        MOTOR=-1
0015 4      RETURN
0016        END
COMPILED
```

STPLD

```
0001 C---- SUBROUTINE TO STOP LOAD TO SPECIMEN ----
0002 C---- SWITCHING VIA 8 CHANNELS CLP051 ANALOGUE OUTPUT INTERFACE --
0003 C---- POWER ON VIA CHANNEL 1  20 MILLIAMPS ----
0004 C---- POWER OFF VIA CHANNEL 1   4 MILLIAMPS ----
0005 C---- FORWARD VIA CHANNEL 2  20 MILLIAMPS ----
0006 C---- REVERSE VIA CHANNEL 2   4 MILLIAMPS ----
0007 C
0008        SUBROUTINE STPLD(MOTOR)
0009 C      SWITCH OFF
0010        CALL ANOUT(0,1,0)
0011        MOTOR=0
0012        RETURN
0013        END
COMPILED
```

```
  COMP TEMP,1.
0001 C---- SUBROUTINE TO CALCULATE THE TEMP. DEGREES C FOR CHROMEL/ALUMEL
0002 C     THERMOCOUPLES UP TO 950 DEGREES C ----
0003 C---- AMBIENT TEMPERATURE CORRECTION AND LINEARISATION BY POLYNOMIAL----
0004 C
0005 C     A(1) TO A(11) CONTAIN POLYNOMIAL COEFFICIENTS
0006 C     A(12) AND A(13) CONTAIN COEFFICIENTS OF BEST STRAIGHT LINE FOR
0007 C     AMBIENT CONVERSION TO VOLTAGE.
0008 C     A2 IS NORM 6 SLOPE IN MICROVOLTS/DEGREE
0009 C     B2 IS NORM 6 OFFSET IN MICROVOLTS
0010 C     COLD JUNCTION IS CHANNEL NO. 420
0011 C
0012       DIMENSION A(13)
0013       SUBROUTINE TEMP(ICHAN,ITEMP)
0014       A(1) = -.2175252E+00
0015       A(2) =  .2641917E+02
0016       A(3) = -.1334961E+01
0017       A(4) =  .3502843E+00
0018       A(5) = -.4650688E-01
0019       A(6) =  .3607113E-02
0020       A(7) = -.1752132E-03
0021       A(8) =  .5418762E-05
0022       A(9) = -.1037811E-06
0023       A(10)=  .1122928E-08
0024       A(11)= -.5249913E-11
0025       A(12)=  .1192093E-06
0026       A(13)=  .4000000E-01
0027       A2   =  2570.0
0028       B2   =  0.0
0029 C
0030       ICR=420
0031       CALL CHAN(ICR,5,1,6)
0032       CALL DVM(ID2,IFLAG)
0033       VM=(FLOAT(ID2)*16.66667-B2)*A(13)/A2+A(12)
0034 C
0035       CALL CHAN(ICHAN,2,1,4)
0036       CALL DVM(ID2,IFLAG)
0037       IF(IFLAG)11,9,11
0038 11    WRITE(1,2)ICHAN
0039 2     FORMAT(/36HOPEN CIRCUIT ON THERMOCOUPLE CHANNEL:I6)
0040       GOTO 10
0041 9     DA=FLOAT(ID2)*1.666667E-3-VM
0042 C
0043 C     LINEARISE BY HORNERS METHODE
0044 C
0045       ITEMP=(A(1)+DA*
0046      /(A(2)+DA*
0047      /(A(3)+DA*
0048      /(A(4)+DA*
0049      /(A(5)+DA*
0050      /(A(6)+DA*
0051      /(A(7)+DA*
0052      /(A(8)+DA*
0053      /(A(9)+DA*
0054      /(A(10)+DA*
0055      /(A(11))))))))))))
0056 10     RETURN
0057       END
```

LIST OF REFERENCES

Ø1. Abrams H S (1970) — Compressive Strength of Concrete at Temperatures of 1600 F. ACI, SP25, 1970, 15pp.

Ø2. Allen D E (1974) Lie T T — Further Studies of the Fire Resistance of Reinforced Concrete Columns. Technical paper No. 416, Division of Building Research, Ottawa, June 1974.

Ø3. Anderberg Y (1976) — Fire Exposed Hyperstatic Concrete Structures - An experimental and theoretical study. Lund Institute of Technology, Bulletin 55, 1976.

Ø4. Anderberg Y (1983) — Predicted Fire Behaviour of Steels and Concrete Structures. The Three Decades of Structural Fire Safety, (BRE), February 1983.

Ø5. ASTM Standard (1975) — C 617-76 Capping Cylindrical Concrete Specimens. ASTM, 1975.

Ø6. Baldwin R (1973) North M A — A Stress-strain Relationship for Concrete at High Temperatures. Building Research Establishment, Fire Research Station. Magazine of Concrete Research : Vol. 25, No. 85, December 1973.

Ø7. Barnard P R (1976) — Researches into the Complete Stress/strain Curve for Concrete. MCR : Vol. 16, No. 49, 1964.

Ø8. Bazant Z P (1978) Panula L — Practical Prediction of Time Dependent Deformations of Concrete. Part I - Shrinkage and Part II - Basic Creep. Matériaux et Construction, Vol. 11, No. 65, 1978, pp. 307-328. Part III - Drying Creep

and Part IV - Temperature Effect on Basic Creep. Matériaux et Contruction, Vol. 11, No. 66, pp. 415-434. Part V - Temperature Effect on Drying Creep and Pat VI Cyclic Creep, Non Linearity and Statistical Scatter. Matériaux et Construction, Vol. 12, No. 69, pp. 169-183.

09. Becker J (1974a)
Bizri H
Bresler B
FIRES-T. A Computer Program for the Fire Response of Structues - Thermal. Fire Research Group, University of California, Berkeley. Report No. UCB FRG 74-1. January 1974.

10. Becker J (1974b)
Bresler B
FIRES-RC. A Computer Program for the Fire Response of Structues - Reinforced Concrete frames. Fire Research Group, University of California, Berkley. Report No. UCB FRG 74-3, July 1974.

11. Billig K (1963)
Structural Concrete, Macmillan & Co LTD, New York, 1963.

12. Bizri H (1973)
Structural Capacity of Reinforced Concrete Columns Subjected to Fire Induced Thermal Gradients. Structural Engineering Laboratory. Report No. UC SESM 73-1. University of California, Berkley, January 1973.

13. BS1881 (1970)
Part 4 : Methods of Testing Concrete for Strength, BSI, 1970.

14. BS476 (1972)
Part 8 : Fire Tests on Building Materials and Structures. BSI, 15 pp. 1972.

15. Carette G G (1982)
Painter K E
Malhotra V M
Sustained High Temperature Effect on Concretes Made With Normal Portland Cement, Normal Portland Cement and Slag, or Normal Portland Cement and

Fly Ash, Concrete International, July 1982.

16. Chilver A H (1955) Instability of Testing Machines, Proc. I Mech. E, Vol. 169, No. 25, 1955.

17. Collette Y (1976) Etudes de propriétes du béton soumis á des températures élevées. Group de Travail, Comportement du Matériaux Béton en Fonction de la Température, Bruxelles, Novembre 1976.

18. Crook N (1980) The Elevated Temperature Properties of Reinforced Concrete. PhD Thesis University of Aston, September 1980.

19. Cruz C R (1966) Elastic Properties of Concrete at High Temperatures. PCA Research and Development Laboratories, 1966.

20. Cruz C R (1968) Apparatus for Measuring Creep at High Temperatures. Journal PCA, Vol. 10, No. 3, pp. 36-42, 1968.

21. Cruz C R (1980) Gillen M Thermal Expansion of Portland Cement Paste, Mortar and Concrete at High Temperatures. PCA. Fire and Materials, Vol. 4, No. 2, 1980.

22. Davis S H (1967) Effects of High Temperature Exposure on Concrete, Materials Research & Standards, October 1967.

23. Diedrichs U (1981) Schneider U Bond Strength at High Temperatures. Technical University of Brunswick. Magazine of Concrete Research, Vol. 33, No. 115, June 1981.

24. Dorn J E (1954) Some Fundamental Experiments on High Temperature Creep. Journal of the

Mechanics and Physics of Solids, Vol. 3, No. 2, pp. 85-116, 1954.

25. Dorn J E (1961) — Mechanical Behaviour Of Materials At Elevated Temperatures, McGraw-Hill, New York, 1961.

26. Dorn J E (1964) Mote J D — Physical Aspects of Creep. Proc. Of The Symposium on Nowal Structural Mechanics "High Temperature Structures And Materials", Perganon Press, 1964.

27. Dougill J W (1965) — Some Effects of Thermal Volume Changes on the Properties and Behaviour of Concrete. International Conference on the Structure of Concrete, Paper 12, 1965.

28. Dougill J W (1966) — Relevance of the Established Method of Structural Fire Testing to Reinforced Concrete. Applied Materials Research, Vol. 5, No. 4, pp. 235-240, 1966.

29. Dougill J W (1972a) — Modes of Failure of Concrete Panels Exposed to High Temperatures. Magazine of Concrete Research, Vol. 24, No. 79, pp. 71-76, 1972.

30. Dougill J W (1972b) — Conditions for Instability in Restrained Concrete Panels Exposed to Fire. Magazine of Concrete Research, Vol. 24, No. 80, pp. 139-148, 1972.

31. Dougill J W (1975) — Fire Resistance of Concrete Structures : Materials Aspects of Behaviour in Compression. Jubilee Conference on "Structural Design for Fire Resistance", September 1975.

32. Eisenstadt M M (1971) Introduction to Mechanical Properties of Materials, Macmillan, New York 1971.

33. FIP/CEB (1978) Report on Methods of Assessment of the Fire Resistance of Concrete Structural Members, C & CA, No. 15-393, pp. 91, 1978.

34. Fischer R (1970) Über das Verhalten von Zementmörtel und Beton bei Höhreren Temperaturen Deutscher Ausschuss für Stahlbeton (DAS) Heft 214, Berlin, 1970, pp. 60-128.

35. Freudenthal A M (1958) Roll F Creep and Creep Recovery under High Compressive Stress. Journal of the American Concrete Institute, Vol. 54, No. 12, pp. 1111-1142, June 1958.

36. Furamura F (1966) The Stress-strain Curve for Concrete at High Temperatures. Paper No. 7004 for the Annual Meeting of the Architectural Institute of Japan. 1966. (In Japanese, Copy held by the Fire Research Station Library, Ref. D17CT67 23.1966).

37. Gillen M (1981) Short Term Creep of concrete at Elevated Temperatures. Fire Research Dept. PCA, Fire and Materials, Vol. 5, No. 4, 1981.

38. Gross H (1973) Computer Aided Thermal Creep Analysis of Concrete Continua. PhD Thesis, University of London, 1973.

39. Gustaferro A H (1970) Temperature Criteria at Failure. ASTM STP 464, 1970.

40. Harmathy T Z (1967) A Comprehensive Creep Model. ASME

Transactions of the ASNE, Vol. 89, Series D, No. 3, September 1967.

41. Harmathy T Z (1970) — Thermal Properties of Concrete at Elevated Temperatures. National Research Council of Canada. ASTM Journal of Materials, pp. 47-74, Ottawa, March 1970.

42. Harmathy T Z (1966) Berndt J E — Hydrated Portland Cement and Lightweight Concrete at Elevated Temperatures. Proc. ACI, Vol. 63, pp. 93-111, 1966.

43. Harmethy T Z (1970) Lie T T — Fire Test Standard in the light of Fire Research, ASTM, STP-464, Fire Test Performance, 1970.

44. Holmes M (1982) Anchor R D Cook G M E Crook R N — The Effects of Elevated Temperatures on the Strength Properties of Reinforcing and Prestressing Steels. Journal IStructE, Vol. 60B, No. 1, March 1982.

45. Hughes B P (1966) Chapman G P — The Deformation of Concrete and Micro-concrete in Compression and Tension with Particualr Reference to Aggregate size. MCR : Vol. 18, No. 54, March 1966.

46. Intercole Systems Limited (1978) — Manuals for the Compulog Four System data logger. December 1978

47. Institution of Structural Engineers (1975) — Fire Resistance of Concrete Structures. Instn. of Struct. Engrs. London, August 1975.

48. Institution of Structural Engineers (1978) — Design and Detailing of Concrete Structures for Fire Resistance. Instn. of Struct. Engrs. London, April 1978.

49. ISO-834 (1968) — Fire Resistance Tests of Structures, International Organisation of Standardisation. 1968.

50. Issen L A (1970) Gustaferro A H Carlson C C — Fire Tests of Concrete Members, an Improved Method of Estimating Thermal Restraint Forces. ASTM STP 464, pp. 153-165, 1970.

51. Kraus H (1980) — Creep Analysis. Wiley-Interscience, 1980.

52. Kordina K (1977) et al — Jahresbericht 1975-77 Sonderforschungsbereich 148, TU Braunschweig, 1977.

53. Law M (1983) — Fire Exposure of Building Structures A Review of Experiments. Three Decades of Structural Fire Safety (BRE), 1983.

54. Lea F C (1920) — The Effect of Temperature on some of the Properties of Materials. Engineering, Vol. 110, No. 2852, August 1920.

55. Lie T T (1983) — A Procedure to Calculate Fire Resistance of Structural Members. Division of Building Research, National Research Coucil, Ottawa, Canada. Three Decades of Structural Fire Safety (BRE), 1983.

56. Lie T T (1972) Allen D E — Calculation of the Fire Resistance of Reinforced Concrete Columns. Division of Building Research, National Research Council. Technical Paper No. 378, Ottawa, August 1972.

57. Malhotra H L (1956) — The Effect of Temperature on the Compressive Strength of Concrete.

Magazine of Concrete Research, Vol. 8, No. 23, August 1956.

58. Malhotra H L (1982) — Design of Fire Resistance Structures. Surrey University Press, 1982.

59. Maréchal J C (1969) — Le fluage du béton en fonction de la température, Matériaux et Constructions, Vol. 2, No. 8, pp. 111-115, 1969.

60. Maréchal J C (1970a) — Fluage du béton en fonction de la température, Annales de l'Institut Technique du Bâtiment et Travaux Publiques, Vol. 23, No. 266, pp. 12-24, Fev 1970.

61. Maréchal J C (1970b) — Contribution a l'étude des Propriétes thermiques du béton, Annales de l'Institut Technique du Bâtiment et Travaux Publiques, Vol. 23, No. 274, pp. 123-146, Octobre 1970.

62. Maréchal J C (1970c) — Fluage du béton en fonction de la température - Compléments expérimentaux, Matériaux et Constructions, Vol. 3, No. 18, pp. 395-406, 1970.

63. Mackechnie Catalogue — General description and properties of the Mackechnie Loose Wool.

64. Neville A M (1981) — Properties of Concrete. Pitman, 3rd Edition, 1981.

65. Nimonic Alloys (1970) — Physical and Mechanical Properties. Publication No. 3270, January 1970.

66. Phillco R (1958) — Some Physical Properties of Concrete at High Temperature. Proc. ACI Vol. 54, pp. 857-864, 1958.

67. Popovics S (1973) — A Numerical Approach To The Complete Stress/Strain Curve Of Concrete. Cement & Concrete Research, Vol. 3, pp. 583-599, 1973.

68. Purkiss J A (1972) — A Study of the Behaviour of Concrete Heated to High Temperatures under Restraint or Compressive Loading. PhD Thesis, University of London, 1972.

69. Purkiss J A (1973) Dougill J W — Apparatus for Compression Tests on Concrete at High Temperatures, MCR, Vol. 25, No. 83, June 1973.

70. Schneider U (1976) — Behaviour of Concrete under Thermal Steady State and Non-Steady State Conditions. Fire and Materials, Vol. 1, No. 3, pp. 103-115, Sep. 1976.

71. Schneider U (1976) Haksever A — Bestimmung der äquivalenten Branddauer Von Statisch bestimmt gelagerten Stahlbetonbalken bei natürlichen Bränden. Report Of Institute für Baustoffkunde and Stahlbetonbau der TU Braunschweig, 1976.

72. Selvaggio S L (1963) Carlson C C — Effect of Restraint Concrete on Fire Resistance of prestressed Concrete. Fire Test Methods (1962), ASTM STP 344, pp. 1-25, Research Dept. Bulletin 164, PCA 1963.

73. Saemann J C (1957) Washa G — Variation of Mortar and Concrete Properties with Temperature, ACI Proceedings, Vol. 54, November 1957, pp. 385-395.

74. Sullivan P J E (1972) — Behaviour of Building Structures. A Complete Guide to Fire and buildings, Pubn. Lancaster 1972, pp. 150-170.

75. Sullivan P J E (1983)
Khoury G A
Grainger B N

Apparatus for Measuring the Transient Thermal Strain Behaviour of Unsealed Concrete under Constant Load for Temperatures up to 700 C. MCR, Vol. 35, No. 125, December 1983.

76. Sullivan P J E (1983)
Dougill J W

Developments in Design of Structural Concrete under Fire Conditions. Three Decades of Structural Fire Safety (BRE) 1983.

77. Tasmin U A (1975)
Culver C G

Effects of Elevated Temperature on Structural Members. Journal of the Structural Division. July 1975.

78. Thelandersson S (1976)
Anderberg Y

Stress and Deformation Characteristics of Concrete at High Temperatures. 2 Experimental Investigation and Material Behaviour Model. Lund Institute of Technology, Bulletin 54, 1976.

79. Three Decades of (1983)
Structural Fire Safety

International Seminar held at the Fire Research Station. BRE, Feb.1983.

80. Thomas F C (1953)
Webster C T

Fire Resistance of Reinforced Concrete Columns. National Building Studies Research, Paper No. 18, pp. 80, 1953.

81. Timoshenko S (1959)
Woinowsky-Krieger S

Theory of Plates and Shells, McGraw-Hill, New York 1959.

82. Witteveen J (1983)

Trends in Design Methods for Structural Fire Safety. Three Decades of Structural Fire Safety. BRE, February 1983.

83. Wittmann F H (1982)

Creep and Shrinkage Mechanisms, Chapter 6 of Creep and Shrinkage in Concrete Structures. Edited by Z P Bazant and F H Wittmann. John Wiley & Sons Ltd., 1982.

84. Zoldners N G. (1960) Effect of High Temperatures on Concrete Incorporating Different Aggregates. Proc. ASTM Vol. 60, pp. 1087-1108, 1960.